Analysis of IEEE 802.11e and Application of Game Models for Support of Quality-of-Service in Coexisting Wireless Networks

Von der Fakultät für Elektrotechnik und Informationstechnik
der Rheinisch-Westfälischen Technischen Hochschule Aachen zur
Erlangung des akademischen Grades eines Doktors der
Ingenieurwissenschaften genehmigte Dissertation

vorgelegt von

Diplom-Ingenieur
Stefan Mangold

aus Goch

Berichter: Universitätsprofessor Dr.-Ing. Bernhard Walke
Universitätsprofessor Dr. Petri Mähönen

30. Juni 2003

To Hella

Abstract

The *Institute of Electrical and Electronics Engineers, Inc.* (IEEE) is currently developing the *IEEE 802.11e* (802.11e) as an extension of the IEEE 802.11 wireless *Local Area Network* (LAN) standard, to enable wireless LANs to achieve higher data throughput and lower delay constraints, hence, to support *Quality of Service* (QoS). By applying 802.11e, stations are able to carry multimedia and Internet applications with QoS. Home networks with their characteristic applications such as voice, video, and interactive data, typically require QoS.

This thesis provides an overview about this new standard, and analyzes the limits of 802.11e in various network configurations. The new coordination function of the 802.11e *Medium Access Control* (MAC) is described and analyzed, where a variety of enhancements of 802.11e are evaluated by means of analytical approximation and stochastic simulation.

The problem of QoS support in coexistence scenarios of overlapping *Basic Service Sets* (BSSs), i.e., co-located sets of communicating 802.11e stations, is discussed.

In an isolated scenario of one single BSS, QoS is guaranteed by one central coordinator polling other stations for data transmission, similar to the European wireless LAN *High Performance Local Area Network type 2* (HiperLAN/2).

In a coexistence scenario of overlapping BSSs, stations cannot guarantee any QoS because of the uncoordinated access to radio resources. Any utilization of radio resources by a BSS depends on the activities of competing BSSs.

The approach developed in this thesis to allow BSSs to support and guarantee QoS is to apply models derived from the theory of games. The models are used to analyze the mutual influence of coexisting BSSs, and to define means for interaction based on actions, utility functions, and payoffs. The competition scenario is modeled as game, and evaluated with a Nash analysis. In a game, a BSS is modeled as player that attempts to maximize its payoff, which is an abstract representation of QoS.

As result of the game approach, the enhanced protocols are able to follow strategies that allow wireless LANs to significantly improve their QoS support, and the overall spectrum efficiency.

Kurzfassung

Das *Institute of Electrical and Electronics Engineers, Inc.* (IEEE) entwickelt *IEEE 802.11e* (802.11e) als eine Erweiterung des populären IEEE 802.11 Standards für drahtlose *Local Area Networks* (LANs). 802.11e Funkstationen werden zukünftige drahtlose Multimedia- und Internet-Anwendungen wie zum Beispiel Audio- und Videokommunikation ermöglichen.

Die vorliegende Arbeit liefert einen Überblick über den Standard (Stand 2003) und analysiert die Möglichkeiten der Dienstgüte-Unterstützung für unterschiedlichen Szenarien. Der Standard wird mittels eines analytischen Models, das in dieser Arbeit entwickelt wird, und mittels stochastischer Simulation bewertet.

Speziell das Koexistenz-Problem der eingeschränkten Dienstgüte-Unterstützung bei im Spektrum konkurrierenden *Basic Service Sets* (BSSs), also Gruppen von 802.11e Funkstationen, wird analysiert. Da 802.11 Funknetze in lizenzfreien Funkbändern betrieben werden, ist ein solches Wettbewerbs-Szenarium mit der wachsenden Bedeutung von drahtlosen LANs wahrscheinlich. In einem Wettbewerbs-Szenarium können Funknetze, die im isolierten Betrieb auf Grund exklusiven Zugriffs auf Funkresourcen Dienstgüte unterstützen, auf Grund der nun entstehenden Konkurrenz um Funkressourcen Dienstgüte nur noch eingeschränkt unterstützen.

Basierend auf einem Konzept zur Integration von HiperLAN/2 in 802.11e wird die Koexistenz von Funknetzen mit Hilfe spieltheoretischer Modelle abstrahiert, analytisch beschrieben, und simuliert. Als Teil des Spielmodells werden um Funkressourcen konkurrierende Netze als ertragsmaximierende Spieler modelliert, die basierend auf individuellen Nutzenfunktionen in einer wiederholten Interaktion bemüht sind, die eigenen Dienstgüte-Anforderungen so genau wie möglich zu erreichen. Das Spielmodell erlaubt, dass die Aktionen eines Gegenspielers und die Wirkung der eigenen Aktionen auf den Gegenspieler mit in Betracht gezogen werden. Mittels Bestimmung der Nash Equilibria in einem Spiel wird in dieser Arbeit das Szenarium zweier konkurrierender Netze auf Stabilität und Konvergenz untersucht. Für eine wiederholte Interaktion werden unterschiedliche Strategien entwickelt und bewertet. Auf Grund seines Abstraktionsgrades ergeben sich Möglichkeiten zur Nutzung des Spielmodells für beliebige Szenarien, in denen konkurrierende Funknetze, die ihre Funkressourcen selbstständig koordinieren, im unlizenzierten Frequenzband koexistieren müssen.

Table of Contents

Chapter 1

INTRODUCTION

COMMUNCATION is life. Communication serves as key means to the globalized world to establish the fundaments of what is referred to as worldwide information society. The way people are living, working, and interacting with each other will change over the decades during which the information society will grow and develop, hopefully bringing welfare to more people. Wireless communication will help to establish this new society.

This thesis is related to wireless communication. In this thesis, support of *Quality of Service* (QoS) in wireless *Local Area Networks* (LANs) is analyzed. New approaches for radio spectrum coordination of coexisting wireless networks are developed. Focus of interest is the *Institute of Electrical and Electronics Engineers, Inc.* (IEEE) wireless LAN protocol 802.11 (in this thesis referred to as *802.11)* (IEEE 802.11 WG, 1999c) with its enhancements for QoS support. Further, a combination of this protocol with the *High Performance Local Area Network type 2* (in this thesis referred to as *HiperLAN/2)* defined by the *European Telecommunications Standards Institute* (ETSI) project *Broadband Radio Access Networks* (BRAN) (ETSI, 2000a) is discussed.

1.1 Increasing Demand for Wireless QoS

The increasing popularity of wireless networks over the last years, and of wearable, hand-held computing and communicating devices, as well as consumer elec-

tronics, indicates that there will be a demand for communicating devices providing high capacity communication together with QoS. QoS is becoming an important factor in wireless networks. It refers to the ability of a network to provide services to applications with certain requirements such as data delivery delay, delay variation, throughput and reliability.

Considering this increase in demand, the growth of the Internet, and the many initiatives to develop the wireless Internet, it is clear that the necessary radio spectrum will not be available in the future due to the limited nature of the radio resources. Because the radio spectrum is a finite and limited resource, spectrum efficiency is critical. The radio spectrum is the resource that has to be used most efficiently, by at the same time being able to support future applications of wireless networks. This means that not only spectrum efficiency, but also QoS support is required in the future and has to be provided by future wireless networks.

Wireless communication researchers are today at the point where the task of managing the radio spectrum becomes increasingly difficult. Future wireless networks will meet many technical challenges in radio resource control, and QoS support.

1.2 Technical Approach

Usually, spectrum is licensed for the use of a certain type of wireless networks. The fact that a licensed radio spectrum is very often not used all the time in every place often results in low spectrum efficiency, when radio spectrum is exclusively licensed to individual services under the control of a single network operator. It would be more spectrum efficient if different wireless networks could share the radio spectrum, even if they would operate with different types of transmission systems and *Medium Access Control* (MAC) protocols. This is approached by unlicensed bands.

From the approach of unlicensed bands, the problems arise of how to support QoS for particular services, and how to apply radio resource sharing between systems competing for the same radio resources. Coexistence of different wireless networks operating in the same spectrum and competing for radio resources is one of the challenges in the development of future wireless networks.

HiperLAN/2 and 802.11 are different wireless LANs and operate in unlicensed bands. Wireless LANs have to share radio resources among different networks, which is the reason for the problematic support of QoS (Mangold et al. 1999; Mangold and Siebert 1999; Mangold 2000; Mangold et al. 2000). This thesis discusses approaches for QoS support, radio resource sharing, and coexistence of

wireless networks in unlicensed spectra, with focus on IEEE 802.11 wireless LAN and its QoS enhancements defined in the supplement standard 802.11e. The frequency band of interest here is the 5 GHz *Unlicensed-National Information Infrastructure* (U-NII).

QoS support in 802.11e is evaluated by means of an analytical model of the protocol, and stochastic simulation. Spectrum sharing among wireless networks is discussed by applying methods taken from game theory.

1.3 Outline

This thesis is outlined as follows. In the next chapter, regulatory requirements, spectrum issues and transmission schemes applied in the 5 GHz unlicensed band are briefly discussed and summarized. The indoor channel error characteristic and a model for error calculation are highlighted to provide a basic knowledge about the wireless networks and their environment discussed in this thesis.

The popular 802.11 is described in Chapter 3. In Chapter 4, the currently discussed MAC enhancements of 802.11 to support QoS are summarized, based on the status of standardization at the time this thesis was written.

In Chapter 5, a detailed analysis of the new MAC enhancements is given, based on stochastic simulation, and analytical approximation. The 802.11e part of the simulator WARP2, which is described in Appendix A, was developed by the author of this thesis and is used for this purpose.

In Chapter 6, a concept to integrate HiperLAN/2 into 802.11e is developed, which will be used in the rest of the thesis to discuss the coexistence problem. In this discussion of the coexistence problem, a game model is developed in Chapter 7, which is used for a single stage game analysis in Chapter 8, again based on an analytical model and simulation. The simulator YouShi, which is described in Appendix B, was developed by the author of this thesis and is used for this purpose.

Finally, in Chapter 9, a multi stage game analysis is provided which allows to define means for the coexisting networks to support QoS by mutual support when interacting for longer durations. Conditions are developed under which such mutual support will be an expected result of interaction.

This thesis ends with the conclusions in Chapter 10. A table of symbols and the list of abbreviations are available at the end of this thesis, see page 239 and 253, respectively.

Chapter 2

WIRELESS COMMUNICATION IN UNLICENSED BANDS

FOR THE UNDERSTANDING of wireless communication, spectrum issues and the transmission scheme of interest for the 5 GHz unlicensed band are discussed in this chapter. The radio channel characteristics are discussed and a model for error calculation of the *Orthogonal Frequency Division Multiplex* (OFDM) transmission scheme is developed to provide knowledge about wireless communication and the environment the WLANs of interest are operating in. he design of a wireless network requires an accurate characterization of the radio channel, specifically a precise model that can be used in time-consuming computer simulation. With an accurate channel characterization and with a detailed mathematical model of the channel, the performance and attributes of a radio transmission scheme and protocols are predictable by means of simulation. The characteristics of an indoor radio channel vary from with the environment, which must be considered when modeling the indoor radio channel.

2.1 The Indoor Radio Channel

Wireless LANs operate mainly in the indoor environment. Radio propagation in indoor environments is complicated because the direct path between transmitter

and receiver (i.e., *Line of Sight, LOS*) is often obstructed by intervening structures (Mangold, 1997). The result is an effect referred to as multi-path fading.

2.1.1 Multi-path Fading in Indoor Environment

A radio signal transmitted in an indoor environment reaches a receiver by more than only the LOS path, and from various directions. Before arriving at the receiver antenna, all paths except the LOS go through at least one order of reflection, transmission or diffraction. This is known as multi-path fading. Multi-path fading is caused by constructive and destructive interference between the signal waves. They combine at the receiver antenna to a resultant signal, which can vary widely in amplitude and phase. The multi-path phenomenon produces a series of delayed and attenuated echoes for a transmitted signal. Radio channel models describe how this transmitted signal is affected by the radio channel. The frequency band of interest in this thesis is the 5 GHz unlicensed band.

Figure 2.1 shows plots of the amplitude of a typical time domain response $|h(t,x)|$ measured at a receiver location x, and the corresponding frequency response $|H(f,x)|$ obtained from the Fourier transform of $h(t,x)$. The amplitude of the frequency response in dB, and the amplitude of the time response on a linear scale are shown. The frequency response consists of samples at a frequency spacing of *2.5 MHz* for a frequency span of *2.0 GHz*, which is centered at *5.0 GHz*. Such a large frequency span is necessary for a high precision of the time response. The interval between *5.0 GHz* and *5.4 GHz* is shown in the figures to show the frequency selective fading for the discussed frequency band. The frequency selective nature of the channel can be seen at certain frequencies in Figure 2.1, right.

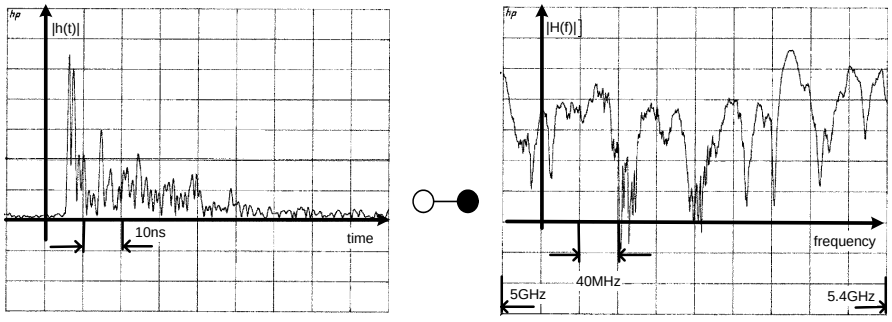

Figure 2.1: (Mangold, 1997) Left: time domain response of the multi-path channel with linear scaling.Right: presentation in frequency domain, amplitude in dB. The normalized signal envelope is indicated with a *5dB/unit* scale.

There are frequencies at which a transmission may be successful, but other frequencies may be useless for transmissions. The channel is referred to as frequency selective radio channel.

From the frequency response, a periodic time response of a maximum duration of *400 ns* can be derived. An impulse response in indoor scenarios is typically smaller than *400 ns*. Figure 2.1, left, is an illustration of such a periodic time response. The effects of the multi-path characteristic of the indoor environment can be clearly seen. The time domain response illustrates the multi-path propagation. Multiple delayed peaks in the signal arrive at the receiver antenna later than the first received signal. This is a result of the multi-path channel, which causes frequency selectivity. The phase is linear for most of the frequency band (Mangold, 1997).

2.1.2 Time Variations of Channel Characteristics

A radio channel can be modeled as time varying linear filter for a given transmitter and receiver location. In indoor environments, when employing local area radio networks with high data rates, it can be assumed that the channel is slowly time varying compared to the transmission cycles[1] of radio networks. For this reason, the impulse response can be assumed time invariant for short time intervals of some milliseconds. The radio channel is interpreted as *Wide Sense Stationary* (WSS) (Höher 1992).

The time varying nature of the indoor radio channel is caused either by the relative motion between the transmitter and the receiver station, or by movements of objects in the transmission path. It is generally described by the Doppler spread B_D. The Doppler effect causes frequency shifts in the received signal, which makes the reception difficult. The Doppler spread B_D is a measure of the spectral broadening caused by the speed of changes of the indoor radio channel. The larger the velocities of moving stations or objects in the environment, the larger the Doppler spread. For example, If a pure sinusoidal harmonic wave is transmitted with frequency f_c, the signal at the receiver will have spectrum components in the range of $f_c \pm B_D/2$ where $B_D = v f_c/c$, where v is the velocity of objects in near distances or of the antenna, and c is the speed of the electromagnetic waves. The coherence time T_c is a measure of the average time duration over which the indoor radio channel is stationary. The Doppler spread and the coherence time are

[1] A transmission cycle of a radio network is a transmission of data by one radio station, for example a data frame exchange in 802.11. Typically durations are less than *1 ms*.

inversely proportional to each other ($T_c \approx 1/B_D$). In indoor environments, the base band signal bandwidth is larger than the Doppler spread and the effects of time variations are negligible at the receiver. Therefore, and in accordance with the WSS channel, the wide-band propagation characteristics of radio waves within buildings can be characterized as slowly fading channels, which are stationary for transmission cycles. What is not stationary, i.e., slowly changing, is the interference caused by neighboring radio transmissions from other transmitting stations. Interferences are the limiting parameter in indoor radio systems and need to be considered in simulation, or analytical models, as accurate as possible.

2.2 Orthogonal Frequency Division Multiplexing

Orthogonal Frequency Division Multiplexing (OFDM) is the transmission scheme used by the wireless LANs that are considered in this thesis. This transmission scheme is discussed in the following.

Radio transmission within buildings typically experience multi-path propagation. In a conventional serial data system, short data symbols are sequentially transmitted. The frequency spectrum of each data symbol is allowed to occupy the entire available bandwidth. As described in the previous section, in indoor environments the received signal arrives as an unpredictable set of reflections and direct waves each with its own degree of attenuation, delay and phase shift. This leads to *Inter-Symbol Interferences* (ISI) between consecutively transmitted data symbols due to the signal delay spread at the receiver. *Multi Carrier Modulation* (MCM) techniques like OFDM transmit data by dividing the high symbol rate stream into several low symbol rate streams, and by using these sub-streams to modulate different sub-carriers (Mangold 1997). The symbol duration of each sub-stream is then higher than the channel delay spread and the maximum excess delay of delayed signals. By using a large number of OFDM sub-carriers, immunity against the multi-path effect can be provided (Cimini, 1985). OFDM, having densely spaced sub-carriers with overlapping spectra of the modulated sub-carriers, abandons the use of steep band pass filters to detect each sub-carrier as it is used in classical *Frequency Division Multiplexing* (FDM) schemes. It offers therefore a high spectral efficiency. There are extensions of OFDM, which are not used in HiperLAN/2 and 802.11a, towards a more flexible MCM. The enhanced MCM is based on Wavelet transforms, where the individual sub-carriers have different bandwidths. This aims to provide an accurate adaptation of the transmission scheme, in terms of data-throughput per sub-carrier, to the time-variant radio channel. In indoor radio environment, signals coming from multiple indirect paths added to the direct path mean that the condition of orthogonality

between sub-carriers is no longer fulfilled, which results in *Inter-Channel Interference* (ICI). However, multi-path propagation can cause ISI as well. The part of the OFDM symbol that carries the information is in the following referred to as block instead of symbol, to distinguish it from the symbols per sub-carrier. Adding a guard interval T_g before the block period T_b can circumvent both effects. A new block duration, $T_b'=T_g+T_b$ is then obtained. This duration represents what is known as OFDM symbol duration. The guard interval is typically smaller than $T_b/4$. If T_g is longer than the maximum channel excess delay, the sub-carriers are still mutually orthogonal inside the effective block interval $(T_g ... T_b')$. Adding a guard interval means that a cyclically extended OFDM symbol is transmitted. Pre-pending a cyclic prefix in an OFDM symbol aids to remove the effects of the multi-path channel by making the OFDM symbol to appear periodic in time. Only with (nearly) periodic discrete-time signals, a convolution of two signals is equivalent to multiplying the Fourier transforms (frequency responses) of the respective signals, here an OFDM symbol and the channel impulse response. OFDM symbols are created by an *Inverse Fast Fourier Transform* (IFFT) of the data to be transmitted. The frequency response of an OFDM symbol generated with an IFFT is the original data, thus each original data symbol is multiplied by a single complex number when it is transmitted over the radio channel. Equalization at the receiver becomes very simple, or even avoidable.

There are two drawbacks of the cyclic prefix worth to be mentioned (Mangold et al., 2001f). One is that redundant data is transmitted over the radio channel reducing the maximum data throughput on top of OFDM. The other drawback is that the cyclic prefix of duration T_g leads to a power loss, as the receiver only uses the energy received during the time T_b. The energy corresponding to T_g is discarded. A power loss α_g must be taken into account:

$$\alpha_g = \frac{T_b}{T_{b'}} \tag{2.1}$$

In HiperLAN/2 and 802.11a, one 52-sub-carrier OFDM symbol occupying *16.6 MHz* has a duration of $4\ \mu s$, and $T_g=800\ ns$ (or, optionally in HiperLAN/2, $T_g=400\ ns$) results in $\alpha_g = 0.8$ (respectively *0.9*). With $T_g=800\ ns$, the useful received signal energy per symbol, E_{av}, is *20 %* less than the received signal energy without cyclic prefix. Now, it is to be differentiated between background noise N and the cumulated interference level ΣI. The interference ΣI is as well created by electromagnetic harmonic sinusoidal waves, as is the wanted signal. Integrating the signal energy and the interference energy over a shorter time, i.e., T_b' instead of T_b reduces the received signal energy by α_g, and to an unknown extend the

cumulated interference level. Note that signals arrive from different locations, and transmitters. Therefore, and because of the tolerant specifications in HiperLAN/2 and 802.11a in terms of frequency accuracy, the worst-case scenario is assumed that ΣI is not affected by the guard interval, and

$$\frac{E_{av}}{N_0} = \frac{\alpha_g C}{(N + \sum I)}. \tag{2.2}$$

The 802.11a and HiperLAN/2 *Physical Layers* (PHY) are almost identical. They apply a 52-carrier OFDM with convolution coding and linear modulation schemes that can be adaptively chosen based on QoS requirements and radio channel conditions. 48 carriers out of 52 are used for data transport (IEEE 802.11 WG, 1999a; ETSI, 2000a). The remaining four sub-carriers of the OFDM symbols are used for pilot symbols. The 802.11a task group of the 802.11 working group accepted the OFDM transmission scheme defined for HiperLAN/2, which facilitates the development of coexistence and interworking mechanisms between the two systems. It is worth noting that the IEEE 802.11 standard specifies a MAC protocol without the definition of the PHY for 5 GHz. 802.11a as a supplement of 802.11 specifies the PHY for the 5 GHz OFDM transmission (IEEE 802.11 WG, 1999a). The Table 2.1 summarizes numerical values for the main parameters of the OFDM transmission system as defined by the two standards.

Table 2.1: Numerical values for the OFDM parameters of 802.11a and HiperLAN/2 (IEEE 802.11 WG, 1999a; ETSI, 2000a)

Parameter	Value
Sampling rate $1/T$:	*20 MHz*
OFDM block duration T_b:	$64 \cdot T = 3.2\ \mu s$
Guard interval duration T_g:	$16 \cdot T = 0.8\ \mu s$ *(0.4 µs optional in HiperLAN/2)*
OFDM symbol duration $T_b' = T_g + T_b$:	$80 \cdot T = 4\ \mu s$
Number of data sub-carriers:	*48*
Number of pilot sub-carriers:	*4*
Total number of sub-carriers N_{total}:	*52*
Sub-carrier spacing D_f:	$1/T_b = 0.3125$ *MHz*
Spacing betw. the outmost sub-carriers:	$(N_{total}-1) \cdot D_f = 15.9375$ *MHz*

2.3 The 5 GHz Band

The 5 GHz unlicensed band comprises frequency bands between *5.15 GHz* and *5.825 GHz*. Figure 2.2 illustrates this spectrum as it is defined for the U.S. and Europe.

A spectrum of *300 MHz* has been released in the U.S. for the *Unlicensed National Information Infrastructure* (U-NII) band. A spectrum of *455 MHz* is available in Europe. In an unlicensed band, regulators permit the operation of any radio communication systems, in contrast to an allocation of spectrum on a licensed base. The restrictions that regulators put on the candidate systems are radio parameters such as limits of the radiated power, out of band emissions, antenna characteristics and the communication services that are supported.

Different center frequencies f_c are defined for the 5 GHz unlicensed band. In the U.S., three U-NII bands are defined between 5.15 GHz and 5.825 GHz leading to 12 frequency channels for operation. In Europe, current regulations allow the operation of wireless LANs at 19 channel frequencies. However, 11 more channels will be available in the U.S. by end of 2003.

The channelization of 20 MHz is not mandatory in the U.S., as part of the regulation. Higher antenna gains are permitted with corresponding reduction of transmitter power. In Europe, wireless LANs must use full spectrum range in order to share the spectrum with radar systems, based on *Dynamic Frequency Selection* (DFS) and *Transmitter Power Control* (TPC). However, in the lower part of the spectrum, below *5350 MHz*, wireless LANs are permitted to operate without these complicated schemes (REGTP, 2002).

2.4 Error Model for the OFDM Transmission applied in the 5 GHz Unlicensed Band

For the OFDM transmission technique applied in the 5 GHz unlicensed band, an error model was developed in Mangold et al. (2001f). This model makes use of an analytical approximation of packet errors of any length, which was developed in Qiao and Choi (2001). This approximation is summarized in Appendix C, and is in this thesis referred to as the Qiao-Choi transmission error probability analysis. The error model for the OFDM transmissions is of importance for this thesis, because it is implemented in the WARP2 simulation tool, as described in Appendix A. The WARP2 simulation tool is used for the analysis of 802.11 in this thesis.

In the following, network elements such as *Access Point* (AP), *Central Controller* (CC), *Wireless/Mobile Terminal* (WT/MT) or *Station* are referred to as a *station*. A combination of coding and modulation schemes is called a *Physical layer Mode* (PHY mode), which may be dynamically selected for transmission by a station. A *burst* is called the single transmission of a frame including preambles and headers initiated by one station. A burst comprises a preamble and a subsequent frame sent as a number of OFDM symbols. Preambles are used for time and frequency synchronization and frame identification. As part of the error calculation, it is assumed that a frame always is transmitted completely at a specific PHY mode and at a constant power level. After a preamble, there follows a number of OFDM symbols sent at the basic and most protected PHY mode, for example, the SIGNAL field as part of the *Physical Layer Control Protocol* (PLCP) header in 802.11a. This is neglected for the sake of simplicity of the model. See Figure 2.3 for an illustration of a burst. The power of a burst received at the addressed station is referred to as *C*; whereas the sum of unwanted interference is generally noted as *ΣI*. Background noise is represented as *N*, which is in the area of *-95dBm* for HiperLAN/2 and 802.11a OFDM receivers.

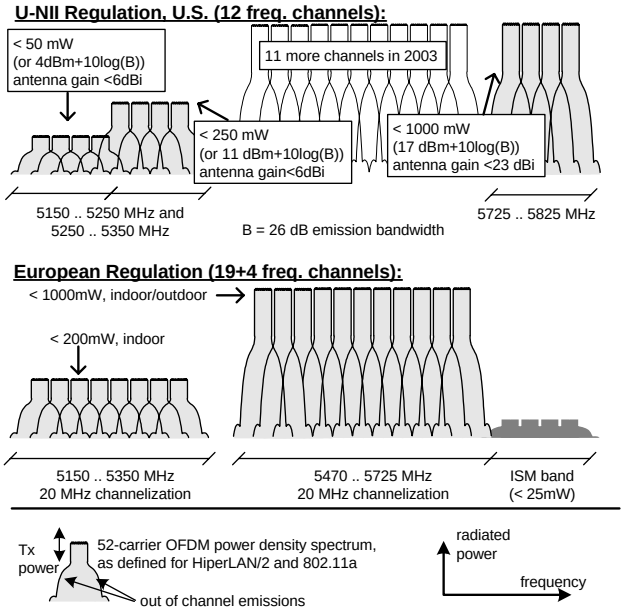

Figure 2.2: The 5 GHz band for wireless LANs in the U.S. and Europe. Higher antenna gains are permitted with corresponding reduction of transmitter power. In Europe, wireless LANs must use the full spectrum in order to share the spectrum with radar systems efficiently (an exception from this rule is defined in REGTP (2002)).

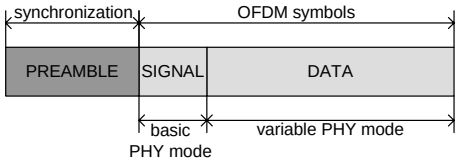

Figure 2.3: 802.11 Burst. The signal field is neglected in the error calculation. See Figure 3.3 for more details.

2.4.1 Interference Calculation

The numerical analysis presented in Section 2.4.3 requires a $C/(\Sigma I+N)$ value for the decision about correct or erroneous reception of frames. This value is calculated as follows. The value of $C/(\Sigma I+N)$ is lower than for the interference free burst when interfering (alien) bursts superpose with the original burst. The original, received burst arrives with signal level C, whereas other bursts contribute to ΣI. Figure 2.4 shows the way of calculating the cumulative interference power. The received power of the burst incoming with the carrier power level is stored in the receiver instance for the length of its transmission. Other bursts that arrive during this time will contribute to the interference power.

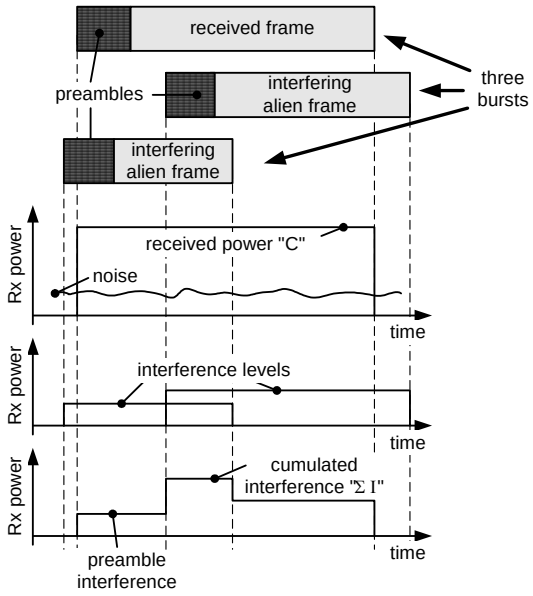

Figure 2.4: (Mangold et al., 2001f) The simplified interference model. A cumulative interference plus the noise is used for the preamble interference and frame interference calculations. A successful frame reception requires individual minimum $C/(\Sigma I+N)$ values, which can be different for synchronization (preamble reception) and frame reception.

Overlapping bursts transmitted at the same time is a typical case when two or more stations try to access a random access channel at the same time in HiperLAN/2 scenarios.

Further, 802.11 stations will transmit at the same time because of the contention-based protocol. Overlapping bursts occur also if 802.11a and HiperLAN/2 operate at the same frequency channel. The case where the original burst arrives later than multiple interfering bursts or signals is also considered.

Assuming the original burst's received signal strength is high enough, compared to the signal strength of the interfering burst; it can correctly be decoded even if the receiver was currently receiving another burst.

The calculation of the received powers is based on the distance d the signal traveled, the actual transmitter power level P_{Tx}, the frequency f_c it was sent at and by assuming certain OFDM- and environmental conditions. The following equation can be used for the path loss calculations between the stations:

$$P_{Rx} = \begin{cases} P_{Tx} g_{Tx} g_{Rx} \left(\dfrac{c}{f_c 4\pi} \right)^2 , d \le 1m & \textit{(free space),} \\ P_{Tx} g_{Tx} g_{Rx} \left(\dfrac{c}{f_c 4\pi} \right)^2 \cdot \dfrac{1}{d^{\gamma}} , d > 1m & \textit{(multi-path).} \end{cases} \tag{2.3}$$

In this equation, the antenna gains g_{Tx} and g_{Rx} are 1 and the path loss coefficient $\gamma = 3.5$, respectively. The cumulative interference power is calculated as the maximum interference power during one received burst by summing up the signal power of all interfering bursts, even if they do not contribute during the complete reception interval.

The interference level that is used for bit error calculations is derived from the simple model. It is not taken into account that in some cases only some of the consecutive OFDM symbols of a received burst may be distorted by a short interfering burst. Using the instantaneously updated cumulative interference level ΣI, the $C/(\Sigma I+N)$ ratio at the receiver antenna is calculated. If the received $C/(\Sigma I+N)$ throughout the burst duration is above a predefined level, the receiver sensitivity, then it is assumed that the frame can be decoded. It is then evaluated according to the $C/(\Sigma I+N)$ for the preamble and the frame, separately.

If another burst arrives during reception of a burst then it contributes to the interference power level, which means that the $C/(\Sigma I+N)$ for the original burst must be re-evaluated. In this case, a receiving station considers the new burst as interference. It waits for the rest of the original burst to arrive and then calculates

the frame error probability with the error calculation discussed in Section 2.4.2. In this calculation, the value E_{av}/N_0 relates to $C/(\Sigma I+N)$.

The following assumptions are made for the error calculations explained in Section 2.4.2:

- The maximum excess delay of the radio channel is always smaller than T_g. T_g=*400 ns* or T_g=*800 ns* => *ISI=ICI=0*.
- The background noise and interferences is interpreted as *Additive White Gaussian Noise* (AWGN), neglecting the fact that interfering signals might well be correlated to the original received signal.
- The energy of a data symbol is evenly spread over all sub-carriers all bits transmitted as part of one OFDM symbol observe the same E_{av}/N_0.
- The radio channel behaves like the WSS channel with constant received power over the burst duration of all bursts.

2.4.2 Error Probability Analysis

The rest of the error calculation is based on the Qiao-Choi transmission error probability analysis (Qiao and Choi 2001). This analysis is summarized in Appendix C, p. 225.

2.4.3 Results and Discussion

The following figures show the results of the analysis presented in Appendix C. Figure 2.5 shows the *Bit Error Ratio* (BER) vs. E_{av}/N_0 for the four linear modulation modes used in HiperLAN/2 and 802.11, comparing single carrier transmission and OFDM multi-carrier transmission. With OFDM, the BER is slightly larger than without, which is obviously due to the introduction of the guard interval in OFDM. With only a small degree of multi-path, there is not much gain from the guard interval, since it is assumed that the maximum excess delay of the radio channel is always smaller than T_g.

Figure 2.6 presents the results for the *Packet Error Ratio* (PER) vs. E_{av}/N_0 for a frame length of *54 byte*, the size of a HiperLAN/2 data frame, assuming OFDM multi-carrier transmission. It can be seen that BPSK3/4 shows roughly the same performance as QPSK1/2, indicating that selecting BPSK3/4 for operation is never the optimal choice. However, the error analysis is based on the AWGN assumption. BPSK3/4 can become more useful than QPSK1/2 in realistic scenarios with multi-path channels. Another reason to select the BPSK3/4 mode although it shows the same error performance as QPSK1/2 is the longer duration required for transmission of data frames, which can be advantageous in resource sharing scenarios.

In Figure 2.7, the PER is shown for different frame lengths. In 802.11, an arbitrary frame length of up to *2304 byte* not including MAC and PHY headers is allowed. Ethernet feeds the MAC with a data packet of a maximum length of *1514 byte*. Typically, long frames are fragmented into shorter frames before transmission in 802.11, mainly in order to increase the utilization of the radio channel.

The resulting PER vs. E_{av}/N_0 for a frame length of 54, 512 and the maximum size of *2304 byte* are shown. As expected, the PER increases with the frame length. Using the results of the analysis presented here, the simulation tool WARP2 works with an error model that models many important radio effects. However, it remains to be investigated how to model the multi-path in office and outdoor scenarios, where the maximum excess delay of the radio channel generally exceeds the guard interval of the OFDM symbols. Results presented in Khun-Jush et al. (1999) indicate that the results that have been calculated here are optimistic for typical office scenarios. In general, with ISI and ICI because of multi-path, a better C/(ΣI+N) is required, however, with the same dependencies between the different PHY modes as presented here.

The analytical approach discussed here does not perfectly represent the real life error characteristics. However, the model takes into account all relevant effects such as the channel characteristics, OFDM parameters, frame lengths, preambles, and modulation and coding schemes, where some necessary simplifications are made. Specifically, the model relies on the AWGN assumption.

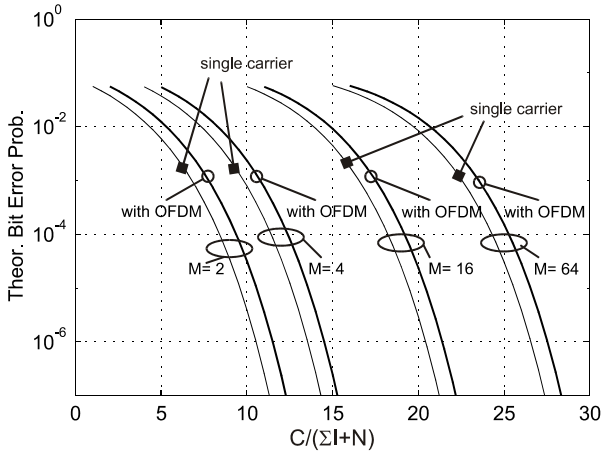

Figure 2.5: (Mangold et al., 2001f) BER vs. E_{av}/N_0 for the linear modulation modes of interest, i.e., BPSK, QPSK, 16QAM, and 64QAM. A guard interval of *800 ns* is assumed for the underlying OFDM. HiperLAN/2 optionally allows the use of a guard interval of *400 ns.*

This way of calculating transmission errors in OFDM transmission schemes with adaptive modulation and coding rates intends to support fast calculations of frame transmission, by allowing to simulate hidden stations, interferences, possible failed synchronization, and signal capture-effects. The channel models have been implemented in the SDL-based simulation environment WARP2, which is capable of accurately modeling the two radio transmission protocols, HiperLAN/2 and 802.11a.

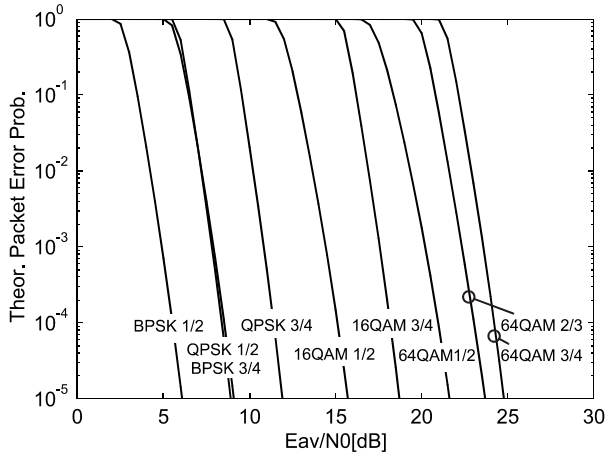

Figure 2.6: (Mangold et al., 2001f) PER vs. E_{av}/N_0 for a frame length of *54 byte*. The PHY mode 64QAM1/2 is not part of 802.11a or HiperLAN/2.

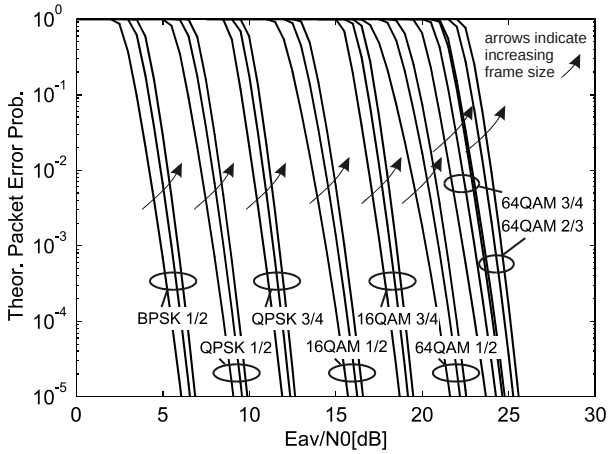

Figure 2.7: (Mangold et al., 2001f) Influence of the frame length on PER in 802.11. The resulting PER vs. E_{av}/N_0 for a frame length of *54 byte*, *512 byte* and the maximum size of *2304 byte* are shown. BPSK3/4 is not shown as it overlays with QPSK1/2. The PHY mode 64QAM1/2 is not part of 802.11a or HiperLAN/2.

Chapter 3

IEEE 802.11

THE IEEE 802 COMMITTEE has established standards for communication systems that have been major contributions to the communications industry, for exampled IEEE 802.3 Ethernet and IEEE 802.5 Token Ring. The most successful IEEE standard for wirless communication is IEEE 802.11. The IEEE published IEEE 802.11 in 1997 as a standard for wireless LANs, and published a revised version in 1999 (IEEE 802.11 WG, 1999c). At the same time, the IEEE 802.11b supplement standard for higher data rates than originally defined has been published (IEEE 802.11 WG, 1999b). This is the best-known wireless LAN today and referred to as IEEE 802.11b. IEEE 802.11b is known under the acronym *Wireless Fidelity* (Wi-Fi). This standard is widely accepted as a wireless LAN that meets the current requirements; see Heegard et al. (2001), Henry and Luo (2002). Wireless LAN IEEE 802.11 is described and analyzed in detail in Hettich (2001) and Walke (2002).

In this chapter, the MAC protocol of 802.11 is briefly described. Problems in QoS support that motivated the 802.11 working group to develop new enhancements for the support of QoS are summarized. This chapter is outlined as follows. In the next section, the reference model is described, and in Section 3.2, the architecture and provided services are discussed. Section 3.3 highlights the details of the 802.11 protocol. For clarification, all supplement standards developed so far are briefly summarized in Section 3.4, at the end of this chapter.

3.1 IEEE 802.11 Reference Model

Like IEEE 802.3 (Ethernet) and IEEE 802.5 (Token Ring), 802.11 is restricted to the lower two layers of the *Open System Interconnection* (OSI) reference model, as indicated in Figure 3.1. In 802.11, the *Data Link Control* (DLC) layer is divided into *Logical Link Control* (LLC) and *Medium Access Control* (MAC) sublayers. 802.11 defines *Physical layer* (PHY) transmission schemes, and the MAC protocol, but no LLC functionality. For LLC, 802.11 relies on already defined protocols that are available for all systems in the 802 context. As the LLC layer is the same for all 802.x LANs, it does not address the specific characteristics of the wireless channel with its typical error characteristics. Therefore, management functions to address the needs of wireless communication are incorporated into the 802.11 MAC. To consider for example radio range aspects, the 802.11 standard contains functions for the management and maintenance of the radio network, which exceed the normal tasks of the MAC sublayer. The LLC layer does not provide association aspects of mobility; consequently, they are also handled in the MAC layer.

802.11 in its original form defines three different types of PHYs, namely 2.4 GHz *Frequency Hopping Spread Spectrum* (FHSS), *Direct Sequence Spread Spectrum* (DSSS) and *Infrared* (IR). Until the time this thesis is written, there are three more PHYs defined in the supplement standards 802.11a, 802.11b, and 802.11g. With FHSS, a set of communicating stations operate with certain center frequency only for short times, before selecting another center frequency ("hopping") for continuing the communication. Which center frequency is used is defined by a pseudo-random list of frequencies, known to all stations.

Different sets of communicating stations use different lists of frequencies, which reduces the probability that they operate with the same radio resources, i.e., at the same center frequency. In contrast to FHSS, in DSSS all stations operate at the same center frequency. In DSSS, different spreading codes allow different sets of communicating stations to reduce the mutual interference.

See Figure 3.1 for the illustration of the 802.11 reference model. The *Physical Medium Dependent* (PMD) sublayer is responsible for sending and receiving data via the wireless channel and defines the transmission scheme, which is different for the different PHYs, whereas the *Physical Layer Convergence Protocol* (PLCP) sublayer adapts the requests of the common MAC to the different PHYs into a format specific to the applied PMD. The MAC user plane is fed with data frames via the *MAC Service Access Point* (MAC-SAP) at the MAC/LLC boundary.

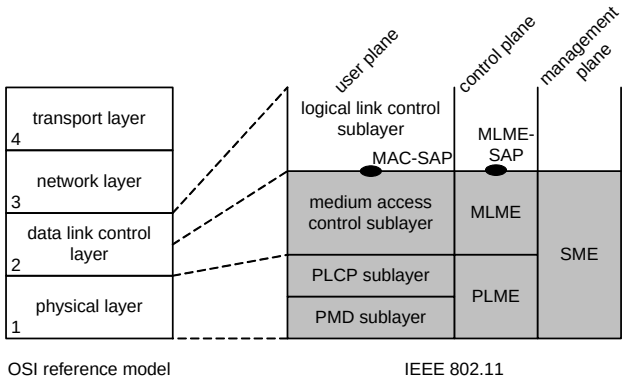

Figure 3.1: IEEE 802.11 reference model in comparison to the OSI reference model.

The control plane incorporates the *MAC Layer Management Entity* (MLME) and *PHY Layer Management Entity* (PLME). The management plane is represented by the *Station Management Entity* (SME). The definition of these entities is very vague in the standard. The reason is that they are implementation dependent and not needed to be standardized to achieve interoperability of different implementations.

3.2 IEEE 802.11 Architecture and Services

The 802.11 network architecture is hierarchical. Its basic element is the *Basic Service Set* (BSS), which is a set of stations controlled by a single *Coordination Function* (CF). The CF manages the access to the radio channel. The *Distributed Coordination Function* (DCF) (Section 3.3.1, p. 20) is mandatory for each BSS, whereas the *Point Coordination Function* (PCF) (Section 3.3.2, p. 35) is optional.

3.2.1 Architecture

An *Independent Basic Service Set* (IBSS) is the simplest 802.11 network type. It is a network consisting of a minimum of two stations, where each station operates with the same protocol. The coordination of the channel access is distributed among the stations. An infrastructure based BSS includes one station that has access to the wired network and is therefore referred to as *Access Point* (AP). In the rest of this thesis, "BSS" is used to refer to both types of service sets, if not stated otherwise.

A BSS may also be part of a larger network, the so-called *Extended Service Set* (ESS). The ESS consists of multiple BSSs interconnected by the *Distribution System* (DS).

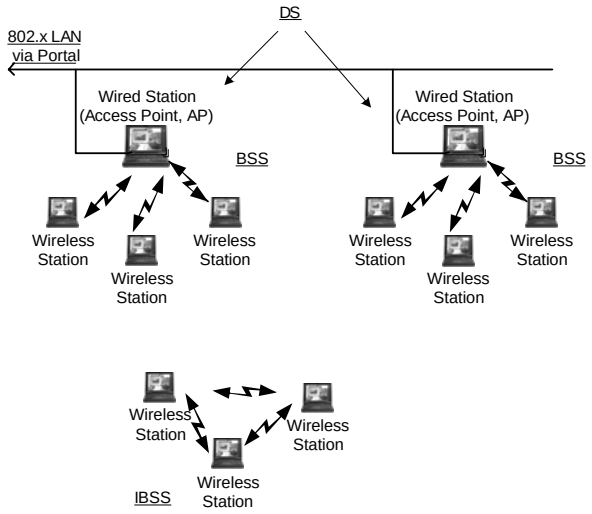

Figure 3.2: IEEE 802.11 architecture

See Figure 3.2 for an illustration of this architecture. The DS provides the service to transport *MAC Service Data Units* (MSDUs) between stations that are not in direct communication. The BSS and the DS work on different media. The BSS operates on the wireless channel whereas the DS uses the *Distribution System Medium* (DSM). As the 802.11 architecture is specified independently of any specific media, DSM may use different variants of IEEE networks for its service. Therefore, the DSM may consist of more than only different wireless LANs and integrate other wired LANs as well.

3.2.2 Services

A station connected to the DS is called AP and provides the *Distribution System Services* (DSS). The DSSs enable the MAC to transport MSDUs between stations that cannot communicate over a single instance of radio channel. A portal is the logical point where a non-802.11 LAN is connected to the DS. This allows the communication across different types of LANs. There are two categories of services in 802.11, the *Station Services* (SS) and the *Distribution System Service* (DSS). DSS services are not available in an IBSS. The main SS of a BSS is the *MAC Service Data Unit* (MSDU) Delivery. Other SSs include (de-)authentication and privacy. DSSs include re-/dis-association and integration. The integration service enables the delivery of MSDUs between non-802.11 LANs and the DS via the so-called *Portal*. DSSs are not discussed in this thesis.

3.2.3 802.11a Frame Format[2]

The 802.11a OFDM PHY consists of two sublayers, the PLCP sublayer and the PMD sublayer, as shown in Figure 3.3. The PLCP sublayer maps the 802.11 MPDUs into a frame suitable for transmitting and receiving user data, control and management information between the associated PMD entities. The PMD describes the method of transmitting and receiving data through the wireless channel. The 802.11a PHY is designed to work with the OFDM transmission scheme. The PLCP maps *MAC Protocol Data Units* (PDUs) into *PHY Service Data Unit* (PSDU) within the PHY PLCP layer. The resulting frame that is requested to transmit over the channel is called OFDM PLCP frame and is started with a PLCP preamble followed by a SIGNAL field and ends with the DATA field. The PLCP Header consists of the following elements: a LENGTH field, a RATE field, one reserved and parity bit, 6 tail bits and a SERVICE field. All of these except for the SERVICE field constitute a separate single OFDM symbol, denoted as SIGNAL, which is transmitted with the most robust combination of modulation and coding rate BPSK1/2. The 12 bits within the LENGTH field of the PLCP Header indicate the length of the PSDU, i.e. the number of bytes inside the PSDU. As stated above, the 802.11a PLCP LENGTH fields has 12 bits, which can theoretically represent up to *4095 byte* for the PSDU. Since *11 bit* cannot represent up to *2346 byte*, which is the maximum length of a *MAC Protocol Data Unit* (MPDU), *12 bit* are required for this field.

Thus, the current 802.11a PHY accepts MPDUs with a frame length of up to *4095 byte*. However, the 802.11 MAC will not feed such a long MPDU to the PHY, MPDUs are limited to *2346 byte* in length. The tail bits in the SIGNAL symbol allow decoding the RATE and the LENGTH fields immediately after their reception. The knowledge of RATE and LENGTH is required for decoding the DATA part of the frame. The resulting OFDM PLCP frame consists of three parts, the PLCP Preamble followed by the SIGNAL field and the DATA field.

Figure 3.3 shows the structure of the frames in all sublayers. The frame body of a data frame consists of the MSDU, which is the data to be delivered across the BSS, or DSS. There are four addresses in the MAC header of an MPDU. These addresses are *Source Address* (SA), *Destination Address* (DA), *Transmitting station Address* (TA), and *Receiving station Address* (RA), denoted as *addr 1* ... *addr 4*, respec-

[2] In this thesis, when PPDUs are transmitted on the channel, this is referred to as MSDU Delivery, frame transmission, or DATA transmission.

tively. The DA (addr 1) identifies the MAC entity or entities intended as the final recipient(s) of the MSDU contained in the frame body. The SA (addr 2) identifies the MAC entity from which the transfer of the MSDU contained in the frame body was initiated. The TA (addr 2) identifies the station that is transmitting the MSDU contained in the frame body. Finally, the RA (addr 4) identifies the intended immediate recipient station on the wireless channel. This address 4 is not necessary if MSDUs are delivered within the BSS. There are three types of frames: management, data, and control frames, as illustrated in the Figure 3.4. The use of these frames is explained in the following section, where the 802.11 MAC protocol is described.

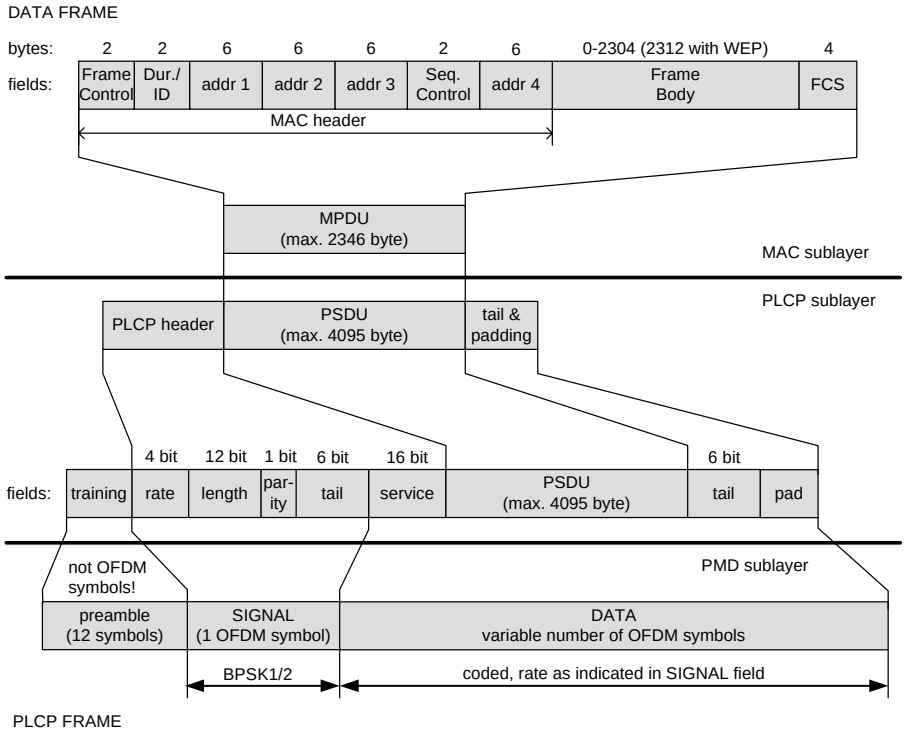

Figure 3.3: MAC DATA frame to PHY PLCP frame mapping for 802.11a.

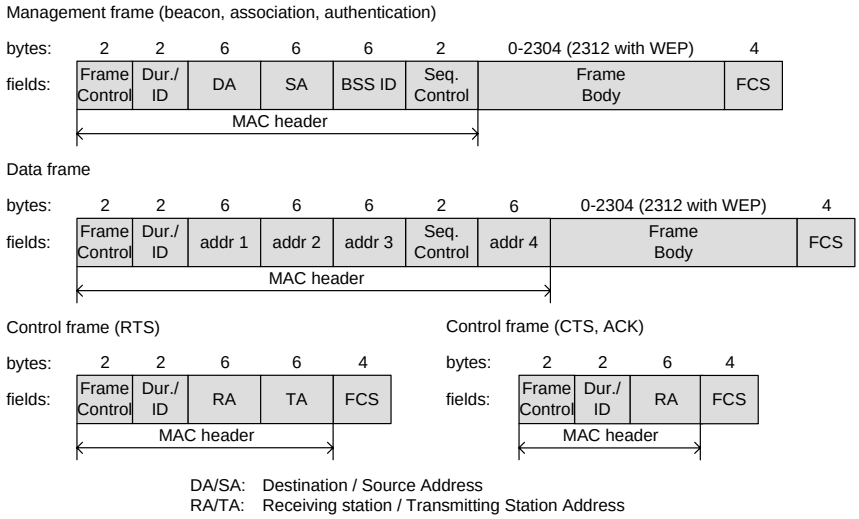

Figure 3.4: 802.11 frame format.

3.3 Medium Access Control

The 802.11 MAC protocol is built with the help of two coordination functions (see Figure 3.5). The two coordination functions are the *Distributed Coordination Function* (DCF) for asynchronous services and the *Point Coordination Function* (PCF) for contention free services. They are discussed in the following.

3.3.1 Distributed Coordination Function

The 802.11 MAC protocol is briefly described in this section. Its limitations in QoS support are shown. An *infrastructure based Basic Service Set* (BSS) of IEEE 802.11 wireless LAN is mainly considered, which is composed of an AP and a number of stations associated with the AP, as explained previously. The AP connects its stations with the infrastructure.

The basic 802.11 MAC protocol is the *Distributed Coordination Function* (DCF) that works as a listen-before-talk scheme, based on the *Carrier Sense Multiple Access* (CSMA) (Bertsekas and Gallager 1992). Stations deliver *MAC Service Data Units* (MSDUs) of arbitrary lengths (up to *2304 byte*), after detecting that there is no other transmission in progress on the radio channel.

The channel sensing function is called *Clear Channel Assessment* (CCA). It uses a single fixed power threshold, which is *-82 dBm* according to 802.11, but may be implementation dependent.

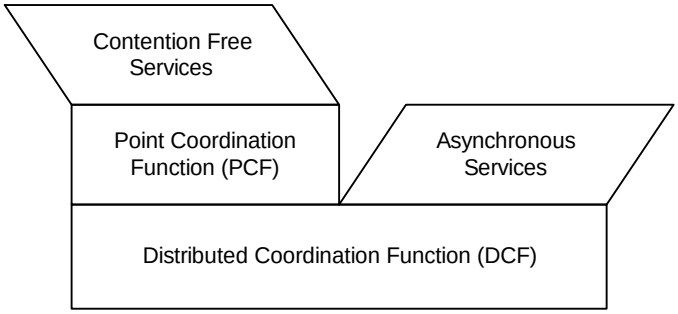

Figure 3.5: 802.11 coordination functions, DCF and PCF.

If the station detects a signal with power larger than this threshold, the radio channel is assumed to be busy and thus unavailable for transmission. Otherwise, the radio channel is assumed to be idle. The *Network Allocation Vector* (NAV) is an addition to the physical sensing of the radio channel. It is used as a means of virtual carrier sensing an in fact has the function of reserving the channel for the time duration it is indicating. The NAV is a timer, which is continuously decremented irrespective of the status of the radio channel.

The NAV is set when a frame is received that includes a duration field that defines how long the following frame exchange may take. As long as the NAV is set or the CCA sensed the radio channel as being busy, a station is not allowed to initiate transmissions. Thus, upon frame reception, the NAV can be eventually set for a duration that is longer than the transmission duration of this frame, and subsequent frame transmissions will be protected.

Each successful reception is acknowledged by the receiving station, as indicated in Figure 3.6. The addressed station transmits an *Acknowledgement* (ACK) immediately after receiving a frame. The time between two MAC frames is called *Interframe Space* (IFS). 802.11 defines four different IFSs.

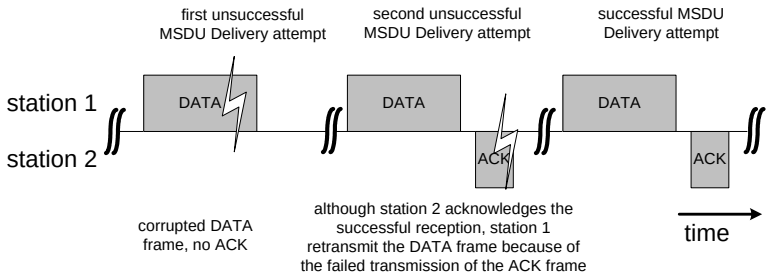

Figure 3.6: Frame exchange. Successful receptions are acknowledged by the receiving station.

Short Interframe Space (SIFS), *Point Coordination Function Interframe Space* (PIFS) and *Distributed Coordination Function Interframe Space* (DIFS) are used under normal conditions and represent three different priority levels for medium access. The shorter the IFS, the higher is the priority in medium access. The fourth IFS, called *Extended Interframe Space* (EIFS), is used when a station detects an on-going transmission as being interfered, assuming that there are some stations that cannot detect each other. A hidden station scenario is then assumed, and the station has to defer from channel access for a longer time.

All interframe spaces are independent of the channel data rate. Due to the different characteristics of the different PHY specifications, the durations of the interframe spaces depend on the used transmission scheme.

The relations between the IFS and the duration aSlotTime (also referred to as slot time) are shown in Figure 3.7. In the following, the durations are listed in order, from shortest to longest.

aSlotTime: The duration aSlotTime is used to calculate the IFSs. SIFS and aSlotTime are the basis of all other durations. In 802.11a, aSlotTime is $9\mu s$. As the name indicates, and as can be seen in Figure 3.7, aSlotTime is used during the *Collision Avoidance* (CA). The CA is explained below.

SIFS: The SIFS is used to prioritize the immediate *Acknowledgement* (ACK) frame of a data frame, the response (*Clear To Send* (CTS) frame) to a *Request To Send* (RTS) frame, a subsequent MPDU of a fragmented MSDU, response to any polling using the PCF, and any frames of the AP during the *Contention Free Period* (CFP). RTS and CTS are explained below. SIFS is $16\mu s$ for 802.11a.

PIFS: The PIFS is used by stations operating under the PCF to obtain channel access with highest priority. PIFS is calculated as: $PIFS = SIFS + aSlotTime$. PIFS is $25\mu s$ for 802.11a.

DIFS: The DIFS is used by stations operating under the DCF to obtain channel access to initiate frame exchanges. DIFS is calculated as: $DIFS = SIFS + 2 \cdot aSlotTime$. DIFS is $34\mu s$ for 802.11a.

EIFS: The EIFS is used instead of DIFS by stations operating under the DCF whenever the PHY indicates that a frame transmission did not result in a correct sequence as denoted in the *Frame Check Sequence* (FCS). The EIFS is therefore used when multiple stations initiated frame exchanges at different starting times.

This occurs typically when these stations are hidden to each other. The EIFS is an extended interframe space resulting in a longer deferral from channel access, which gives other stations clearly a higher priority in medium access. As soon as one other frame is received correctly, DIFS is used again. EIFS is around *200 μs* for 802.11a.

3.3.1.1 Collision Avoidance

As part of the DCF, it may occur that more than one station attempt to transmit at the same time. This is called a collision. In wireless communication, a transmitter cannot detect a collision at a receiver, while transmitting. To account for this, 802.11 is based on *Carrier Sense Multiple Access / Collision Avoidance* (CSMA/CA).

If two or more stations detect the channel as being idle at the same time, inevitably a collision occurs when these stations initiate a frame exchange at the same time. The 802.11 defines a CA mechanism to reduce the probability of such collisions. As part of CA, a station performs the so-called backoff procedure before starting a transmission. A station that has an MSDU to deliver has to keep sensing the channel for an additional random time duration after detecting the channel as being idle for the minimum duration DIFS, which is *34 us* for 802.11a. Only if the channel remains idle for this additional random time duration, the station is allowed to initiate its transmission. The duration of this random time is determined as a multiple of a slot duration (aSlotTime). Each station maintains a so-called *Contention Window* (CW), which is used to determine the number of slot times a station has to wait before transmission. Figure 3.7 shows an example: after a successful frame exchange, i.e., after the ACK transmission, a station starts the next frame exchange (RTS frame followed by CTS frame), because the radio channel has been idle for a duration equal to DIFS and its following backoff slots. The contention window size increases when a transmission fails, i.e., when the transmitted data frame has not been acknowledged.

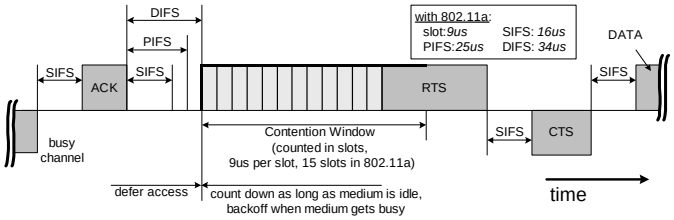

Figure 3.7: Interframe spaces and backoff procedure with random contention window size.

After an unsuccessful transmission, the next backoff is performed with a doubled size of the contention window. This reduces the collision probability in case there are multiple stations attempting to access the channel. The stations that deferred from channel access during the channel busy period do not select a new random backoff time, but continue to count down the time of the deferred backoff in progress after sensing the channel as being idle again. In this way, stations, that deferred from medium access because their random backoff time was larger than the backoff time of other stations, are given a higher priority when they resume the transmission attempt. Figure 3.8 illustrates the increase of the contention window upon unsuccessful transmissions. Note that a station cannot differentiate between collision and failed transmission due to errors on the wireless channels. A missed ACK frame will always be interpreted as collision.

3.3.1.2 Post-Backoff

After each successful transmission, it is mandatory that another random backoff is performed by the transmission-completing station, even if there is no other MSDU to be delivered, as indicated in Figure 3.9.This is referred to as "post-backoff," as this backoff is done after, not before, a transmission. This can be interpreted as the backoff for the next MSDU Delivery. By using this post-backoff, it is guaranteed that any frame (with the exception of the first MSDU in

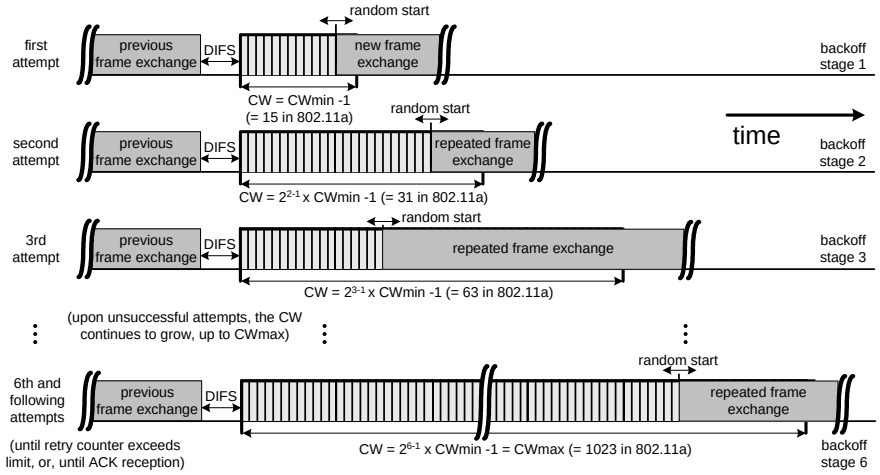

Figure 3.8: Increase of contention window size after unsuccessful frame exchanges. The size is doubled for each new attempt of collided or erroneously received MSDUs, up to a certain limit. The actual numbers vary with the PHY specifications.

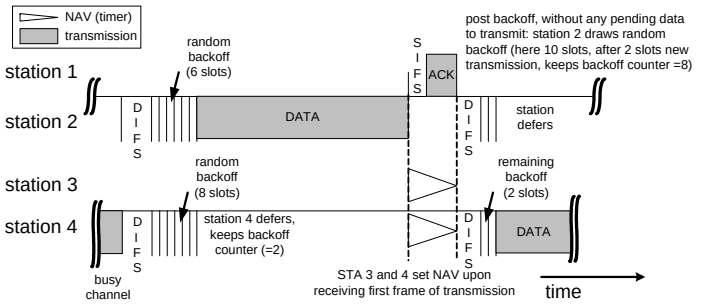

Figure 3.9: Post-backoff. A post-backoff is performed after each successful frame exchange, regardless of the station has MSDUs to deliver or not.

a burst, arriving at an empty queue and during an idle phase) will be delivered with backoff. An MSDU arriving at the station from the higher layer may be transmitted immediately without waiting any time, if the transmission queue is empty, the latest post-backoff has been finished already, and at the same time, the channel has been idle for a minimum duration of DIFS. This helps to reduce the delivery delay in lightly loaded systems.

3.3.1.3 Recovery Procedure and Retransmissions

When a frame exchange is not successful, i.e., when a transmitting station does not receive an ACK frame immediately after the frame transmission, the frame size of the transmitted frame is compared against a threshold value before retransmission.

All unsuccessful transmissions of frames with a frame size shorter than the threshold value, and all failed RTS transmissions, increment the *Short Retry Counter* (SRC). If the SRC reaches a limit (default: 7), the frame is discarded.

All unsuccessful transmissions of frames with a frame size larger than the given threshold, increment the *Long Retry Counter* (LRC). Again, no more retransmission attempts are made, when LRC is equal to a limit (default: 4). Whenever an MSDU is successfully transmitted, SRC and LRC are reset. The actual value of the threshold is implementation dependent.

3.3.1.4 Fragmentation

To reduce the duration the channel is occupied when frames collide, data frames (MSDUs) can be transmitted in more than one MPDU, if their length exceeds a certain threshold. The process of partitioning an MSDU into smaller MPDUs is called fragmentation. See Figure 3.10 for an illustration of fragmentation, where

also the complicated protection of frames by the NAV vectors is illustrated. An MPDU protects the subsequent transmissions of its ACK responses within its duration field, see Figure 3.4, and in addition, when fragmentation is used, the following MPDU.

Fragmentation creates MPDUs smaller than the original MSDU length to limit the probability of long MPDUs colliding and being transmitted more than once. With fragmentation, a large MSDU can be divided into several smaller data frames, i.e., fragments, which can then be transmitted sequentially as individually acknowledged frames. The benefit of fragmentation is, that in case of failed transmission, the error is detected earlier and there is less data to retransmit. It also increases the probability of successful transmission of the MSDU in scenarios where the radio channel characteristics cause higher error probabilities for longer frames than what can be expected for shorter frames. Each fragment can be transmitted sequentially as individually acknowledged data frame. The obvious drawback is the increased overhead. The process of recombining MPDUs into a single MSDU is called defragmentation, which is accomplished at each receiving station. Only MPDUs with a unicast receiver address may be fragmented. Broadcast/multicast frames may not be fragmented even if their length exceeds the implementation dependent threshold. Note the maximum length of an MSDU is limited to *2346 byte*.

3.3.1.5 Hidden Stations and RTS/CTS

In wireless communication systems that use carrier sensing, the so-called hidden station problem can occur, depending on the locations of the stations. This problem arises when a station is able to successfully receive frames from two different stations but the two stations cannot detect each other.

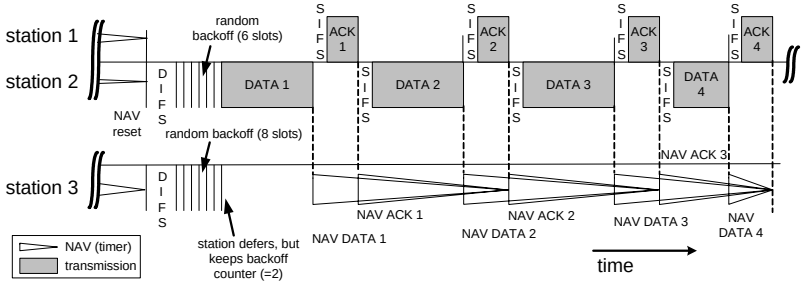

Figure 3.10: Fragmentation. Data frames protect the subsequent transmissions of their ACK responses and the following data frame with the NAV.

When stations cannot detect each other, a station may sense the channel as idle even when other hidden stations are transmitting. It may initiate a transmission while the other station is transmitting already. This may result in a collisions and severely interfered frames at stations that can detect coinciding transmissions of hidden stations.

To reduce throughput reduction owing to hidden stations, 802.11 allows the optional use of a *Request-to-Send/Clear-to-Send* (RTS/CTS) mechanism. Before transmitting a frame, a station has the option to transmit a short RTS frame, which must be followed by a CTS frame transmission by the receiving station. Between two consecutive frames in the sequence of RTS, CTS, data, and ACK, a *Short Interframe Space* (SIFS), which is 16 us for 802.11a, gives transceivers time to turn around. It is a decision made locally by the transmitting station, if or if not RTS/CTS is used. Upon receiving an RTS frame, the receiving station has to reply with a CTS frame. The RTS and CTS frames include the information of how long it does take to transmit the next data frame, e.g., the first fragment, and the corresponding ACK frame. Hence, other stations close to the transmitting station and hidden stations close to the receiving station will not start any transmissions; their NAV timer is set. A hidden stations close to the receiving station might not receive the RTS due to the large distance, but will in most cases receive the CTS frame.

See Figure 3.11 for an example of the DCF using RTS/CTS. It is important to note that SIFS is shorter than DIFS, which gives CTS and ACK always the highest priority for access to the radio channel.

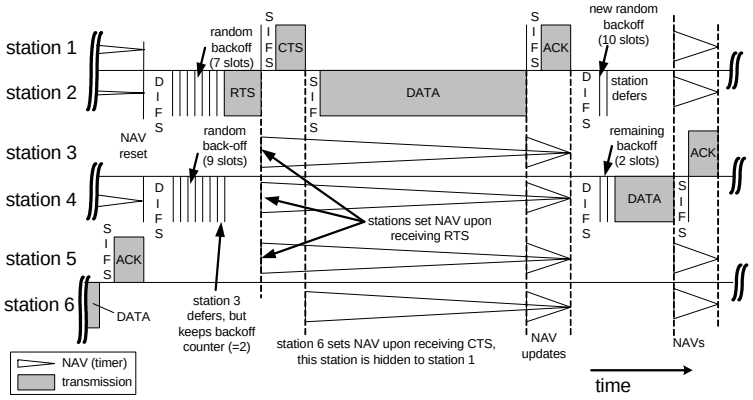

Figure 3.11: Timing of frame exchanges and NAV settings of the 802.11 DCF. Station 6 cannot detect the RTS frame of the transmitting station 2, but the CTS frame of station 1. Although station 6 is hidden to station 1, it refrains from channel access because of NAV.

3.3.1.6 Synchronization and Beacons

All stations within a single BSS are synchronized to a common clock by maintaining a local timer. by using the *Timing Synchronization Function* (TSF). To synchronize the stations, a management frame, the beacon, is used.

Beacons are transmitted periodically, hence, every station knows when the next beacon frame will arrive; this time is called *Target Beacon Transmission Time* (TBTT). The TBTT of each beacon is announced in the previous beacon.

The TSF's original function is to support various PHYs that require synchronization, and management functions such as a station joining a BSS, and saving power through sleep modes. Local timers are updated by the information received from other stations as part of a beacon. In order to give beacon transmissions highest priority of medium access, stations stop initiating frame exchanges upon reaching a TBTT. However, ongoing frame exchanges are completed, even this means that beacon transmissions are delayed. Note that beacons are transmitted after the channel was idle for PIFS (which is 25 us in 802.11a), and in a BSS without backoff. Thus, if a frame exchange is ongoing at TBTT, then the beacon is delayed. In BSS and IBSS, the synchronization is maintained by broadcasting the TSF timer in the beacon. The decision about if the local timer in a station has to be updated or not upon reception of the beacon, is different for BSS and IBSS.

Figure 3.12, left, illustrates the TSF in an infrastructure BSS[3]. Only the AP generates beacons in a BSS. At each TBTT, the AP schedules a beacon as the next frame to be transmitted.

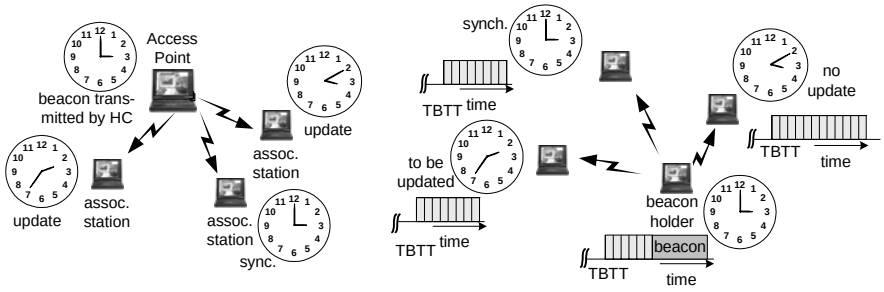

Figure 3.12: Left: Stations 2 and 3 change their TSF timers to the value received in the beacon of the AP. Right: In IBSS, station 2 transmits the beacon because of the smaller backoff counter.

[3] An infrastructure BSS is referred to as BSS and an independent BSS is referred to as IBSS.

If the channel has been idle for at least PIFS before TBTT, the AP transmits the beacon right at TBTT, otherwise the beacon is transmitted PIFS after the current transmission, without contention. All stations associated to this AP update their local timers with the information received from the beacon.

Figure 3.12, right, illustrates the TSF in an IBSS. There, the TSF is distributed over all stations. All stations take part in the generation of beacons. The beacon generation is distributed using a mechanism similar to the backoff mechanism.

At the TBTTs, stations that are part of an IBSS attempt to transmit a beacon in contention, with small CWmin and after PIFS. Stations stop attempting to transmit a beacon when they receive a beacon from another station of the IBSS. However, beacons transmitted with contention window may collide, which is allowed as part of the standard. Beacons are not retransmitted; the next beacon will be transmitted at the next TBTT. Note that beacons are not acknowledged by other stations. A station that transmitted a colliding beacon will not detect this collision, as it is not waiting for a subsequent ACK frame.

In BSS and IBSS, upon receiving a beacon, a station updates its local timer with the information from the beacon only if the received value represents an earlier time than the value currently maintained in the local timer. This is indicated in Figure 3.12. This distributed synchronization results in the shared information about the slowest running clock, with which the complete IBSS will synchronize.

Among the timing information needed to synchronize stations, the beacon delivers other parameters related to the protocol and to radio regulations. In addition to the timing information needed to synchronize the BSS, the beacon delivers protocol related parameters, for example

- the *Basic Service Set Identification* (BSSID)
- the beacon interval (next TBTT)
- PHY depending parameters
- the duration of the *Contention Free Period* (CFP)
- regulatory and spectrum management information, such as the available channels and the power limits.

Depending on the type of the BSS, not all information may be contained in what is broadcasted across the BSS in the beacon. In case of an infrastructure BSS the AP uses the beacon for instructions to its associated stations and announcements of future transmissions, e.g. delivery of multicast traffic to stations in power save mode. Stations may also use the signal strength of the received beacons to decide when to disassociate, because of channel conditions, and to which AP to associate again.

3.3.2 Point Coordination Function

To support time-bounded services, the IEEE 802.11 standard defines the *Point Coordination Function* (PCF) to let stations have priority access to the radio channel, coordinated by a station called *Point Coordinator* (PC). The PC typically resides in the AP.

3.3.2.1 Contention Free Period and Superframes

The PCF has higher priority than the DCF, because the period during which the PCF is used is protected from the DCF access by the NAV. The time during which 802.11 stations operate is divided into repeated periods, called superframes. A superframe starts with a beacon. With an active PCF, a *Contention Free Period* (CFP) and a *Contention Period* (CP) alternate over time, where a CFP and the following CP form a superframe. During the CFP, the PCF is used for accessing the channel, while the DCF is used during the CP. It is mandatory that a superframe includes a CP of a minimum length that allows at least one MSDU Delivery under DCF. A superframe starts with a beacon frame, regardless if the PCF is active or not. The beacon frame is a management frame that maintains the synchronization of the local timers in the stations and delivers protocol related parameters, as explained earlier. The PC, which is typically co-located with the AP, generates beacon frames at regular beacon frame intervals, thus every station knows when the next beacon frame will arrive. During CFP, there is no contention among stations; instead, stations are polled. See Figure 3.13 for a typical frame exchange sequence during CFP. The PC polls a station asking for a pending frame. Because the PC itself has pending data for this station, it uses a combined data and poll frame by piggybacking the *CF-Poll* frame into the data frame. Therefore, no idle period longer than PIFS occurs during CFP.

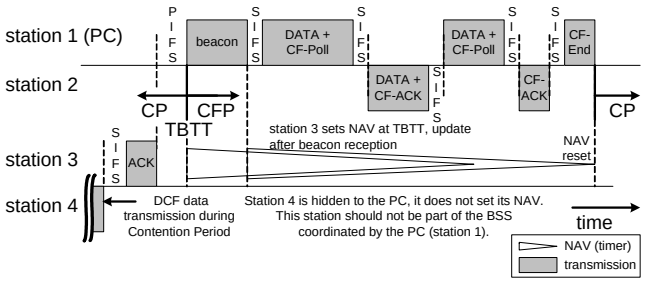

Figure 3.13: Example for the PCF operation. Station 1 is the PC and polls station 2. Station 3 detects the beacon frame and updates the NAV for the whole CFP.

The PC continues with polling other stations until the CFP expires. A *CF-End* control frame is transmitted by the PC as the last frame within the CFP to signal the end of the CFP.

3.3.2.2 QoS Support with PCF

There are problems with the PCF that motivated to the current activities to enhance the protocol. Among others, the main problems are the unpredictable beacon delays and unknown transmission durations of the polled stations. See Figure 3.14 for an illustration of the problems. At TBTT, a PC schedules the beacon as the next frame to be transmitted, and the beacon can be transmitted when the channel has been determined to be idle for at least PIFS. Depending on the radio channel at this point in time, i.e., whether it is idle or busy around the TBTT, a delay of the beacon frame may occur. The time the beacon frame is delayed, i.e., the duration it is sent after the TBTT, delays the transmission of time-bounded MSDUs that have to be delivered in CFP. From the legacy 802.11 standard, stations can start their transmissions even if the MSDU Delivery cannot finish before the upcoming TBTT. This may severely affect the QoS as this introduces unpredictable time delays in each CFP. Beacon frame delays of around *4.9 ms* are possible in 802.11a in the worst case.

In simulation of the PCF that have been performed, a mean beacon frame delay of up to *250 us* was observed, depending on frame lengths, fragmentation, and the offered traffic (Mangold et al., 2002a). There is another problem with the PCF, the unknown transmission time of polled stations. A station that has been polled by the PC is allowed to send a single frame that may be fragmented and of arbitrary length, up to the maximum of *2304 byte* (*2312 byte* with *Wired Equivalent Privacy* (WEP) encryption due to the overhead that results from the encryption). Further, different modulation and coding schemes are specified in 802.11a, thus the duration of the MSDU Delivery as response to the CF-Poll frame is not under the control of the PC. This destroys any attempt to provide QoS to other stations that are polled during the rest of the CFP.

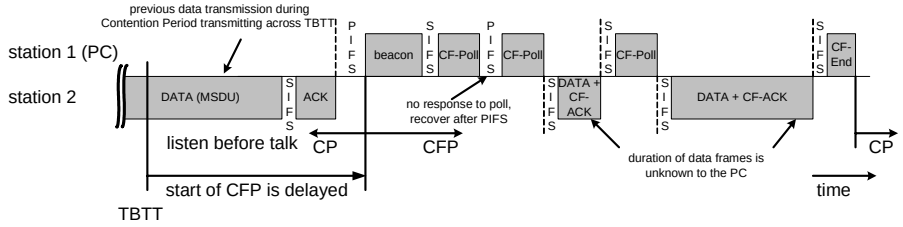

Figure 3.14: Frame exchanges with the Point Coordination Function (PCF).

3.4 The 802.11 Standards

To conclude this chapter on 802.11, this section outlines briefly all supplement standards (amendments) under the roof of 802.11 that have been developed or are being developed at the time this thesis is written. General information about the structure of the standards can be found in Mittag (2002), Gast (2002), and Geier (2002).

3.4.1 IEEE 802.11

The 802.11 standard is considered as the root standard, defining operation and interfaces at MAC and PHY for data networks such as the popular TCP/IP network. Three PHY layer interfaces are defined that are not compatible with each other. One is based on *Infrared* (IR) communications, and the other two use the *2.4 GHz* unlicensed band, which is more or less, harmonized over the world. One is based on *Frequency-Hopping Spread Spectrum* (FHSS) and the other uses *Direct Sequence Spread Spectrum* (DSSS).

802.11 was published in 1997, an updated version is available since 1999, see IEEE 802.11 WG (1999c).

3.4.2 IEEE 802.11a

This extension defines the PHY that allows up to *54 Mbit/s* by operating in the 5 GHz unlicensed band, making use of the *Orthogonal Frequency Division Multiplexing* (OFDM), equivalent to HiperLAN/2. This PHY is mainly considered in this thesis. IEEE 802.11a is also sometimes referred to as *Wi-Fi5*, to highlight that 802.11a networks operate in the 5 GHz band, and to reduce the apparent confusions of the many abbreviations.

3.4.3 IEEE 802.11b

This extension is defined in the IEEE 802.11 supplement standard "Higher-Speed Physical Layer Extension in the 2.4 GHz Band", known as IEEE Standard 802.11b-1999. IEEE 802.11b defines the *High Rate Direct Sequence Spread Spectrum* (HR/DSSS) transmission mode with a chip rate of *11 Mchip/s*, providing the same occupied channel bandwidth and channelization scheme as DSSS. The higher data rate is achieved through a transmission mode based on 8-chip *Complementary Code Keying* (CCK) modulation. The code set of complementary codes is richer than the set of Walsh codes. At *11 Mbit/s*, the spreading code length is *8* and the symbol duration is 8 instead of 11 chips, as it was with the DSSS. Data bits encode the symbols with *Quaternary Phase Shift Keying* (QPSK) and *Differential*

QPSK (DQPSK). IEEE 802.11b is known under the acronym *Wireless Fidelity* (Wi-Fi).

3.4.4 IEEE 802.11c

This task group of the 802.11 working group finished its work by not developing an additional supplement standard, but providing information for changes in other standards. The results of 802.11c were modifications of other standards, not a separate document. The 802.11c task group defined protocols for what is referred to as AP bridging. 802.11 APs can communicate which each other across networks within relatively short distances.

3.4.5 IEEE 802.11d

This standard is related to radio regulation in an international context. The use of the frequency spectrum is regulated by nations and is different from one nation to another. 802.11d provides procedures and protocols to let 802.11 networks operate compliantly to what is regulated, by introducing regulatory domains. If a station does not comply with the rules defined for a specific regulatory domain, it will not initiate transmissions, and not associate with a network. The domains are identified by information elements that are broadcasted by the AP.

3.4.6 IEEE 802.11e

The 802.11e task group is defining enhancements to 802.11 to allow QoS support. It is described in detail in Chapter 4 of this thesis. 802.11e will work with any PHY extension.

3.4.7 IEEE 802.11f

AP handovers are supported by the *Inter AP Protocol* (IAPP), defined by 802.11f. A constant operation while the station is actually moving is supported when the IAPP is used. The concept of handovers is familiar to cellular networks, and will need to be standardized, as APs and stations will be provided by different vendors.

3.4.8 IEEE 802.11g

IEEE 802.11g combines the advantages of 802.11b (relatively large coverage) and 802.11a (higher throughputs) by defining the application of the multi carrier 802.11a OFDM transmission scheme in the *2.4 GHz* band, in which originally 802.11b stations are operating. Therefore, 802.11g will provide up to *54 Mbit/s* at

the air interface. There is also an extended rate PHY mode based on DSSS single carrier (802.11b), which allows up to 33Mbit/s. Further, because 802.11g and 802.11b stations are likely to operate at the same time in many scenarios, it is possible to use the DSSS based preambles and headers together with the remainder of a frame being transmitted with extended rate PHY modes (single carrier or multi carrier). With this multi-mode operation, 802.11g stations will be able to interwork and coexist with 802.11b networks, which makes 802.11g attractive for increasing the capacity of already rolled-out 802.11b networks.

3.4.9 IEEE 802.11h

Dynamic Frequency Selection (DFS) and *Transmitter Power Control* (TPC) are defined by this group, with focus on 802.11a and the 5 GHz band. The reasons for applying these schemes are spectrum sharing and efficiency, QoS support, and energy consumption.

To select the frequency channel to operate its BSS, an AP needs to know the status of all frequency channels. While the status of the current channel is available to the AP, the AP needs to collect the information about other channels as well, in order to initiate a channel selection. This will be performed via the standardized channel measurements by other station and the AP itself. The channel measurement by the AP does not need to be standardized, as it does not need to report the measurement results to other stations. However, the AP measurement should be performed in such a way that the service disruption is minimized. Any other measurements must be standardized in the context of 802.11h. The channel measurements by stations will be (1) detection of other BSSs (2) measurement of *Clear Channel Assessment* (CCA) busy periods, and (3) measurement of received signal strength statistics.

TPC is a difficult task in 802.11 networks, since as part of the DCF; every station needs to detect all transmissions of frames within its BSS. Thus, there are no peer links between two stations that are subject to TPC. However, to meet future regulatory requirements, and for increased spectrum efficiency, and in order to reduce interference imposed on other networks, TPC is standardized in 802.11h.

3.4.10 IEEE 802.11i

Security and privacy becomes increasingly important with the growing popularity of 802.11. There are problems in the algorithms for providing security defined in the legacy 802.11 protocol. 802.11i is tasked with improving the security by enhancing the *Wired Equivalent Privacy* (WEP) protocol.

Chapter 4

IEEE 802.11E HYBRID COORDINATION FUNCTION

QUALITY OF SERVICE (QoS) is a synonym for service characteristics that are provided by a MAC layer service to higher layer applications, within a layered data transport system. QoS may or may not be required by an application, and may or may not be provided by the service. The service of interest here and in the rest of this thesis is the *MSDU Delivery*, which is an 802.11 station service available at the *MAC Service Access Point* (MAC-SAP) at the *Logical Link Control* (LLC)/MAC boundary. For this service, QoS involves achieving at least a minimum MSDU Delivery throughput as well as achieving MSDU Delivery delays not exceeding a maximum limit. Additionally, MSDU Delivery delay variation and MSDU loss rate are often considered as part of QoS.

The legacy 802.11 DCF is a distributed contention-based channel access protocol and cannot deliver MSDUs under QoS constraints.

The legacy 802.11 PCF is centralized and provides contention-free channel access. It is inefficient and provides only limited QoS for MSDU Delivery.

For these reasons, IEEE 802.11 *Task Group E* (TGe) defines enhancements of the legacy 802.11 MAC. The enhancements are defined in the supplement stan-

dard referred to as IEEE 802.11e. In this thesis, the drafts 3.3 and 4.0 (IEEE 802.11 WG, 2002a, 2002c) are considered, together with some newer notations of TGe working documents.

The main element of the QoS enhancements of 802.11 is the new coordination function called *Hybrid Coordination Function* (HCF). This HCF is described in this chapter.

After an overview in Section 4.1, the contention-based channel access of the HCF is described in detail in Section 4.2. The contention-based channel access is also referred to as *Enhanced Distributed Coordination Function* (EDCF) and can be understood as enhancement of the legacy DCF. In Section 4.3, the controlled channel access of the HCF is described in detail. This controlled channel access relies on the contention-based channel access (the EDCF). It can be interpreted as enhancement of the legacy PCF, which relies on the DCF. In the last part of this chapter, Section 4.4, additional enhancements that are considered to be included in the 802.11e standard for improving the efficiency of the protocol are described.

It is emphasized that this thesis does not provide a complete description of the 802.11e standard, as the standardization process is still ongoing at the time this thesis is written. In this and the following chapter, MAC enhancements are described and evaluated, which are not necessarily part of the standard. For details about the standard, the reader is referred to the original documentation, see IEEE 802.11 WG (2002a, 2002c).

4.1 Overview and Introduction

The MAC enhancements of 802.11e enable the support of QoS for a wide variety of applications. However, non-802.11e conformant stations, in this thesis referred to as legacy stations, can operate in parallel to 802.11e stations. 802.11e stations and legacy stations can exchange data under the rules of the legacy coordination functions DCF and PCF (if available). All frames of the 802.11e standard are defined in a way that they do not violate the operation of the legacy stations operating in parallel to the new 802.11e stations.

4.1.1 Naming Conventions

A station that operates according to 802.11e is referred to as *802.11e station* in this thesis. Other stations are referred to as *legacy stations*. If the difference between 802.11e stations and legacy stations is not important in a discussed context, or if it is obvious which kind of station is discussed, an 802.11e station is referred to

as *station* in this thesis. In the 802.11e standard, an 802.11e station is denoted as *QoS supporting Station* (QSTA), and a legacy station is denoted as *Station* (STA). These abbreviations are not used in this thesis.

An 802.11 station, which may optionally work as the centralized coordinator for all stations in the *QoS supporting BSS* (QBSS), including the legacy stations, is referred to as *Hybrid Coordinator* (HC). A QBSS is an infrastructure-based BSS, which includes an 802.11e-compliant HC and stations. The HC will typically reside within an 802.11e AP. Such an AP is referred to as 802.11e-AP in this thesis only if it is necessary to highlight that it is 802.11e-compliant, otherwise AP is used. In the 802.11e standard, an 802.11e AP is referred to as *QoS supporting Access Point* (QAP). This abbreviation is not used in this thesis.

802.11e stations comprise multiple backoff entities in parallel, as explained in detail later in this chapter. For this reason, in this thesis it is often referred to a transmitting *backoff entity* instead of transmitting station. Legacy stations comprise one backoff entity; therefore, *legacy backoff entity* and legacy station may be used as synonym for each other.

The HCF incorporates two access mechanisms, namely, the contention-based channel access and the controlled channel access. The contention-based channel access is also referred to as EDCF:

> *"The contention-based channel access mechanism of the HCF is referred to as the »EDCF«. It is closely related to the DCF channel access mechanism being viewed as an enhanced version of that mechanism. Despite the presence of »CF« in its name, the EDCF is part of the HCF and is not a separate coordination function." (IEEE 802.11 WG, 2002c)*

The EDCF is part of the HCF and is not a separate coordination function.

A QBSS is an 802.11-compliant infrastructure-based BSS, which includes the HC. The 802.11-compliant independent BSS is referred to as *QoS supporting IBSS* (QIBSS).

With 802.11e, there may still be two phases of operation within the superframes, i.e., a *Contention Period* (CP) and a *Contention Free Period* (CFP). The contention-based channel access, i.e., EDCF, is used in the CP only, while the controlled channel access is used in both phases. This is the reason why the new coordination function is called hybrid. Because the controlled channel access can be used during CP, the CFP is not necessary in 802.11e for QoS support.

4.1.2 Enhancements of the Legacy 802.11 MAC Protocol

4.1.2.1 Transmission Opportunity

As part of 802.11e, a station that obtained channel access must not allocate radio resources for durations longer than a specified limit. This important new attribute of the 802.11e MAC is referred to as a *Transmission Opportunity* (TXOP). A TXOP is an interval of time during which a station has the right to initiate transmissions. A TXOP is defined by a starting time and a maximum duration. TXOPs can be obtained via the contention-based channel access. Such TXOPs are referred to as EDCF-TXOPs. Alternatively, a TXOP can be obtained by the HC via the controlled channel access. In this case it is referred to as *Controlled Access Phase* (CAP). The duration of an EDCF-TXOP is limited by a QBSS-wide parameter called *TXOPlimit*. This TXOPlimit is distributed regularly by the HC in an information field of the beacon. The HC broadcasts the beacon at the beginning of each superframe. Legacy stations will only understand the fields known from the legacy standard, whereas 802.11e stations will understand all new information fields. The new information fields are ignored by legacy stations. Therefore, legacy stations may transmit for longer durations than allowed by the TXOPlimit.

4.1.2.2 Beacon Protection

As part of 802.11e, no backoff entity is allowed to transmit across the TBTT. Frame exchanges are only to be initiated if they can be completed before the next TBTT. This reduces the expected beacon delay, which gives the HC a better control over the channel, especially if the optional CFP is used after the beacon.

4.1.2.3 Direct Link

As part of 802.11e, any backoff entity can directly communicate with any other backoff entity in a QBSS, without communicating first with the AP. In the legacy 802.11 protocol, within an infrastructure based BSS (which is denoted as BSS), all data frames are sent to the AP, and received from the AP. This however consumes at least twice the channel capacity compared to the direct communication. Only in an independent BSS (which is denoted as IBSS), station to station communication is allowed in the legacy protocol, due to the absence of the AP. The direct communication is referred to as *Direct Link* (DiL) in 802.11e. A set-up procedure, the *Direct Link Protocol* (DLP) is defined to establish a DiL between 802.11e backoff entities.

4.1.2.4 Use of RTS/CTS

As part of 802.11e, transmissions of data frames can be protected by RTS/CTS whenever required, without considering any threshold in the frame body size. Hence, even small MSDUs can be delivered with the additional NAV protection using RTS/CTS. It is a local decision taken by the transmitting backoff entity if RTS/CTS is used or not. However, RTS/CTS increases the duration of frame exchanges. This duration must not exceed the TXOPlimit, if the respective frame exchange is initiated in an EDCF-TXOP.

4.1.2.5 Fragmentation

As part of 802.11e, fragmentation of an MSDU into multiple MPDUs is allowed with any fragmentation size, and any number of fragments, whenever required by an 802.11e backoff entity. The fragmentation threshold known from the legacy protocol can still be used by 802.11e backoff entities, as part of the implementation. However, the 802.11e standard does not explicitly require that a backoff entity uses this threshold to decide if a MSDU should be fragmented into multiple MSDUs or not. As with RTS/CTS, fragmentation may significantly increase the duration of frame exchanges. This duration must not exceed the TXOPlimit.

4.2 Hybrid Coordination Function, Contention-based Channel Access

The EDCF as the contention-based channel access of 802.11e is the basis of the HCF, as illustrated in Figure 4.1. It is indicated that the contention-based channel access of the HCF, i.e., the EDCF, is part of the HCF. It is used to support differentiated services with priorities. The controlled channel access of the HCF is based on the EDCF and is used for time-bounded services with strict QoS guarantees. The details of the EDCF are described in the following sections.

4.2.1 Traffic Differentiation, Access Categories, and Priorities

The QoS support in EDCF is realized with the introduction of *Access Categories* (ACs) and parallel backoff entities. MSDUs are delivered by multiple parallel backoff entities within one 802.11e station, each backoff entity parameterized with AC-specific parameters, the so-called EDCF parameter sets. There are four different ACs, thus, four backoff entities exist in every 802.11e station, with four priorities AC 0…3. See Figure 4.2 for an illustration of the backoff entities.

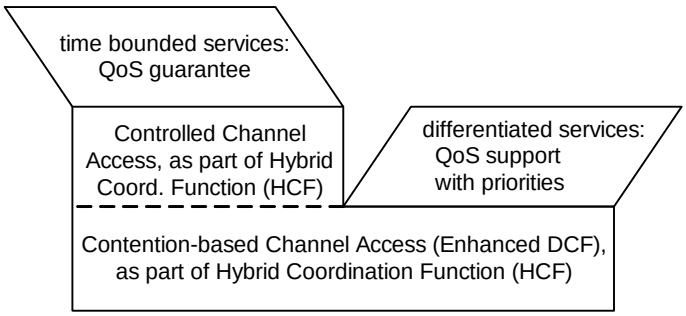

Figure 4.1: 802.11e coordination function HCF.

The priorities correspond to Annex H.2 of IEEE 802.1D (1998), and are summarized in Table 4.1. The EDCF parameter sets define the priorities in channel access by modifying the backoff process with individual interframe spaces, contention windows and many more parameters per AC, as explained in the following.

4.2.2 EDCF Parameter Sets per AC

The contention-based channel access is realized with the EDCF parameter sets per AC. Which values to be used by which backoff entity is defined by the HC. The EDCF parameters can be adapted over time by the HC, and are announced via information fields in the beacon frames. Figure 4.3 illustrates the distributed nature of this approach. A QBSS with some activities on the radio channel is shown in the figure. The identical EDCF parameters must be used by the different backoff entities of the same AC. Any active schedule of MSDUs waiting in different queues, and any individual change of EDCF parameters within a station will violate the standard.

Table 4.1: Priority – AC mapping (IEEE 802.11 WG, 2002a)

802.1D Priority	802.1D Interpretation	802.11e AC	Service Type
0	*Best Effort*	*0*	*best effort*
1	*Background*	*0*	*best effort*
2	-	*0*	*best effort*
3	*Excellent Effort*	*1*	*video probe*
4	*Controlled Load*	*2*	*video*
5	*Video < 100ms delay and delay variation*	*2*	*video*
6	*Voice, video < 10ms delay and delay variation*	*3*	*voice/video*
7	*Network Control*	*3*	*network control*

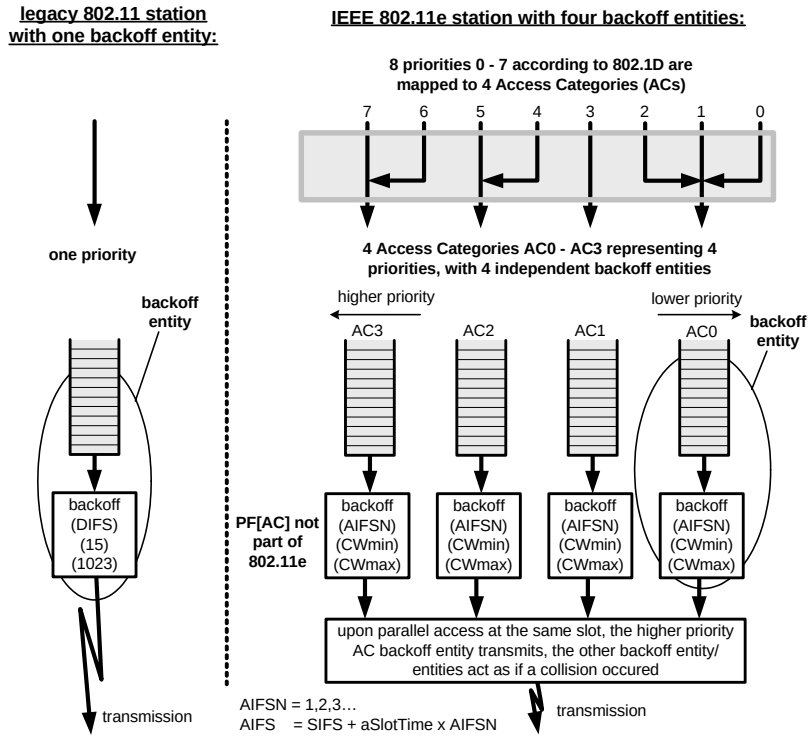

Figure 4.2: Legacy 802.11 station and 802.11e station with four ACs within one station. The abbreviations used in the figure are explained in Section 4.2.2.

This violation will break the consistency of the protocol because in this case MSDUs delivered by backoff entities of different stations but within one AC will observe different QoS. In an QIBSS, the beacon holder is responsible for defining the EDCF parameters.

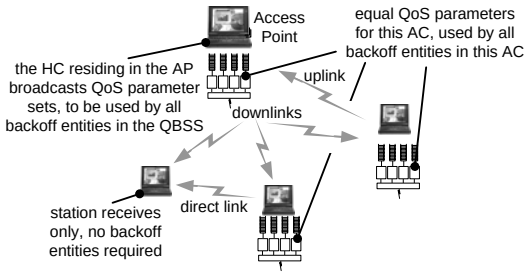

Figure 4.3: Multiple backoff entities in each 802.11e station. Any scheduling or optimization of the EDCF parameters within one station will violate the standard and introduce fairness problems.

4.2.2.1 Arbitration Interframe Space and Arbitration Interframe Space Number as EDCF Parameters per Access Category

Each backoff entity within the stations contends for a TXOP independently. It starts down-counting the backoff-counter after detecting the channel being idle for an *Arbitration Interframe Space* ($AIFS[AC]$). The $AIFS[AC]$ is at least PIFS, and can be enlarged per AC with the help of the *Arbitration Interframe Space Number* ($AIFSN[AC]$). The $AIFSN[AC]$ defines the duration of $AIFS[AC]$ according to

$$AIFS[AC] = SIFS + AIFSN[AC] \cdot aSlotTime, \quad 1 \le AIFSN[AC] \le 10 .$$

$AIFSN[AC]$ can be any number between *1* and *10*. The smaller $AIFSN[AC]$, the higher the channel access priority. It is emphasized that with $AIFSN[AC] = 1$, the earliest channel access time after the channel became idle is DIFS, similar to the legacy protocol, because of a different interpretation of the contention window. This different interpretation will be explained in the next section.

4.2.2.2 Minimum Contention Window as Parameter per Access Category

The minimum size of the contention window, $CWmin[AC]$, is another parameter dependent on the AC. The initial value for the backoff counter is a random number taken from an interval defined by the *Contention Window* (CW), similar to legacy DCF. The contention window may be the initial minimum size $CWmin[AC]$, or higher values in case MSDU Delivery failures occurred during the last frame exchange. Different to the legacy DCF, an 802.11e backoff entity selects its counter as a random number drawn from the interval $[1, CW+1]$ instead of $[0, CW]$ for the following reason. When many backoff entities contend for channel access, it occurs often that backoff entities defer from channel access upon detecting that at least one other backoff entity initiated a frame exchange at a particular slot. However, only backoff entities that did not count down to *0* defer. Any other backoff entity that reaches *0* at this slot will also transmit. After the channel becomes idle again, backoff entities that deferred will have to count down at least one more slot. This means that in legacy DCF, in scenarios with high offered traffic, in most of the cases the earliest channel access is *DIFS+aSlotTime*, and not DIFS, as expected. This can be easily confirmed with simulation, by evaluating the CCA pattern in scenarios with high load and many contending stations. To eliminate this unwanted behavior, 802.11e backoff entities select a slot from the interval $[1, CW+1]$ instead of $[0, CW]$.

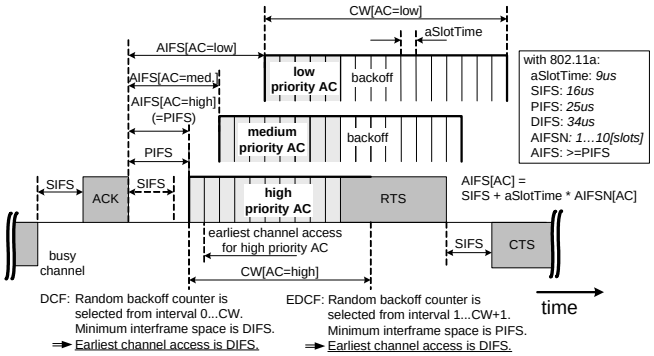

Figure 4.4: In EDCF, multiple backoff entities contend for channel access with different priorities in parallel. The earliest possible channel access time after a busy channel is DIFS.

With the minimum $AIFS[AC]$ being PIFS, the earliest channel access time for backoff entities that did not defer from access is DIFS, similar to legacy stations.

Further, the earliest channel access time for backoff entities is $AIFS[AC] + aSlotTime = DIFS$ after any deferrel, however, only in the case when $AIFSN[AC] = 1 \Rightarrow AIFS[AC] = PIFS$.

See Figure 4.4 for an illustration of the $AIFS[AC]$ and $CWmin[AC]$. Three priorities are shown in the figure[4].

The smaller $CWmin[AC]$, the higher the priority in channel access. However, the collision probability increases with smaller $CWmin[AC]$ if there are more than one backoff entities of the respective AC operating in the QBSS. Priority over legacy stations can be supported by setting $CWmin[AC] < 15$ (in case of 802.11a PHY), and $AIFSN[AC] = 1$, which means that the earliest channel access time is DIFS, similar to the legacy DCF.

Obviously, the positions of the contention windows relative to each other, as defined per AC by the EDCF parameters, are the important factors to define the relative priority in channel access per AC. Different settings are possible, as illustrated in Figure 4.5 and Figure 4.6.

---

[4] Throughout this thesis, if not stated otherwise, EDCF and HCF priorities are labeled with expressions such as "highest," "higher," "medium," and "lower." This is motivated by the fact that there is no absolute priority 1 or 2 in the contention-based channel access of the HCF. What can be identified is the legacy priority, and relative to that, "higher" and "lower" priorities. The legacy priority is often referred to as "medium" priority in this thesis. In addition, "highest" priority denotes the most aggressive channel access with smallest possible AIFS and CWmin (equivalent to the controlled channel access).

In Figure 4.5, the initial CWs do not overlap at all (in the figure, intervals X1, X2, X3), which makes the QoS differentiation between the ACs of different priorities more strictly.

However, as soon as CWs increase upon collisions, this strict priority differentiation is lost. In a scenario of multiple backoff entities contending for access, not all backoff entities increase their CWs at the same time. Thus, a backoff entity of the higher priority AC may operate with increased CWs while at the same time a medium priority backoff entity operates with *CW=CWmin*, for example after a successful transmission. The EDCF cannot support strict priorities between ACs, as long as increasing backoff stages lead to overlapping CWs. Figure 4.6 illustrates another possible case where the initial CWs overlap in the initial stage, making the QoS differentiation less strictly.

4.2.2.3 Maximum Contention Window Size as Parameter per Access Category

The contention window increases upon unsuccessful frame exchanges, but never exceeds the value of $CWmax[AC]$, which is the maximum possible value. This parameter is defined per AC as part of the EDCF parameter set. The smaller the $CWmax[AC]$, the higher the channel access priority. However, a small $CWmax[AC]$ may increase the collision probability. Note that any value $CWmin[AC] \leq CWmax[AC] \leq 65535$ is possible. Further, it should be highlighted that the retry counters limit the number of retransmissions and can therefore limit the maximum size of the CW.

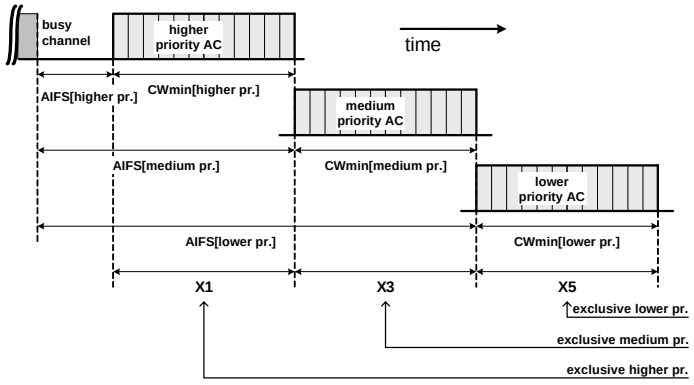

Figure 4.5: Non-overlapping contention windows of three Access Categories (ACs), higher, medium, lower priority.

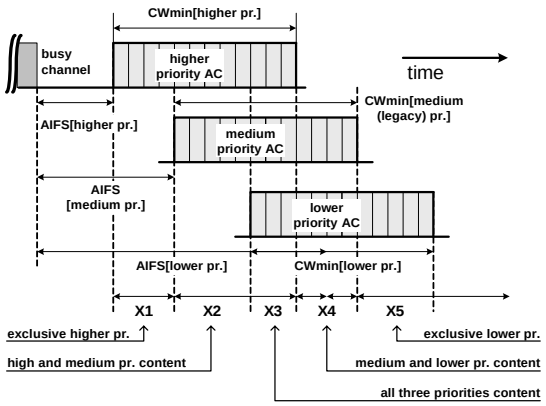

Figure 4.6: Overlapping contention windows of three ACs, higher, medium, lower priority. The initial contention windows of higher and lower priority overlap.

4.2.2.4 Maximum TXOP Duration as Parameter per Access Category

In addition to the backoff parameters, the $TXOPlimit[AC]$ is defined per AC as part of the EDCF parameter set. The larger $TXOPlimit[AC]$, the larger the share of capacity for this AC.

4.2.3 Collisions of Frames

As described above, four backoff entities reside inside an 802.11e station with different EDCF parameters. During contention, when the counters of two or more backoff entities in the same station reach zero at the same time, a collision is avoided as explained in the following. Upon access to the same slot by more than one backoff entity, the backoff entity with the higher priority will transmit, whereas all other backoff entities will act as if a collision occurred on the channel. See Figure 4.2 for an illustration. There is still a chance that the frame transmitted by the backoff entity with the higher probability will collide with another frame transmitted by backoff entities of other stations.

4.2.4 Other EDCF Parameters per AC that are not Part of 802.11e

4.2.4.1 Retry Counters as Parameter per Access Category

The retry counter $RetryCnt[AC]$ defined per AC is a candidate to be included in the EDCF parameter set. The larger $RetryCnt[AC]$, the more often a backoff entity of this AC will attempt to deliver MSDUs. In general, also the maximum

size of the contention window is determined by the $RetryCnt[AC]$. Since the influence of the retry counter can be mitigated by setting the $CWmax[AC]$ accordingly, a differentiation of the retry counter per AC, i.e., $RetryCnt[AC]$, is not included in the 802.11e standard.

4.2.4.2 Persistence Factor as Parameter per Access Category

In legacy 802.11, a new contention window is used after any unsuccessful transmission attempt. This contention window is twice as large as the previously used contention window. A new backoff counter out of this enlarged contention window is drawn to reduce the probability of a new collision.

In 802.11e, instead of increasing the contention window by the factor *2*, a *Persistence Factor* ($PF[AC]$), can be used to support priorities between ACs. Whereas in legacy 802.11, the contention window is always doubled after any unsuccessful transmission attempt (equivalent to $PF=2$), 802.11e may use $PF[AC]$ to increase the contention window differently for each AC. The contention window size is calculated as

$$CW(i) = min\left(CWmax[AC],\quad \left(CWmin[AC]+1\right)\cdot PF[AC]^{i-1}-1\right),$$

where i indicates the backoff stage. This calculation of the contention window upon unsuccessful transmission attempts is illustrated in Figure 4.7.

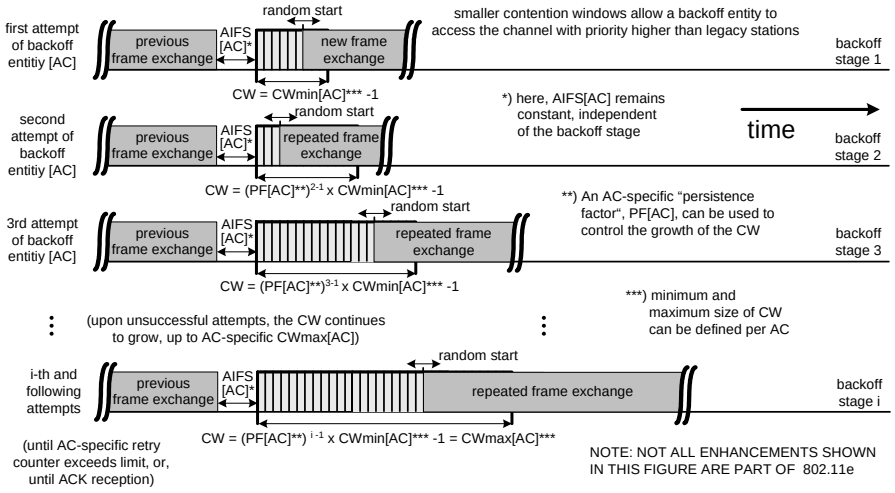

Figure 4.7: Increase of contention window size in EDCF, after unsuccessful frame exchange attempts. The growth of the contention window per attempt depends on many parameters. Not all parameters shown in this figure will be part of the 802.11e standard.

How the $PF[AC]$ may help to support QoS in 802.11e is illustrated in Figure 4.8 and Figure 4.9, for a scenario with three priorities labeled with "higher," "legacy" and "lower". In Figure 4.8, all ACs use the same $PF[AC]$ as the legacy priority. i.e., $PF[AC] = 2$ for all ACs. In contrast, in Figure 4.9, the higher priority AC uses a smaller and the lower priority uses a larger $PF[AC]$.

The figures indicate that $PF[AC]$ is a help to support QoS especially in scenarios with a high number of collisions. For example, in case of collisions, a high priority backoff entity does not need to increase its contention window by factor *2*. This is helpful to give this high priority backoff entity the chance to access the channel earlier than other backoff entities, to retransmit the collided frame.

The $PF[AC]$ is not included in the 802.11e standard, but may be an important means to support QoS against legacy stations, as will be shown in Chapter 5, where 802.11e is evaluated.

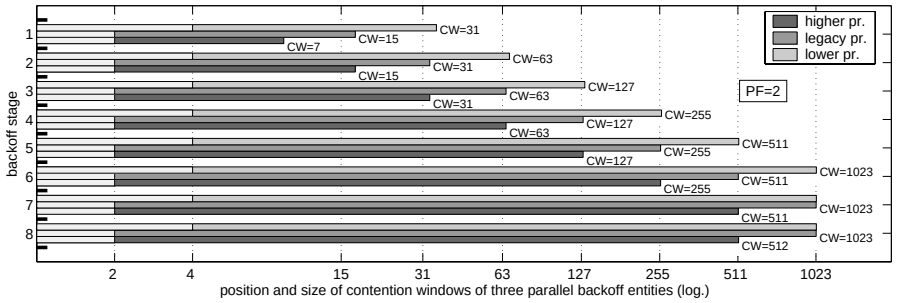

Figure 4.8: Change of contention window size with increasing backoff stage, PF=2 for all ACs.

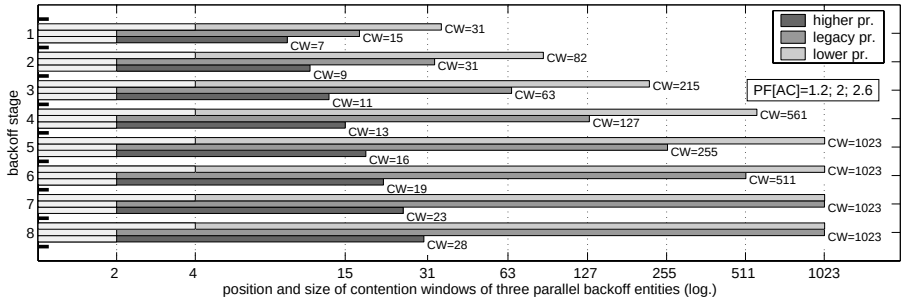

Figure 4.9: Change of contention window size with increasing backoff stage. Here, different PFs are used for the 3 priorities (ACs): PF[AC=high, legacy, low]=1.2, 2, 2.6.

4.2.5 Traffic Streams

To determine and classify MSDUs that are delivered within a QBSS with certain QoS requirements, 802.11e stations use so-called *Traffic Streams* (TSs) that are identified by *Traffic Stream Identifiers* (TSID). A TS is a set of MSDUs that are delivered using a certain EDCF parameter set. A TS is in this thesis referred to as *stream*. An 802.11e station has to be capable of supporting 8 streams from the HC to itself and 8 streams from itself to any other station, including the HC, at the same time. Before a stream is delivered, 802.11e stations have to negotiate with the HC the so-called *Traffic Specification* (TSPEC) for this stream. The TSPEC includes objectives and limits for traffic characteristics such as the MSDU frame body sizes, arrival rates, maximum MSDU Delivery delay, and variance. A so-called *Traffic Classification* (TCLASS) is used between the 802.11e MAC and the higher layer at the MAC SAP, in order to classify MSDUs into the TSPECs, by using the *Traffic Identifier* (TID). TID structure and TCLAS specification is implementation dependent and beyond the scope of the standard, as is the classification process itself.

4.2.6 Default EDCF Parameter Set per Draft 4.0, Table 20.1

Table 4.2 is a short version of a table in IEEE 802.11 WG (2002c), and shows recommended default values for the EDCF parameter sets for the four ACs, as defined by 802.11e. An HC may use these values when setting up a QBSS, and may change them dynamically upon change of channel and traffic condition.

Table 4.2: 802.11e recommended default values (IEEE 802.11 WG, 2002c).

AC	CWmin *	CWmax *	TXOPlimit* (802.11a, 802.11g)	*AIFSN*	*AIFS*	earliest channel access	PF
0	*CWmin*	*CWmax*	*0*	*2*	*DIFS*	*DIFS+aSlotTime*	*32/16=2*
1	*CWmin*	*CWmax*	*1.5 ms*	*1*	*PIFS*	*PIFS+aSlotTime*	*32/16=2*
2	*(CWmin+1) /2-1*	*CWmin*	*3.0 ms*	*1*	*PIFS*	*PIFS+aSlotTime*	*32/16=2*
3	*(CWmin+1) /4-1*	*(CWmin+1) /2-1*	*1.5 ms*	*1*	*PIFS*	*PIFS+aSlotTime*	*32/16=2*

*) PHY dependent

4.3 Hybrid Coordination Function, Controlled Channel Access

The controlled channel access of the HCF extends the EDCF access rules by allowing the highest priority channel access to the HC during the contention free period and the contention period (CFP and CP). The details about the controlled channel access are summarized in this section.

4.3.1 Controlled Access Period

In 802.11e, a TXOP can be obtained by the HC via the controlled channel access. In this case the TXOP is referred to as *Controlled Access Phase* (CAP).

The HC may allocate TXOPs to itself to initiate MSDU Deliveries whenever it requires, after detecting the channel as being idle for PIFS, and without backoff. To give the HC the higher priority over the legacy DCF and the EDCF access, $AIFSN[AC]$ cannot have a value smaller than one for any AC. During CP, each TXOP begins either when the channel is determined to be available under the EDCF rules, i.e., after $AIFS[AC]$ plus the random backoff time of at least one slot, or when a backoff entity receives a polling frame, the *QoS CF-Poll*, from the HC, hence, starting a CAP. The QoS CF-Poll from the HC can be transmitted after a PIFS idle period, without any backoff, by the HC. Therefore, the HC can issue polled TXOPs, referred to as CAPs, in the CP using its prioritized channel access. During the CFP, the starting time and maximum duration of each CAP is also specified by the HC, again using the QoS CF-Poll frames. During CFP, 802.11e backoff entities will not attempt to access the channel without being explicitly polled, hence, only the HC can allocate CAPs by transmitting QoS CF-Poll frames, or by immediately transmitting downlink data. CAP allocations may be delayed by the duration of an EDCF-TXOP, as illustrated in Figure 4.10.

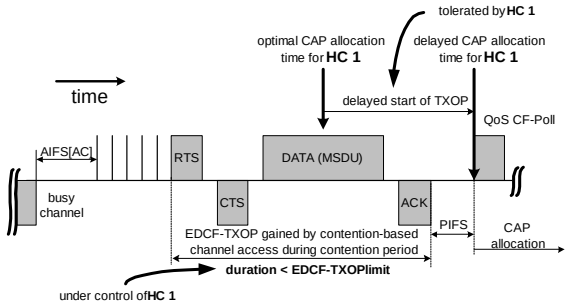

Figure 4.10: CAP allocation. Note that any 802.11e frame exchange will not take longer than the TXOPlimit, which is the limit for all EDCF-TXOPs and under control of the HC.

The HC controls the maximum duration of EDCF-TXOPs within its QBSS by announcing the $TXOPlimit[AC]$ for all ACs via the beacon. Therefore, it can allocate CAPs at any time during the CP, and the optional CFP. When very small MSDU Delivery delays are required, CF-Polls may be transmitted a duration of $TXOPlimit[AC]$ earlier than the optimal CAP allocation time to avoid any MSDU Delivery delay imposed by EDCF-TXOPs at all. The largest $TXOPlimit[AC]$ of the four ACs must be considered, however.

Figure 4.11 illustrates an example of a superframe that includes a CFP and a CP. The superframe starts with a beacon transmitted by the HC, see Figure 4.11, (1). During the CFP, i.e., the first part of the superframe, the backoff entities only transmit upon being polled by the HC. Indicated with (2) is the transmission of a fragmented MSDU within CFP. The CFP is optional and ends with the CF-End frame transmitted by the HC as shown at (3).

During the following CP, all backoff entities attempt to transmit through the contention-based channel access of the HCF, i.e., the EDCF. EDCF-TXOPs are obtained through contention, and two such EDCF-TXOPs are indicated with (4). During the CP, the HC can also poll backoff entities to allocate CAPs. This is in the figure shown as an example. Following the two EDCF-TXOPs, the HC polls a backoff entity to obtain a CAP during which a fragmented MSDU is transmitted as shown at (5). The duration of CAPs is not limited by any parameter specified in the standard. The HC is responsible for determining the duration of a CAP. However, any CAP must not exceed the TBTT. In addition, regulatory requirements may limit the duration of a CAP if 802.11e stations operate in certain regulatory domains.

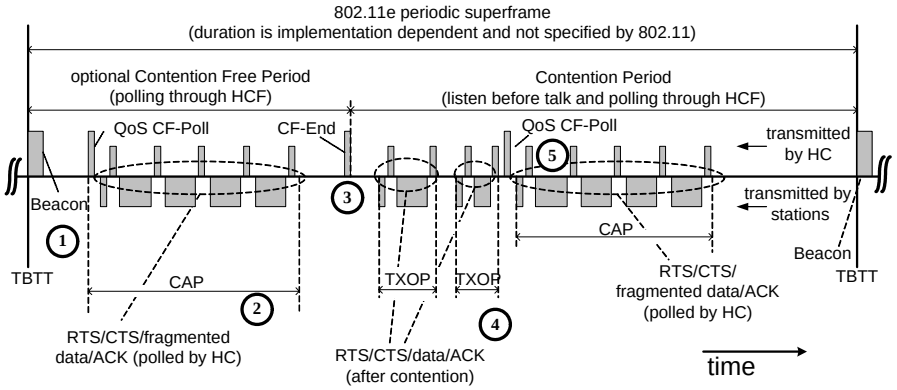

Figure 4.11: Example of an 802.11e superframe where the HC grants TXOPs in Contention Free Period and Contention Period. The duration of the superframe is not specified in the standard.

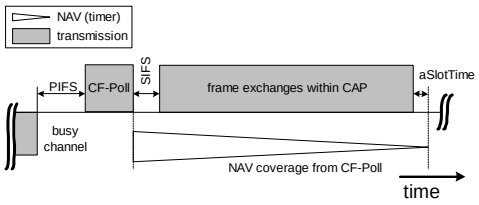

Figure 4.12: NAV protection of a CAP.

CAPs are protected by the NAV, as indicated in Figure 4.12. Through the longer NAV setting, the HC can grab the channel again without colliding with other frames, and continue to allocate the channel.

4.4 Improved Efficiency

In this last section about 802.11e, four important schemes to improve the efficiency of the protocol, that are under discussion at TGe, are briefly described and summarized. Contention free bursts help to improve the achievable throughput, they are described in the next section. The optional block acknowledgement allows an higher throughput and is described in the Section 4.4.2. The controlled contention is an additional random access scheme that was proposed at TGe but not accepted. It is described in Section 4.4.3. Controlled contention can be compared to the random access in HiperLAN/2, and enables stations to react more dynamically on changes of the radio environment, or on changes of the offered traffic. Finally, Section 4.4.4 summarizes a concept that will allow higher layers to exchange time information between different stations, for the purpose of synchronization.

4.4.1 Throughput Improvement: Contention Free Bursts

The concept of transmitting more than one MSDU after winning the EDCF contention is referred to as *Contention Free Bursts* (CFBs). Figure 4.13 illustrates the CFB concept. With CFBs, a backoff entity may transmit many MSDUs within one EDCF-TXOP, however, for a duration that must not exceed the $TXOPlimit[AC]$. The advantage of CFBs is the increased maximum achievable throughput at the cost of potentially increased MSDU Delivery delays in other streams, which do not necessarily utilize their complete EDCF-TXOP until the maximum allowed duration, because they deliver only one MSDU per TXOP. With CFBs, the number of collisions can be reduced (Tourrilhes, 1998).

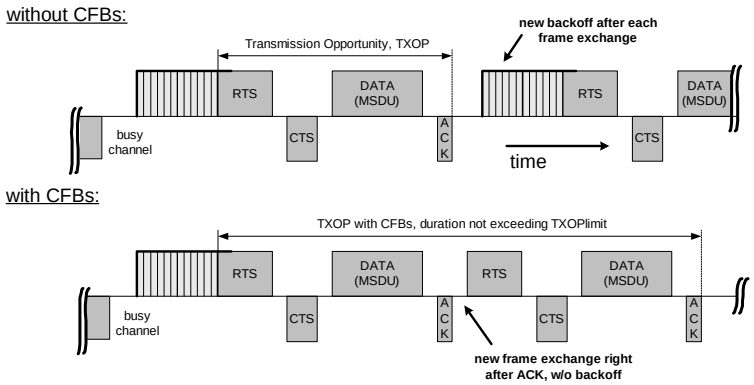

Figure 4.13: One MSDU per EDCF-TXOP (top) and Contention Free Bursts (CFBs) (bottom).

4.4.2 Throughput Improvement: Block Acknowledgement

With this concept, the MSDU Delivery throughput efficiency of the protocol is improved. The block acknowledgement frame exchange is an optional enhancement defined in 802.11e. Block acknowledgements allow a backoff entity to deliver a number of MSDUs being transmitted during one TXOP, separated by SIFS, and transmitted without individual ACK frames, consequently reducing the protocol overhead. The MSDUs that are delivered during the TXOP are referred to as block of MSDUs.

At the end of the block, all MSDUs are individually acknowledged through a bit pattern delivered in the block acknowledgement frame, thus reducing the overhead of control exchange sequences to a minimum of one acknowledgement frame per number of MSDUs delivered in a block. Each data frame in a block protects its succeeding frame by setting the NAV as illustrated in Figure 4.14. The subsequent frame may either be another data frame or a frame requesting the acknowledges for the preceding data frames.

The following block acknowledgement that is transmitted by the receiving station in response to the request includes the pattern bitmap of acknowledges for all received MSDUs. The block acknowledgement may be transmitted immediately after the request, or alternatively later, in the next available TXOP.

It is possible to transmit blocks of MSDUs over more than one TXOP. Before using the block acknowledgement, the transmitting backoff entity and the receiving station need to set up the block acknowledgement by exchanging some primitives as defined in the 802.11e.

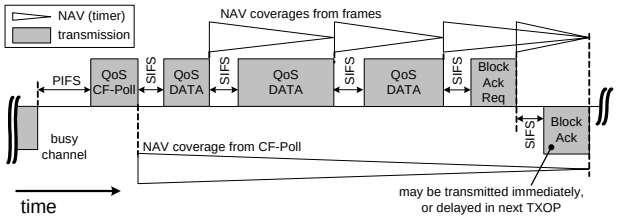

Figure 4.14: A block acknowledgement frame exchange may consist of up to 16 data frames before the actual acknowledgement pattern is requested.

After the block acknowledgement mechanism was successfully established, the receiving station will not send individual ACK frames upon reception of data frames with a registered address. If the transmitting backoff entity has only a limited number of MSDUs to deliver to the particular receiving station, it may temporarily request individual acknowledgements for the sake of higher flexibility.

4.4.3 Delay Improvement: Controlled Contention

With controlled contention, the MSDU Delivery delay efficiency of the protocol is improved. The controlled contention is not part of the 802.11e draft 4.0, but was an early proposal at TGe (draft 2.0). It is here briefly summarized because of its similarity to the HiperLAN/2 random access protocol. An additional random access protocol that allows fast collision resolution is referred to as controlled contention. In order for the HC to grant TXOPs for MSDU Delivery, it requires information about the data that is pending in the queues of the stations. In a dynamic environment, this information has to be updated from time to time. The controlled contention interval as illustrated in Figure 4.15 is a means for the HC to update which backoff entity requires radio resources, at what times and for what durations. The controlled contention interval is initiated by the HC via a frame referred to as controlled contention frame, as shown in the figure. Following this frame, backoff entities may request TXOPs by transmitting resource

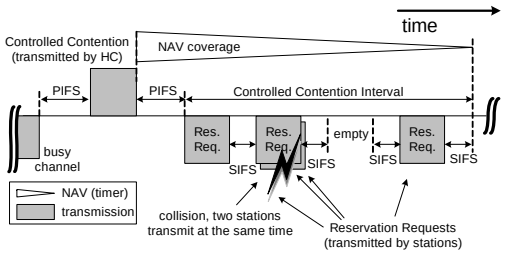

Figure 4.15: Controlled contention.

requests, without contending with other backoff entities. The controlled contention frame defines the number of so-called opportunity intervals available for the random access (i.e., intervals separated by SIFS) and some access priorities for the ACs. Each backoff instance that is allowed to transmit resource requests selects one opportunity interval and transmits a resource request frame containing the requested AC and TXOP duration, or the queue size of the requested AC. Resource requests are transmitted within randomly selected opportunity intervals, and may therefore collide when two or more backoff entities select the same opportunity interval. For fast collision resolution, the HC acknowledges the receptions by generating another control frame with a feedback field so that the requesting backoff entities identify collisions in the preceding controlled contention interval. Upon the successful reception of the initiating controlled contention frame, the EDCF backoff entities, but also legacy 802.11 stations set the NAV until the end of the controlled contention interval, as illustrated in the figure.

4.4.4 Support of Time-Bounded Data: Improved Timer Synchronization

With this concept, an accurate synchronization of timers that are maintained by applications on top of MAC is supported. Time-bounded data of some audio- and video applications such as IEEE 1394 require an accurate synchronization across stations. Different timers running in the layers on top of the 802.11 MAC may have to be mutually synchronized with each other. This requires that the information about other timers is provided by the MAC layer to the higher layer. The actual implementation of how these timers are synchronized is not focus of the standard and therefore implementation dependent. However, what needs to be included in the standard are additional primitives that have to be exchanged between the MAC layers and the higher layers via the *MAC Layer Management Entity – Service Access Point* (MLME-SAP). Further, management frames are defined by 802.11e that allow the set-up of the improved timer synchronization, if required. After setting-up the timer synchronization by determining which stream requires such a precise synchronization, all data frames transmitted within the respective stream carry an additional time field. This field includes the timer information from the transmitting backoff entity of the point in time when the last symbol of the transmitted data frame was transmitted. The receiving station will deliver this information to its higher layer, after adding some processing delay to that time. How this processing delay, which depends on the receiver only, is determined by the MAC layer, is again implementation dependent and not standardized.

Chapter 5

EVALUATION OF IEEE 802.11E WITH THE IEEE 802.11A PHYSICAL LAYER

THIS CHAPTER provides the analysis of the main 802.11e MAC enhancements, and identifies problems in QoS support in 802.11. It further highlights the advantage of *Contention Free Bursts* (CFBs), and shows that a coexistence problem exists when multiple *Hybrid Coordinators* (HCs) use the *Hybrid Coordination Function* (HCF) with controlled channel access at the same time. The contention-based channel access, i.e., the *Enhanced Distributed Coordination Function* (EDCF) is analyzed based on an analytical approach to model the achievable throughput per AC of the contention-based channel access, and with the help of stochastic simulation. As part of this analysis, a new analytical model is developed and evaluated. This new model allows calculating the achievable throughput per ACs and the mutual influences when different ACs with arbitrary EDCF parameter sets are at the same time used by an arbitrary number of backoff entities.

The used simulation tool is described in Appendix A. The analytical approach makes use of a modified version of the analytical model described in Appendix D. This chapter is outlined as follows. In Section 5.1 a performance evaluation of the EDCF medium access is presented, where an analytical approach for ap-

proximating the system saturation throughput per *Access Category* (AC), when multiple backoff entities of different ACs operate in parallel, is introduced. In Section 5.2 a new concept, the CFB, is discussed, and its importance in scenarios of overlapping *QoS supporting Basic Service Sets* (QBSSs) in unlicensed bands is evaluated. In Section 5.3 some known capture effects in 802.11 are analyzed. In Section 5.4 a performance evaluation of the HCF contention-based channel access and a discussion of coexistence of overlapping QBSSs is provided. This chapter ends up with a conclusion in Section 5.5.

5.1 HCF Contention-based Channel Access

Four different approaches are taken in this section to evaluate the HCF contention-based channel access. In Section 5.1.1 the maximum achievable throughput is calculated. In Section 5.1.2, the achievable throughput (here referred to as system saturation throughput) for an arbitrary number of contending backoff entities all operating with the same EDCF parameter set is discussed. When all backoff entities operate with the same EDCF parameter set, the same AC is used by all backoff entities. For the analysis, a known model for the legacy 802.11 is modified to capture all relevant effects of the new MAC enhancements. With the modified model, the saturation throughput in 802.11e can be calculated. In Section 5.1.3, this modified model is extended to approximate the saturation throughput per AC in scenarios where an arbitrary number of backoff entities operate in parallel, but with different EDCF parameter sets. When backoff entities operate with different EDCF parameter sets, multiple ACs are used and the resources are shared among backoff entities of different ACs according to their relative priorities. Finally, in Section 5.1.4 the specific problem of QoS support under contention with legacy 802.11 stations is discussed.

5.1.1 Maximum Achievable Throughput

The maximum achievable throughput depends on a large number of parameters when all parameters such as channel errors with respect to the PHY modes, frame body sizes, fragmentation, the use of RTS/CTS, and many more are considered. However, it is of interest to know the maximum achievable throughput with the EDCF, in case all protocol parameters are adjusted such that the achievable throughput in a single point to point downstream is maximized. This throughput is discussed in this section for the three different PHY modes BPSK1/2 (*6 Mbit/s*), 16QAM1/2 (*24 Mbit/s*), and 64QAM3/4 (*54 Mbit/s*). An ideal environment without transmission errors is assumed. The simple scenario is illustrated in Figure 5.1.

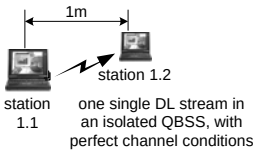

Figure 5.1: A single stream is simulated to measure the achievable throughput with EDCF using the EDCF parameters given in Table 5.1.

The maximum achievable throughput is calculated as

$$Thrp\left[{}^{Mbit}/_{s}\right] = \frac{frame\ body\ size\ [Mbit]}{expected\ backoff\ time[s] + frame\ exchange\ time[s]}.$$

With one single transmitting backoff entity, collisions never happen, and the expected backoff time is given by $CWmin/2$. The frame exchange time includes the *PHY Protocol Data Unit* (PPDU) durations including the headers and PHY overheads according to the applied PHY mode, and all interframe spaces, including *AIFS*. The frame exchange time increases when RTS/CTS is used.

In the following, results for three different priorities with three different EDCF parameter settings are compared with each other. EDCF parameters as defined in Table 5.1 are used.

Figure 5.2, left, shows the resulting throughput as a function of the MPDU frame body size for the most optimistic scenario, where RTS/CTS is not used, and neither the optional encryption *Wired Equivalent Privacy* (WEP) nor the address 4 is used (see p. 65). Note that without encryption, and without address 4, an MPDU can be transmitted with the smallest overhead. In terms of maximum throughput, RTS/CTS can be considered as overhead as well. Therefore, it is not used here.

Table 5.1: Used EDCF parameters with legacy backoff.

AC (priority):	highest	legacy	lower
AIFSN[AC]:	*2*	*2*	*4*
AIFS[AC]:	*DIFS (34us)*	*DIFS (34us)*	*52us*
CWmin[AC]:	*0*	*14*	*31*
CWmax[AC]:	*N/A*	*N/A*	*N/A*
PF[AC]:	*N/A*	*N/A*	*N/A*
RetryCnt[AC]:	*N/A*	*N/A*	*N/A*

The legacy priority uses *AIFS=DIFS (AIFSN=2)*[5], and an initial contention window size known from the legacy standard, that means *CWmin=15* (valid for 802.11a). The results are similar to what a legacy DCF backoff entity may theoretically achieve. The lower priority uses AIFSN=4 and *CWmin=31*, and shows a smaller throughput than the legacy priority due to larger AIFSN and longer backoff durations. In contrast, the highest priority shows clearly the largest throughput. With *AIFSN=2*, and *CWmin=0*, the backoff entity always transmits with highest priority. Without contention, the maximum achievable throughput can therefore be increased, as long as no other contending backoff entity operates in the near environment. In this scenario it is assumed that the receiving station is not allowed to contend for medium access.

Results of a stochastic simulation study are also shown and prove the analysis to be sufficiently accurate. The right hand graph in Figure 5.2 shows results for the same parameters, but now including RTS/CTS, WEP encryption, and the address 4 in the MAC header of the directed MPDU are necessary. The resulting achievable throughput is smaller, but show qualitatively the same characteristics: with small *AIFSN* and small *CWmin*, the maximum achievable throughput can be increased as long as there is only one transmitting backoff entity.

To understand the overhead that results from the 802.11 MAC protocol, it is worth to discuss the maximum achievable throughput for the 802.11a physical layer in scenarios assuming PHY modes with higher modulations than defined in 802.11. The higher the modulation of a transmitted PPDU, the shorter the transmission duration of a PPDU. A frame is also referred to as PPDU, see Figure 3.4, p. 25. A PPDU consists of the preamble, the PHY header, and the MPDU as payload. Parts of the PPDU are transmitted with the basic PHY mode (BPSK1/2). However, the interframe spaces SIFS and AIFS are independent of the used PHY mode. Therefore, and because of the limited frame body size, the maximum achievable throughput converges to a finite limit when using higher modulations of up to an infinite amount of bits per second. This is indicated in Figure 5.3. It can be seen that the maximum throughput with improved PHY modes is around *111 Mbit/s* with RTS/CTS and *188 Mbit/s* in the most optimistic case. Obviously, assuming an error free channel is not realistic with such unre-

[5] In this analysis, the legacy DCF backoff is used for the EDCF discussion. Specifically, the earliest channel access time of the EDCF backoff entities is DIFS, which is here interpreted as AIFS=DIFS and AIFSN=2. This is consistent with the interpretation of the legacy DCF backoff, but not with the interpretation of the EDCF backoff. However, since comparisons of DCF and EDCF are presented in this chapter, only the legacy interpretation is used.

alistically high modulation values. The results in this section are obtained through analytical calculations and stochastic simulation, without taking the capacity loss through regular beacon transmissions into account. The small variations of the throughput curves in Figure 5.2 are the results of the bit padding into OFDM symbols. A perfect radio channel is assumed.

5.1.2 System Saturation Throughput

The system saturation throughput $Thrp_{sat}$ is defined as expected sum of all MSDU throughputs of contending backoff entities that are saturated with traffic load so that all entities have always MSDUs to deliver, queues are never empty.

In Appendix D, an approximate analysis is presented based on a Markov model to calculate the saturation throughput of a number of contending backoff entities. The approximation is based on Bianchi (1998a, 1998b, 2000) and in this thesis referred to as Bianchi's legacy 802.11 model. Hettich (2001) uses Bianchi's legacy 802.11 model and extends it for the analysis of not only the throughput, but also the backoff delay. To evaluate the concepts of the EDCF contention window, Bianchi's legacy 802.11 model is modified in the following. The focus of the discussion is the throughput approximation.

5.1.2.1 Modifications of Bianchi's Legacy 802.11 Model

To model the saturation throughput of an EDCF backoff entity instead of a legacy station, some modifications of Bianchi's legacy 802.11 model are required.

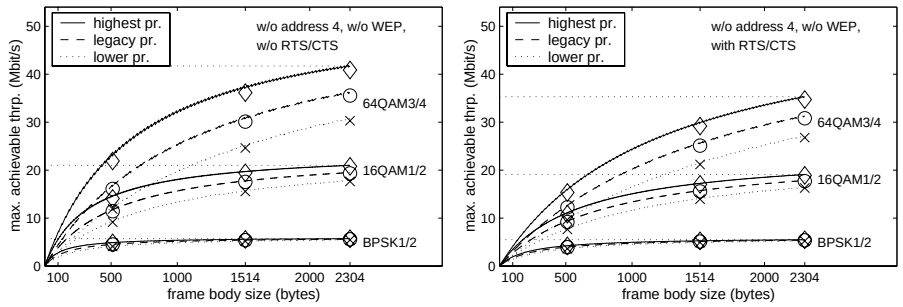

lines: analytics, markers: WARP2 simulation results

Figure 5.2: Maximum achievable throughput for three PHY modes, and three EDCF parameter settings. Left: most optimistic situation. Right: realistic situation with RTS/CTS, WEP encryption and use of optional address 4. Analytical and simulation results.

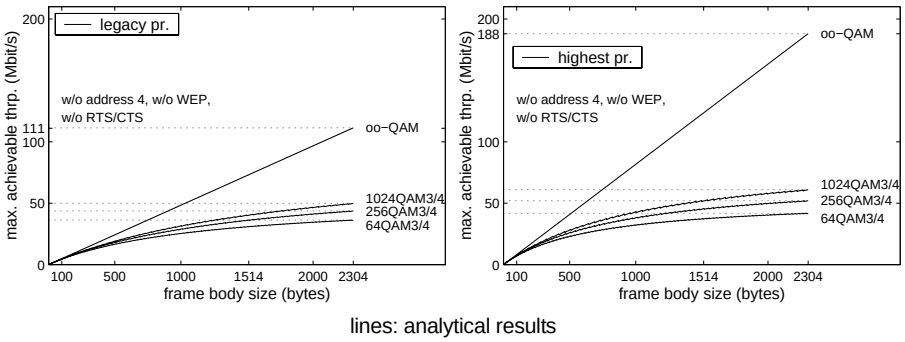

Figure 5.3: Maximum achievable throughput and its upper limit for higher PHY modes, which are not part of the 802.11 standard. Left: DCF (legacy priority) configuration. Right: EDCF (highest pr.) configuration. The results are obtained with the analytical model only.

In Equation (D.1), the parameter i is the backoff stage, and m is the maximum value of the backoff stage. The contention window sizes $W_i, i = 0 \ldots m$ and the maximum number of backoff stages m are dependent on the EDCF parameter set, individually defined per AC. Further, since the *Persistence Factor* (PF) can also be included in the modified model as well -although it is not part of 802.11e- this parameter has to be considered in the equation. The modifications are as follows. The size of the contention window in 802.11e is calculated by

$$W_i[AC] = PF[AC]^{min(i,m[AC])} \cdot W_0, \quad i \in 0,1,\ldots m[AC]. \tag{5.1}$$

The probability that transmission attempts of a single backoff entity at a particular slot are unsuccessful due to collision is denoted by p. As in the approach to model the legacy 802.11, it is in the following assumed that this probability is independent of the contention window size. For $W_i \geq 1$, the persistence factor is incorporated in Equation (D.4) by considering Equation (5.1):

$$\begin{aligned} 1 &= \sum_{i=0}^{m} \left(b_{i,0} \cdot \sum_{k=0}^{W_i - 1} \frac{W_i - k}{W_i} \right), \quad W_i \geq 1 \quad \forall\, 0 \leq i \leq m, m \geq 0 \quad \Rightarrow \\ 1 &= \frac{1}{2} \cdot \sum_{i=0}^{m} b_{i,0} \cdot (W_i + 1) \\ &= \frac{b_{0,0}}{2} \cdot \left[W_0 \cdot \sum_{i=0}^{m-1} \left(PF[AC] \cdot p \right)^i + \frac{1}{1-p} + W_0 \cdot \frac{\left(PF[AC] \cdot p \right)^m}{1-p} \right], \\ & \text{with } m \geq 0, W_0 \geq 1. \end{aligned} \tag{5.2}$$

Considering all these modifications, the stationary probability distribution $b_{0,0}$ of an idle system is calculated as

$$b_{0,0} = \begin{cases} \dfrac{2\cdot(1-p)}{W_o\cdot(1-p)\cdot m\cdot(PF[AC]\cdot p)^{m+1}+W_o\cdot(PF[AC]\cdot p)^m+1}, & \begin{cases} p=\dfrac{1}{PF[AC]}, \\ m>0 \end{cases} \\ \dfrac{2\cdot(1-p)}{W_o\cdot(1-p)\cdot\dfrac{1-(PF[AC]\cdot p)^m}{1-PF[AC]\cdot p}+W_o\cdot(PF[AC]\cdot p)^m+1}, & \begin{cases} p\neq\dfrac{1}{PF[AC]}, \\ m>0 \end{cases} \\ \dfrac{2}{2+(1-p)\cdot(W_o-1)}, & m=0 \end{cases} \quad (5.3)$$

The probability τ that a backoff entity is transmitting in a generic slot is calculated by the summation of all stationary distributions $b_{i,0}$, as in Bianchi's legacy 802.11 model, given by

$$\tau=\sum_{i=0}^{m} b_{i,0}=\begin{cases} 1, & p=1, \\ b_{0,0}\cdot\dfrac{1}{1-p}, & else. \end{cases}$$

In 802.11e, with the controlled channel access, $p=1$. In this case, all slots are busy at any time, and therefore $\tau=1$.

All the rest of the analysis of the saturation throughput can be taken from Appendix D. Note that a generic slot is different to a backoff slot in this thesis. A generic slot may be an idle generic slot during the contention phase, or a busy generic slot during which a frame exchange is completed, or, alternatively, during which a collision occurs. It is referred to as generic slot to differentiate it from the backoff slots, because a generic slot can be a backoff slot or a busy phase with a longer duration than the backoff slot duration.

5.1.2.2 Throughput Evaluation for Different EDCF Parameter Sets

The saturation throughput of a number of backoff entities that operate all according to the same AC can be approximated by modifying Bianchi's legacy 802.11 analysis as explained in the previous Section 5.1.2.1. These approximations are evaluated in this section and compared to WARP2 simulation results. In

addition to the legacy EDCF parameters, two other EDCF parameter sets are defined in the following. One is referred to as the "higher priority AC" and the other as the "lower priority AC," as they will allow higher and lower priority in channel access than the legacy priority, respectively. The legacy priority AC is also referred to as "medium priority AC." The saturation throughput for the medium priority AC can be found in Appendix D, and the results for the higher and lower priority AC are shown in this section. Table 5.2 summarizes the EDCF parameter sets selected for the three ACs. The medium priority AC follows the legacy DCF protocol. The higher priority AC operates with a smaller $CWmin[AC]$ and a smaller $PF[AC]$, the lower priority AC operates with a larger $CWmin[AC]$ and a larger $PF[AC]$ than what is defined for the legacy DCF. All other EDCF parameters remain equal to the medium priority EDCF parameters.

The contention window sizes for the three priorities for the first four backoff stages are presented in Figure 5.4. It can be seen that the parameter PF has a considerable impact on the resulting contention window sizes. The relative large value of $AIFSN$ for the lower priority ($AIFSN[lower] = 9$) together with the larger contention window sizes will give this AC only a very limited priority in channel access.

Larger contention window sizes have also positive effects on the saturation throughput. shows the probability τ that a backoff entity transmits in a generic slot versus the number of backoff entities.

Furher, Figure 5.5 illustrates the probability p that transmission attempts at a particular slot are unsuccessful due to collision, as function of the number of backoff entities. The probabilities are shown for the three known priorities. As expected, the larger the number of backoff entities, the larger the collision probability. Further, the probability that a backoff entity is transmitting at a generic slot decreases with increasing number of backoff entities.

Table 5.2: EDCF parameter sets for the three ACs, as selected for the analysis. The TXOPlimit per AC is not used in this thesis; one value is used for all ACs. Note that the legacy DCF backoff is assumed.

AC (priority):	higher	medium(=legacy)	lower
AIFSN[AC]:	*2*	*2*	*9*
CWmin[AC]:	*7*	*15*	*31*
CWmax[AC]:	*1023*	*1023*	*1023*
PF[AC]:	*24/16*	*32/16*	*40/16*
RetryCnt[AC]:	*7*	*7*	*7*

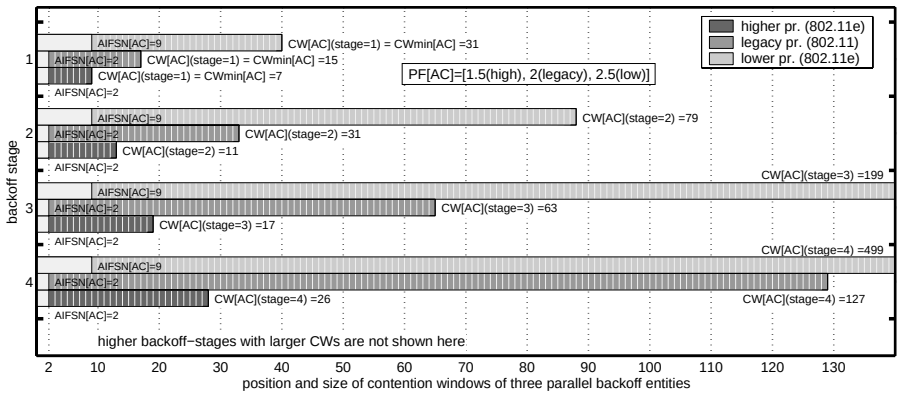

Figure 5.4: EDCF QoS-parameter setting for the three priorities, contention windows of the first four backoff stages.

Remarkably, with any number of backoff entities, the collision probability is higher for the higher probability AC than for the legacy and lower probability ACs, which is a result of the large contention window sizes. With a small number of backoff entities, the probability that a particular backoff entity is transmitting at a generic slot is higher for the higher priority AC than for the other ACs.

Figure 5.6 illustrates three other probabilities of the modified model as functions of the number of backoff entities. The probability that a generic slot is idle is referred to as *prob(CCAidle)*, the probability that a collision occurs, if a generic slot is busy is referred to as *prob(collision|CCAbusy)* and the probability that a frame exchange is successful, provided that a generic slot is busy, is referred to as *prob(success|CCAbusy)*.

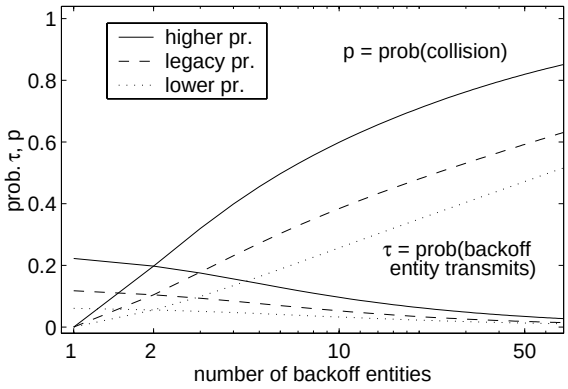

Figure 5.5: Collision and transmission probability (p, τ) for a single backoff entity in a generic slot, as functions of the number of backoff entities.

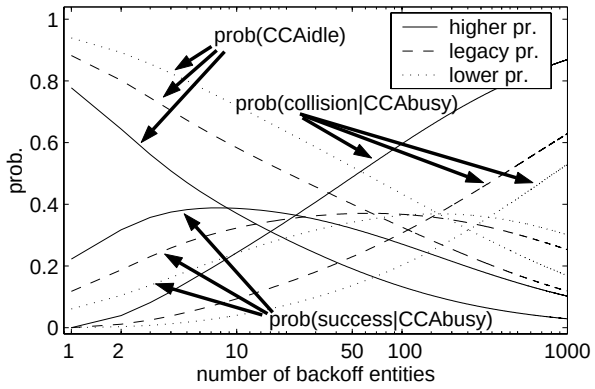

Figure 5.6: Probability that a generic slot is idle, busy with an collided frame, or busy with a successfully transmitted frame, as functions of the number of backoff entities.

The probabilities are defined in Appendix D.2 as $P_{CCAidle}$, P_{coll}, and $P_{success}$, respectively. The index "CCA" refers to *Clear Channel Assessment* (CCA), which is the carrier sense process in the 802.11 protocol. It can be observed from Figure 5.6 that with increasing number of backoff entities the probability that a generic slot is idle, $P_{CCAidle}$, decreases, as expected. In addition, the collision probability P_{coll} increases with increasing number of backoff entities, which is again an expected result. An interesting observation is that the probability $P_{success}$ shows maxima for all ACs, which are at different numbers of backoff entities for the different ACs. The higher the priority, the smaller the number of backoff entities that define the unique maximum, which is an expected result.

In the next two sections, Section 5.1.2.2.1 and Section 5.1.2.2.2, the saturation throughput calculated for the two priorities "lower" and "higher" are discussed and evaluated. The figures can be compared also to the figures that show the results for the legacy AC, see Figure D.3, p. 237, and Figure D.4, p. 238.

5.1.2.2.1 Lower Priority AC Saturation Throughput

Figure 5.7 and Figure 5.8 illustrate the resulting saturation throughput obtained through simulation and analytical approximation with the modified model for the lower priority AC. Shown is the saturation throughput for different PHY modes, and a varying number of backoff entities for the frame body sizes *48*, *512*, *1514*, and *2304 byte*. The EDCF parameters as defined in Table 5.2 are used. Figure 5.7 shows the saturation throughput for scenarios without use of RTS/CTS, Figure 5.8 shows results for the same scenarios, with the use of RTS/CTS. The results show the expected characteristics.

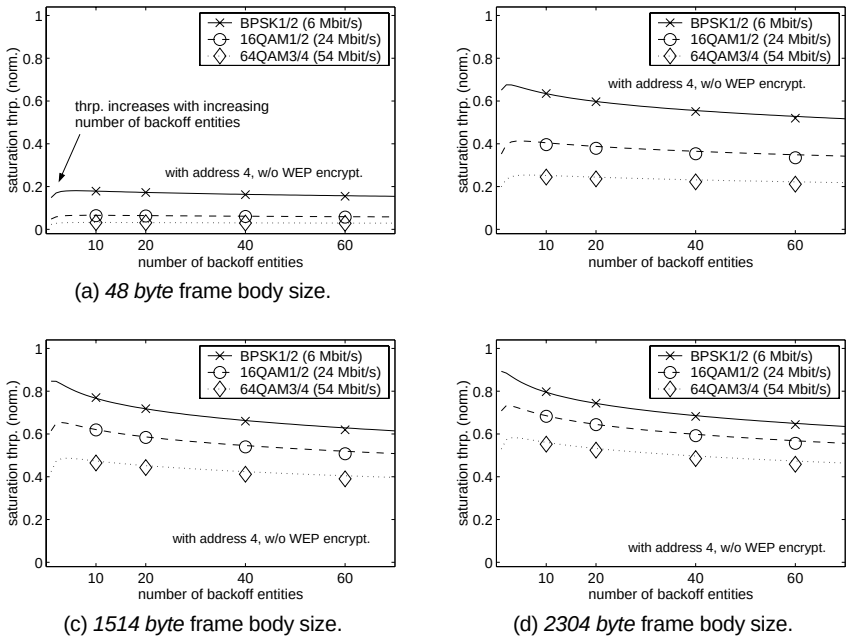

(a) *48 byte* frame body size.

(c) *1514 byte* frame body size.

(d) *2304 byte* frame body size.

lines: modified Bianchi approx.; markers: WARP2 simulation results

Figure 5.7: Normalized saturation throughput for different PHY modes, and a varying number of backoff entities, for lower priority (AC="lower"). EDCF parameters as defined in Table 5.2. RTS/CTS are not used. The respective legacy saturation throughput is illustrated in Appendix D.4, Figure D.3, p. 237.

The throughput increases with increasing frame body sizes. The higher the number of backoff entities, the lower the saturation throughput. The higher the PHY mode, the smaller the efficiency of the carrier sense protocol.

RTS/CTS increase the saturation throughput for long frame body sizes, but not for short frame body sizes. For small numbers of backoff entities, the saturation throughput increases with increasing number of backoff entities.

This is an expected result for the lower priority AC with its large initial contention window: as long as the collision probability is not too high, more contending backoff entities result in shorter idle phases and thus higher saturation throughput. Comparing the figures to the results of the legacy priority AC (Figure D.3, p. 237, and Figure D.4, p. 238), the saturation throughput is higher for the lower priority than for the legacy priority, which again is an effect resulting from the lower collision probability at the lower priority AC.

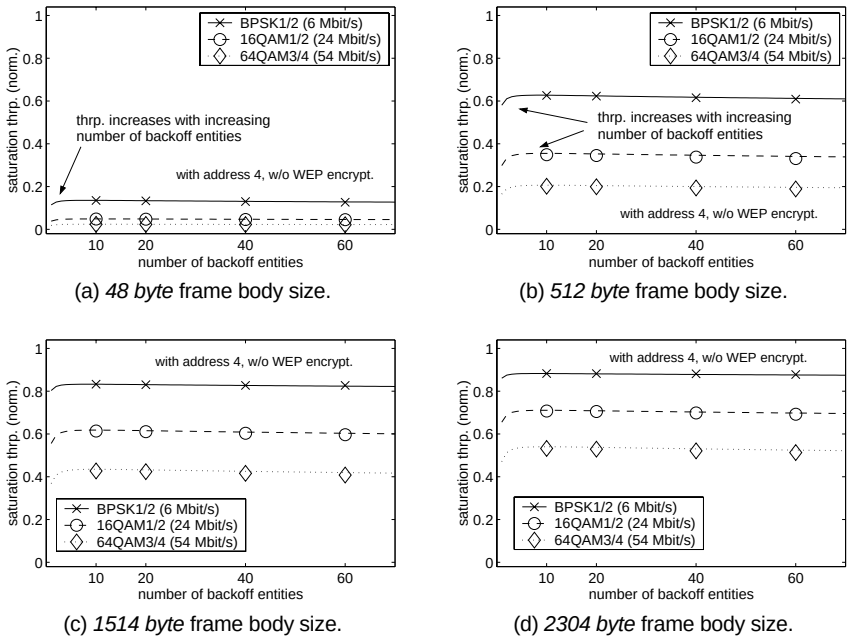

lines: modified Bianchi approx.; markers: WARP2 simulation results

Figure 5.8: Normalized saturation throughput for different PHY modes, and a varying number of backoff entities, for lower priority (AC="lower"). EDCF parameters as defined in Table 5.2. RTS/CTS are used. The respective legacy saturation throughput is illustrated in Appendix D.4, Figure D.4, p. 238.

5.1.2.2.2 Higher Priority AC Saturation Throughput

Figure 5.9 and Figure 5.10 illustrate the resulting saturation throughput for the same scenarios as discussed in the last section, but now for the higher priority AC. As before, results for scenarios without the usage of RTS/CTS, and results with the use of RTS/CTS are given in the two figures.

When comparing the results with the lower and legacy priorities, it can be observed that the higher priority AC shows a larger saturation throughput for a smaller number of backoff entities. However, with an increased number of backoff entities, the saturation throughput for the higher priority AC decreases considerably, because of the higher collision probability.

It worth noting that for this AC with its high probability of collisions, simulation results and analytical approximation do not always show the same saturation throughput.

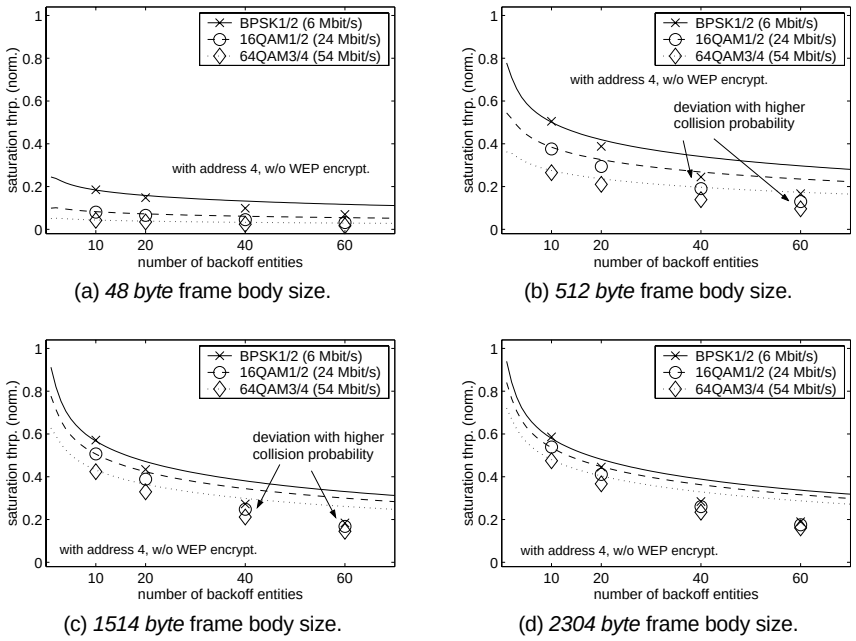

(a) *48 byte* frame body size.

(b) *512 byte* frame body size.

(c) *1514 byte* frame body size.

(d) *2304 byte* frame body size.

lines: modified Bianchi approx.; markers: WARP2 simulation results

Figure 5.9: Normalized saturation throughput for PHY modes, and a varying number of backoff entities, for higher priority (AC="higher"). EDCF parameters as defined in Table 5.2. RTS/CTS are not used. The equivalent legacy saturation throughput is illustrated in Appendix D.4, Figure D.3, p. 237.

For a larger number of backoff entities, simulation results and analytical approximation deviate from each other and show not the same results with the accuracy as observed for the lower and legacy priority AC.

This effect results mainly from the definition of the collision duration in Bianchi's legacy 802.11 model. In the analytical approximation, the collision time T_{coll} is defined without considering the ACK timeout; see Section D.3, p. 234.

This is a valid assumption only for the backoff entities that are not transmitting the colliding frames, but not accurate enough for backoff entities that are transmitting colliding frames. The higher the collision probability, the less accurate is the approximation.

However, it can be observed from Figure 5.9 and Figure 5.10 that the analytical approximation and the simulation results show at least qualitatively the same saturation throughput.

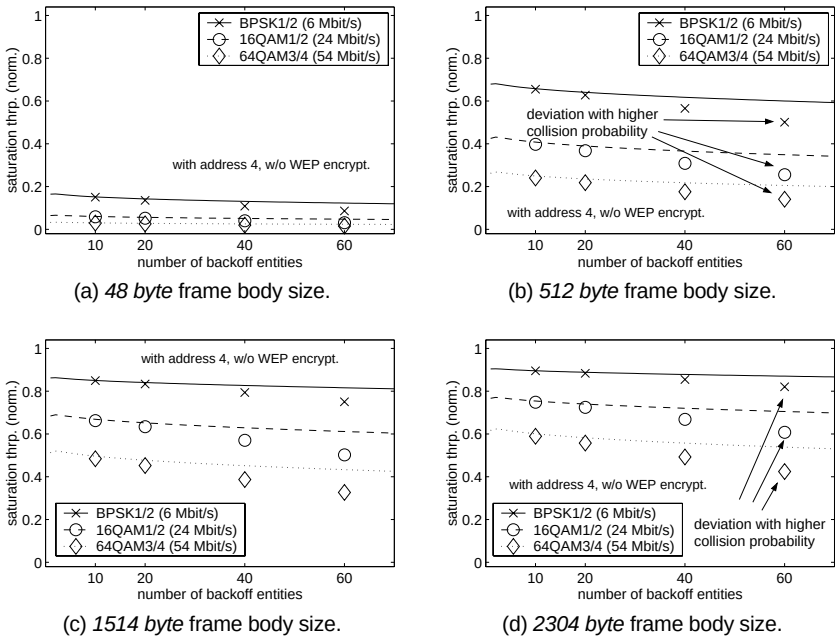

(a) *48 byte* frame body size. (b) *512 byte* frame body size.

(c) *1514 byte* frame body size. (d) *2304 byte* frame body size.

lines: modified Bianchi approx.; markers: WARP2 simulation results

Figure 5.10: Normalized saturation throughput for different PHY modes, and a varying number of backoff entities, for higher priority (AC="higher"). EDCF parameters as defined in Table 5.2. RTS/CTS are used. The equivalent legacy saturation throughput is illustrated in Appendix D.4, Figure D.4, p. 238.

5.1.3 QoS Support with the HCF Contention-based Channel Access

Focus of interest in this EDCF performance evaluation is to develop a method to control the channel access priorities between the different ACs, when backoff entities are operating in parallel and according to different ACs. This is referred to as share of capacity per AC and more relevant for the QoS analysis than the saturation throughput in isolated operation. The saturation throughput in isolated operation, where all contending backoff entities operate with the same EDCF parameter set, i.e., within the same AC, are discussed in the previous section. In contrast, in this section the achievable throughput per AC (share of capacity per AC) and the mutual influences between the ACs are investigated for the shared operation. In shared operation, backoff entities operate with different EDCF parameter sets, according to the different ACs.

5.1.3.1 Share of Capacity per Access Category

A method to quantify the mutual influences between the ACs is developed in the following, based on the expected idle time duration when operating in saturation.

Recapturing the model described in Appendix D including all modifications described earlier in this chapter, the probability that the channel is busy in a generic slot time is given by

$$P_{CCAbusy} = 1 - P_{CCAidle} = 1 - \left(1 - \tau\left[AC\right]\right)^{N\left[AC\right]},$$

equivalent to what is defined for legacy 802.11 in Equation (D.6), p. 234. $N\left[AC\right]$ is the number of backoff entities of a particular AC and $\tau\left[AC\right]$ is the probability that a backoff entity of this AC transmits at a generic slot time.

The number of consecutive idle slots in this model depends on the expected duration of the idle backoff phase, i.e., the expected contention window length, given in slots, until the first backoff entity attempts its resource allocation by initiating a transmission. This can be expressed by $P_{CCAbusy}$ and $P_{CCAidle}$. For example, the probability that one single generic slot is idle between two busy generic slots is given by $P_{CCAbusy} \cdot P_{CCAidle}$. However, the probability that *n* consecutive generic slots are idle and thus form a longer idle period between two busy generic slots is $P_{CCAbusy} \cdot P_{CCAidle}^{\ n}$. Therefore, the expected contention window length, $E\left[CW\left[AC\right]\right]$,can be calculated to

$$E\left[CW\left[AC\right]\right] \Big/ _{slot} =$$

$$E = P_{CCAbusy} \cdot \left[1 \cdot P_{CCAidle}^{\ 1} + 2 \cdot P_{CCAidle}^{\ 2} + 3 \cdot P_{CCAidle}^{\ 3} + \ldots\right]$$

$$\Leftrightarrow \frac{E}{P_{CCAidle}} = P_{CCAbusy} \cdot \left[1 + 2 \cdot P_{CCAidle}^{\ 1} + 3 \cdot P_{CCAidle}^{\ 2} + \ldots\right]$$

$$\Leftrightarrow \frac{E}{P_{CCAidle}} - E = P_{CCAbusy} \cdot \left[1 + P_{CCAidle}^{\ 1} + 2 \cdot P_{CCAidle}^{\ 2} + \ldots\right]$$

$$= P_{CCAbusy} \cdot \frac{1}{1 - P_{CCAidle}}$$

$$\Leftrightarrow E = P_{CCAbusy} \cdot \frac{P_{CCAidle}}{\left(1 - P_{CCAidle}\right)^2}.$$

As a result, with Equation (D.6), the expected number of consecutive idle slots, i.e., the expected size of the contention window is written as

$$E[CW[AC]]/_{slot} = (1 - P_{CCAidle}) \cdot \frac{P_{CCAidle}}{(1 - P_{CCAidle})^2} = \frac{P_{CCAidle}}{1 - P_{CCAidle}}$$
$$= \frac{(1 - \tau[AC])^{N[AC]}}{1 - (1 - \tau[AC])^{N[AC]}}.$$

Again, the parameter τ is the probability that a backoff entity is transmitting at a generic slot, and $N[AC]$ defines the number of backoff entities.

It is well known that σ-persistent CSMA (Kleinrock and Tobagi, 1975) results in the following expected duration of the idle phase, when N backoff entities operate at the same time:

$$E[idle] = \frac{(1 - \sigma)^N}{1 - (1 - \sigma)^N} \cdot aSlotTime .$$

This is confirmed by Calì et al. (2000b). Three known types of CSMA are often distinguished.

- In persistent CSMA, MSDUs arriving while the channel is busy have to wait for the channel to become idle again (backlogging), before being delivered immediately. This leads to a relatively high probability of collisions in scenarios with many backoff entities.
- In nonpersistent CSMA, in contrast, MSDUs arriving during a busy channel are also backlogged, but when the channel becomes idle again, MSDUs are delivered with a certain probability at this particular time. Bertsekas and Gallager (1992) refer to this type of CSMA to CSMA slotted ALOHA. If they are not delivered at this time, then a delivery attempt will start at the next slot with the same probability.
- Finally, in σ-persistent CSMA, MSDUs that collided before and are waiting for retransmission while the channel is busy, and MSDUs arriving while the channel is busy are delivered with different probabilities, once the channel becomes idle again.

In Calì et al. (2000a, 2000b), the 802.11 DCF is approximated by σ-persistent CSMA. The difference between the 802.11 (E)DCF and the σ-persistent CSMA lies in the selection process of the backoff interval, i.e., the size of the contention window. Whereas 802.11 EDCF adopted a binary exponential backoff, the size of the contention window in σ-persistent CSMA is calculated from a geometric

distribution[6] with the parameter σ (Calì et al., 2000b). However, Calì et al. (2000a, 2000b) show that in the case the system of contending backoff entities is in saturation, the throughput results of the σ-persistent CSMA approximate the achievable throughput of the 802.11 EDCF, if the average backoff intervals, i.e., the expected size of the contention window, $E[CW[AC]]$, of the two different CSMA types are equal. For this reason, the mutual influences between the different ACs in the 802.11 EDCF are in this thesis evaluated based on the assumption that the saturation throughput of the EDCF can be approximated with the saturation throughput of σ-persistent CSMA. In the following, the mutual influences of σ-persistent CSMA backoff entities with different σ-parameters are analyzed instead of the mutual influences of backoff entities that operate with the binary exponential backoff CSMA. The results of this analysis will be compared to 802.11 EDCF simulation results with binary exponential backoff.

For each individual AC, the expected size of the contention window, i.e., $E[CW[AC]]$, is used to parameterize σ-persistent CSMA per AC

$$\underbrace{E[CW[AC]] = \frac{1}{\sigma[AC]}}_{\substack{\sigma\text{-persistent CSMA with } N \\ \text{contending backoff entities per AC}}} \overset{!}{=} \underbrace{\frac{\left(1-\tau[AC]\right)^{N[AC]}}{1-\left(1-\tau[AC]\right)^{N[AC]}} = E[CW[AC]]}_{\substack{\text{Bianchi approximation with } N \\ \text{contending backoff entities per AC}}}. \quad (5.4)$$

The left side of this equation shows the expected value for the contention window from the geometric distribution in σ-persistent CSMA, and the right side shows the expected value for the contention window as calculated from Bianchi's model. This assumption is used in the following, to calculate the mutual influences between the different ACs. Figure 5.11 and Figure 5.12 show the access probabilities of the three ACs that are parameterized according to Table 5.2, for 3 and 8 backoff entities per AC, respectively. The shape of the geometric distribution is clearly visible. As expected, with a higher number of backoff entities, the expected size of the contention window decreases, as a result, the probability of access at earlier slots increases.

---

[6] The probability density function of the geometric distribution is defined as $p(x) = 1-(1-\sigma)^{\lfloor x \rfloor}\ \forall x \geq 1$, and $p(x) = 0$ else, with the parameter $\sigma \in (0..1)$. The expected value is directly obtainable from σ as $E[X] = 1/\sigma$. The operator $\lfloor \cdot \rfloor$ rounds towards minus infinity, hence, the distribution is discrete and memoryless. The cumulative probability function is defined as $P(x) = \sigma(1-\sigma)^{x-1}$ with $x = 1, 2, 3...$, and $P(x) = 0$ else; (Görg, 1997).

5.1.3.2 Calculation of Access Priorities from the EDCF Parameters

With the assumption of σ-persistent CSMA, it is now possible to derive a method to determine the access priorities from the EDCF parameters. A scenario of three rather than the available number of four ACs is used for the sake of simplicity. The ACs are labeled with "High," "Medium," and "Low," according to their priorities. A fundamental approximation taken here is that, once the characteristics of the backoffs of the ACs are found with the modified Bianchi model, these characteristics are assumed to remain constant even in contention with other ACs.

That means that for example the expected size of the contention window per AC are as found in the isolated scenario, mutual influences between the ACs on this expected size are neglected. Note that this assumption is taken for all ACs. What is determined here is the access priority, not the actual resulting capacity share (throughput). This resulting capacity share is calculated based on the access priorities by considering all ACs.

When calculating the access priorities, care must be taken about the fact that the different ACs start their backoffs at different slots, according to the AIFSN parameter. As a first step, the contention windows are therefore shifted by the AIFSN parameters, hence,

$$E\left[AIFS\left[AC\right]+CW\left[AC\right]\right]=AIFS\left[AC\right]+E\left[CW\left[AC\right]\right]$$
$$=AIFS\left[AC\right]+\frac{1}{\sigma\left[AC\right]}.$$

The access probability of the backoff entities of an AC at a certain slot is in the following referred to as $\xi_{slot}\left[AC\right]$ with $1\le slot\le max\left(CWmax\left[AC\right]\right)+1$.

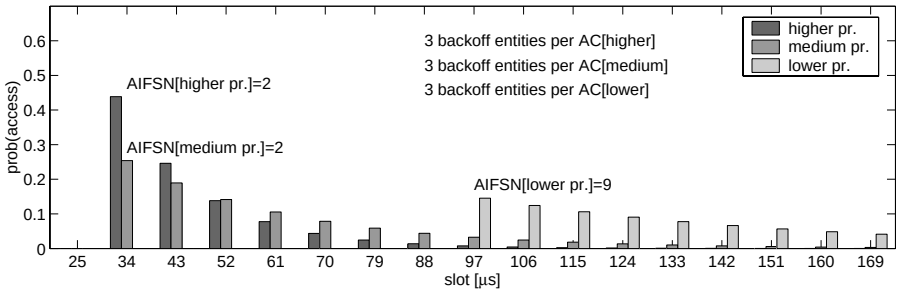

Figure 5.11: Access probability per slot for 3 backoff entities per AC, each AC operating isolated. Three ACs with EDCF parameter sets as defined in Table 5.2. Note that a legacy backoff is assumed, i.e., earliest backoff is DIFS when AIFSN=2.

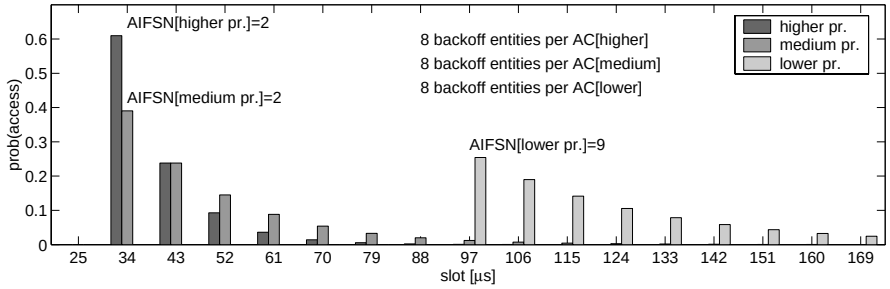

Figure 5.12: Access probability per slot for 8 backoff entities per AC, each AC operating isolated. Three ACs with EDCF parameter sets as defined in Table 5.2.

The largest value of the maximum size of the contention window defines over how many slots the access probabilities are calculated. Usually this is the value of the lowest priority AC. Of course, in saturation, ACs with smaller CWs and thus typically higher priorities access the channel with probability *1* within their CWs. The access probability for $slot < AIFS[AC]$ is $\xi_{slot}[AC] = 0$, because for slots earlier than $AIFS[AC]$, backoff entities of this AC will not access the channel. However, the access probability for $slot > CWmax[AC] + AIFS[AC]$ is also given by $\xi_{slot}[AC] = 0$, because for slots later than $CWmax[AC]$, backoff entities of the respective AC will not access the channel neither. It is again emphasized that $CWmax[AC]$ is in this study defined by not only the EDCF parameters known from 802.11e, but also depending on a number of parameters such as the $RetryCounter[AC]$, the $PF[AC]$, and the initial contention window size, $CWmin[AC]$[7]. See Section 4.2.2.3, p. 50, for the definition of $CWmax[AC]$ in 802.11e. Using the assumption explained in the previous section, especially Equation (5.4), the access probability to a particular slot follows from the geometric distribution

$$\xi_{slot}[AC] = 1 - \left(1 - \left(\sigma[AC] \cdot \left(1 - \sigma[AC]\right)^{slot - AIFS[AC]}\right)\right)^{N[AC]} \qquad (5.5)$$

if $AIFS[AC] < slot \leq CWmax[AC]$, and *0* otherwise.

5.1.3.2.1 Markov Chain Analysis

The access probability functions of the three ACs, and thus the share of capacity per AC can be derived from a Markov model, illustrated in Figure 5.13. It represents the process $s(t)$ of all contending backoff entities of the three considered

[7] More parameters than defined in the 802.11e MAC enhancements are evaluated in this thesis.

priorities. In what follows, this process is referred to as *CSMA regeneration cycle*. The system alternates between states representing idle phases during which the backoff phase is ongoing and a busy phase during which at least one backoff entity transmits a frame. Takagi and Kleinrock (1985) call this a regeneration cycle. Each alternation is a "probabilistic replica" (Takagi and Kleinrock, 1985) of the previous alternation.

Four states "C," "H," "M," and "L," represent the system in the busy phase during ongoing transmissions, and a number of states "1," "2,"..., "CWmax+1" represent the system during the backoff (idle phase). There is one state for each slot of the backoff, beginning with $slot = 1$, which is equivalent to $AIFSN=1$ and thus $AIFS=PIFS = 25\mu s$. According to 802.11e, the earliest time when backoff entities access the channel is one slot after $AIFS$. Thus, the second slot represents the first possible access time $SIFS+2\times aSlotTime$ for backoff entities that operate according to the HCF contention-based channel access, without regard to the individually selected $AIFSN[AC]$ parameter. The access probability per slot of the set of backoff entities of one AC is given by Equation (5.5), The access probability for slots earlier than $AIFSN[AC]$ is 0.

The last slot possible for access is determined by the value of $CWmax+1$; it is calculated as the maximum of all contention window sizes per ACs:

$$CWmax = max\left(CWmax[High], CWmax[Medium], CWmax[Low]\right).$$

Typically, but not necessarily, $CWmax = CWmax[Low]$, since a large value implies a lower priority in channel access. If the backoff entities of one AC operate with a smaller value for $CWmax[AC]$ than given in Equation (5.5), then the access probability for this slot is set to 0. If at least one backoff entity of the AC "High" attempts to transmit by accessing the channel as the first backoff entity, for example by accessing the channel at the first slot, and if no other backoff entity from the other ACs accesses the channel at this slot or earlier, then the system changes from state *slot* (idle) to state "H" (busy). At least one high priority frame exchange is then ongoing. Note that this includes collisions of frames transmitted by backoff entities that belong to this priority "High." The states "M" and "L" represent the busy periods for the ACs "Medium" and "Low," respectively. However, if more than one backoff entity of different ACs start their transmission attempts at the same slot, a collision of frames transmitted by backoff entities that belong to different ACs occurs and the system changes to the state "C." From the four states "C," "H," "M," and "L," the system always transits back to state "1."

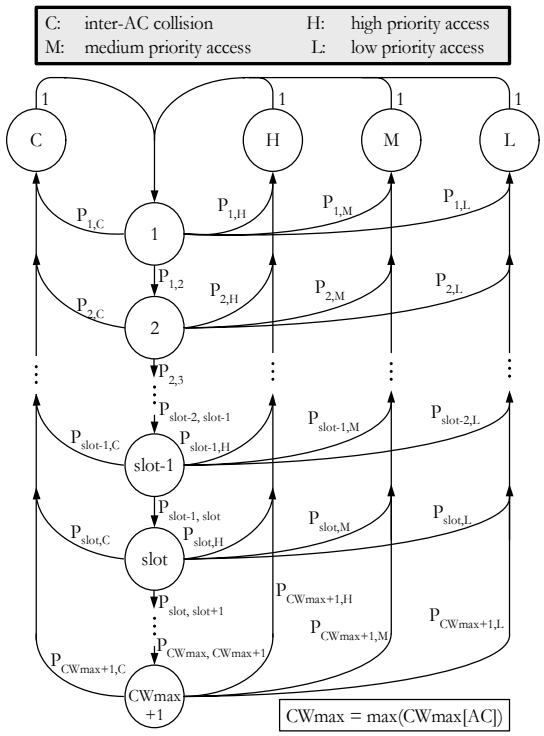

Figure 5.13: State transition diagram for the Markov chain of the CSMA regeneration cycle process. There are states C, H, M, L representing a busy system. There are states 1, 2, 3..., CWmax+1 representing an idle system. Time is progressing in steps of a slot. The state of the chain changes with the state transition probabilities indicated here.

5.1.3.2.2 State Transition Probabilities

Let

$$P\{s(t+1) = AC \mid s(t) = slot\} = P_{slot,AC}, \quad AC \in H, M, L,$$
$$P\{s(t+1) = C \mid s(t) = slot\} = P_{slot,C},$$
$$P\{s(t+1) = slot+1 \mid s(t) = slot\} = P_{slot,slot+1}, \quad slot = 1 \ldots CWmax+1$$

be the transition probabilities as indicated in Figure 5.13, and let

$$\lim_{t\to\infty} P\{s(t) = AC\} = p_{AC}, \quad AC \in H, M, L,$$
$$\lim_{t\to\infty} P\{s(t) = C\} = p_C,$$
$$\lim_{t\to\infty} P\{s(t) = slot\} = p_{slot}, \quad slot = 1 \ldots CWmax+1$$

be the stationary distributions of all states of the backoff process $s(t)$. The transition probabilities in this model can be easily derived from the definitions given earlier in this section. At a particular slot, the probability that the system changes to one of the three states "H," "M," "L" is given by the probability that at least one backoff entity of this AC accesses the channel at this slot, and none of the backoff entities of the other ACs access this same slot:

$$P_{slot,H} = \xi_{slot}[High] \cdot (1 - \xi_{slot}[Medium]) \cdot (1 - \xi_{slot}[Low]),$$
$$P_{slot,M} = \xi_{slot}[Medium] \cdot (1 - \xi_{slot}[High]) \cdot (1 - \xi_{slot}[Low]),$$
$$P_{slot,L} = \xi_{slot}[Low] \cdot (1 - \xi_{slot}[High]) \cdot (1 - \xi_{slot}[Medium]).$$

The probability that at a particular slot, a collision of frames transmitted by backoff entities of different ACs occurs, is given by

$$\begin{aligned} P_{slot,C} = {} & \xi_{slot}[High] \cdot \xi_{slot}[Medium] \cdot (1 - \xi_{slot}[Low]) + \\ & \xi_{slot}[High] \cdot \xi_{slot}[Low] \cdot (1 - \xi_{slot}[Medium]) + \\ & \xi_{slot}[Medium] \cdot \xi_{slot}[Low] \cdot (1 - \xi_{slot}[High]) + \\ & \xi_{slot}[High] \cdot \xi_{slot}[Medium] \cdot \xi_{slot}[Low]. \end{aligned}$$

Finally, the probability that the system changes from one idle slot to the next idle slot state is derived from the probability that no backoff entity attempts to transmit at this slot:

$$P_{slot,slot+1} = \begin{cases} 0, & slot > CWmax \\ 1 - (P_{slot,H} + P_{slot,M} + P_{slot,L} + P_{slot,C}), & else \end{cases}.$$

Note that, depending on the position of the backoff windows, some transition probabilities are *0* for the respective *AC:*

$$(slot < AIFSN[AC]) \, or \, (slot > CWmax[AC]) \Rightarrow P_{slot,AC} = 0 \, .$$

5.1.3.2.3 The Priority Vector

The stationary distributions of the states of the Markov model are not needed to calculate the access priorities of the ACs. Instead, it is sufficient to calculate a vector that determines the transition probabilities per AC to states {C, H, M, L} from a particular idle state {1, 2, ..., CWmax+1}. From the definitions of the stationary distributions, the transition probabilities from state "1" to the states "H," "M," "L," and "C" can be derived. These four transition probabilities define the actual priority in channel access. The stationary distribution of state "H" is given by

$$p_H = \underbrace{\left\{ P_{1,H} + \sum_{slot=2}^{CWmax+1} P_{slot,H} \cdot \prod_{i=1}^{slot-1} P_{i,i+1} \right\}}_{=: \eta[AC=High]} \cdot p_1 =: \eta[AC=High] \cdot p_1 . \qquad (5.6)$$

(this defines the relative priority of the AC "High")

In this equation, a new parameter $\eta[High]$ is defined that determines the relative priority of the AC "High." The stationary distributions of the states "M," "L," and "C" are similarly defined:

$$\begin{aligned} p_M &= \left\{ P_{1,M} + \sum_{slot=2}^{CWmax+1} P_{slot,M} \cdot \prod_{i=1}^{slot-1} P_{i,i+1} \right\} \cdot p_1 =: \eta[Medium] \cdot p_1, \\ p_L &= \left\{ P_{1,L} + \sum_{slot=2}^{CWmax+1} P_{slot,L} \cdot \prod_{i=1}^{slot-1} P_{i,i+1} \right\} \cdot p_1 =: \eta[Low] \cdot p_1, \\ p_C &= \left\{ P_{1,C} + \sum_{slot=2}^{CWmax+1} P_{slot,C} \cdot \prod_{i=1}^{slot-1} P_{i,i+1} \right\} \cdot p_1. \end{aligned} \qquad (5.7)$$

The priority vector η is found as

$$\eta = (\eta_H, \eta_M, \eta_L) = \frac{1}{\sum_{AC} \eta[AC]} \left(\eta[High], \eta[Medium], \eta[Low] \right). \qquad (5.8)$$

The stationary distribution p_1 is given in the following equation as

$$p_1 = p_H + p_M + p_L + p_C .$$

The priority vector η determines the relative priorities of the three ACs. Once the system changes from ongoing transmission to the backoff phase *s(t)*, the system will change to one of the states "H," "M," "L" according to the priority vector η. With the help of the priority vector η, the saturation throughput $Thrp_{share}$ (or the share of capacity) that an arbitrary number of backoff entities of each of the three ACs may achieve when all backoff entities operate in parallel, can be calculated. Any number of backoff entities per AC is possible in this model, and any setup of the EDCF parameters. The achievable saturation throughput $Thrp_{share}$ for the three ACs is approximated by

$$Thrp_{share} = Thrp_{sat} \cdot \eta = \begin{pmatrix} Thrp_{sat}[High] \cdot \eta_H \\ Thrp_{sat}[Medium] \cdot \eta_M \\ Thrp_{sat}[Low] \cdot \eta_L \end{pmatrix}. \qquad (5.9)$$

Equation (5.9) neglects the mutual influences of the ACs to each other the shared operation implies on the individual changes of maximum saturation throughput per AC. This will be discussed in the next section, where the results of the analytical approximations are compared to simulation results for a large number of parameter combinations.

5.1.3.3 Results and Discussion

The example with the three ACs and four backoff entities per AC as defined in Table 5.2, p. 68, and illustrated in Figure 5.11 and Figure 5.12, is used to evaluate the approximation of the saturation throughput $Thrp_{share}$ in a shared scenario. The backoff entities of one of the three ACs are assumed to apply a range of EDCF parameters: the EDCF parameters are changed gradually from the higher to the lower priority such that many different parameter combinations are analyzed. The other two ACs apply always the same EDCF parameters: the backoff entities of the two other ACs are assumed to operate according to the legacy and lower priority EDCF parameter setups. Many different combinations of EDCF parameters and relative priorities can be studied under these assumptions. The definitions of the EDCF parameters of the higher, legacy, and lower priority ACs can be found in Table 5.2. A constant frame body size of *512 byte* for all ACs is selected here, RTS/CTS is not used. Note that the parameters *CWmax* and *RetryCnt* remain constant for all ACs at any time and are not varied.

The following figures show the resulting throughput per AC as a result of simulation and analytical approximation, where a different numbers of backoff entities per AC have been assumed. Figure 5.15 shows the results for the scenarios with four backoff entities per AC, i.e., 12 backoff entities in total. Figure 5.17 shows results for scenarios with 10 backoff entities with variable EDCF parameter setup, 2 legacy priority backoff entities, and 4 lower priority backoff entities. Therefore, 16 backoff entities in total share a common channel in these scenarios.

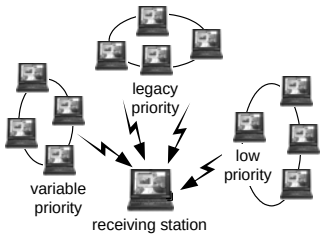

Figure 5.14: Scenario. One backoff entity per station. All stations detect each other. If two or more stations transmit at the same time, a collision occurs.

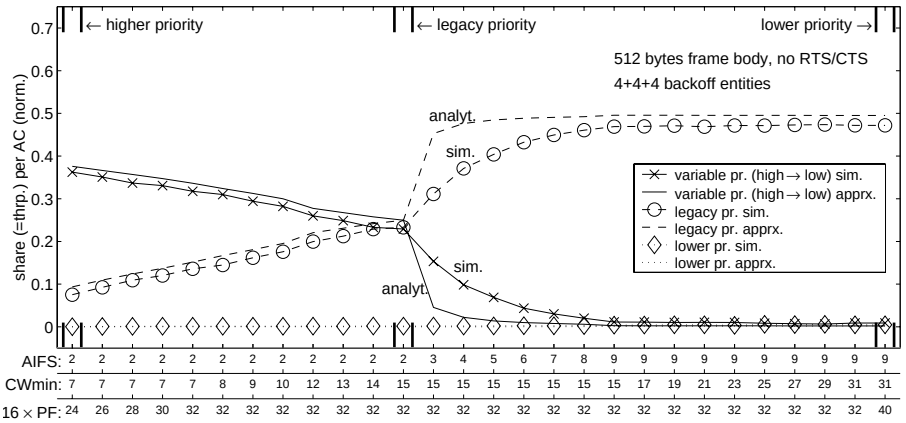

lines w/o markers: analytical approx.; lines with markers: WARP2 sim. results

Figure 5.15: Saturation throughput per AC with 4 backoff entities per AC.

Finally, Figure 5.19 shows results for scenarios with 2 backoff entities with variable EDCF parameter setup, 10 legacy priority backoff entities, and 4 lower priority backoff entities. Hence, 16 backoff entities in total are again assumed here. Figure 5.15 is discussed in the next Section 5.1.3.3.1, Figure 5.17 is discussed in Section 5.1.3.3.2, and Figure 5.19 is discussed in Section 5.1.3.3.3.

5.1.3.3.1 4 Variable Priority Backoff Entities against 4 Legacy and 4 Low Priority Backoff Entities

Figure 5.15 shows simulation and analytical results for 28 parameter combinations, where the EDCF parameters of one AC (used by 4 of 12 backoff entities) are varied from higher (left hand side in the figure) to legacy priority, and down to the lower priority (right hand side in the figure), according to Table 5.2. The scenario is depicted in Figure 5.14.

The other 8 backoff entities of the other ACs operate with legacy and lower priority. It can be seen that the analytical results approximate for all the priorities the simulated results with a sufficient accuracy. This result indicates that the Markov model can be used to sufficiently approximate the backoff process from which the saturation throughput has been calculated.

It can be observed from the left hand side of Figure 5.15 that the AC with the variable priority observes the largest throughput (shares of capacity) in scenarios with higher priority EDCF parameters (*AIFSN=2, CWmin=7, PF=24/16*). However, this share decreases with changed EDCF parameters towards legacy priority. If the 4 backoff entities of the AC with the variable EDCF parameters

operate according to the legacy priority, then the observed share of capacity is the same as for the 4 legacy backoff entities. This is indicated by the simulation results, and confirmed by the analytical approximations (center of Figure 5.15, *AIFSN=2, CWmin=15, PF=32/16*). As expected, when changing the EDCF parameters down to the lower priority, the share of capacity of this AC decreases down towards the share that is observed by the backoff entities of the lower priority AC (right hand side of Figure 5.15, *AIFSN=9, CWmin=31, PF=40/16*). In parallel, the legacy priority backoff entities observe increased shares in theses scenarios. This is an expected result: in these scenarios, the legacy priority AC is parameterized such that the 4 legacy backoff entities access the channel with highest priority relative to the other 8 backoff entities, because those backoff entities all operate with the lower priority EDCF parameters. This again is confirmed by the simulation results as well as the analytical approximations.

5.1.3.3.2 10 Variable Priority Backoff Entities against 2 Legacy and 4 Low Priority Backoff Entities

In contrast to the previous scenario, a different number of backoff entities per AC is assumed in the following, as shown in Figure 5.16. Figure 5.17 shows simulation and analytical results for parameter combinations with 10 backoff entities with variable EDCF parameter setup, 2 legacy priority backoff entities, and 4 lower priority backoff entities, thus, 16 backoff entities operate in parallel here. The observed shares are the same as in the previous scenario from the last section, illustrated in Figure 5.15. The main difference to the previous scenario is that now the backoff entities that slowly reduce their priority from parameter combination to parameter combination (i.e., from the left to the right in the figure), keep their maximum share a longer time (for more parameter combinations).

After some more parameter combinations (left to right), an immediate reduction of throughput share suddenly happens (indicated in the center of the figure).

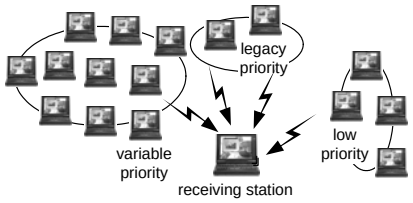

Figure 5.16: Scenario. One backoff entity per station. All stations detect each other. If two or more stations transmit at the same time, a collision occurs.

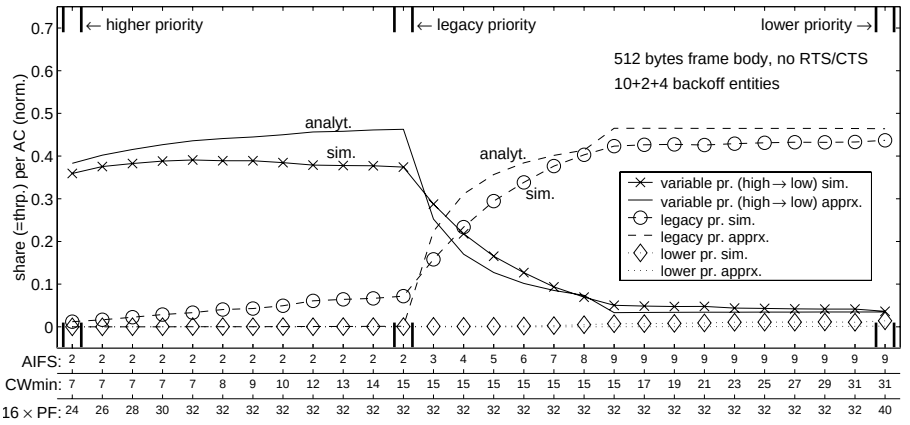

lines w/o markers: analytical approx.; lines with markers: WARP2 sim. results

Figure 5.17: Saturation throughput per AC with 10 backoff entities with varying EDCF parameters, contending with 2 legacy and 4 lower priority backoff entities.

This is an obvious result. The 10 backoff entities are more dominant than the 4 backoff entities of the previous scenario. Note that of course the capacity share per backoff entity in the AC with variable priority is less than before, as 10 instead of 4 backoff entities are operating according to this AC. In contrast, only 2 instead of 4 legacy backoff entities operate in the scenario shown here. Thus, these 2 backoff entities will observe an increased resulting throughput when they operate with higher priority, relative to the other 10+4 backoff entities (towards the right in the figure). As before, the analytical results and the simulation results confirm each other with sufficient accuracy.

5.1.3.3.3 2 Variable Priority Backoff Entities against 10 Legacy and 4 Low Priority Backoff Entities

Figure 5.19 shows results for a scenario with 2 backoff entities with variable EDCF parameter setup, 10 legacy priority backoff entities, and 4 lower priority backoff entities, as illustrated in Figure 5.18. 16 backoff entities in total are assumed as in the last sections. The results are again obvious. Although the 2 variable priority backoff entities operate with highest priority at the beginning (indicated in the left of the figure), they do not observe a considerable share. However, the share per backoff entity is larger for any of the 2 backoff entities than the share observed by any of the 10 legacy backoff entities. It should be emphasized that the analytical results and the simulation results deviate more from each other with such parameter combinations, although the approximations show qualitatively the same shares.

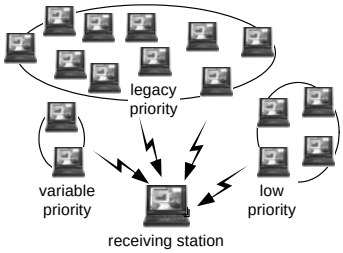

Figure 5.18: Scenario. One backoff entity per station. All stations detect each other. If two or more stations transmit at the same time, a collision occurs.

The analytical results overestimate the share of the legacy stations for the parameter combinations shown in the left hand side of the figure. This is a result of the assumption that the binary exponential backoff of 802.11 can be approximated by the σ-persistent CSMA, even for such a small number of backoff entities. With reduced priority in the more right hand side parameter combinations, the 10 dominating legacy backoff entities obtain the largest throughput and all other backoff entities are suppressed entirely.

5.1.4 QoS Support with EDCF Contending with Legacy DCF

The earliest access time of EDCF backoff entities cannot be smaller than DIFS. Thus, the question arises if EDCF backoff entities do really have a chance to achieve a higher channel access priority than legacy DCF stations.

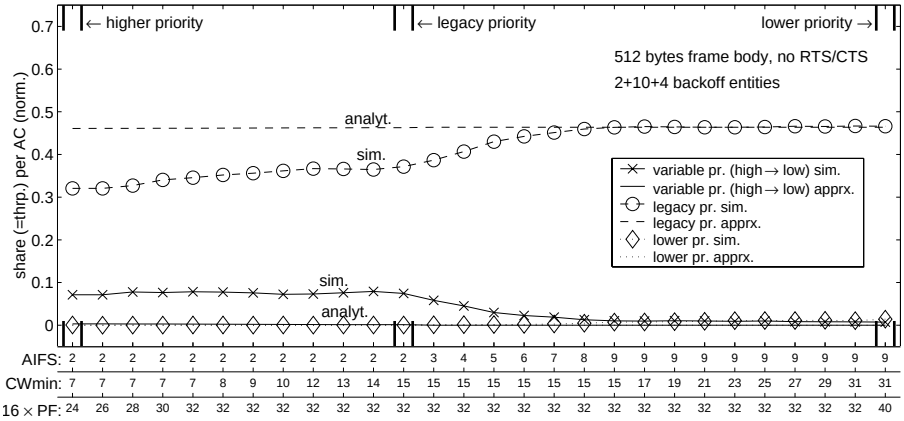

lines w/o markers: analytical approx.; lines with markers: WARP2 sim. results

Figure 5.19: Saturation throughput per AC with 2 backoff entities with varying EDCF parameters, contending with 10 legacy and 4 lower priority backoff entities.

In the following, the resulting throughput for backoff entities of the AC with higher priority (EDCF backoff entities) and with legacy priority (legacy DCF stations[8]) are discussed for different scenarios. It is shown that EDCF backoff entities do not achieve the desired priority over the legacy DCF stations. Two measures to support a better priority over legacy stations are therefore discussed in this context: the PF and the use of EIFS instead of DIFS. Legacy stations can be forced to use EIFS instead of DIFS by using *Frame Check Sequences* (FCSs) that are different from the DCF (Hiertz, 2002). This is one of the concepts used in the context of interworking of different wireless LANs and discussed in detail in Section 6.2.1.2.

Three different scenarios are examined in the following sections. In Section 5.1.4.1, scenarios with one EDCF backoff entity and one legacy DCF station operating in parallel are discussed. In Section 5.1.4.2, the more problematic case when one EDCF backoff entity operates in parallel to multiple legacy DCF stations is discussed. Finally, in Section 5.1.4.3, scenarios with multiple EDCF backoff entities and multiple DCF stations operating in parallel are discussed.

In all simulated scenarios, all stations can detect each other. Hence, there is no hidden station. All frame bodies are *512 byte* long, neither RTS/CTS nor fragmentation is used. Inter-arrival times are negative-exponentially distributed. The 16QAM1/2 PHY mode is used; the radio channel is error free.

5.1.4.1 1 EDCF Backoff Entity Against 1 DCF Station

Figure 5.20 illustrates the scenario and Figure 5.21 shows the resulting throughput per AC vs. the offered traffic per backoff entity (a-c), and the distribution of backoff delay in saturation (d).

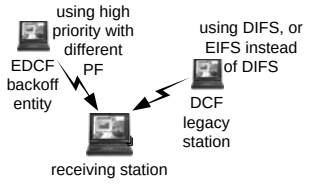

Figure 5.20: Scenario. All stations detect each other. If the two stations transmit at the same time, a collision occurs.

[8] For legacy 802.11, "DCF station" and "DCF backoff entity" can be used as synonym for each other, because there is one backoff entity per station in legacy 802.11.

5.1.4.1.1 Discussion

Figure 5.21(a) shows the results for the standard configuration, where the EDCF backoff entity operates with the higher priority EDCF parameters defined in Table 5.2, but with the persistence factor set as defined in 802.11e, i.e., *PF=2*. *(AIFSN=2*, *CWmin=7*, *CWmax=1023*, *PF=2*, *RetryCounter=7)*. Note that *PF=2* is the only value used in 802.11e, according to draft 4.0 (IEEE 802.11 WG, 2002c). Shown are simulation results and results obtained with the analytical model that is described in the previous section. It can be seen that the EDCF backoff entity achieves a higher throughput than the legacy DCF station, because of the smaller size of the initial contention window, i.e., CWmin.

It is interesting to investigate additional concepts that are not 802.11e conformant, to increase the relative priority of EDCF over legacy DCF. In the following, the influence of the PF and an increase of the interframe space from DIFS to EIFS are evaluated.

Figure 5.21(b) shows the results for scenarios where the EDCF backoff entity operates with the high priority EDCF parameters, now including the PF. The PF is now *1.5* instead of *2*. With only two contending backoff entities, a smaller PF is not helpful, as the number of collisions is relatively small. Thus, the results in Figure 5.21(b) do not significantly diverge from the results in Figure 5.21(a). With a small number of collisions, the influence of the PF on the achievable throughput is negligible. Figure 5.21(c) shows the results for scenarios where the legacy DCF station is forced to operate with EIFS instead of DIFS all the time. Now, the priority of the EDCF backoff entity is clearly visible, thanks to the increased interframe space used by the legacy DCF station.

The analytical results in Figure 5.21(a-c) deviate from the simulation results because of the used assumption that the access probability per slot is geometrically distributed. This is not the case with one backoff entity per AC. With one backoff entity per AC, the access probability per slot is uniformly distributed. However, the analytical results show at least the same characteristics of the saturation throughput per AC relative to each other. The analytical model described in the previous section gives the saturation throughput per AC in a shared scenario, which is here the throughput per backoff entity when the offered traffic is high (overload scenario). Instead of illustrating the results as one single point in the figure, they are indicated as maximum achievable throughput when the offered traffic is increased (indicated as line).

Figure 5.21(d) illustrates the *Complementary Cumulative Distribution Functions* (CCDFs) of the backoff delay for all three scenarios. The EDCF backoff entity

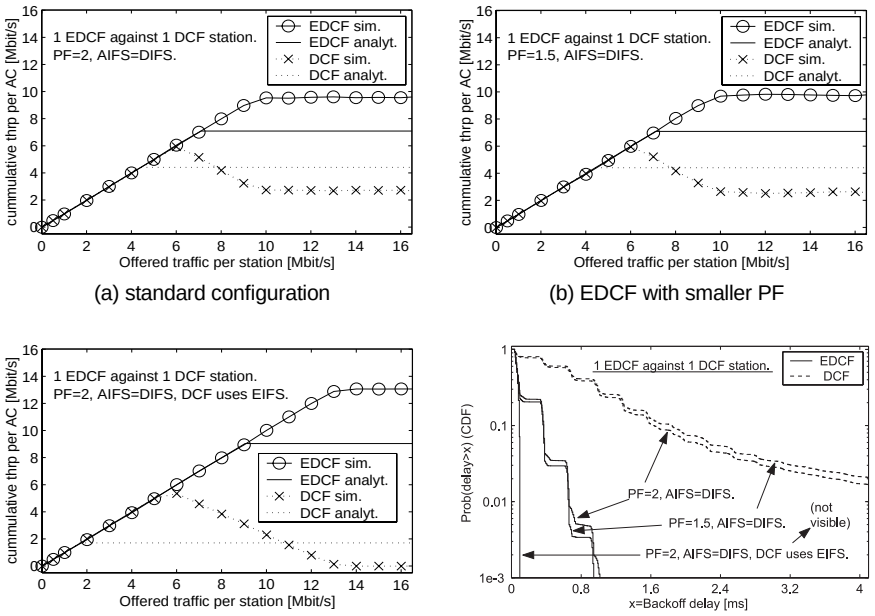

(a) standard configuration

(b) EDCF with smaller PF

(c) DCF with extended interframe space

(d) backoff delays in saturation (simulation results)

lines w/o markers: analytical results (a-c), lines with markers: WARP2 simulation results

Figure 5.21: Throughput and backoff delay results for one EDCF backoff entity contending with one legacy DCF station. The analytical results give the saturation throughput per AC only, which is here and in the following figures of this section indicated as maximum achievable throughput when the offered traffic is increased.

observes always a smaller backoff delay than the legacy DCF station. It can be further observed that in the last scenario, where the legacy DCF station uses EIFS instead of DIFS, the EDCF backoff entity observes significantly smaller backoff delays.

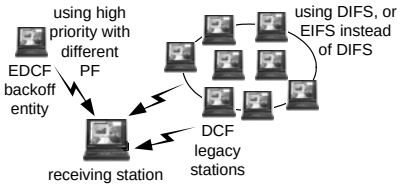

Figure 5.22: Scenario. All stations detect each other. If two or more stations transmit at the same time, a collision occurs.

5.1.4.1.2 Summary

The results can be summarized as follows. The PF is not a helpful measure to increase the priority of EDCF over legacy DCF, as long as a small number of backoff entities operate at the same time, i.e., as long as the collision probability is relatively small. However, the priority of EDCF over legacy DCF is significantly improved by forcing the legacy DCF station to operate with EIFS instead of DIFS.

5.1.4.2 1 EDCF Backoff Entity Against 8 DCF Stations

Figure 5.22 illustrates the scenario where the EDCF backoff entity now operates in parallel to 8 legacy DCF stations. As before, Figure 5.23 shows the resulting throughput per AC vs. offered traffic per backoff entity (a-c), and the distribution of backoff delays in saturation (d).

5.1.4.2.1 Discussion

The PF and the interframe spaces are used similarly to the previous scenarios. Figure 5.23(a) shows the results for the standard configuration with *PF=2*. Figure 5.23(b) shows the results for scenarios where the EDCF backoff entity operates with *PF=1.5*. Figure 5.23(c) shows the results for scenarios where all 8 legacy DCF stations operate with EIFS instead of DIFS at any time. Finally, as before, Figure 5.23(d) illustrates the CCDFs of the backoff delays for the three scenarios.

It can be observed from Figure 5.23(a) that in contention with 8 instead of 1 legacy DCF station, the achievable saturation throughput for the EDCF backoff entity with standard configuration is considerably lower than in contention with 1 legacy DCF station.

However, the single EDCF backoff entity is still achieving a higher throughput than a single legacy DCF station (the total sum of the results of all 8 legacy DCF stations are shown in the figure), but this throughput is lower than what was achieved before, when contending against 1 legacy DCF station (see Figure 5.23(a) and Figure 5.21(a)). Figure 5.23(b) shows the results for scenarios where the EDCF backoff entity operates with the high priority EDCF parameters, now including *PF=1.5*. This has now more impact than before, as there are more contending backoff entities in total, and the number of collisions is higher. Thus, Figure 5.23(b) indicates saturation throughput improvements for the EDCF backoff entity as a result of the usage of the smaller PF. However, comparing Figure 5.23(b) with Figure 5.21(b), it can be seen that the 8 legacy DCF stations still have an undesirable effect on the throughput results for the single EDCF backoff entity.

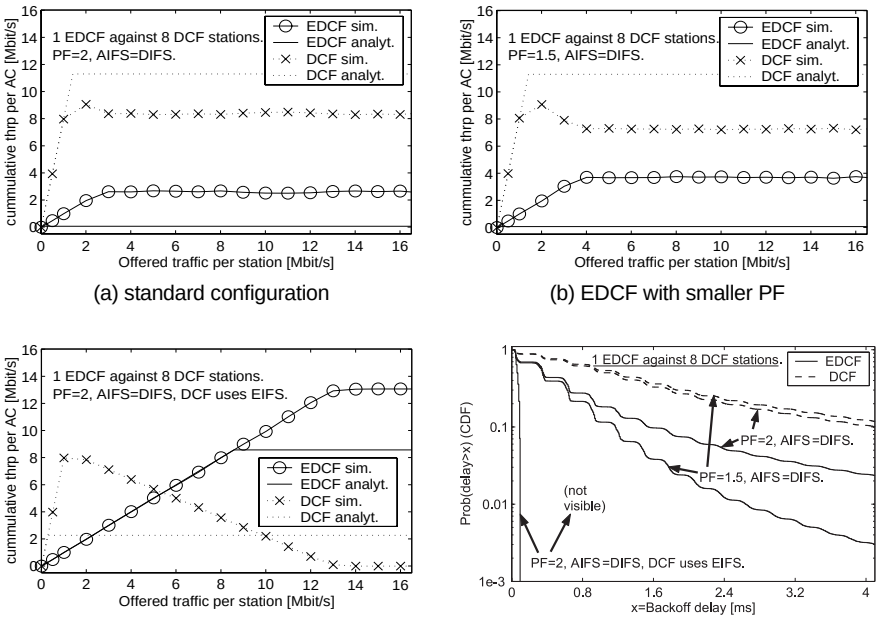

(a) standard configuration

(b) EDCF with smaller PF

(c) DCF with extended interframe space

(d) backoff delays in saturation (simulation results)

lines w/o markers: analytical results (a-c), lines with markers: WARP2 simulation results

Figure 5.23: Throughput and backoff delay results for one EDCF backoff entity contending with eight legacy DCF stations.

A clear priority over the 8 legacy DCF stations can be achieved only by forcing the 8 legacy DCF stations to operate with EIFS instead of DIFS all the time, as can be seen in Figure 5.23(c). As before, the analytical results in Figure 5.23(a-c) show only the same trends as the simulation results due to the assumption of geometrically distributed access probabilities per slot.

Figure 5.23(d) illustrates the CCDFs of the backoff delays for all three scenarios. The delays are in general larger than before, due to the higher number of backoff entities. As before, when the legacy DCF stations use EIFS instead of DIFS, the EDCF backoff entity observes very small backoff delays.

5.1.4.2.2 Summary

The results can be summarized as follows. The achievable saturation throughput of an EDCF backoff entity in contention with legacy DCF stations depends considerably on the number of legacy DCF stations that operate in parallel.

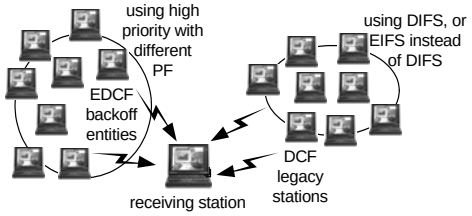

Figure 5.24: Scenario. All stations detect each other. If two or more stations transmit at the same time, a collision occurs.

The higher the number of legacy DCF stations, the lower is the achievable saturation throughput of the EDCF backoff entity. When operating in parallel to many legacy DCF stations, a smaller PF is helpful to increase the priority of EDCF over legacy DCF. In addition, the priority of EDCF over legacy DCF is significantly improved by forcing the legacy DCF station to operate with EIFS instead of DIFS.

5.1.4.3 8 EDCF Backoff Entities Against 8 DCF Stations

Figure 5.24 illustrates the scenario and Figure 5.25 shows the resulting throughput per AC vs. the offered traffic per backoff entity (a-c), and the distribution of backoff delays in saturation (d).

5.1.4.3.1 Discussion

The PF and the interframe spaces are used similarly to the previous scenarios. It can be observed from Figure 5.25(a) that 8 EDCF backoff entities in total achieve a higher priority over 8 legacy DCF station than a single EDCF backoff entity. With an increased offered traffic, the influence of the PF becomes even more significant, as can be seen in Figure 5.25(b).

A clear priority of the 8 EDCF backoff entities over the 8 legacy DCF stations can be again achieved by forcing the 8 legacy DCF stations to operate with EIFS instead of DIFS, as can be seen in Figure 5.25(c). The analytical results in Figure 5.25(a-c) conform more precisely than before to the simulation results, because the assumption of geometrically distributed access probabilities per slot is more accurate with a larger number of backoff entities. Figure 5.25(d) illustrates the CCDFs of the backoff delay for all three scenarios. The delay increases again, since the number of contending backoff entities is now 16 in total. It must be highlighted that, when the legacy DCF stations use EIFS instead of DIFS, the 8 EDCF backoff entities now observe an increased backoff delay as well. The reason for this is as follows. Transmissions by EDCF backoff entities may collide more often than before because of the small contention window size.

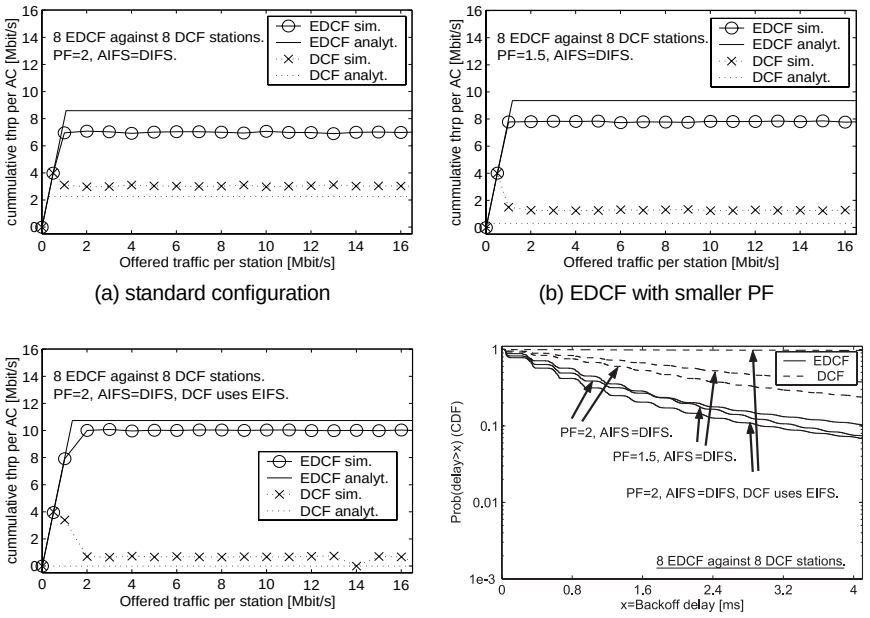

(a) standard configuration

(b) EDCF with smaller PF

(c) DCF with extended interframe space

(d) backoff delays in saturation (simulation results)

lines w/o markers: analytical results (a-c), lines with markers: WARP2 simulation results

Figure 5.25: Throughput and backoff delay results for eight EDCF backoff entities contending with eight legacy DCF stations.

Therefore, the EDCF backoff entities have to use higher backoff stages, and more retransmissions. With higher backoff stages used by the EDCF backoff entities, there is a smaller influence of the legacy DCF stations using EIFS instead of DIFS.

5.1.4.3.2 Summary

The results can be summarized as follows. The achievable saturation throughput of a number of EDCF backoff entities in contention with legacy DCF stations is supported with a smaller PF. As before, when operating in parallel to many legacy DCF stations, a smaller PF is helpful to increase the priority of EDCF over legacy DCF. In addition, the priority of EDCF over legacy DCF is improved by forcing legacy DCF stations to operate with EIFS instead of DIFS. Because of the small initial contention window size in the EDCF, collisions occur more often for transmissions initiated by EDCF backoff entities, which increases the resulting backoff delays even when the legacy DCF stations operate with EIFS instead of DIFS.

5.2 Contention Free Bursts

This section is based on Mangold et al. (2002d). Here, fairness problems between QBSSs are discussed that exist when coexisting, overlapping QBSSs share the radio channel. By applying a new 802.11e mechanism, called *Contention Free Bursts* (CFBs), it is shown that wireless LANs gain from intelligent radio resource control in a fair manner.

A simple radio resource control scheme based on the dynamic selection of PHY modes is introduced in the next section. The combination of this scheme with CFBs, and the gain of spectrum efficiency when using this combination are discussed in the following sections.

5.2.1 Contention Free Bursts and Link Adaptation

The CFB concept is defined in 802.11e and described in detail in Section 4.2.5, p. 54.

Link Adaptation (LA) is the process of dynamically selecting a combination of PHY modes for the transmission of frames, under certain conditions such as the channel error probability, and required QoS. For example, the throughput optimization in the 802.11a wireless LAN via LA is presented in Qiao and Choi (2001).

For the analysis in this section, a simple open loop LA process is used, which counts the number of successful and failed transmissions and switches the PHY mode after a certain number of transmission successes or failures. A transmitting station that carries data for more than one station selects the PHY mode with respect to the addressed receiving station. Such a station is typically the AP. It has to alternate the PHY mode from frame exchange sequence to frame exchange sequence with high dynamics. Applying this simple LA process, a station ends up transmitting with the PHY mode that optimizes the throughput, by periodically attempting to increase it. This attempt occurs after 25 successful transmissions. This may then lead to higher probability of failed transmissions, which means that the station has to fall back to the original PHY mode, here after 4 unsuccessful transmission attempts. Finding an optimal algorithm for LA is beyond the scope of this discussion. The used algorithm is limited but allows to investigate the combination of CFBs with the radio resource control, i.e., with LA.

In principle, a frame can be transmitted with an individually optimized PHY mode, but in case of control frames under the following restriction. The 802.11a standard defines mandatory PHY modes, i.e., *6, 12,* and *24 Mbit/s*, which every 802.11 station must be able to operate with. As control frames (e.g.,

RTS/CTS/ACK) should be received not only by the addressed station but also by other active stations in the area close to the transmitting and receiving station, they must be transmitted using one of the mandatory PHY modes.

By applying dynamic LA, a station can select the optimal PHY mode in order to use the radio spectrum more efficiently. The duration of a frame exchange can be minimized when using dynamic LA. When CFBs are used in addition, the station may be able to transmit more MPDUs per TXOP. The advantages of the combination of LA and CFBs are discussed in the following.

5.2.2 Simulation Scenario: two Overlapping QBSSs

Event-driven stochastic simulation is used for the analysis of CFBs. Figure 5.26 shows the scenario of two overlapping QBSSs with three stations in each QBSS. The two stations 2.1 and 1.1 are HCs, which deliver MSDUs to the other stations. Each HC generates the same mix of offered traffic of three data streams per station.

The three data streams are labeled with *"high"*, *"medium"*, and *"low"*, according to their priorities. The HC 1.1 transmits three data streams to station 1.2 and three data streams to station 1.3; the HC 2.1 transmits three data streams to station 2.2 and three data streams to station 2.3.

At the high priority AC, MSDUs of *80 byte* are transmitted. The negative-exponentially distributed inter-arrival time has a mean of *2.5 ms* for the offered traffic of *256 kbit/s*. The high priority streams offer *256 kbit/s* per stream throughout all simulation campaigns. The medium and low priority streams each transmit MSDUs of *1514 byte* with negative-exponentially distributed inter-arrival times, each stream with variable rates.

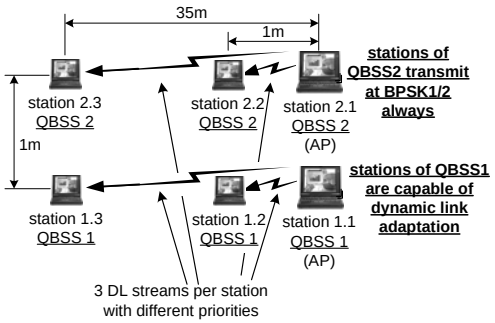

Figure 5.26: Simulation scenario. The two larger stations are the HCs that deliver MSDUs with three different priorities to their associated stations. All stations are in range to each other (no hidden stations).

Table 5.3: EDCF parameters Used for three ACs.

AC(priority):	High	Medium	Low
AIFSN [AC]:	*2*	*4*	*5*
AIFS[AC]:	*34μs*	*52μs*	*61μs*
CWmin [AC]:	*7*	*10*	*15*
CWmax [AC]:	*7*	*31*	*255*

Table 5.3 shows the EDCF-parameters chosen for the three priorities. Because of the overlapping QBSS coexistence scenario, station *1.1* and *2.1* do not make use of their highest priority as an HC in accessing the channel, but rely on a prioritized random backoff as part of the EDCF to avoid collisions of transmitted frames.

Distances between stations are chosen in a way that all stations are able to detect all transmissions by other stations. No station is hidden to another one. A radio channel error model as described in Appendix C is used. This error model was developed in Qiao and Choi (2000) and evaluated in Mangold et al. (2001f). With a path loss coefficient $\gamma=3.5$ and constant transmission power of *200mW*, PHY mode 64QAM3/4 (*=54 Mbit/s*) for the stations close to the HCs (*1 m*) and the PHY mode 3 (*=12 Mbit/s*) for the stations far from the HCs (*35 m*) are the best combinations to optimize the throughput.

The offered traffic in the simulated scenarios includes three streams with different priorities from the two HCs to each of their associated stations.

Only HC 1.1 of QBSS *1* is capable of operating with LA. The PHY modes of control frames are sent at *6 Mbit/s* all the time. The stations of QBSS *2* always transmit data frames and control frames at *6 Mbit/s*.

Channel errors are rare with the selected PHY modes. The stations at larger distances (*35 m*) have an error probability at the channel similar to the stations close to the HCs (*1 m*). For this reason, the throughput results given in the following figures are shown as throughput per priority stream, where for each QBSS the stream to the close station and the stream to the far station are averaged, without loss of relevant information. Hence, there are three resulting throughputs for each QBSS, i.e., one per priority class.

5.2.3 Throughput Results with CFBs

5.2.3.1 Throughput Results with Static PHY mode 1

The resulting throughput when all stations transmit at *6 Mbit/s*, i.e., PHY mode *1*, without operating with CFBs, is shown in Figure 5.27, left (left subfigure). Here,

QBSS *1* does not apply dynamic LA; therefore, both QBSSs show equal throughput results. The offered traffic is varied for the medium priority and low priority streams. The offered traffic of the four high priority streams stays at *256 kbit/s* per stream, which can be carried by the two QBSSs at any time. As expected, the low priority streams suffer from the increased offers at medium priority. Note that in the figures the throughput between the station near to the AP and the station far from the AP is shown as an average throughput.

5.2.3.2 Unwanted Throughput Results with LA used in one QBSS, without CFBs

An interesting observation can be taken from Figure 5.27, left (right subfigure). In contrast to before, now QBSS *1* is applying LA. Although only QBSS *1* is applying LA, both QBSSs gain from it. The improved throughput of the medium priority streams within QBSS *2* even exceeds the resulting throughput of the QBSS *1*. The reason for this is as follows. Because of the simplicity of the applied algorithm for LA, the HC in QBSS *1* attempts to transmit to its far station at higher PHY modes than *6 Mbit/s* from time to time. After a number of failed transmissions, it switches back towards the basic mode, before trying again to increase the PHY mode. This reduces the throughput of the medium and low priority streams in QBSS *1* compared to QBSS *2*. Interestingly, the throughput is still improved compared to static PHY mode *1*. For the transmissions to the closer station, the HC of QBSS *1* switches to *54 Mbit/s* and then transmits very efficiently with a small number of errors. As transmissions at this PHY mode require short times, the radio resources are efficiently utilized. However, both QBSSs can improve their resulting throughput performance. The probability that station *1.1* or station *2.1* wins the contention is still the same.

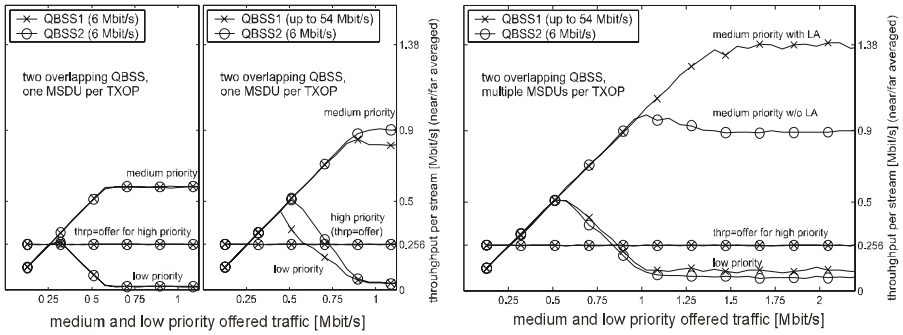

Left: all *6 Mbit/s*. Right: LA in QBSS *1*. LA applied in QBSS *1*. CFBs in both QBSSs.

Figure 5.27: Resulting throughput vs. offered traffic. Left: without CFBs, right: with CFBs.

The fact that QBSS *2* gains from dynamic LA that is applied in QBSS *1* is an undesirable result. There is no motivation to apply spectrum efficient and complicated techniques if the gain from such an effort is shared between coexisting wireless LANs. From the regulatory perspective, radio systems that operate spectrum efficiently must benefit from it. To attract vendors to implement dynamic LA or other radio resource control schemes into their radio systems, other co-located radio systems should not gain equally from its usage.

This problem is known as the "tragedy of commons" in game theory and especially important for radio systems that share unlicensed bands (Salgado-Galicia et al., 1997).

5.2.3.3 Throughput Results with Link Adaptation applied in one QBSS and CFBs applied in both QBSSs

Figure 5.27, right, shows the resulting throughput when CFBs are used by both QBSSs. QBSS *1* is capable of applying dynamic LA. Now the throughput of the medium priority streams in QBSS *1* exceeds the throughput of the medium priority streams in QBSS *2*. The reason is obvious: after a short transmission of an MSDU, the HC of QBSS *1* is allowed to deliver another MSDU without contending for the access to the channel again, as long as the TXOPlimit is not exceeded (here, *TXOPlimit=2.88 ms)*. Therefore, it is now mainly QBSS *1* that notably improves its performance by applying dynamic LA, compared to the previous scenario. The QBSS *1* improves its performance by efficiently utilizing a given TXOP because of transmitting frames at *54 Mbit/s* when possible.

5.2.4 Delay Results with CFBs

Figure 5.28 (a) and (b) show the MSDU Delivery delay distributions for both QBSSs in a lightly loaded scenario, i.e., *320 kbit/s* for medium and low priority streams, *256 kbit/s* for high priority streams. In each figure, the results for one QBSS are shown, where two *Complementary Cumulative Distribution Functions* (CCDFs) per priority class are given, one for the near station and one for the far station, respectively. It is visible that the LA within QBSS *1* results in considerable shorter minimum MSDU Delivery delays than in QBSS *2*.

Due to the higher error probability with the higher PHY modes, retransmissions are more likely in QBSS *1*. This is the reason for the higher probability of larger delays in QBSS *1*. The near and far stations show different delays in QBSS *1* due to different PHY modes. Figure 5.28 (c) and (d) present the delays when CFBs are applied. It is visible that in a lightly loaded scenario, CFBs have minor impacts on the MSDU Delivery delay.

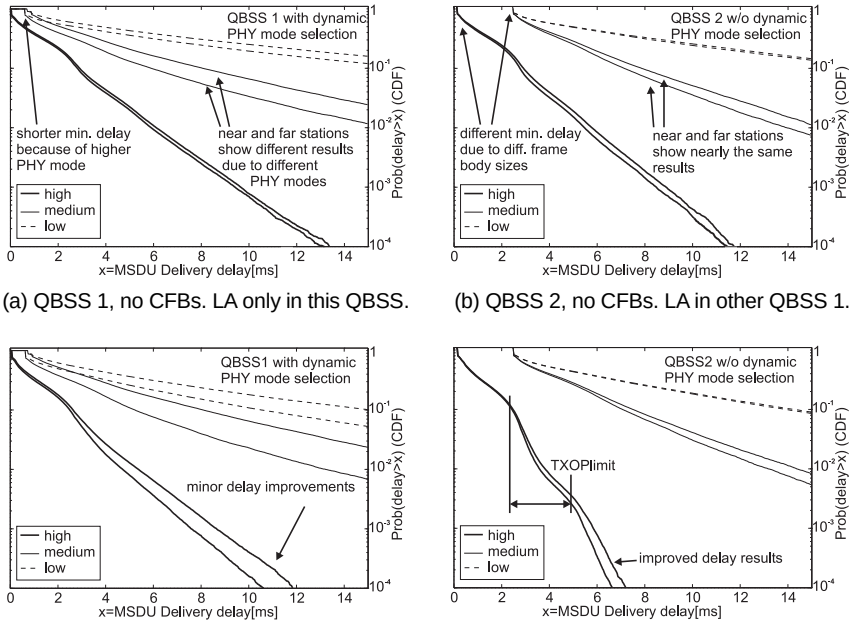

(a) QBSS 1, no CFBs. LA only in this QBSS.

(b) QBSS 2, no CFBs. LA in other QBSS 1.

(c) QBSS 1, CFBs in both QBSSs. LA in this QBSS.

(d) QBSS 2, CFBs in both QBSSs. LA in other QBSS 1.

Figure 5.28: MSDU Delivery delays. Left: QBSS *1*, Right: QBSS *2*.

As before, QBSS *1* always shows smaller delays than QBSS *2*, as the transmission times in QBSS *1* are reduced with the higher PHY modes. Figure 5.28 (d) indicates that QBSS *1* fills its TXOPs often up to the TXOPlimit of *2.88 ms*, which is the reason for the shape of the curve of the high priority streams within QBSS *2*.

5.2.5 Conclusion

The concept of CFBs is an attractive element of IEEE 802.11e in terms of spectrum efficiency, and economy. In overlapping QBSS coexistence scenarios, a wireless LAN takes advantage of applying dynamic link adaptation when CFBs are used. A wireless LAN that uses CFBs can improve its performance compared to other wireless LANs that operate without CFBs. With CFBs, future wireless LANs will apply dynamic link adaptation in order to achieve an higher throughput. Without CFBs, future wireless LANs will not necessarily apply dynamic link adaptation. Without CFBs, coexisting wireless LANs achieve the same throughput results. The use of the CFB mechanism motivates for the application of link adaptation, which as a result increases the spectrum efficiency of radio systems in the unlicensed 5 GHz band.

5.3 Radio Resource Capture

This section is based on Mangold et al. (2002c). Stations that are hidden to each other operate simultaneously, without mutually synchronized transmission, contention and CCA procedures. The contention-based channel access works only efficiently if all stations are in detection range of each other. There, if the channel gets idle at a specific point in time, the CCA processes of all stations indicate the channel idle. Then, stations will start their backoff procedures synchronously, and the backoff entity that first counts down its backoff counter determines the station which transmits next. The other backoff entities will defer from channel access. If this synchronized contention for channel access is not maintained owing to hidden stations, some stations may capture the radio channel for long time durations. This leads to problems in QoS support, as discussed in the following, where two scenarios are discussed. Note that the resource capture phenomenon exists with or without the 802.11e MAC enhancement.

5.3.1 Radio Resource Capture by Hidden Stations

The resource capture by hidden stations was identified in Benveniste (2001; 2002), and there referred to as neighborhood capture. A station that is located in the detection range of other stations that are hidden to each other can only initiate a transmission if all of the hidden stations are idle.

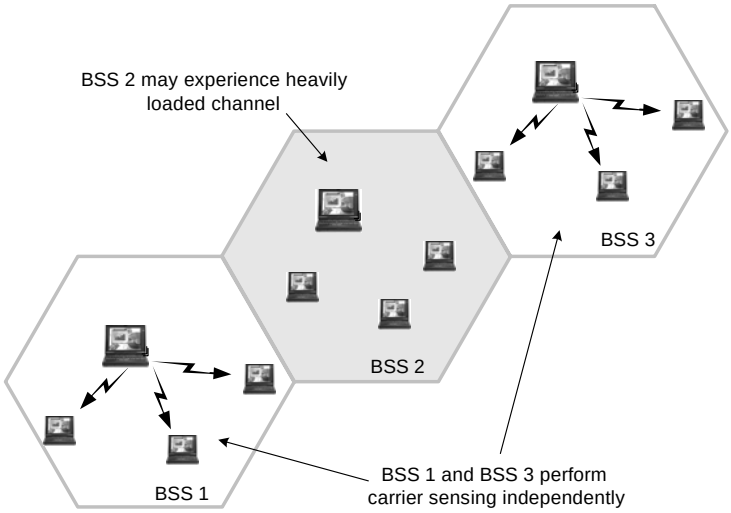

Figure 5.29: Scenario where two (Q)BSSs that are not in receive range of each other (BSS *1* and BSS *2*) perform their CCA independently. Stations of (Q)BSS *2* may not detect an idle channel for undesirable long periods.

However, this is usually not the case, especially at times of high traffic load. See Figure 5.29 for an illustration of this problem. Three BSSs are shown, where each BSS can only detect transmissions of its respective neighbor BSSs. BSS *1* and BSS *3* are hidden to each other. Hence, BSS *1* and BSS *3* can independently operate at the same time and are uncoordinated without synchronized channel access. Once a station of BSS *1* started a frame exchange, stations of BSS *2* will defer from channel access. However, this implies that a station of BSS *3*, which does not detect the ongoing frame exchange in BSS *1*, starts its frame exchanges independently during the ongoing frame exchange. This can continue with any following frame exchange as long as BSS *1* and BSS *3* have data to deliver. As a result, the stations of BSS *2* may not be able to transmit for longer time durations, and the channel is captured by stations in the neighborhood of BSS *2*. This leads to increased MSDU Delivery delays and reduced throughput in BSS *2*.

5.3.2 Radio Resource Capture through Channels that Partially Overlap in the Spectrum

Similarly, the same capture effect can occur also when frequency channels overlap in the frequency domain. See Figure 5.30 for an illustration of this problem. Now all stations are in close vicinity to each other such that any transmission is detected by any station, across all BSSs. However, it is here assumed that every BSS operates at a different frequency channel, as indicated in Figure 5.30. This implies that the three BSSs can operate without mutually interfering each other, as long as the used frequency channels are orthogonal, i.e. as long as frequency channels do not overlap in the frequency domain. When frequency channels overlap, the same resource capture as described in the last section may occur. In the example of Figure 5.30, stations of BSS *1* operating at channel *2* and stations of BSS *3* operating at channel *4* can initiate frame exchanges without mutual interference. The two BSSs can operate independently. The BSS *2* operates on channel *3*, which overlaps with the two other channels. Therefore, the CCA processes of all stations in BSS *2* may not find an idle channel for longer time durations, for the same reason as explained in the last section. Note that overlapping frequency channels are not standardized for the 5 GHz band.

5.3.3 Solution

To reduce the unwanted effects of the resource capture, Benveniste (2001) proposes an efficient and simple solution based on synchronous time division, here referred to as slotting. In the following, a way to introduce such a slotting in 802.11(e) is presented.

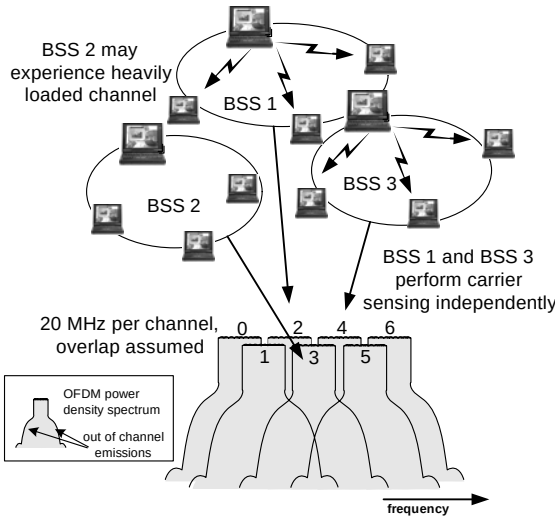

Figure 5.30: Resource capture with frequency channels that overlap in the frequency domain. As before, stations of (Q)BSS *2* may not detect an idle channel for undesirable long periods.

5.3.3.1 Mutual Synchronization across QBSSs and Slotting

Two modifications of the 802.11e protocols are required to enable coexisting QBSSs or coexisting IBSSs to synchronize the access. Figure 5.31 illustrates the two modifications. One is that beacons must be transmitted in contention by all stations of a QBSS, as is the case in an IBSS. Stations that are associated to an HC also must transmit the beacon. It is not necessary for such stations to deliver all information an HC usually transmits with its beacon. For the purpose of synchronization of neighbored BSSs, only the TSF information is required.

The second modification to the standard is that all stations, regardless of whether they are an AP or a station of a QBSS or IBSS, must update their timers according to the rules of the IBSS. Exactly this will guarantee the synchronization of neighbored BSSs. By applying these two modifications in 802.11, overlapping QBSSs are mutually synchronized without loosing any functionality of the protocol. Synchronous time division, i.e., slotting, is possible by defining a slot dwell time. With a slot dwell time, frame exchanges of a BSS are allowed to start only if they can be finished before the end of the respective slot, i.e., without exceeding the slot dwell time. After expiry of a slot dwell time, stations of the BSSs contend for the next frame exchange in parallel. Because the slot dwell times are synchronized, all stations of all BSSs content at the same time, which provides a fair ac-

cess. As a result, the channel cannot be captured for time durations longer than a slot duration. In the simulation discussed in the following, a slot duration of *4 Time Units* (TUs), i.e., *4.096 ms*, is used. An immediate drawback of the slotting is the throughput degradation in each BSS. To mitigate this, it is here proposed to apply CFBs as explained in the next section.

5.3.4 Evaluation

A symmetric scenario is selected to investigate the effects of slotting and CFBs in 802.11e. A circle of *12* stations forms a QBSS where all stations operate according to EDCF, see Figure 5.32. All frames are transmitted with the *12 Mbit/s* PHY mode. Each station generates the same offered traffic comprising three single hop data streams, labeled as high, medium and low, according to their priorities.

By means of these streams, stations deliver MSDUs with three different priorities to one direct neighbor station, and also receive three streams from the other neighbor station. In total, $12 \cdot 3 = 36$ data streams are simulated. All MSDUs arrive with negative-exponentially distributed inter-arrival times.

The three priorities are always offered the same traffic. At the different backoff entities in the simulated system model, MSDUs with a size of either *600 byte* or *128 byte* arrive such that the queues are always full. Another traffic load is derived from an Ethernet traffic trace file that offers *1 Mbit/s* with typical Ethernet frame sizes of up to *1514 byte* as traffic source for each data stream.

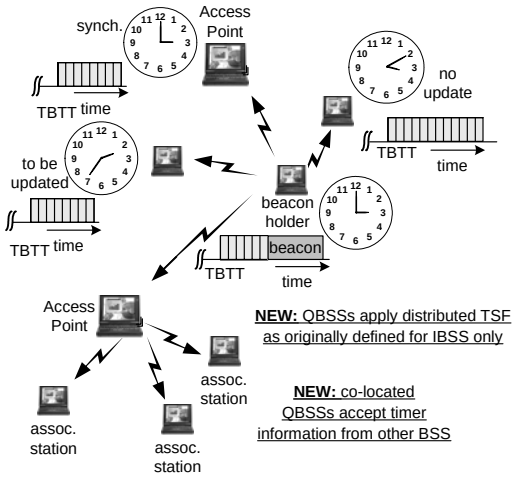

Figure 5.31: Two modifications in 802.11e to allow mutual synchronization for the reduction of the radio resource capture and to support multi-hop traffic.

Table 5.4 shows the relevant EDCF parameters selected for the three priority classes, summarizing the parameters that are mainly used. RTS/CTS is used for MSDUs larger than *512 byte*. MSDUs are delivered in single *MAC Protocol Data Units* (MPDUs), i.e., MSDUs are not fragmented. The TXOPlimit is larger than the slot dwell time.

5.3.4.1 Simulation Results and Discussion

The three simulated protocol configurations are the standard configuration labeled "*with (resource) capture*" being the protocol specified in the standard, the slotted configuration labeled "*slotted*," and the slotted configuration with CFBs, labeled "*bursted*." Table 5.5 presents the maximum achievable throughput for a load, where one station transmits to its neighbor and all other stations remain idle. Thus, no collisions occur at the radio channel. The results are given for the three configurations and three different types of traffic load. It can be seen that slotting reduces the throughput compared to non-slotting, whereas the CFBs has a better throughput. For shorter frame body sizes, CFB achieves even the highest throughput.

Table 5.6 shows the maximum achievable throughput in the hidden station scenario of Figure 5.32. It can be seen how severe the throughput is degraded in 802.11 by hidden stations without using slots plus CFBs.

Figure 5.33 (a) and (b) show the resulting backoff delays for the three ACs as CCDF. Here the MPDU frame body size is *600 byte*. All stations together are evaluated, as the scenario is symmetric. The advantage of the slotting is clearly visible. For all ACs, the backoff times are reduced. As expected, CFBs increase the delay compared to slotting. The shapes of the curves in both figures are modulated by the slotting with a duration of *4.096 ms*.

Figure 5.33 (c) and (d) show the resulting backoff delay for the Ethernet traffic trace files. Here, the positive effect of the slotting is again visible, although the advantage is not as high as before. In general, the longer the MPDUs, the more probable are channel captures, and thus, the more efficient is the slotting.

Table 5.4: Used EDCF parameters for the three ACs.

AC (priority):	high, AC6	medium, AC5	low, AC0
AIFS[AC]:	*34µs*	*34µs*	*34µs*
CWmin[AC]:	*7*	*14*	*15*
CWmax[AC]:	*127*	*175*	*255*
PF[AC]:	*2*	*2*	*2*

Table 5.5: Achievable throughput (all ACs) with two isolated stations [kbit/s].

frame body size:	600 byte	200 byte	Ethernet trace
with resource capture*:	*7153.5*	*4213.7*	*=load (1Mbit/s)*
slotted:	*6831.8*	*2998.2*	*= load (1Mbit/s)*
bursted:	*6977.9*	*4987.1*	*= load (1Mbit/s)*

*) although labeled as "with capture," captures do not occur here, as this is an isolated scenario where no hidden stations exist.

Table 5.6: Max. achievable throughput saturation throughput (all ACs) [kbit/s].

frame body size:	600 byte	200 byte	Ethernet trace
with resource capture:	*236.1*	*162.4*	*220.3*
slotted:	*232.2*	*160.3*	*205.6*
bursted:	*285.0*	*201.1*	*267.8*

5.3.4.2 Conclusion

The results indicate that resource channel capture by coexisting BSSs can be efficiently reduced when applying the slotting scheme as described in Benveniste (2001) together with CFBs. This modified protocol may especially have a potential for multi-hop communication and the efficient forwarding of MSDUs across multiple (Q)BSSs under QoS constraints.

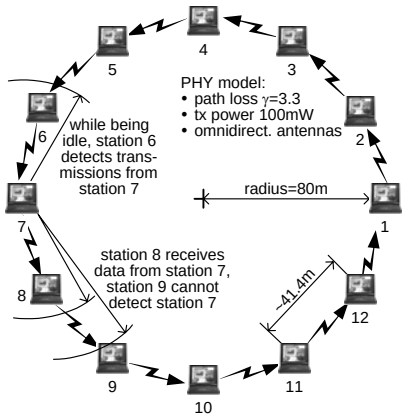

Figure 5.32: Symmetric hidden station scenario. Each station detects its two neighbors. Each station carries three parallel streams of data with high, medium, low priority.

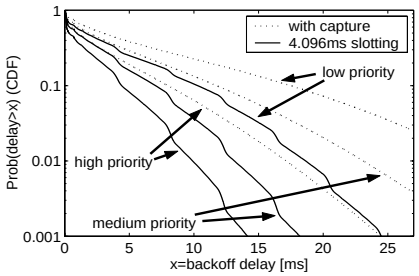

(a) “Slotted”, *600 byte* frame body size.

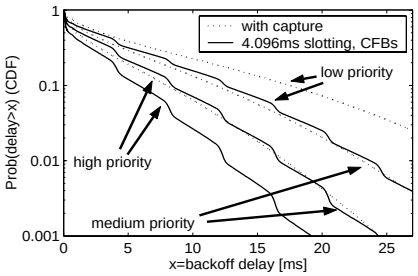

(b) “Bursted”, with CFBs, *600 byte* frame body size.

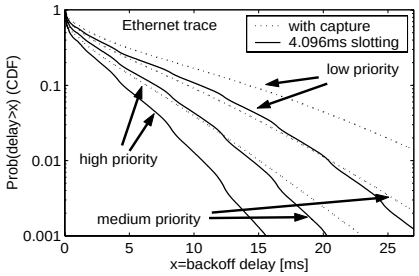

(c) “Slotted”, Ethernet trace.

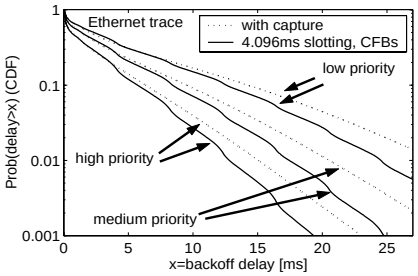

(d) “Bursted”, with CFBs, Ethernet trace.

Figure 5.33: Backoff delays for different offered traffics, standard 802.11 (“with capture”), with slotting, and with slotting incl. CFBs.

5.4 HCF Controlled Channel Access, Coexistence of Overlapping QBSSs

The controlled channel access of the HCF provides the highest possible priority in channel access to a backoff entity. Usually, the HC makes use of the controlled channel access by periodically polling various backoff entities during the contention period. A time interval during which the channel is allocated with the controlled channel access is referred to as *Controlled Access Phase* (CAP).

At any time during the contention free period (which is optional) or during the contention period, the HC can allocate a CAP, as soon as the channel is idle for a duration of PIFS. This works sufficiently only as long as one HC operates at the channel. When two or more HCs of overlapping QBSSs operate at the same time in a coexistence scenario, the controlled channel access cannot provide the required QoS, as will be discussed in the following.

5.4.1 Prioritized Channel Access in Coexistence Scenarios

Figure 5.34 gives an example where more than one HC operate at the same time, in a coexistence scenario. A typical EDCF frame exchange is shown. One MSDU is delivered through contention-based channel access, during an EDCF-TXOP. Within this EDCF-TXOP, RTS, CTS, the data frame that is carrying the MSDU and the ACK are transmitted. In an isolated QBSS, the length of this EDCF-TXOP is limited by the TXOPlimit to guarantee that the channel will be sufficiently often idle to allow the allocation of CAPs with some required delays.

The TXOPlimit is under control of the HC in that isolated QBSS. When QBSSs overlap, however, HCs can only control the duration of the EDCF-TXOPs within their own QBSS. That means that if one HC requires a small TXOPlimit, but the coexisting backoff entities of the overlapping QBSSs follow the larger TXOPlimit of a second HC, then the first HC will not meet its delay requirements.

In addition, after the end of an EDCF-TXOP, two or more HCs may attempt to allocate a CAP to deliver data immediately after the ongoing EDCF-TXOP with highest priority, as indicated in the right hand side of Figure 5.34. In this case, the first frames transmitted in the CAPs will collide, which is a substantial problem for the controlled channel access. In general, the probability of collisions increases with increasing durations of the EDCF-TXOPs, i.e., with an increased TXOPlimit. Note that the two HCs may require different TXOPlimits in their respective QBSSs.

Figure 5.35 illustrates another obvious problem that occurs when more than one HC operate at the same time, in a coexistence scenario. The HC *1* needs to allocate a CAP at a point in time when the other HC *2* allocated a CAP already.

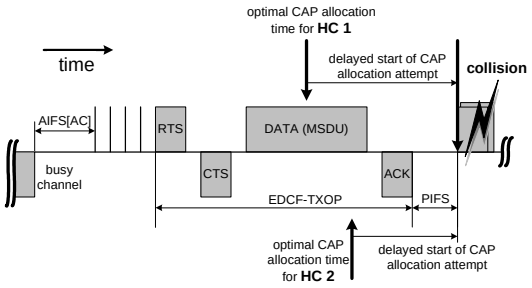

Figure 5.34: One of the problems in overlapping QBSSs: after the end of an EDCF-TXOP, both HCs may attempt to transmit immediately with highest priority. In this case, frames collide.

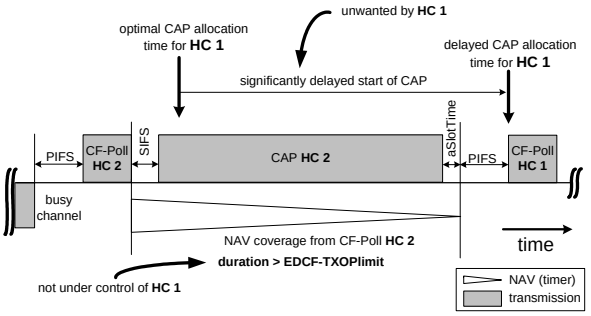

Figure 5.35: One of the problems in overlapping QBSSs: HC *1* needs to allocate resources while the other HC *2* allocates resources through a granted TXOP already. The duration of the ongoing TXOP is not limited by the TXOPlimit. As a result, the HC *1* may observe large delays.

The duration of the ongoing CAP is not limited by the TXOPlimit, and therefore not under control of the HC *1*. As a result, the HC *1* observes significant delays when attempting to allocate a CAP, and may even have to give up the CAP allocation attempt due to the increased delays.

No HC operating in overlapping QBSSs can meet its requirements, as soon as coexisting HCs allocate CAPs with durations larger than the TXOPlimit that is individually defined by the respective HC.

5.4.2 Saturation Throughput in Coexistence Scenarios

The modified version of Bianchi's legacy 802.11 model is used here to analyze the identified problems, see Section 5.1.2.1, p. 65. Figure 5.36 shows the collision and transmission probabilities p, τ in a generic slot time for an HC, as a function of the number of HCs in overlapping QBSSs. This figure should be compared to Figure 5.5, p. 69, where the same probabilities are shown for the contention-based channel access of the HCF, i.e., the EDCF, versus the number of contending backoff entities. As expected, due to the lack of contention in the controlled channel access, the collision probability is $p = 0$ for one HC, and $p = 1$ if more than one HC allocate CAPs. As slots are never idle when one or more HCs allocate as many CAPs as possible (in saturation), the probability that the HC transmits at a generic slot is $\tau = 1$ for any number of HCs.

Figure 5.37 shows the respective probabilities that a generic slot is idle, busy with a collided frame, or busy with a successfully allocated CAP, versus the number of HCs. This figure should be compared to Figure 5.6, p. 70, where the same probabilities are shown for the EDCF. As expected, in saturation, slots are never idle. Further, the channel is always busy with unsuccessful transmissions, as soon as

more than one HC attempt to allocate CAPs. One isolated HC will always successfully allocate its CAPs. Figure 5.38 shows the resulting saturation throughput for different frame body sizes and PHY modes, vs. the number of HCs in overlapping QBSSs. It is assumed that one frame per CAP is exchanged. One HC can achieve different saturation throughput for different frame body sizes and PHY modes, similar to the EDCF. However, in contrast to the EDCF, as soon as the number of HCs increases beyond one, the throughput drops down to zero, since all CAP allocation attempts will fail if two or more HCs operate in saturation in the coexistence scenario.

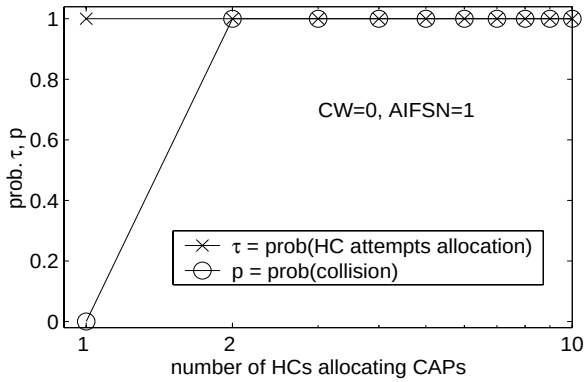

Figure 5.36: Collision and transmission probability p, τ in a generic slot time for an HC, as functions of the number of HCs in overlapping QBSSs.

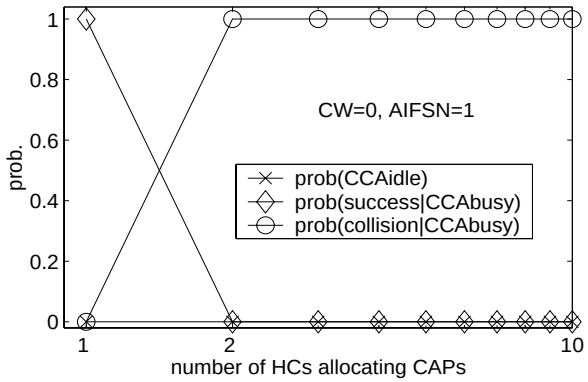

Figure 5.37: Probability that a generic slot is idle, busy with a collided frame, or busy with a successfully transmitted frame, as functions of the number of HCs in overlapping QBSSs.

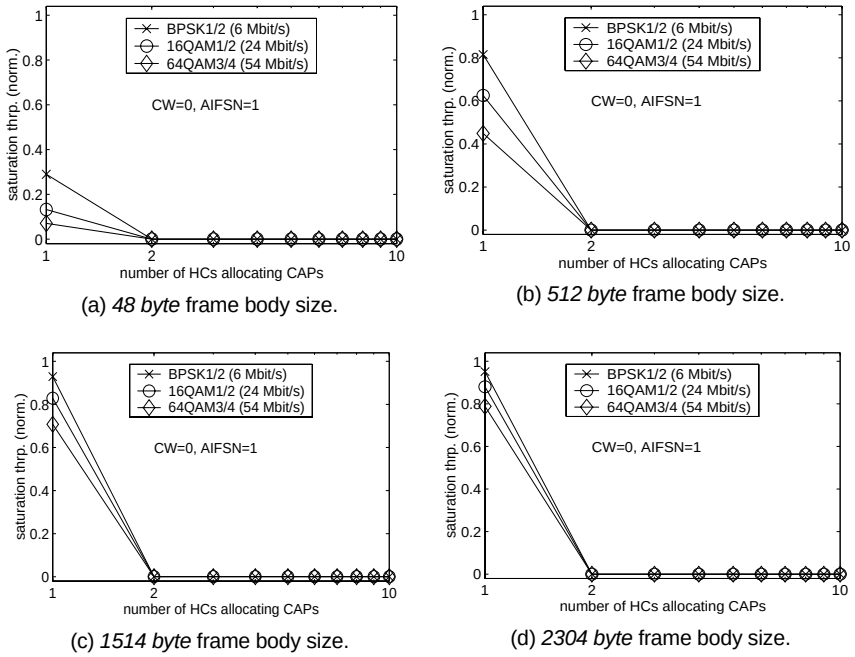

(a) *48 byte* frame body size.

(b) *512 byte* frame body size.

(c) *1514 byte* frame body size.

(d) *2304 byte* frame body size.

Figure 5.38: Saturation throughput for different frame body sizes, PHY modes, vs. the number of HCs in overlapping QBSSs.

5.4.3 MSDU Delivery Delay in Coexistence Scenarios

The previous results were obtained with the analytical model, and show the saturation throughput. In addition to the saturation throughput analysis, it is worthwhile to look -by means of simulation- at the MSDU Delivery delay that can be expected in realistic scenarios.

5.4.3.1 Scenario

Two fully overlapping QBSSs as indicated in Figure 5.39 or one of the two QBSSs in an isolated environment are investigated in the following. Transmission powers and distances between stations are chosen in such a way that they are not hidden to each other with the selected PHY modes. All frames but the data frames are transmitted with the PHY mode BPSK1/2 (*6 Mbit/s*). Data frames are transmitted with the PHY mode 16QAM1/2 (*24 Mbit/s).* Each station generates the same mixture of offered traffic of three data streams, which are labeled "*high (AC 6)*", "*medium (AC 5)*" and "*low (AC 0),*" according to their priorities. At the high priority AC, MSDUs with a frame body size of *80 byte* arrive periodically to

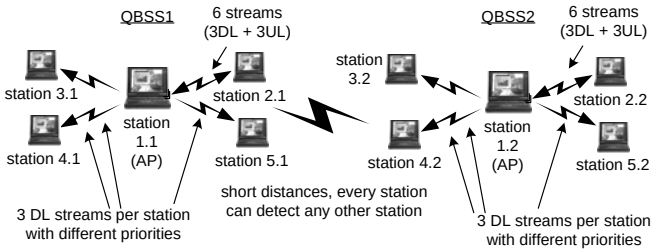

Figure 5.39: Coexistence scenario of overlapping QBSSs.

model isochronous traffic that is usually served with CAPs as part of the controlled channel access in the HCF. The repetition period depends on the offered traffic, and is *5 ms* for the *128 kbit/s* traffic stream. The medium and low priority ACs carry MSDUs with a constant frame body size of *200 byte* with negative exponentially distributed inter-arrival times, each stream with *160 kbit/s*. Table 5.7 shows the EDCF parameters used for the three priorities. If not stated otherwise, neither RTS/CTS nor fragmentation is used. The fragmentation threshold is set to *256 byte*. The TXOPlimit is set to allow backoff entities to exchange a single data frame with the contention-based channel access of the HCF.

5.4.3.2 Simulation Results and Discussion

Figure 5.40(a) shows the resulting MSDU Delivery delay distributions for an isolated QBSS. All backoff entities including the AP contend for medium access via EDCF. The HC resides in the AP. In addition, the AP carries one isochronous downstream (*80 byte* frame body size per MSDU, *128 kbit/s*) which is delivered with the controlled channel access of the HCF by allocating CAPs with highest priority, higher than AC6, and therefore labeled as "AC7". The data frames of this stream are immediately transmitted after PIFS when the channel is detected idle. As stated earlier, the controlled channel access of the HCF achieves its strict delay requirements by setting a maximum TXOP duration with the TXOPlimit for all other priority classes. The different QoS levels achieved by the priority classes are clearly visible: the higher the priority, the smaller the delay. The minimum delay in the figure results from the MSDU Delivery time, and depends on the duration of the respective frame. The delay is dependent on the offered traffic. With increased offered traffic, the delay of the three contention-based channel access AC 0, 5, 6 increase, whereas the maximum delay of the controlled AC 7 stays constant. The scenario is only slightly loaded. AC 6 is partially served better than AC 7 because there is only one AC 7 stream, whereas multiple streams in AC 6.

Figure 5.40(b) shows the resulting MSDU Delivery delay distributions for an isolated QBSS, but in comparison with Figure 5.40(a) with an increased offered traffic at the low and medium priority streams; the offered traffic is *320 kbit/s* per stream instead of *160 kbit/s* per stream. The line labeled as "AC7" corresponds to the stream that is served with CAPs. Only this stream stays within its maximum delay limit.

In contrast, if longer MSDUs are transmitted through the medium and lower priority streams, i.e., if the TXOPlimit is increased, then the maximum MSDU Delivery delay of the highest priority, served with CAPs, increases as well. This is shown in Figure 5.40(c). The same offered traffic as in the previous scenario (a) is simulated, but with longer data frames. The frame body size of MSDUs delivered in AC0 and AC5 now exceeds the fragmentation threshold. Since the HC has the control on the TXOPlimit duration it can avoid a high priority AC to exceed its delay by appropriate setting of the limit value.

A significantly increased MSDU Delivery delay occurs with coexisting QBSSs, as indicated in Figure 5.39. The delay is not under the control of the HC in this scenario. Here, two identical overlapping QBSSs are co-located to each other, so that they interfere. All traffic parameters remain as described for the isolated QBSSs. This coexistence scenario has been discussed in the previous section. The MSDU Delivery delay distributions in this scenario are shown in Figure 5.40(d). It can be seen that now the delay of the high priority AC 7 exceeds the TXOPlimit of $300\mu s$ defined by the HC to meet the needs of AC 7.

This example shows that a variety of delays and throughputs that are observed in overlapping QBSSs depend on the degree of overlap. One extreme example of this is when two HCs always attempt to allocate CAPs at the same time. Then all CAPs would collide, and the throughput of all streams in AC 7 would be significantly reduced. In this case the delay of AC 7 would be infinite.

Table 5.7: EDCF parameters used for the analysis of the overlapping QBSS scenarios.

AC (priority):	highest (AC 7)	higher (AC 6)	medium (AC 5)	lower (AC 0)
AIFSN[AC]:	*1*	*2*	*4*	*7*
CWmin[AC]:	*0*	*7*	*10*	*15*
CWmax[AC]:	*0*	*7*	*31*	*255*
PF[AC]:	*N/A*	*2*	*2*	*2*
RetryCnt[AC]:	*1*	*7*	*7*	*7*

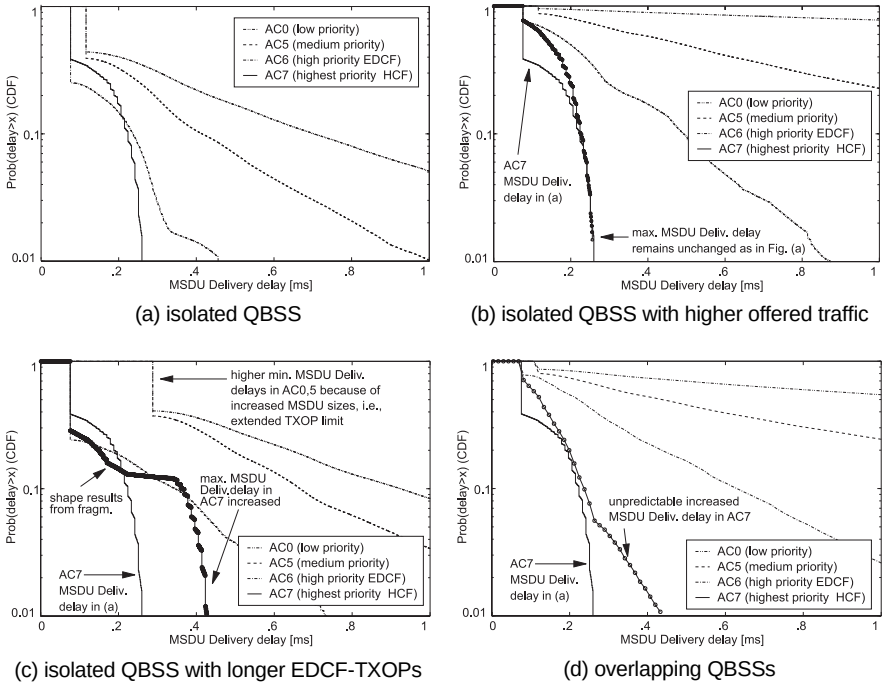

(a) isolated QBSS

(b) isolated QBSS with higher offered traffic

(c) isolated QBSS with longer EDCF-TXOPs

(d) overlapping QBSSs

Figure 5.40: (Mangold et al., 2002a) MSDU Delivery delay for the four ACs in isolated and overlapping scenarios.

5.4.4 Conclusions about the HCF Controlled Channel Access

The controlled channel access of the HCF allows allocating resources with highest priority, and to guarantee a maximum MSDU Delivery delay only if the QBSS operates in isolation. If backoff entities of overlapping QBSSs allocate TXOPs that are longer than the specified TXOPlimit, the MSDU Delivery delay of the controlled channel access of the HCF increases unpredictably.

Further, if HCs of overlapping BSSs allocate CAPs as well, allocation attempts may often fail due to colliding frames, and MSDU Delivery delays may increase dramatically. As a result, QoS guarantees are not possible then.

5.5 Summary and Conclusion

The upcoming 802.11e standard is an efficient means for QoS support in wireless LANs for a wide variety of applications, although open problems such as the overlapping QBSSs remain to be solved. This chapter provides an in-depth analy-

sis of potential 802.11e enhancements. The maximum achievable throughput as well as the saturation throughput for the HCF contention-based channel access (EDCF) have been calculated analytically, and validated by simulation, see Section 5.1.2.

A new model to approximate the resulting share of capacity per AC, i.e., the relative priority between different ACs when backoff entities operate with different EDCF parameters, has been developed and validated by simulation in Section 5.1.3. The model sufficiently approximates the simulation results for nearly all studied load scenarios.

The specific problem of providing EDCF backoff entities a higher priority in channel access over the legacy DCF stations has been discussed, and means based on the Persistence Factor and the EIFS to support EDCF in congestion with DCF were proposed and evaluated, see Section 5.1.4.

The importance of applying contention free bursts together with radio resource control schemes in coexistence scenarios have been highlighted in Section 5.2. Radio resource capture scenarios have been investigated in Section 5.3 and have been shown to be sensitive in that they might affect the ability of 802.11e to guarantee QoS support.

The controlled channel access of the HCF has been analyzed in Section 5.4. It provides in an isolated QBSS the means for delivering time-bounded traffic, and requires all backoff entities within the range of the HC to follow its coordination. QoS support appears to be problematic when multiple QBSSs overlap.

Chapter 6

COEXISTENCE AND INTERWORKING BETWEEN 802.11 AND HIPERLAN/2

WIRELESS networks are able to coexist if they operate with the same radio resources at the same time and location, i.e., in an overlapping scenario (Mangold et al., 2001h). Wireless networks that coexist with each other operate in the same coverage area without harmful interference. With successful coexistence, individual wireless networks that overlap with each other generally see a reduced capacity of the radio resources but still have full access to the available radio resources. Without a successful coexistence strategy, wireless networks are not able to successfully control their access to radio resources. It is worth mentioning that coexisting wireless networks not necessarily must follow the same standard. Further, the capability to exchange information between overlapping wireless networks is not a required characteristic for establishing successful coexistence, as will be shown in this chapter. Wireless networks are able to interwork rather than to coexist if they are able to exchange information across the different networks. When interworking, wireless networks are able to coordinate the usage of radio resources. This is achieved by exchanging spectrum coordination information. To be capable of exchanging information, it is required that overlapping wireless networks operate with the same transmission scheme through a protocol that is common between these wireless networks.

Coexistence and interworking of two different types of wireless networks are discussed in the following. This chapter introduces a concept for interworking of wireless LANs in the 5 GHz unlicensed band, HiperLAN/2 and 802.11. As explained in Chapter 2, the 802.11a wireless LANs operate with an OFDM based transmission scheme defined in IEEE 802.11 WG (1999a) in the 5 GHz. We refer to this 802.11a in the following, when referring to 802.11. HiperLAN/2 operates with the same transmission scheme and channelization, with some minor modifications (ETSI, 2000a). Since 802.11 and HiperLAN/2 operate at the same frequency band, and because the transmission schemes are so similar, it is therefore natural to look at MAC enhancements that allow for interworking or coexistence.

This chapter provides in the next section a brief overview on HiperLAN/2, based on (Walke 2002; Walke et al. 2001). In Section 6.2, an interworking concept based on the integration of HiperLAN/2 into the 802.11 MAC protocol is developed, which was proposed as interworking solution between HiperLAN/2 and 802.11 in Mangold et al. (2001a), Mangold et al. (2001b), Mangold et al. (2001c), and Mangold et al. (2001d). One single communicating device coordinating a QBSS and being able to operate alternatively in 802.11 and HiperLAN/2 mode of operation is proposed to realize interworking there. Section 6.3 describes how this concept can serve as generic solution for the general coexistence problem. If this device can coexist with another co-located device of the same type, the coexistence problem of overlapping QBSSs, and between HiperLAN/2 and 802.11 stations is mitigated. As this is the focus of this thesis, Section 6.3 leads up to the following chapters, in which a game theoretic approach is developed and evaluated. This approach uses new adaptive methods for radio resource control for communicating devices in the presence of competing devices, with focus on radio spectrum sharing and QoS support for all coexisting wireless LANs.

6.1 ETSI BRAN HiperLAN/2

ETSI BRAN HiperLAN/2 (referred to as HiperLAN/2) is a radio system for Wireless LAN and Home Networking applications. HiperLAN/2 is a standard for wireless transport systems including layer 1 and layer 2 protocols. A so-called convergence layer on top of the protocol allows the wireless extension of applications like Ethernet, IP, and IEEE 1394. For *Logical Link Control* (LLC), which is referred to as *Error Control* (EC) at ETSI BRAN, HiperLAN/2 defines its own EC scheme, which aims to provide a high level of QoS support. In the following, the reference model, the architecture, and the MAC protocol are summarized.

For more details than given here, Walke (2002) provides an overview and performance evaluation of the HiperLAN/2 protocol.

6.1.1 Reference Model (Service Model)

The HiperLAN/2 reference model is also referred to as service model, which is illustrated in Figure 6.1. The reference model comprises the *Physical layer* (PHY) and the *Data Link Control layer* (DLC) for stations and APs. A station is in HiperLAN/2 referred to as *Mobile Terminal* (MT), or if it is not mobile, as *Wireless Terminal* (WT). In this thesis, "station" is used instead of MT/WT. Various network types like *Internet Protocol* (IP), Ethernet, IEEE 1394 and the *Asynchronous Transfer Mode* (ATM) can be connected to the DLC layer by the *Convergence Layer* (CL) that performs the adaptation of the packet formats to the requirements of the DLC layer. For higher layers other than ATM, the CL contains a *Segmentation and Reassembly* (SAR) function.

The physical layer provides the basic transport functions for the DLC *Protocol Data Units* (PDU), that are equivalent to the MSDUs in 802.11. The DLC layer is divided into two parts, the control plane and the user plane. In the user plane, data are handled that arrive from higher layers via the *User Service Access Point* (U-SAP). This user plane contains the EC that implements the *Automatic Repeat Request* (ARQ) protocol. Therefore, HiperLAN/2 comprises a MAC and a LLC protocol; the combination of the two is referred to as DLC protocol. The HiperLAN/2 DLC protocol is connection oriented and provides multiple connection end points in the U-SAP. The control plane consists of the *Radio Link Control* (RLC) protocol that includes the connection control, the radio resource control, and association control functions. The HiperLAN/2 RLC is equivalent to a combination of MLME and SME in 802.11. Both planes access the physical medium via the MAC protocol.

6.1.2 System Architecture

HiperLAN/2 is centrally controlled. An AP that is typically connected to a core network or a distribution system consists of an *Access Point Controller* (APC) and up to sixteen *Access Point Transceivers* (APTs). Each APT operates on a different frequency channel.

Two operation modes are defined for the HiperLAN/2 DLC: centralized mode and direct mode. In the centralized mode, stations communicate via the AP with other stations. In the direct mode, stations communicate user data under the control of the AP directly over direct links with each other, similar to what is

defined for 802.11e DiL. In both modes, the AP assigns radio resources, schedules the transmission times, and controls the communication in the radio cell. A radio cell in HiperLAN/2 is equivalent to a (Q)BSS in 802.11(e).

Data are transmitted via an RLC connection either between station and AP or between directly communicating stations. A connection must be established prior to the data transmission, using signaling functions of the HiperLAN/2 control plane. Therefore, HiperLAN/2 is centrally controlled, like the PCF in 802.11. Point-to-point connections are bidirectional, point-to-multipoint and broadcast connections are unidirectional from the AP to stations in the radio cell. Connections are realized by means of logical channels.

Because of the centralized approach and the connection orientation of HiperLAN/2, support of QoS is achieved. Each connection can be associated to QoS parameter requirements that define throughput, delay, delay variation, bit error probability, and others.

6.1.3 Medium Access Control

In HiperLAN/2 the controlling station transmits a beacon every *2 ms*, providing the timing of the *Medium Access Control frame* (MAC frame) that follows the beacon. Whereas in 802.11, a MAC frame refers to a data frame, in HiperLAN/2 a MAC frame refers to the periodic time interval of *2 ms*.

The station that coordinates the MAC frame is referred to as *Central Controller* (CC) and has the full control over the frequency channel it is operating at. The CC is equivalent to an HC in 802.11e, and typically resides in an AP, but might reside in any other station.

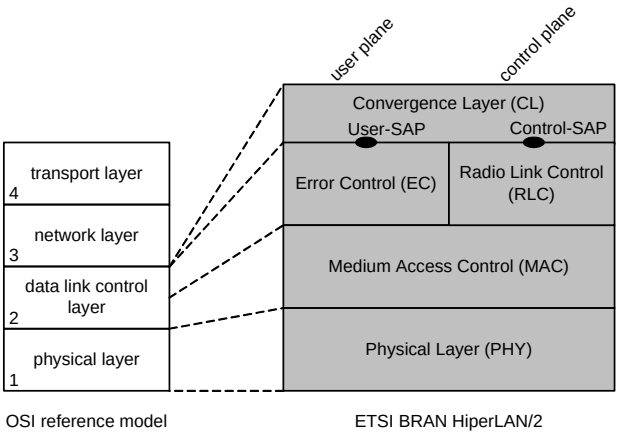

Figure 6.1: HiperLAN/2 reference model.

For the exclusive medium access, *Dynamic Frequency Selection* (DFS) is required in the HiperLAN/2 standard. With DFS, HiperLAN/2 systems are able to avoid that co-located CCs operate at the same frequency channel.

The HiperLAN/2 MAC frame comprises four generic phases, all controlled by the CC. Order and duration of the phases are determined by the CC and may change from MAC frame to MAC frame depending on the instantaneous QoS requirements. Typically, after the beacon sent to the associated stations, the unicast data from the CC to the stations follows in downlink, before transmissions from stations are scheduled for data in uplink direction. In HiperLAN/2, data transmission is performed by transmitting so-called *Protocol Data Unit* (PDU) trains, i.e., groups of consecutive DLC PDUs that carry the user data. The lengths of the PDU trains vary depending on what duration is scheduled by the CC for data transmission. The direct link phase, during which data is transmitted directly from station to station, is optionally allowed at any time during the MAC frame. During the random access phase of the MAC frame, stations may send short control frames, called *Resource Requests* (RRs) to ask for transmit capacity for the subsequent MAC frame. A random access phase ends a MAC frame and the next MAC frame starts immediately with the beacon data transmitted. The assignment of resources to the individual stations and to their connections is not static but may change dynamically from one MAC frame to the next MAC frame, depending on what the CC will schedule.

Figure 6.2 illustrates the operation of HiperLAN/2. The CC transmits the beacon (broadcast channel) at the start of a periodic MAC frame even if there is no user data to be transmitted. The beacon contains control information like network identity, transmission power levels, scheduled transmission starting points, and durations of random access phases. It is transmitted using the most robust modulation scheme available, i.e., BPSK1/2.

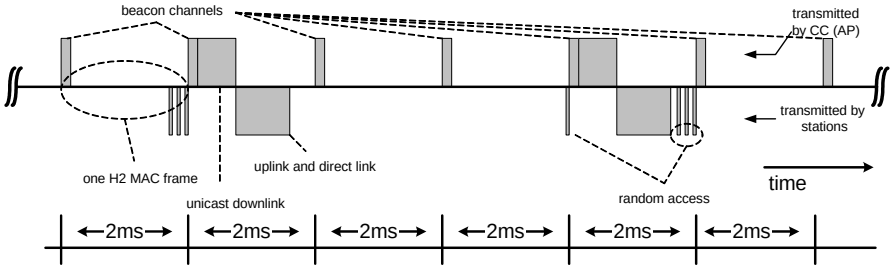

Figure 6.2: HiperLAN/2 timing. The MAC frame comprising beacon (broadcast) phase, down-, direct- and up-link phase, and random access phase, is repeated every *2 ms*. The access to the radio channel is centrally controlled by one station, the CC. HiperLAN/2 requires an exclusive frequency channel.

6.2 Interworking Control of ETSI BRAN HiperLAN/2 and IEEE 802.11

In this section, a concept to integrate HiperLAN/2 into 802.11 is described in detail. The concept is developed and introduced in Mangold et al. (2001a), Mangold et al. (2001b), Mangold et al. (2001c), and Mangold et al. (2001d). As explained in Chapter 2, 802.11 and HiperLAN/2 apply nearly the same OFDM-based transmission scheme and channelization, which facilitates interworking.

Interworking of 802.11 and HiperLAN/2 implies the communication between stations of similar and different types in a common integration protocol. The concept discussed in the following realizes this integration by a centrally coordinating device that is capable of operating in both, an 802.11 and HiperLAN/2 mode. As part of the interworking concept, regular HiperLAN/2 MAC frames with durations of *2 ms* are integrated into the superframe of 802.11e. The concept is based on the QoS enhancements of 802.11 that are defined in the 802.11e MAC enhancements (IEEE 802.11 WG, 2002a). Interworking is realized by applying the HCF of the upcoming IEEE 802.11e QoS-enabled MAC. A combination of a HiperLAN/2 *Central Controller* (CC) and 802.11a/e *Hybrid Coordinator* (HC), referred to as CCHC, is proposed for the interworking of 802.11a/e and HiperLAN/2 systems. The CCHC is placed in a device that must have 802.11a/e MAC/PHY and in addition, the HiperLAN/2 MAC/PHY implemented. The CCHC works as the HC to 802.11a/e stations and as the CC to HiperLAN/2 stations. The proposed CCHC relies on the HCF including QoS CF-poll as described in IEEE 802.11 WG (2002a).

Once this interworking concept is established, it can serve as a basis for also providing support for coexistence of HiperLAN/2 and 802.11, as well as coexistence of overlapping 802.11e QBSSs. It has been shown in Chapter 5 that 802.11e QBSSs suffer from unpredictable QoS reductions if they overlap and if more than one QBSS applies the HCF for controlled channel access.

6.2.1 CCHC Medium Access Control

The CCHC as a single device is proposed that operates at one single frequency channel to coordinate the HiperLAN/2 and 802.11 networks, i.e., a HiperLAN/2 cell and an 802.11 QBSS. Within the limit of each radio resource allocated to stations under control of the CCHC, a station itself decides what data to transmit. This is exactly the concept used in 802.11e, when stations are polled by an HC. It appears natural to extend this concept for defining HiperLAN/2 MAC frames by the CCHC to cover the needs of HiperLAN/2 stations in an inter-

working scenario. It is assumed that the CCHC is able to execute both protocols completely to organize the interworking between any stations.

6.2.1.1 CCHC Scenario

Figure 6.3 shows a CCHC based scenario, including the combined protocols used by the CCHC. One CCHC and one controlled station of each wireless network type are shown. The control over the stations is guaranteed by regularly allocating radio resources for some predefined duration to the 802.11 and HiperLAN/2 stations, by the CCHC that has full control over the radio channel.

Allocated time intervals are here referred to as resource allocations. A resource allocation is interpreted by an 802.11 station as a TXOP according to the 802.11e protocol, and by a HiperLAN/2 station as one or more consecutive HiperLAN/2 MAC frames, i.e., time intervals of *2 ms* length that are started by a beacon (i.e., broadcast channel).

The interworking scenario addressed in Figure 6.3 allows the exchange of information between HiperLAN/2 and 802.11 stations via the CCHC device. If a HiperLAN/2 station has data to deliver to an 802.11 station, and if both stations are associated with the BSS that is coordinated by the CCHC, then the HiperLAN/2 station delivers this data during a MAC frame to the CCHC, which then forwards the data within a later resource allocation to the addressed 802.11 station, by using the respective communication protocol. The CCHC comprises the MAC layers of both communication protocol stacks, with an harmonized PHY and some common services on top of the two user planes of the MAC layer. An adaptation layer or convergence layer may be required, as it is already available in HiperLAN/2 (ETSI, 2000c). A central management entity within the CCHC MAC layer controls the alternating turns of operation of the two parallel user planes.

6.2.1.2 CCHC and Legacy 802.11

Besides using a HiperLAN/2 MAC frame and the high priority access through 802.11e HCF, 802.11 stations may wish to operate in the prominent EDCF mode, by contending for medium access whenever they want to transmit. This mode of operation would be no problem for the CCHC concept proposal, as long as stations follow the EDCF instead of the legacy DCF. The EDCF does not allow stations to allocate the radio channel for longer durations than the TXOPlimit, and thus can be easily coordinated by the CCHC. Stations that operate according to the legacy DCF are here referred to as legacy 802.11 stations and should not be allowed to associate with a QBSS coordinated by a CCHC, because

they would violate the TXOPlimit, see Chapter 4, p. 41. Besides to not allowing legacy 802.11 stations to associate with a QBSS coordinated by the CCHC, a function existing in 802.11 is proposed to keep legacy stations silent. The function helps to prevent legacy 802.11 stations from interfering with CCHC resource allocations. The *Extended Interframe Space* (EIFS) specified to be able to operate under hidden station interference is proposed to be exploited by the CCHC, in order to silence down legacy duration stations. There is a mechanism specified in the IEEE 802.11 MAC protocol that allows QBSSs coordinated by a CCHC that are co-located with 802.11 stations to force 802.11 stations to defer from medium access for a long time, i.e. EIFS duration. This mechanism has been originally defined to reduce interference of hidden stations. The 802.11 MAC protocol specifies a concept called virtual carrier sensing, as explained in Chapter 3.

An 802.11 station that detects a valid preamble, but that is not able to successfully receive the complete frame, assumes a hidden station scenario and is forced to defer from medium access for a long duration, called EIFS. A *Frame Check Sequence* (FCS) that is part of any frame in 802.11 is incorrect in case of unsuccessful frame reception. The CCHC should take advantage of this. By using the same preambles and headers, but different FCSs or different PHY modes for the rest of the frames, legacy stations that detect frames from the CCHC will operate with EIFS instead of DIFS.

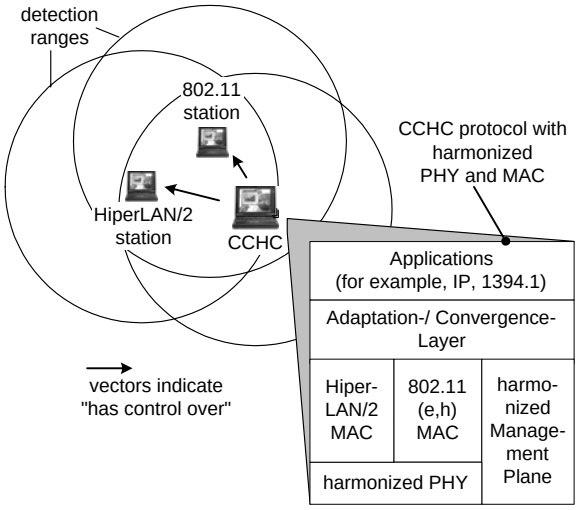

Figure 6.3: CCHC coordinating 802.11 and HiperLAN/2 stations. The detection ranges indicate that all stations are in the range of CCHC, which is required for QoS support. Note that this requirement exists for all standard QBSSs.

It is possible for a QBSS coordinated by a CCHC to protect itself from interference of legacy 802.11 stations by regularly transmitting preambles and PLCP headers[9] during the EIFS duration, which then would set the NAV in the 802.11 stations again for another EIFS duration.

6.2.1.3 CCHC Working Principle

Figure 6.4 shows the proposed CCHC frame structure. It can be seen that within the CCHC superframe with optional *Contention Free Period* (CFP), the CCHC allocates TXOPs in order to allow the periodic resource allocation for HiperLAN/2 MAC frames.

To enable the alternated operation of 802.11 and HiperLAN/2 in subsequent resource allocations, the HiperLAN/2 stations receive a periodic *AP-Absence* announcement by the CCHC, a concept in HiperLAN/2 to allow the HiperLAN/2-AP or CC to stop transmitting the periodic beacon for some defined time interval. Originally, AP-Absence is defined to let the AP/CC perform channel measurements (ETSI, 2000c).

The HCF is the basis for the new CCHC interworking concept. The QoS CF-Poll can be used by the CCHC to allocate TXOPs within the *Contention Period* (CP) with high priority, i.e., after PIFS idle time. The CCHC may initiate a frame exchange right after PIFS during the CP by immediately transmitting a data frame, preceded by or without RTS/CTS followed by an HiperLAN/2 MAC frame. One HiperLAN/2 MAC frame is shown to be transmitted after a CF-Poll in the CFP in Figure 6.4.

According to Figure 6.4, a superframe between two TBTTs is starting with an 802.11 beacon as the first frame. Information fields in the beacon announce the superframe duration and inform all stations whether a CFP will start right after the beacon. Further, the TXOPlimit and the EDCF parameters are broadcasted by the CCHC via information fields in the beacon and can be used to control the impact of the EDCF background traffic on the resource allocations scheduled by the CCHC.

In the example shown in Figure 6.4, there is a CFP with two HiperLAN/2 MAC frames, ending with the CF-end frame. This example will be discussed in the following.

---

[9] See Chapter 3, p. 19, for the explanation of the frame structure in 802.11, including the PLCP and MAC headers.

6.2.1.4 CCHC Frame Structure

After the beacon, four TXOPs are related to four resource allocations in Figure 6.4. The first TXOP is a resource allocation by the CCHC during the optional CFP. The CCHC uses a *Controlled Access Phase* (CAP) to allocate the channel, as part of the controlled channel access of the HCF. Because the CAP is allocated by the CCHC and not through contention-based channel access by any other 802.11 station, the maximum duration of this resource allocation is not restricted by the TXOPlimit. The only limit is that the resource allocation has to be finished before the end of the CFP. However, the length of CFP is under control of the CCHC. This first resource allocation (in the figure indicated as CAP) is used to operate HiperLAN/2 by means of two MAC frames. As explained before, in 802.11e the CFP is not mandatory and not needed for QoS support by the HCF.

Another three resource allocations, which fall in the CP after the CF-end frame, are shown in Figure 6.4. The second and the third resource allocations (in the figure indicated as TXOPs) are allocated by stations through contention-based channel access, and therefore their durations must not exceed the TXOPlimit. Based on what is defined for the HCF, the CCHC may use various techniques to allocate resources during the CP. One way is illustrated for the fourth resource allocation (indicated as CAP in Figure 6.4). There, the CCHC uses its high priority in channel access as part of the controlled channel access of the HCF and transmits a QoS CF-Poll frame addressed to itself in advance right after the end of the preceding TXOP.

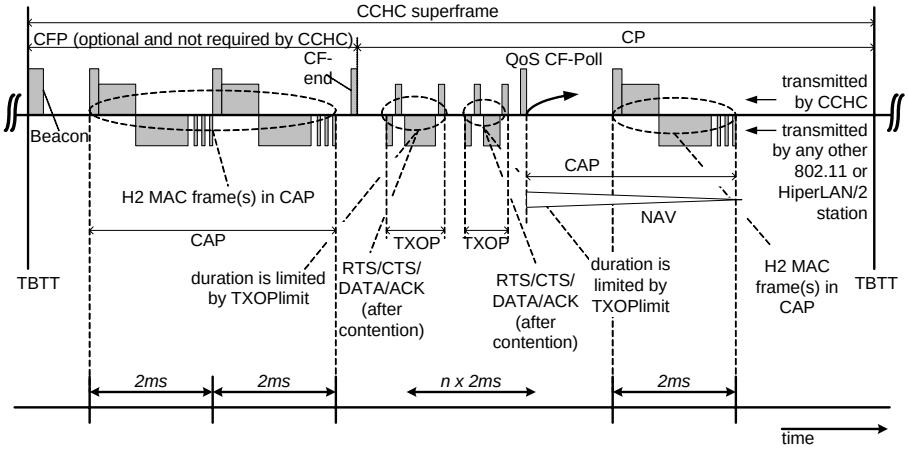

Figure 6.4: The structure of the CCHC superframe. One superframe between two TBTTs is illustrated. HiperLAN/2 MAC frames are scheduled within periodically repeated TXOPs.

It then schedules the next HiperLAN/2 MAC frame, now within the CP. By transmitting the QoS CF-Poll, the CCHC can force all the stations within the QBSS to refrain from access during the period it wants to reserve for the HiperLAN/2 MAC frames. The NAV setting from the poll frame is indicated in the figure.

The CCHC schedules the time instances in advance where HiperLAN/2 frames would need access to the channel. Since the TXOPlimit is system widely known the CCHC must allocate the channel when a CP transmission has ended and the time instance of the next HiperLAN/2 MAC frame is closer than a duration of TXOPlimit apart. Some unused time interval of a duration less than TXOPlimit might result after the CF-Poll before the HiperLAN/2 frame starts.

There are alternative possibilities available for the CCHC to allocate radio resources. One alternative possibility is to transmit downlink frames (i.e., CCHC to an 802.11 station, with or without RTS/CTS), or to transmit a QoS CF-Poll frame to grant a resource within a TXOP directly to an associated station. Once the CCHC allocated radio resources, it can continue to allocate resources by not allowing more than PIFS time between two resource allocations.

Another alternative possibility for allocating radio resources with highest priority during the CP is to follow a proposal by Sobrinho and Krishnakumar (1996, 1999). They propose an energy signal to be transmitted by the CCHC, as soon as the channel gets idle, for the support of real time traffic. The energy signal results in all contending stations to detect the channel as busy and therefore to defer from access. In the CCHC approach, the duration of this energy signal must be chosen such that the HiperLAN/2 frame to be started after this signal ends at the scheduled point in time.

6.2.2 Requirements for QoS Support

The proposed interworking concept requires that the CCHC has full control over the stations of the co-located 802.11a/e and HiperLAN/2 networks. This requires both protocols implemented in the CCHC. Because the HiperLAN/2 standard requires periodic transmissions of beacons every *2 ms*, the HiperLAN/2 MAC frames have to be allocated according to fixed periods of multiples of *2 ms*. All stations have to be located in the receive range of the beacon for understanding the management and control frames from the CCHC. Legacy stations operating in the same radio channel must be prevented, for example by using the schemes described in Section 6.2.1.2.

6.3 Coexistence Control of ETSI BRAN HiperLAN/2 and IEEE 802.11

The CCHC concept as discussed before has the potential to serve as basic approach to solve the coexistence problem between 802.11 and HiperLAN/2 stations, as well as the overlapping QBSS problem identified in Section 5.4, p. 108. Coexistence of WLANs using different protocols is difficult to achieve as long as the stations are not coordinated by a single device that is capable of all protocols. This is exactly what the CCHC approach offers. The CCHC as central coordinator of all stations within a QBSS allows a time-sharing of one frequency channel by two (or more) different WLANs. The coexistence control is difficult to perform when more than one CCHC operate at the same frequency channel, in the same area, as explained in Section 5.4, p. 108, for the coexistence of HCs in 802.11e networks, i.e., overlapping QBSSs each employing their own centrally controlled resource coordination.

6.3.1 Conventional Solutions to Support Coexistence of WLANs

Until today, coexistence is handled by using DFS and by selecting different frequency channels upon detecting a competing QBSS. As described earlier, DFS is available for HiperLAN/2 as part of the standard. DFS is available too for 802.11 as part of the 802.11h supplementary standard defined in IEEE 802.11 WG (2002b), an extension to the 802.11 MAC and the 802.11a PHY. For this reason, DFS will be available to be applied for coexistence control in an integrated protocol as well; the CCHC would also be capable of applying DFS. Handling the coexistence problem based on DFS requires a number of free frequency channels to be available. This may not always be the case: under high traffic load or with a large number of active stations, or with many overlapping QBSSs, it may be advantageous and spectrum efficient that stations of different wireless networks share a single frequency channel instead of occupying different frequency channels. If all the frequency channels are already occupied by colocated WLANs, it appears to be advantageous to share a single frequency channel by stations of different WLANs. Of course, the same or similar level of QoS should be available then as if they would operate on exclusive frequency channels.

Developing a new technique to allow coexistence of CCHCs operated on the same frequency channel, is focus of the rest of this thesis.

6.3.2 Coexistence as a Game Problem

In the following, a scenario of two overlapping QBSSs coordinated by CCHCs is assumed, as illustrated in Figure 6.5.

The CCHCs are assumed to be able to detect each other all the time, and all stations operate at the same frequency channel. Two CCHCs with their QBSSs share a finite capacity radio channel. For each CCHC, independent QoS requirements are assumed to exist, that both CCHCs attempt to serve throughout a certain communication phase. This phase is a time interval with finite duration, as is the continuing resource allocation process in the coexistence scenario.

CCHCs in general are able to allocate resources whenever required. However, when both CCHCs attempt to allocate resources at the same time, both experience significant QoS degradations in what they observe after the resource allocation process.

This mutual interdependency of the CCHCs is considered as a game problem (Mangold, 2000). It is therefore proposed to analyze the CCHC coexistence problem with the theory of games, as explained in detail in the next chapter. A competition for resources across QBSSs exists with and without information exchange between CCHCs, i.e., with and without their interworking.

The game problem exists also when the CCHCs that interact with each other are capable to interwork and are able to notify each other about their individual QoS requirements. They still would have to negotiate how to allocate resources: the actual competition remains present.

In what follows, exchanging information between CCHCs is assumed to be not permitted at any time in the coexistence scenario. The use of radio resources allocated by one CCHC is observed by the opponent CCHC. Any spectrum coordination by announcing the actual QoS requirements and/or upcoming radio resource allocations is excluded here.

The reason for this restriction is that in the following the thesis is established that, in order to achieve successful coexistence between interfering CCHCs, it is not required that an explicit communication by data exchange between the CCHCs must take place. The CCHC coexistence scenario discussed in the following, and the control concepts derived from game theory that will be presented in the next chapters, will serve as example for tackling the problem of WLAN coexistence in the unlicensed spectrum. In the unlicensed spectra, WLANs following different air interface standards should be able to share radio resources similarly to how the CCHCs share resources. However, different radio networks in an unlicensed spectrum are generally not capable of exchanging information because of the

lack of a common protocol. Therefore, although technically feasible, the exchange of information for spectrum coordination between CCHCs is assumed to be not allowed, throughout the analysis in the rest of this thesis.

The following chapters provide an in-depth analysis of the CCHC coexistence problem, and offer candidate solution concepts for the general problem of coexistence of radio networks that operate in unlicensed bands.

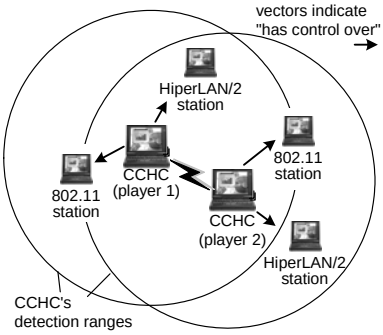

Figure 6.5: Two QBSSs each coordinated by a CCHC, both operating at the same frequency channel. Each CCHC coordinates both, interworking HiperLAN/2 and 802.11 stations and coexistence of the respective QBSSs.

Chapter 7

THE GAME MODEL

THIS CHAPTER introduces a model derived from game theory, that describes the CCHC coexistence problem as a game of decision makers. A game model is based on a set of decision makers (here entities within a CCHC device) that are called players (Fudenberg and Tirole 1991). The model will be used to analyze the coexistence problem that was identified in the previous chapters. After an overview about the approach taken in the next Section 7.1, Section 7.2 introduces the *Single Stage Game* (SSG) including the concepts of action, utility, preference and behavior. Section 7.3 introduces the *Multi Stage Game* (MSG), which will serve for the investigation of static and dynamic strategies, and rational behavior versus cooperation. Further, the prediction method that allows coexisting entities to estimate the demands of other coexisting entities is described in Section 7.4. This prediction method serves as estimator of QoS requirements of different coexisting CCHCs throughout the analysis that follows in the next chapters. The SSG will be used in Chapter 8 for an in-depth analysis of the problem, and for the definition of various kinds of so-called behaviors for coexisting entities.

The MSG will finally serve as the rational behind the concept of cooperation of coexisting entities, as studied in Chapter 9 in the context of the CCHC coexistence problem.

The vocabulary of game theory is not standardized. In this thesis, the notation and terminology of Osborne and Rubinstein (1994) and Neumann and Morgenstern (1953) are used, with many definitions taken from Fudenberg and Tirole (1991), Debreu (1959), and Green and Heller (1981).

7.1 Overview

A dynamic game model is applied to study the CCHC coexistence. The game model comprises a set of players that choose their actions in each stage of the game to maximize their expected own utility in the stage, given their assessment of their opponent's actions in that particular stage. Utilities are defined in Section 7.2.3. An action of a player is the selection of a certain way of resource allocation by a CCHC. The game model is called dynamic as players periodically adapt their action to the environment after each period of the game. At each game stage a player observes the action of its opponent together with its own utility, which is measured in the CCHC case based on the mutual influence of the player's interactions, see Section 7.2.3.

The SSG competition model that is discussed in the next section, describes one such stage of the game. Based on that model, the MSG competition model covers the dynamic effects in repeated SSGs. Whereas an SSG is played once, the MSG represents a repeated interaction of players. The MSG competition model helps to understand social phenomena between players that interact for a longer time. Section 7.2 introduces the competition model of the SSG. Section 7.3 extends the SSG to the multi stage case.

In Section 7.4, a prediction method is described that allows a player to estimate the demands of its opponent player. This approach gives way for the usage of game models with complete knowledge, i.e., games where each player determines its action after observing past actions of its opponent players and determining the demands of those opponent players from the observed actions[10]. However, knowing the demands does not imply that the actual requirements are known to the opponent players. This differentiates the coexistence scenario from an interworking scenario, as discussed earlier in this thesis.

[10] Games where the interacting players do not have any means to determine the requirements of their opponent player from their observation are referred to as games without complete knowledge.

7.2 The Single Stage Game (SSG) Competition Model

To study the coexistence between competing wireless networks, and specifically overlapping QoS-supporting QBSSs that are coordinated by CCHCs, a competition model approach is taken that is motivated by the theory of games (see Mangold 2000; Mangold et al. 2000; Mangold et al. 2001h; Mangold et al. 2002b). The problem is modeled as a strategic game. A game in a strategic form consists of a finite set of players, a set of actions for each player, a utility function that is common knowledge between the players, and individual requirements per player that parameterize the utility function, to allow the calculation of payoffs for each game stage. Competing CCHCs are modeled as rational players attempting to maximize their payoffs within the game. A payoff is a measurable quantity related to QoS a player observes after playing the game.

In the following, deterministic decision-taking processes are assumed that select a single action out of the set of actions. A single action is also referred to as pure action. Often, game models allow nonsingle, so-called mixed actions to be taken by the decision-taking processes. A player that selects mixed actions relates probabilities to actions instead of selecting one single action. A decision taken by a player in this case is an allocation of a probability to each single action. The reason for the wide use of this type of action is that often games do not converge to stable operation points if mixed actions are not part of the set of actions. This thesis is limited to game models with pure actions, to reflect that the competing CCHCs attempt to guarantee QoS by setting fixed maximum tolerable QoS thresholds. Specifically for the scheduling of isochronous, time-bounded services, or coordinating HiperLAN/2 MAC frames, the points in time when the respective TXOPs start must be accurately defined, only small delays are tolerated. Therefore, in the SSG model of competition, an action taken corresponds to one choice of resource utilization after having some knowledge about the action the opponent player may select.

Sections 7.2.2-7.2.4 describe the details of the SSG, which is the mean to analyze the coexistence of CCHCs.

7.2.1 The Superframe as SSG

A CCHC is modeled as player. Within the CCHC protocol stack, the SME includes a decision taking player entity. A CCHC's utilization of the radio channel is motivated by the requirement of all stations within its QoS supporting BSS, i.e., QBSS. This utilization of the radio channel is attained through selected actions

and determines the player's observed payoff. A successfully transmitted beacon marks the begin of each single stage of the game, where a superframe defines the duration of one single stage. Suppose that the beacon is successfully transmitted by one of the competing CCHCs. The length of the superframe, i.e., the period between two subsequent beacons (*Superframe Duration,* SFDUR), defines the capacity of the radio channel per stage of the game. The requirement for resource allocations per CCHC i (per player i) determines the number $L^i(n)$, durations $d^i_{1..L}(n)$ and starting times $t^i_{1..L}(n)$ of the TXOPs that players attempt to allocate. The starting times are determined by the allocation intervals $D^i_{1..L}(n)$. In these definitions, n is the superframe number and L^i the number of resource allocations of player i.

Figure 7.1 illustrates an 802.11 superframe that is interpreted as the SSG of two players. Player *1* (CCHC *1*) allocates three TXOPs within the n^{th} superframe, and player *2* allocates two TXOPs. Note that in addition to the high priority TXOPs, additional TXOPs may be allocated through EDCF by all contending stations. The duration of those EDCF-TXOPs are limited by the TXOPlimit, which is typically smaller than *1 ms*. They are not indicated in the figure.

As already discussed for the interworking approach in Chapter 6, the TXOPs that are considered are the TXOPs that are directly allocated by a CCHC with highest priority, i.e., without collision avoidance. These TXOPs are typically relatively long (*2…10 ms*) (Mangold et al., 2001d; ETSI, 2000c), and here particularly used to schedule HiperLAN/2 MAC frames, as well as delivering high priority MSDUs. However, there are other TXOPs offering limited QoS support that are allocated in contention under the rules of the EDCF. Those EDCF-TXOPs are not part of the analytical game model that is used to calculate stable operating points (equilibria).

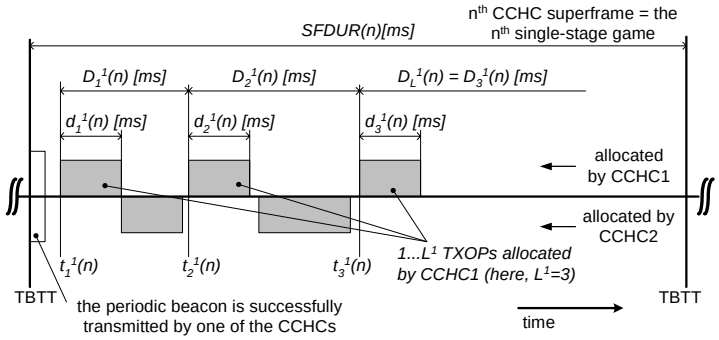

Figure 7.1: One superframe is modeled as single shot (i.e., single stage) strategic game of two players (two CCHCs).

For accurate evaluation, they are included in the simulation model where they carry background traffic for applications that require limited QoS support (modeled by Ethernet traffic traces).

7.2.2 Action, Action Space A, Requirements vs. Demands

The action defines the actual operation a player performs, based on requirements. A player that attempts to allocate resources must be aware of the fact that there are competing players, i.e., the player's opponents that also try to meet their individual requirements. An action is taken based on the expected actions of all involved players. The selection process that assigns an action to particular requirements is called the decision-taking process. This decision-taking process implements what is called behavior and strategy, i.e., the way it aims to meet certain requirements. Behaviors are discussed in Section 8.3 as part of the SSG. Strategies are discussed in the context of MSGs in Section 9.1.

Let N be the number of players, in a simplified case, $N=2$.[11] The periodic superframes define discrete time stages numbered by n. In each superframe, i.e., time stage, a player $i \in \mathbf{N} = 1,...,N$ decides to take an action $a^i(n)$, i.e., to select a certain demand, as explained in the following.

7.2.2.1 Abstract Representation of QoS

The QoS requirements that are important in the CCHC coexistence problem are (*1*) the share of capacity that determine any throughput within a QBSS, (*2*) the resource allocation periods that determines any MSDU Delivery delay within a QBSS, and (3) the variation of the delays of allocated resources. This variation of the delays of allocated resources can be calculated as time derivation of the resource allocation periods. The player's QoS requirements are taken from the traffic specifications of isochronous MSDU streams that are carried within the QBSS, as well as the HiperLAN/2 activity that a CCHC tries to support. From the perspective of a CCHC, HiperLAN/2 MAC frames are an application that it tries to carry. Here, it is assumed that the way of resource allocation changes slowly in comparison to the speed of the game, i.e., the decision-taking processes. This assumption allows claiming stationarity of the underlying decision processes.

---

[11] In this thesis, the CCHC coexistence problem is analyzed for the two player scenario only. In general, the approach taken here can be extended to games with more than two players.

Three abstract and normalized representations of the QoS parameters are defined in the following.

1. The normalized share of capacity $\Theta^i(n) \in \mathbb{R}$ at stage n, a real number without dimension, which is required $(\hat{=} \Theta^i_{req})$, demanded $(\hat{=} \Theta^i_{dem}(n))$, or observed $(\hat{=} \Theta^i_{obs}(n))$ by a player i. See Section 7.2.2.2 for the definition of QoS demand. It is always assumed that the QoS requirements stay constant throughout the game, therefore, the requirement Θ^i_{req} is not dependent on n. $\Theta^i(n) \in [0...1] \in \mathbb{R}$, where the extreme cases $\Theta^i(n) = 0$ and $\Theta^i(n) = 1$ mean the full deferral of resource allocation throughout the game stage n and the complete allocation of all resources of game stage n, respectively.

2. The normalized resource allocation period $\Delta^i(n) \in \mathbb{R}$, i.e., the time between the starting points of two consecutive resource allocations at stage n, a real number without dimension, which also can be required $(\hat{=} \Delta^i_{req})$, demanded $(\hat{=} \Delta^i_{dem}(n))$, or observed $(\hat{=} \Delta^i_{obs}(n))$ by a player i. Again, the requirement Δ^i_{req} is not dependent on n. As before, $\Delta^i(n) = [0...1] \in \mathbb{R}$. With $\Delta^i(n) \to 0$, the number of resource allocations increases, and with $\Delta^i(n) = 1$, only one resource allocation per game stage n is allocated. As part of the realistic models, a minimum number of TXOPs per superframe is required, which means that $\Delta^i(n) < 0.1$ in all stages. However, $\Delta^i(n) > \varepsilon > 0$ in all stages, with ε being defined by the precision of the medium access, which is in this thesis determined through the value of *aSlotTime* ($9\,\mu s$ in the 5 GHz wireless LAN 802.11a). Typically, $\varepsilon = 9\,\mu s / SFDUR = 4.5 \cdot 10^{-5}$ when $SFDUR = 200\,ms$.

3. The normalized delay variation $\Xi^i_{obs}(n) \in \mathbb{R}$ at stage n, a real number without dimension, which is observed, but never demanded. An upper bound for the tolerable variation can be given as requirement. Here, delay means the delay of a resource allocation, which is related to the common definition of delay, for example the MSDU Delivery delay in 802.11, but is not the same.

The normalized QoS is represented through three real numbers,

$$QoS \triangleq \begin{pmatrix} \Theta = [0...1] \in \mathbb{R} \\ \Delta = [0...1] \in \mathbb{R} \\ \Xi = [0...1] \in \mathbb{R} \end{pmatrix},$$

where Ξ is an optional parameter as explained below. All three parameters can have values between 0 and 1, without dimensions. The definitions of the QoS parameters Θ, Δ, Ξ are given with the following Equations (7.1)…(7.5).

The parameter $\Theta^i(n)$ represents the share of capacity a player *i* requires, demands, or observes at game stage *n*:

$$\Theta^i(n) = \frac{1}{SFDUR(n)} \sum_{l=1}^{L^i(n)} d_l^i(n), \tag{7.1}$$

where $L^i(n)$ is the number of allocated TXOPs of player *i* per game stage *n*, and *SFDUR(n)* the duration of the superframe in ms within this stage. Note that this value is assumed to remain constant throughout all games, in this thesis. A typical value for the SFDUR is *200 ms*. The parameter $d_l^i(n)$ describes the length of resource allocation l (duration of TXOP l) of player *i* at stage *n*, $l=1...L^i$, given in ms.

The parameter $\Delta_{max}^i(n)$ specifies the resource allocation period between subsequent resource allocations of one player *i* (TXOPs allocated by one player that follow each other), that a player *i* attempts to get allocated at game stage *n*:

$$\Delta_{max}^i(n) = \frac{1}{SFDUR(n)} max\left[D_l^i(n) \right]_{l=1...L^i(n)-1} \quad , \tag{7.2}$$

where $D_l^i(n) = t_{l+1}^i(n) - t_l^i(n)$ is the time between the starting points of the two TXOPs l and l+1 of player i in superframe n, again measured in ms. Note that $D_{L^i}^i(n) = t_1^i(n+1) - t_{L^i}^i(n)$ exceeds the superframe n. In particular, this parameter is related to the expected maximum delay of MSDU Deliveries.

The mean delay per game stage *n* for player *i*, i.e., $\Delta_{mean}^i(n)$, is defined as

$$\Delta_{mean}^i(n) = \frac{1}{SFDUR(n) \cdot (L^i(n)-1)} \sum_{l=1}^{L^i(n)-1} D_l^i(n). \tag{7.3}$$

Note that in this equation, the last resource allocation interval of stage n is not considered, as it is exceeding the superframe, and thus is dependent on duration of the beacon that is transmitted at the beginning of the next frame.

The third QoS parameter that is an optional part of the model represents the maximum tolerable delay variation of the resource allocation times for player *i*. It is defined as

$$\Xi^i_{max}(n) = \frac{1}{SFDUR(n)} max\left[\left|D^i_l(n) - D^i_{l+1}(n)\right|\right]_{l=1\ldots L^i(n)-1} \quad , \qquad (7.4)$$

and given in ms.

For the sake of completeness, the mean delay variation, also referred to as jitter, is defined as

$$\Xi^i_{mean}(n) = \frac{1}{SFDUR(n)\cdot(L^i(n)-1)} \sum_{l=1}^{L^i(n)-1} \left|D^i_l(n) - D^i_{l+1}(n)\right| . \qquad (7.5)$$

The variation of the delays of allocated resources can be interpreted as time derivation of the resource allocation period. The focus of interest in the coexistence problem is a predictable support of QoS. Therefore, the maximum instead of the mean values of Δ and Ξ are used and evaluated in the following:

$$\Delta^i(n) \overset{!}{:=} \Delta^i_{max}(n), \quad \Xi^i(n) \overset{!}{:=} \Xi^i_{max}(n) .$$

Figure 7.2 illustrates how the three QoS parameters, the share of capacity Θ, the resource allocation period Δ, and the delay variation Ξ are related to the actual allocations within an SSG. In the example, some allocations of CCHC 2 are delayed due to the busy channel through earlier resource allocations. Note that the parameter Θ can only be observed, but is never demanded.

While the SSG is discussed in the rest of this section, attention to the index n is only paid where necessary. The QoS parameter Ξ is not used for determining an actual demand of a player. Further, the decision-taking processes that will be defined later do not consider this parameter. Only a maximum tolerable delay will be part of the game model.

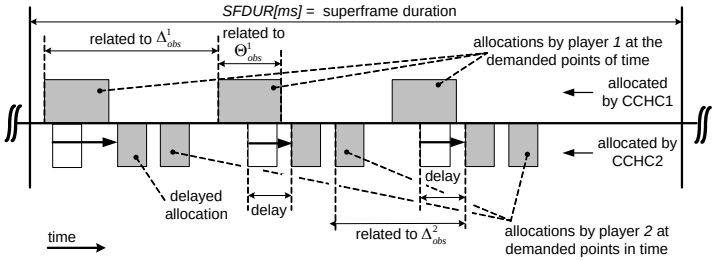

Figure 7.2: Illustration of the QoS parameters and their relation to the resource allocations.

Despite this maximum tolerable delay, the QoS parameter Ξ is neglected in the following for the sake of readability. The parameters L^i, D^i, d^i determine the times of the resource allocations of player i. They are illustrated in Figure 7.1. It is possible to express these parameters as functions of the QoS parameters:

$$\begin{aligned} L^i &= \left\lceil \frac{1}{\Delta^i} \right\rceil, \quad \Delta^i > 0; \\ D^i &= SFDUR \cdot \Delta^i; \\ d^i &= SFDUR \cdot \Theta^i \cdot \Delta^i. \end{aligned} \tag{7.6}$$

The operator $\lceil \cdot \rceil$ rounds to the nearest integer towards plus infinity. This operator is neglected in the following for the sake of analytical tractability of the model. Any value $L>0$ is allowed in the analytical model (this model is introduced in Chapter 8, p. 159). In real life and simulation, integer values are used only, i.e., $L \in 1, 2, 3, \ldots$.

7.2.2.2 Definition of Action; Required, Demanded, and Observed QoS parameters Θ, Δ

Using the abstract QoS parameters, it is possible to define what is called an action $a^i(n)$ of player i at stage n. A player i takes its action $a^i(n)$ at the beginning of an SSG with the purpose to achieve in this SSG the level of QoS that is required. This requirement is not dependent on the stage n of the game and given by the QoS requirement $(\Theta^i_{req}, \Delta^i_{req})$ of a player i.

An action is the selection of a set of QoS parameters that determine the resource allocations in this SSG. The selected QoS parameters are called the QoS demand $(\Theta^i_{dem}(n), \Delta^i_{dem}(n))$ of a player i and may vary significantly from the player's QoS requirement. As an outcome of an SSG, the resulting QoS parameters are called the QoS observations $(\Theta^i_{obs}(n), \Delta^i_{obs}(n))$ of a player i.[12] Demand and observation change dynamically in repeated SSGs and are therefore depending on the

[12] This violates the terminology of game theory. The results of a game are usually referred to as "outcome" instead of the here used term "observation". In this thesis, "observation" is used as synonym for "outcome" to highlight the wireless characteristic of the game. What is an outcome in a game of two players may be partially observed by other players that are located in the same area. These other players are not part of the game as it is defined here, but may face their own coexistence scenario in the near vicinity. From a cellular perspective on coexisting networks, the games that are developed in this thesis may be extended to models of societies of a large number of interacting individuals. Then, outcomes may be observed by neighbors, which is the motivation for referring to the game results as "observation" rather than "outcome".

stage *n*. The action of a player is to determine the QoS demand taking into consideration its QoS requirement, the estimated demands of the opponent player *-i*, $(\tilde{\Theta}^{-i}_{dem}(n), \tilde{\Delta}^{-i}_{dem}(n))$, and the history of observations, here the observations of the previous stage *n-1, i.e.,* $(\Theta^{i}_{obs}(n-1), \Delta^{i}_{obs}(n-1))$. The superscript "~" indicates that the demands of any opponent player *-i* are not known to a player *i*, but estimated from the history of observations.

Note that optimizing the estimation accuracy by taking into account a long history of past stages is out of the scope of this thesis.

An action of player *i* at stage *n* is formally defined as

$$\begin{pmatrix} \Theta^{i}_{dem}(n) \\ \Delta^{i}_{dem}(n) \end{pmatrix} := \left(\begin{pmatrix} \Theta^{i}_{req} \\ \Delta^{i}_{req} \end{pmatrix}, \begin{pmatrix} \Theta^{i}_{obs}(n-1) \\ \Delta^{i}_{obs}(n-1) \end{pmatrix}, \begin{pmatrix} \tilde{\Theta}^{-i}_{dem}(n) \\ \tilde{\Delta}^{-i}_{dem}(n) \end{pmatrix} \right) \rightarrow a^{i}(n),\ a^{i} \in \mathcal{A}^{i}, \quad (7.7)$$

where $\mathcal{A}^{i}$ is an infinite set of actions out of which a player *i* selects its action. This set represents a domain of an infinite number of alternatives from which a player selects an action. Player *i* selects its action out of $\mathcal{A}^{i}$, player *-i* selects its action out of $\mathcal{A}^{-i}$. In accordance with the notation in literature, the index *-i* refers to the opponent of a player *i*. Possible actions are taken from intervals of real numbers,

$$a^{i} \in \mathcal{A}^{i} = \begin{pmatrix} \Theta = [0...1] \in \mathbb{R} \\ \Delta = [0...0.1] \in \mathbb{R} \end{pmatrix}, \quad i \in \mathbf{N}. \quad (7.8)$$

The set of actions $\mathcal{A}^{i}$ is a single coherent[13] subset of $\mathbb{R}^{2}$, and it is thus an Euclidean space of two dimensions, $\mathcal{A}^{i} \subseteq \mathbb{R}^{2}$. The set of actions $\mathcal{A}^{i}$ is infinite and nonempty because it allows an uncountable number of actions.

The set of actions $\mathcal{A}^{i}$ is further defined as being (i) compact and (ii) convex as explained in the following. To (i): the set $\mathcal{A}^{i}$ is compact if any sequence in this space has a subsequence that converges to a limit point, which is a member of the set $\mathcal{A}^{i}$ (Bronstein and Semendjajew 1992). In other words, the bounds of the set $\mathcal{A}^{i}$ are members of $\mathcal{A}^{i}$, and $\mathcal{A}^{i}$ describes one single coherent subset of $\mathbb{R}^{2}$. This is true for the set of actions $\mathcal{A}^{i}$ defined in Equation (7.8). To (ii): the set $\mathcal{A}^{i}$ is convex if, for any $a^{i}, b^{i} \in \mathcal{A}^{i}$ and any real number $\alpha \in (0,1)$, $(\alpha \cdot a^{i} + (1-\alpha) \cdot b^{i}) \in \mathcal{A}^{i}$ (Bronstein and Semendjajew 1992). In other words, $\mathcal{A}^{i}$ has the property that all points lying at the line joining any pair of two points

[13] If any two arbitrary points of a set $S \subseteq \mathbb{R}^{n}$ can be connected through a curve that is completely a member of S, then the set S is said to be coherent.

of $\mathcal{A}^i$ are all members of $\mathcal{A}^i$ (Green and Heller 1981:37). This is true for the set of actions $\mathcal{A}^i$ defined in Equation (7.8).

Let

$$\mathbf{A} = \times_{i \in N} \mathcal{A}^i, i \in \mathbf{N} \tag{7.9}$$

be the Cartesian product (or direct product) of all N sets of actions, here $N=2$ [14]. Note that in the following, games with two players are considered. The outcome of the game at stage *n*, i.e., the observations, are the result of the resource allocation process throughout the superframe at stage *n*. This stochastic process can be analytically described and simulated with the simulator YouShi, see Appendix B. In general,

$$\left(\begin{pmatrix}\Theta^i_{dem}(n)\\ \Delta^i_{dem}(n)\end{pmatrix},\begin{pmatrix}\Theta^{-i}_{dem}(n)\\ \Delta^{-i}_{dem}(n)\end{pmatrix}\right) \Rightarrow \begin{pmatrix}\Theta^i_{obs}(n)\\ \Delta^i_{obs}(n)\end{pmatrix}, \tag{7.10}$$

which depends on the demands of all involved players *i, -i* at stage *n*. An analytical approximation of the resource allocation process of two interacting players is developed for the equilibrium analysis and described in Chapter 8. The following Figure 7.3 illustrates the concept of requirement, demand, and observation as well as the decision taking process of a player *i* in repeated SSGs.

The requirement of player *i* in all stages is given by the QoS a player *i* is trying to achieve. This requirement does not change throughout the repeated games. Player *i* selects its demand at stage *n* as part of its action within the SSG *n*.

The demand is calculated based on the estimated demand of the opponent player *-i*, which is derived from the history of past observations. The observation, i.e., the outcome of an SSG *n*, is used to calculate the demand of the SSG *n+1*. In Figure 7.3, the label "z^{-1}" denotes a time shift of one stage duration. Here, the outcome of a single previous stage *n* is used by the player at a particular stage *n+1* to determine what action to take at this stage *n+1*.

---

[14] The Cartesian product (or the direct product) is defined as $\mathcal{A}^i \times \mathcal{A}^{-i} = \{(a,b) : a \in \mathcal{A}^i \text{ and } b \in \mathcal{A}^{-i}\}$. A denotes therefore a subset of an Euclidean space of four dimensions, $\mathcal{A} \subseteq \mathbb{R}^4$, as $a = (\Theta^i, \Delta^i)$, and $b = (\Theta^{-i}, \Delta^{-i})$.

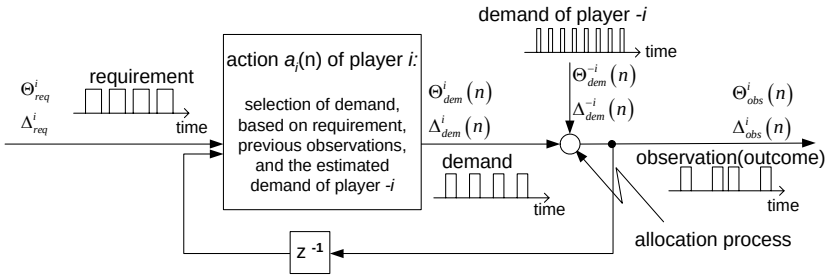

Figure 7.3: The different QoS parameters of player *i* in repeated SSGs. The requirement is given by the QoS a player is trying to support. As part of its action within a game, a player selects its demand based on the estimated requirements of the opponent player, taken from the history of observations.

7.2.3 Utility

The utility $U^i \in \mathbb{R}_0^+$ of player *i* defines what a player *i* gains from its action $a^i(n)$. This utility is a set-based function over the set A^i, and defined as follows. The definition takes into account all relevant aspects of what a CCHC actually requires, and whether or not the observed QoS is satisfying a particular QoS. In general, utility functions represent a "measure of satisfaction" (Goodman and Mandayam 2000:48) an individual player is experiencing. In the CCHC coexistence game, this level is determined by the QoS requirements in an overlapping QBSS.

7.2.3.1 Utility as Function of Observed Share of Capacity and Observed Resource Allocation Interval

Based on the selection of an action, a player *i* obtains a utility that is dependent on two normalized utility terms $U_\Theta^i \in \mathbb{R}_0^+$ and $U_\Delta^i \in \mathbb{R}_0^+$ that represent the utility as a nonnegative real number with respect to the share of capacity and with respect to the observed resource allocation interval, respectively:

$$U^i = U_\Theta^i(\Theta_{dem}^i, \Theta_{obs}^i, \Theta_{req}^i) \cdot U_\Delta^i(\Delta_{obs}^i, \Delta_{req}^i), \quad U^i \in \mathbb{R}^+. \tag{7.11}$$

Both utility terms can have values between *0* and *1*, thus $0 \le U^i \le 1$. To maximize its utility, a player has to consider both, share of capacity as well as delays. The utility as it is defined in this section reflects all relevant characteristics of the CCHC requirements in terms of QoS. There are many approaches to reflect such characteristics with different functions. In this thesis, an approach based on rational functions is selected to simplify the analytical game analysis. However,

other utility functions may be applicable when modeling the preferences of a player in the CCHC coexistence game.

The first utility term U^i_Θ, which is related to the share of capacity, is defined as

$$U^i_\Theta := \left(\Theta^i_{dem}, \Theta^i_{obs}, \Theta^i_{req}\right) \rightarrow \left(1 - \frac{1}{\left(1 + u \cdot \left(\Theta^i_{obs} - \Theta^i_{req} + \Theta^i_{tolerance}\right)\right)}\right) \cdot \left(1 + v \cdot \left(\Theta^i_{req} - \Theta^i_{dem}\right)\right) \tag{7.12}$$

if $\Theta^i_{obs} \geq \Theta^i_{req} - \Theta^i_{tolerance}$ and *0* other wise. The observations and demands in this equation (and in the following Equation (7.13)) vary with *n*, whereas the requirement stays constant over the repeated SSGs.

The *u* and *v* parameters in Equation (7.12) define what is referred to as elasticity, i.e., tolerable deviation of the share of capacity, as

$$\Theta^i_{tolerance} = \frac{\sqrt{v^2 + u \cdot v} - v}{u \cdot v}, \quad u, v \in \mathbb{R}^+, \quad u, v > 0 \,.$$

This parameter is indicated in Figure 7.4. It is dependent on the two shaping parameters $u, v \in \mathbb{R}^+$, $u, v > 0$ as is $U^i_\Theta(\Theta^i_{dem}, \Theta^i_{obs}, \Theta^i_{req})$. Figure 7.4 illustrates the first utility term $U^i_\Theta(\Theta^i_{dem}, \Theta^i_{obs}, \Theta^i_{req})$ and the influence of the shaping parameters u, v with a requirement $\Theta^i_{req} = 0.4$ as example.

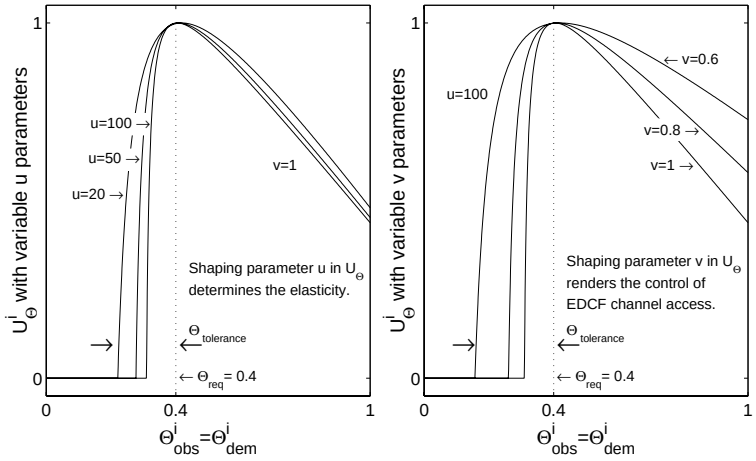

Figure 7.4: First utility term $U^i_\Theta(\Theta^i_{dem}, \Theta^i_{obs}, \Theta^i_{req})$ of a player *i* vs. observation $\Theta^i_{obs} = \Theta^i_{dem}$, with $\Theta^i_{req} = 0.4$. Left: varying *u*, right: varying *v*. Maximum utility is observed if the requirement is reached. The share of capacity can be any value between *0* and *1*.

Note that $U^i_\Theta(\Theta^i_{dem}, \Theta^i_{obs}, \Theta^i_{req})$ is a function of the demand as well as observation, violating a pure game theoretical approach. The utility a player observes decreases with increasing demand for share of capacity. There is no obvious reason for the utility to decrease in case of high capacity demand, i.e., $\Theta^i_{dem} \to 1$.

However, demanding higher capacity for the highest priority access would result in poor EDCF results due to its lower priority.

To influence a player not to overload the channel by demanding all available resources, the v parameter shapes the function to decrease the resulting utility with increasing demand, for the benefit of the EDCF based medium access.

This is related to the demand-driven cost of resource in economic competition models, which determines a price to be paid when demanding an individual share of common good. The cost of resources is a result of the cumulative demand of all involved players for that particular resource. The phrase "price" suggests a monetary transaction, but it does not involve real money; it is an abstract model of cost.

The u-parameter allows modeling what is referred to as elasticity: depending on this parameter, a player may strictly demand what it requires, or it may be satisfied with observations that actually differ to a certain extent from the requirement. Both shaping parameters are assumed constant throughout the game, and known by all players.

The same shaping parameters as before, u and v are used for the definition of the second utility term U^i_Δ, which is related to the resource allocation period, see Equation (7.13). The shaping parameters are now multiplied by 10 to consider smaller Δ-parameters. Note that in typical situations, all $\Delta = [0 \ldots 0.1]$, whereas all $\Theta = [0 \ldots 1]$.

$$U^i_\Delta := \left(\Delta^i_{obs}, \Delta^i_{req}\right) \to \left(1 - \frac{1}{1 - 10 \cdot u \cdot \left(\Delta^i_{obs} - \Delta^i_{req} + \Delta^i_{tolerance}\right)}\right) \cdot \left(1 + 10 \cdot v \cdot \left(\Delta^i_{obs} - 2 \cdot \Delta^i_{req} + \Delta^i_{tolerance}\right)\right) \tag{7.13}$$

if $\Delta^i_{obs} \le \Delta^i_{req} - \Delta^i_{tolerance}$ and 0 otherwise. The parameter $\Delta^i_{tolerance}$ is related to the maximum extension of the allocation periods and is defined as

$$\Delta^i_{tolerance} = \frac{\sqrt{(10 \cdot v)^2 + 10 \cdot u \cdot 10 \cdot v} - 10 \cdot v}{10 \cdot u \cdot 10 \cdot v}, \quad u, v \in \mathbb{R}^+, \quad u, v > 0 . \tag{7.14}$$

The value of this parameter is given by the tolerated variation of the delay of resources allocations Ξ^i that was discussed in Section 7.2.2.1.

Figure 7.5 illustrates the second utility term $U^i_\Delta(\Delta^i_{obs},\Delta^i_{req})$. As in $U^i_\Theta(\Theta^i_{dem},\Theta^i_{obs},\Theta^i_{req})$, the v parameter models a decrease in utility with decreasing observation, i.e., $U^i_\Delta \to 0$ if $\Delta^i_{obs} \to 0$. This is motivated by the fact that real-time applications, as well as HiperLAN/2 MAC frames integrated into the 802.11 protocol require constant time periods that should not be extended by unpredictable delays.

If $\Delta^i_{obs} > \Delta^i_{req}$, QoS support is limited. In addition, too short resource allocation intervals are not useful as well, i.e., when $\Delta^i_{obs} \ll \Delta^i_{req}$. This is represented by the utility function discussed here. The utility function therefore decreases for small resource allocation intervals.

The *v* parameter in $U^i_\Delta(\Delta^i_{obs},\Delta^i_{req})$ has thus a different intention, although it is used the same way as in $U^i_\Theta(\Theta^i_{dem},\Theta^i_{obs},\Theta^i_{req})$. However, $U^i_\Delta(\Delta^i_{obs},\Delta^i_{req})$ does not depend on the demand Δ^i_{dem}.

In the next chapters, where the utility defined here is extensively used for the analysis of the SSG and the discussion of behaviors and strategies, the *u* and *v* parameters are set to these common values:

$$u = 10, \qquad v = 1. \tag{7.15}$$

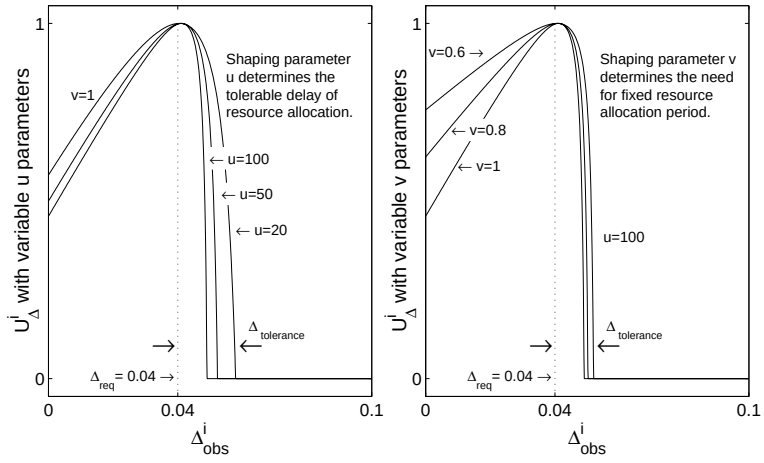

Figure 7.5: Second utility term $U^i_\Delta(\Delta^i_{obs},\Delta^i_{req})$ of a player *i* vs. observation Δ^i_{obs}, with $\Delta^i_{req} = 0.04$. $U^i_\Delta(\Delta^i_{obs},\Delta^i_{req})$ is not dependent on the demand. Left: varying *u*, right: varying *v*. This figure is shown for $\Delta^i_{obs} = 0 \ldots 0.1$, as the minimum number of resource allocation attempts per player and stage is *10*.

In the approach that is taken in this thesis it is assumed that these numbers are used by all players, and further they are assumed common knowledge among the players. In real life, individual players may have different preferences and therefore may implement autonomous shaping parameters, which vary from player to player. However, in this thesis the players attempt to establish a share of resources between networks instead of traffic classes with individual preferences in terms of the shaping of the utility functions. Therefore, u and v are equally used as defined in Equation (7.15).

As stated above, the observations and demands in Equation (7.12) and (7.13) vary with n, whereas the requirement stays constant over the repeated SSGs.

Figure 7.6 shows the resulting utility U^i as a function of the observation for a requirement of $(\Theta^i_{req}, \Delta^i_{req}) = (0.4, 0.04)$. It can be seen that there is one single observation that – if it is selected by the player i – maximizes the utility. In the ideal case that is shown here, the player observes what it is demanding, i.e., there is no competition for resources.

Therefore, the optimal action $a^i* = (\Theta^i_{dem}*, \Delta^i_{dem}*)$ here is to demand the requirement $(\Theta^i_{req}, \Delta^i_{req}) = (0.4, 0.04)$. Note that the utility U^i is strictly concave in $(\Theta^i_{obs}, \Delta^i_{obs})$ for all $U^i > 0$ and concave in $(\Theta^i_{obs}, \Delta^i_{obs})$ for any utility U^i.[15]

The principle of a utility as a function of observation and demand is used to inspire players not to overload the channel by selecting actions without taking into account the effect of their decisions on the opponent players. Accurately defined utility functions will lead to the selection of demands that allow co-located CCHCs to coexist. A utility function is a tool to encourage players to act in a way that optimizes the usage of shared resources. Interacting players are forced by the utility to use shared resources most efficiently. As part of the game approach, it is supposed that there is a common knowledge about the utility function, i.e., all players know the utility function as part of radio regulations or as part of standardized protocols. A fundamental assumption that is taken for the underlying game model is that the utility function including the shaping parameters of the utility function is common knowledge, i.e., a player knows the utility function, and "knows that its opponents know it, and knows that its opponents know that it knows, and so on ad infinitum" (Fudenberg and Tirole 1991:4). This is true if all CCHCs follow the game model. However, this does necessarily re-

[15] A function $f:\mathbb{R}\rightarrow\mathbb{R}$ is concave if $f(\alpha\cdot x+(1-\alpha)\cdot x') \geq \alpha\cdot f(x)+(1-\alpha)\cdot f(x')$, and strictly concave if $f(\alpha\cdot x+(1-\alpha)\cdot x') > \alpha\cdot f(x)+(1-\alpha)\cdot f(x')$ for all $x, x' \in \mathbb{R}$, and all $\alpha \in (0,1)$ (Osborne and Rubinstein 1994:7). In particular, a linearly increasing function is concave.

quire that players know the QoS requirement of their opponents. Because of the coexistence approach without interworking, i.e., without information exchange, players observe actions of their opponent player and with the help of a prediction method the demands of their opponent player, but do not have access to the QoS requirements their opponent player is attempting to achieve. The prediction method to determine the demand of the opponent player from the observations is explained in Section 7.4.

It is assumed that one common utility function is used by all players, where the individual players do not know the parameters of the utility functions of their respective opponents.

For the game approach to be successfully applied, all involved radio systems have to follow it.

It is not the intention of this approach to allow a CCHC to improve its performance against legacy stations, i.e., stations that do not follow the game approach. However, upon detecting a co-located legacy station, a CCHC does model this opponent as a so-called myopic, persistent player, which does not consider any utility, but attempts to allocate its requirement. There are strategies that optimize the utility against such players, as will be shown in Chapter 9.

7.2.3.2 Preference and Behavior

The utility U^i represents the preference relation $\succsim^i$ of player i in the sense that $U^i(a) \geq U^i(b)$ whenever $a \succsim^i b$, with $a, b \in A^i$. In this case it is said that a is preferred over b, a weakly dominates b. If $U^i(a) > U^i(b)$, a strictly dominates b, i.e., $a \succ^i b, a, b \in A^i$. The binary operator "$\succsim^i$" can be understood as a function from A to A^i (Debreu 1959:6).

A behavior that a player actually is following is based on such preferences. For example, a player may attempt to maximize its utility within the current stage n by selecting a demand that optimizes its own utility. In contrast, it may prefer to select a demand that allows the opponent player to achieve a certain utility as well. Various kinds of behavior are introduced in Section 8.3.

7.2.4 Payoff, Response and Equilibrium

So far, the utility was introduced as a value that represents the QoS a player observes. Because the observed utility is dependent on the actions of all involved players, another term is introduced that highlights this dependency.

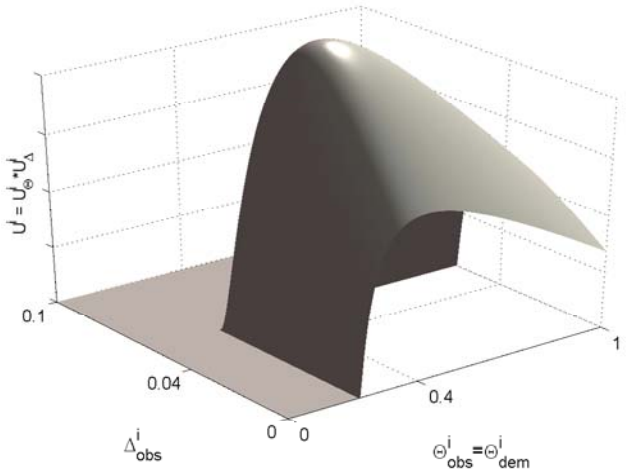

Figure 7.6: Utility U^i of a player i vs. observation $(\Theta^i_{obs}, \Delta^i_{obs})$, with $(\Theta^i_{req}, \Delta^i_{req}) = (0.4, 0.04)$. There is no impact of any opponent player -i in this example, the player i observes its demands. To demand the requirement is the action that maximizes the observed utility.

The resulting utility as the outcome of an SSG at stage *n* is called the observed payoff V^i:

$$V^i(\underline{a}(n)) := (a^i(n), a^{-i}(n)) \quad \rightarrow \quad U^i(n), \qquad a(n) \in \mathrm{A} = \times_{i \in N} \mathrm{A}^i \qquad (7.16)$$

Here, $\underline{a}(n) = (a^i(n), a^{-i}(n))$ is a vector of actions, which is also referred to as action profile. The principle of an observed payoff completes the SSG model. The payoff describes what a player receives as utility for selecting an action, as function of the demand of all involved players. It denotes the single stage payoff of the player i as function of the actions, or demands, of all involved players i, -i. Figure 7.7 shows the payoff $V^i(\underline{a}(n))$ of player i for the utility function presented above. In this example, the same requirements as before are assumed, whereas player -i demands $(\Theta^{-i}_{dem} = 0.4, \Delta^{-i}_{dem} = 0.04)$. Comparing the payoff in Figure 7.7 with the utility in Figure 7.6, the mutual impact of the allocation processes of the players can be clearly seen. The optimal action of player i, i.e., the action that maximizes the observed payoff, differs significantly from its requirement, i.e., the action that maximizes the utility when no other player demands any resources.

In contrast to decision problems, in a game each player has only partial control over the environment. The payoff of each player depends not only upon its actions but also upon the actions of other players. As consequence, when demanding resources, a player must therefore act by taking into account the possible demand of resources of its opponent. This may be interpreted as response or

reaction to the opponent's actions. A best response is the action that maximizes the player's expected payoff. A player that selects this action is in this thesis referred to as acting rationally by responding to the correct expectation about its opponent player's actions. Figure 7.7 shows the payoff of player *i* in stage *n*, $V^i(\underline{a}(n)) = V^i(a^i(n), a^{-i}(n))$, where in this example it is assumed that the opponent player takes the action $a^{-i}(n) = (0.4, 0.04)$. When players interact, there is another payoff $V^{-i}(\underline{a}(n))$ for the opponent player *-i*, which also depends on the action of both players. This payoff is not shown in Figure 7.7. In an SSG without history, and without information exchange between players, the players cannot estimate the upcoming actions of their opponents. What action their opponent player will take is not known to any player.

For successful QoS support, demands must be selected, i.e., actions must be taken, that allow a minimum level of observed QoS, i.e., a minimum payoff, regardless what action the opponent takes. This leads to inefficient usage of resources. In contrast, if there is mutual knowledge about the opponents, this can be used to coordinate the actions. Such knowledge may be taken from the history of interaction of earlier games (as it is assumed in this thesis), or through dedicated information exchange (for example via a common spectrum coordination channel).

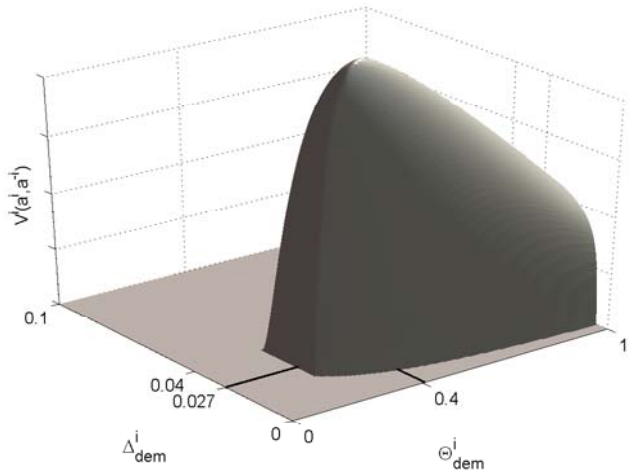

Figure 7.7: Payoff $V^i(\underline{a}(n))$ of player *i* vs. demand $a^i = (\Theta^i_{dem}, \Delta^i_{dem})$, with the same requirements as before, $(\Theta^i_{req}, \Delta^i_{req}) = (0.4, 0.04)$. The player *i* does not observe its requirements and does not observe its demands due to the implications of the actions taken by the opponent player *-i*. Indicated is the optimal action $a^i* = (\Theta^i_{dem}* = 0.4, \Delta^i_{dem}* = 0.027)$. In this example, the opponent player *-i* demands $(\Theta^{-i}_{dem} = 0.4, \Delta^{-i}_{dem} = 0.04)$. The figure is based on the analytical model of the SSG, as described in Section 8.1.

The possibility of information exchange does not contradict the game approach that is taken here. There are still competing entities that have different interests. The question arises if there is an action of a player that is optimal in the sense that it maximizes the observed payoff of a player. Further, it is of interest if there exists an action vector $\underline{a}^*(n) = (a^i*(n), a^{-i}*(n))$, with $\underline{a}^*(n) \in \mathrm{A}$, that maximizes the payoff for all players in the sense that no player can improve its payoff by unilaterally changing its action. If such an action vector exists, it is of interest if it is unique, and a stable operation point, i.e., equilibrium point in $\mathrm{A} = \times_{i \in N} \mathrm{A}^i$. It is further not necessary that this operation point is efficient, which means that there can be another action vector that leads to higher payoffs for all players, but requires that all players take this action, with the individual risks for each player of observing very poor payoff results.

These questions that are most relevant for solutions to the problem of coexisting CCHCs are discussed in Chapter 8 with the help of an analytic approximation of the SSG. A deeper look is taken in the context of repeated interaction in Chapter 9.

7.3 The Multi Stage Game (MSG) Competition Model

Repeated SSG are referred to as *Multi Stage Games* (MSGs) and introduced in this section. Coexisting CCHCs operate in relatively time-invariant radio environment. Due to the nomadic mobility in wireless LANs, coexisting CCHCs interact for such long durations that a large number of repeated SSGs can be assumed as representation of a typical CCHC coexistence scenario. The QoS requirements a player attempts to support may more dynamically change than the positions of the involved radio stations. The mobility of stations in a wireless network characterizes the dynamics of changes of the radio environment. This mobility is known to be small in indoor scenarios of wireless LANs. Here specifically the coordination of CCHCs that support integrated protocols such as HiperLAN/2 are in the focus of interest, not the direct support of any particular application. The changes of QoS requirements of CCHCs are not as dynamic as the changes of QoS requirements of characteristic applications.

It is therefore assumed in the following that the QoS requirements of a CCHC change slowly compared to speed of the decision processes. In the simulation that will be discussed later, this is taken into account by changing the actions from one profile to the other not in one step, but taking a number of stages for slow changes.

Throughout the play of an MSG, the QoS requirements of each player will stay constant. In case the QoS requirements change, another MSG will be used to analyze the subsequent time for which the selected actions of the involved players have to adapt to the new QoS requirements.

MSGs allow the analysis of the dynamic effects of competition. In an MSG, players are able to condition their actions on the way their opponent played in previous stages.

This is done by applying strategies: a strategy completely describes how a player plays an MSG from the first stage to the final stage of the MSG (Shubik 1982:34). Based on a strategy, players select behaviors upon certain events, hence a dynamic interaction can be established where the players adapt their behavior. Still operating in the domain of alternatives that are available in the SSG, in an MSG, players are concerned with rapidly achieving a certain level of payoff that is stable until the end of interaction. While interacting, the moment when the MSG will end is not known to the individual players. The MSG is a finite game with unknown end.

In the context of the CCHC coexistence scenario, not the outcome after an SSG with its short duration is to be optimized by a player, but the resulting outcome over the complete time of interaction, i.e., the complete MSG. In addition, strategies must provide means to allow a player to assess in advance what level of QoS can be supported in a certain environment. For this purpose, a player has to understand the influence of any upcoming actions of the opponent player on the own payoff results. Once this influence of the opponent is known, mutual support may help to optimize the observed payoffs in the game, which often is beneficial for all players. This is called cooperation (Shubik, 1982). The concept of cooperation –in some publications referred to as mutuality– between players is helpful to understand what can be gained by mutual support and will be analyzed in the Chapter 9. See Stephens and Anderson (1994) for some interesting discussions about cooperation, and mutuality. A cooperating player implements a strategy that does not select a behavior for its best response (called rational behavior). Instead, it deviates towards a behavior that, if the opponent player also deviates from its best response, results in a larger payoff for both players. This is referred to as efficient behavior, see Section 8.3. With this behavior, based on mutual support, players may achieve a better outcome in an action profile that is not necessarily a stable operation point and thus requires what is referred to as cooperation. The next Chapter 8 will show that in the game of coexisting CCHCs, such an efficient action profile indeed exists. If a player knows from the past interaction that its opponent player also implements a similar rationale for coop-

eration in the MSG, strategies should be applied by the player to achieve cooperation with the opponent. Because of cooperation, the grade of QoS that can be supported by a CCHC may become predictable by interacting players, after having successfully established a stable cooperation.

An in-depth analysis of strategies in the MSG and the concept of cooperation is given in Chapter 9.

7.4 Estimating the Demands of the Opponent Player

The MSG model relies on the assumption of interacting players that attempt to maximize their payoff. Maximizing a payoff implies that players select the best response to their believes of what action the opponent players take. This requires that a player has knowledge about the actions of its opponents before the decision of what action to take. This is in general not a realistic assumption. However, if it is taken into account that the SSG is played repeatedly, and if players adapt their demands slowly, this assumption can be made if there are means to mutually predict the opponent's demands. Such a prediction requires that players estimate the upcoming actions of their opponent players from their past observations.

7.4.1 Description of the Estimation Method

In this section, an algorithm to estimate the demand of a player's opponent from an observation is described. The estimation is used as prediction method during simulation with the simulation tool YouShi (see Appendix B for a description of the simulator). In the game approach taken here, a player predicts at the end of each stage n that the opponent will take the same actions in stage $n+1$ as it is estimated based on the observations of stage n.

To predict the action, i.e., the demand of the opponent player -i at stage $n+1$, it is necessary for a player i to calculate the parameters that actually determine the demanded resource allocations:

$$D^{-i}(n), d^{-i}(n), L^{-i}(n) \quad \Rightarrow \quad \begin{pmatrix} \tilde{\Theta}^{-i}_{dem}(n+1) \\ \tilde{\Delta}^{-i}_{dem}(n+1) \end{pmatrix}.$$

See Figure 7.1 for an illustration of these parameters. Whereas $d^{-i}(n)$ can be accurately observed, $D^{-i}(n), L^{-i}(n)$ can only be estimated. Allocations may have been delayed, or failed through collisions. Thus, the observation may considerably

differ from what a player may have demanded. For the estimation of the demand, the prediction algorithm selected in this thesis uses the time correlation of the resource allocations that have been successfully allocated in the past stage n by the opponent player *-i*. The information for the prediction are (*1*) the times $t_1^{-i}(n), t_2^{-i}(n), \ldots$ when resources have been allocated in the past, and (*2*) the time of the last *TBTT*, i.e., the begin of the last SSG. The history of the resource allocations is transformed into a discrete sequence of elements $s(k)$, where $s(k)=1$ if a start of a resource allocation was detected in the time interval $[k \cdot aTimeUnit; (k+1) \cdot aTimeUnit]$, and $s(k)=0$ otherwise:

$$s(k) \in [0;1], \quad k = 0 \ldots K, \quad K = \frac{SFDUR}{aTimeUnit}. \tag{7.17}$$

The value of *aTimeUnit* determines the precision of the sequence and is set to a value below the TXOPlimit, typically $100\,\mu s$. The TXOPlimit defines the maximum duration of resource allocations based on EDCF. In Equation (7.17), The SFDUR determines the boundaries defining the interval that is represented by $s(n)$. With an appropriate window size W, the autocorrelation properties of $s(n)$ are used to calculate the estimated times of resource allocations of the opponent player. With

$$\varphi(l) = \frac{1}{2W+1} \sum_{m=K-W}^{W} s(m) \cdot s(m+l),$$

any local maximum of the right-hand side of $\varphi(l)$, $max\left[\varphi(l)\big|_{l>0}\right] \Rightarrow l = l_{max}$ indicates a periodic detection of resource allocations. The value of l indicates how often this period was detected: the larger the value the higher the number of detections. The first maximum towards *0* determines the estimated resource allocation period $l_{max} \Rightarrow D^{-i}(n)$, which then can be used to calculate $L^{-i}(n)$.

7.4.2 Evaluation

Figure 7.8 and Figure 7.9 illustrate the capability of the prediction method. In the figures, the QoS parameters of one player *i* and their predictions by player *-i* are shown for 40 repeated SSGs. Figure 7.8 illustrates the demanded, observed, and predicted shares of capacity Θ. Figure 7.9 illustrates the demanded, observed, and predicted resource allocation intervals Δ. The observations differ from the demands in some stages because of the competing allocation processes of the two players. The share of capacity Θ_{dem}^{i} demanded by player *i* varies from stage to stage, as can be seen in Figure 7.8.

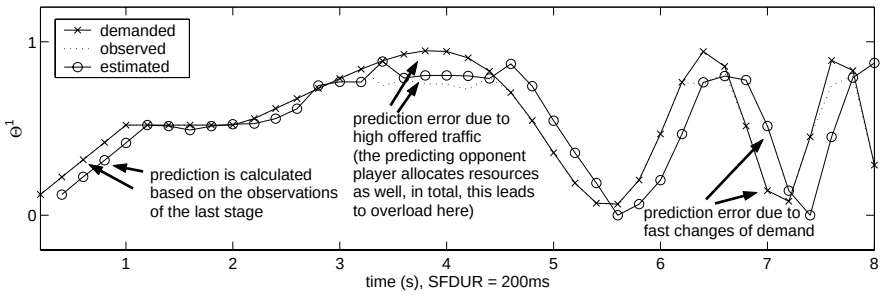

Figure 7.8: Demanded, observed, and predicted shares of capacity Θ in 40 repeated SSGs (equivalent to *8 s*), with changing demands. The prediction is an estimation of the demands. The opponent player demands $(\Theta^{-i}_{dem} = 0.3, \Delta^{-i}_{dem} = 0.03)$ constantly throughout all games. EDCF background is modeled with Ethernet traffic trace (*5 Mbit/s* offered traffic).

In addition to its varying Θ^{i}_{dem}, player *i* demands further varying resource allocation intervals between $\Delta^{i}_{dem} = 0.03$ and $\Delta^{i}_{dem} = 0.05$ for the first *2 s*. After *2 s*, the demand remains constant at $\Delta^{i}_{dem} = 0.04$ for the rest of the stages, as can be seen in Figure 7.9.

However, player *-i* also attempts to allocate resources while estimating demands of player *i*. In this example, player *-i* demands $(\Theta^{-i}_{dem} = 0.3, \Delta^{-i}_{dem} = 0.03)$ continuously throughout all games. In addition, EDCF background traffic is present at all stages, modeled with an Ethernet traffic trace offering *5 Mbit/s*.

It can be observed from the figures that the prediction is accurate as long as the channel is not overloaded (see for example the times of high offered traffic around *4 s)*. Further, as long as the demand remains constant (as for examples around *1.5 s*) over some stages, the prediction is relatively successful. In contrast, as soon as it changes dynamically (as for example around *0.5 s*), the prediction is less successful. This results from the fact that the estimating player *-i* predicts the demands of player *i* based on the history of observations of earlier stages. This problem is clearly visible in Figure 7.8 for the last stages of the repeated SSGs (at around *6...8 s*). Here, the player *i* changes its demands very fast with a high dynamic, thus, the prediction errors become unacceptable. The two failed predictions indicated in Figure 7.9 occur because the number of resource allocations by player *i* has dropped down to $\Theta^{i}_{dem} \rightarrow 0$ at the respective stages because of its small demands for shares of capacity. Hence, estimating the demanded resource allocation interval of player *i* is less successful at these stages. It can be concluded from the example illustrated in the figures that, as long as the channel is not overloaded, and as long as the QoS demands do not change too fast, the estimation method is sufficiently accurate for predicting the demands of an opponent player.

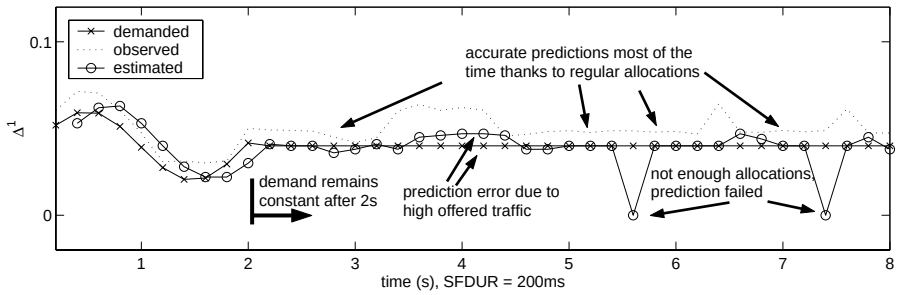

Figure 7.9 Demanded, observed, and predicted resource allocation intervals Δ in the same 40 repeated SSGs as shown in Figure 7.8. The demands change during the first *2 s*. The prediction is an estimation of the demands. The two failed predictions result from the small demands for Θ at these stages.

Clearly, the prediction method as it is realized here relies on the correlation in time of resource allocation attempts. The more regular the opponent allocates resources, the more accurate the prediction. If a player cannot successfully allocate its resources at its demanded times, it is more difficult to estimate its demand from the history of its allocations. Further, the more dynamic a player adapts its demands to the environment and to any change in requirements, the less useful the prediction of this player's demand becomes. In the MSGs discussed in this thesis, the requirements do not change throughout the course of an MSG. This must be kept in mind when dynamic strategies are discussed in the context of MSGs, see Chapter 9.

The way the predictor uses the algorithm described in the previous section is illustrated for one example in Figure 7.10, p. 157. In this example, the mutual prediction with the resource allocation interval predictor is shown. It is indicated how the right hand sides of the auto correlation functions are used to predict the upcoming actions of opponent players. In the figure, it is shown that even when the players mutually delay their allocations, a reliable prediction is possible as long as the allocation attempts occur regularly with constant periods. This is the reason for the accuracy of most of the predictions in the example illustrated in Figure 7.8 and Figure 7.9.

7.4.3 Application and Improvements

By applying the predictor as it is introduced here, the knowledge of the opponent's demand enables the player to interact during an MSG. It depends on the player's strategy if they mutually support each other, or if they aim to optimize their own payoff only. Knowing the opponent's demands, a player is able on the

one hand to prevent the opponent from successful allocation by taking an action that reduces the observed payoff of the opponent. On the other hand, a temporary withdraw of allocations may be preferred by a player, in order to let the opponent player achieve a maximum utility. In any case, it is of importance that a player has knowledge about the current demands, which is realized by applying the predictor.

There are other ways to predict the demands the opponent player has which may lead to more accurate results, as they have been used in a different context in Kyriazakos (1999) and Mangold and Kyriazakos (1999).

The improvement of the estimation method to predict demands from the history of allocations is not within the scope of this thesis. Possible improvements of the prediction accuracy by for example averaging the history of past observations within a number of SSGs. See Berlemann (2002) for an in-depth analysis of the prediction as well as a discussion of the gain of a common spectrum coordination channel that allows information exchange between players, and thus eliminates the need for the mutual prediction of demands. This gain is given through the limitations of the predictor. The less accurate the prediction, the more helpful becomes a spectrum coordination channel that is common to all players.

7.5 Concluding Remark

When viewing the CCHC coexistence problem as a game of players, several questions can be answered by applying the model, such as whether there exists a stable operation point, whether this stable point is unique, whether the dynamic system actually converges to this point, and if it converges, how fast does it converge.

In the context of the wireless LAN 802.11e, it is important to understand the level of QoS that can be supported by overlapping QBSSs that operate on a shared medium in the unlicensed band. Further, as part of the MSG discussion, it is beneficial to analyze possible behaviors of overlapping networks. With the help of the game model, sharing rules, or a spectrum etiquette can be defined for particular frequency bands and radio systems.

The fundamental question is which action should be taken by each player in order to meet their requirements as close as possible in the presence of competing players.

This problem exists regardless of the ability of players to exchange information about their individual requirements. Solutions to this problem are developed in the following chapters.

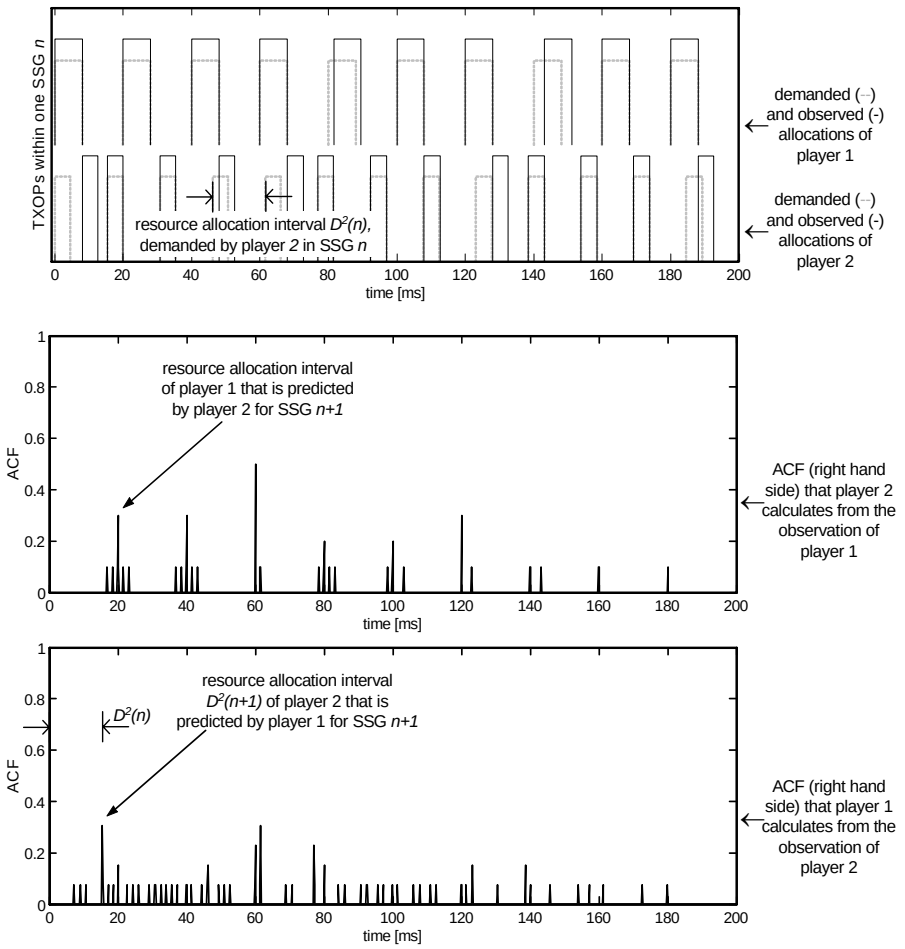

Figure 7.10: An SSG example illustrating the prediction of the opponents demand with the help of the resource allocation interval predictor. Top: resource allocations of two players within one SSG *n*, duration *200 ms*. Center and bottom: right hand sides of the auto correlation functions that are used to predict the upcoming actions of player *1* and player *2*, respectively.

Chapter 8

THE SUPERFRAME AS SINGLE STAGE GAME

BEFORE the actual play of a *Single Stage Game* (SSG), players must take their actions for that particular stage. A player i takes its action based on its own QoS requirements that are given by Θ^{i}_{req}, Δ^{i}_{req}, with the consideration of the opponent player's demands $\widetilde{\Theta}^{-i}_{dem}, \widetilde{\Delta}^{-i}_{dem}$. As before, the index $-i$ refers to the opponent of a player i. Note, that the superscript "~" indicates the fact that the demands of any opponent player $-i$ are not known to a player i, but estimated from the history of earlier stages of repeated SSGs. A player attempts to optimize its expected utility that depends on the QoS observations $\Theta^{i}_{obs}, \Delta^{i}_{obs}$. For this reason, a player must be able to estimate the expected QoS observations, i.e., the outcome of a game in advance, while decision taking. It has to approximate the expected observations based on its own demands and the demands of the opponents. An analytical approximation of the SSG that can be used by a player for this purpose is developed in the next Section 8.1. In this section, after the approximation is explained in detail, it will be demonstrated that it is accurate enough to allow players to capture the statistical characteristics of the current stage of a game, i.e., an upcoming SSG. The analytical approximation of the SSG results in values for the observed share of capacity and for the observed resource allocation period. For the observed resource allocation period an upper bound is given. Such an upper bound of the resource allocation period is the relevant information that is required for the support of QoS.

Whereas the model is simple enough to allow players to estimate the outcomes in a game in advance, this model is also used for the equilibrium analysis of the SSG, see Section 8.2. This equilibrium analysis will show the characteristics of the competition scenario of two CCHCs operating with the same radio resources.

Based on this analysis, various behaviors are defined in Section 8.3, where the efficiency of equilibria in the SSG is discussed. These behaviors are the base for the strategies that are investigated in Chapter 9.

8.1 Approximation of the QoS Observations of the Single Stage Game

8.1.1 The Markov Chain P

In this section, a model for the game of two players that allows an analytical approximation of the expected observations as functions of the demands is presented:

$$\left(\begin{pmatrix}\Theta^{i}_{dem}\\ \Delta^{i}_{dem}\end{pmatrix},\begin{pmatrix}\tilde{\Theta}^{-i}_{dem}\\ \tilde{\Delta}^{-i}_{dem}\end{pmatrix}\right) \Rightarrow \begin{pmatrix}\Theta^{i}_{obs}\\ \Delta^{i}_{obs}\end{pmatrix}, \qquad i,-i \in \mathrm{N} = \{1,2\}\,. \tag{8.1}$$

The approximation is calculated by means of a Markov chain with five states, which will be explained in the following sections. Note that in the rest of this chapter, the dependency of some game parameters on the game stage n is not indicated, since it is the SSG that is analyzed in this chapter.

8.1.1.1 Illustration and Transition Probabilities

In an SSG of two players, the calculation of the QoS observations is performed using the discrete-time Markov chain P illustrated in Figure 8.1 and defined by Equation (8.2). The Markov chain P is the model of the stochastic process, which approximates the SSG of two players. This Markov chain P is irreducible, as each state communicates with each other (Bertsekas and Gallager 1992).

It is assumed that the single stage game is stationary. The longer the duration of an SSG and the higher the number of allocation attempts per stage, the more stationary the process becomes. In a short SSG with relatively long and few resource allocations, the stationary distribution may depend on the starting state, or may even not exist. Therefore, a minimum of 10 resource allocations per player is required, i.e., $\Delta^{i,-i}_{dem} < 0.1$. With this restriction, stationary of the SSG can be generally assumed. Further, it is assumed that none of the states is periodic.

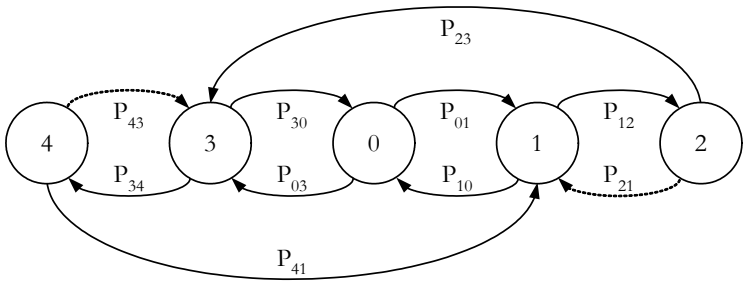

Figure 8.1: Discrete-time Markov chain P with five states to model the game of two players that attempt to allocate common resources. The default state in which the channel is idle or an EDCF frame exchange is ongoing is denoted as state 0. In case of high offered traffic, $P_{43} \to 0$, $P_{21} \to 0$, as explained in Section 8.1.2.

The aperiodic characteristic of *P* is a necessary condition for the game analysis, and cannot be assumed in general. The influence of the assumption that *P* is aperiodic is discussed in Section 8.1.3, when discussing the delay of resource allocations during an SSG, see Equation (8.12).

With $P_{03}=1-P_{01}$, $P_{10}=1-P_{12}$ and $P_{30}=1-P_{34}$, and by approximating $P_{21} \to 0$ and $P_{43} \to 0$, the corresponding transition probability matrix is denoted with

$$P = \begin{bmatrix} 0 & P_{01} & 0 & P_{03} & 0 \\ P_{10} & 0 & P_{12} & 0 & 0 \\ 0 & P_{21} & 0 & P_{23} & 0 \\ P_{30} & 0 & 0 & 0 & P_{34} \\ 0 & P_{41} & 0 & P_{43} & 0 \end{bmatrix} = \begin{bmatrix} 0 & P_{01} & 0 & 1-P_{01} & 0 \\ 1-P_{12} & 0 & P_{12} & 0 & 0 \\ 0 & 0 & 0 & 1 & 0 \\ 1-P_{34} & 0 & 0 & 0 & P_{34} \\ 0 & 1 & 0 & 0 & 0 \end{bmatrix}. \quad (8.2)$$

8.1.1.2 Definition of Corresponding States and Transitions

The five states the SSG process, which is modeled by P, can be in are:

0: The channel is idle or allocated by low priority EDCF-TXOPs that are allocating the radio channel after successful contention. It is not modeled which station is operating in this phase.

1: Player *1* successfully allocates resources with highest priority, i.e., after PIFS, without backoff. Player *2* does not attempt to allocate resources, i.e., player *2* does not wait for the channel to become idle again.

2: Player *1* successfully allocates resources with highest priority, player *2* waits for the channel to become idle, in order to allocate resources immediately.

3: Player *2* successfully allocates resources with highest priority, player *1* does not attempt to allocate resources. This state is equivalent to state p_1 that models the same situation for the opponent player *1*.

4: Player *2* successfully allocates resources with highest priority, player *1* waits for the channel to get idle, to allocate resources immediately. This state is equivalent to state p_2 that models the same situation for the opponent player *1*.

Let

$$P\left\{state\left(t+1\right)=i \mid state\left(t\right)=slot\right\}=P_{ki}, \quad i,k=0\ldots4$$

be the transition probabilities of *P*.

The transition probabilities with $P_{ki} \geq 0,\ i,\ k=0\ldots4$ are identified as:

P_{01}: Probability that player *1* allocates resources while the channel is idle or allocated by low priority EDCF-TXOPs that allocate resources via contention.

P_{03}: Probability that player *2* allocates resources while the channel is idle or allocated by low priority EDCF-TXOPs that allocate resources via contention. In a game with *2* players, $P_{03}=1-P_{01}$.

P_{10}: Probability that player *2* does not attempt to allocate resources during an ongoing resource allocation of player *1*.

P_{12}: Probability that player *2* does attempt to allocate resources during an ongoing resource allocation of player *1*, thus, $P_{12}=1-P_{10}$.

P_{21}: Probability that player *2* gives up its attempt to allocate resources before player *1* finishes its resource allocation.

P_{23}: Probability that player *2* allocates resources right after player *1* finished its resource allocation, if it attempted to allocate resources during an ongoing allocation of player *1*.

P_{30}: Probability that player *1* does not attempt to allocate resources during resource allocation of player *2*.

P_{34}: Probability that player *1* does attempt to allocate resources during resource allocation of player *2*, thus, $P_{34}=1-P_{30}$.

P_{41}: Probability that player *1* gives up its attempt to allocate resources before player *2* finishes its resource allocation.

P_{43}: Probability that player *1* allocates resources right after player *2* finished its resource allocation, if it attempted to allocate resources during an ongoing allocation of player *1*.

8.1.1.3 Solution of P

The stationary distributions of the Markov chain *P* are defined by

$$\lim_{t\to\infty} P\{state = i\} =: p_i, \quad i = 0\ldots 4,$$

and can be calculated to

$$\begin{aligned}
p_0 &= 1 - p_1 - p_2 - p_3 - p_4, \\
p_1 &= \frac{1}{2}\cdot\frac{P_{34} + P_{01}\cdot(1 - P_{34})}{1 + P_{34} + P_{01}\cdot(P_{12} - P_{34})}, \\
p_2 &= P_{12}\cdot p_1, \\
p_3 &= \frac{1}{2}\cdot\frac{P_{12} + (1 - P_{01})\cdot(1 - P_{12})}{1 + P_{12} + (1 - P_{01})\cdot(P_{34} - P_{12})}, \\
p_4 &= P_{34}\cdot p_3.
\end{aligned}$$

Here, $P_{23}\to 1$ and $P_{41}\to 1$, assuming that players tolerate delays of their resource allocation attempts, which occur when the opponent player allocates resources. It is assumed that a player never gives up its attempt to allocate resources when it waits for the opponent player to finish its resource allocation. This implies the simplification that a player does not attempt to allocate more than one resource during one single ongoing resource allocation by the opponent player. The model actually fails to represent an SSG in situations where the two players demand very dissimilar resource allocation periods. On the other hands, numerical results show that even in such unlikely configurations, the observations are still qualitatively represented by *P*.

8.1.1.4 Collisions of Resource Allocation Attempts

The two players may attempt to allocate a resource at nearly the same point in time, thus, the first MPDUs that are transmitted during resource allocation by each player may collide. It is obvious that the probability of collision does increase with decreasing $\Delta^{i,-i}$. The smaller the resource allocation period of any player, the higher the probability of medium access and collision. Further, the TXOPlimit that defines the maximum duration of a resource allocation through contention-based medium access, i.e., under the rules of the EDCF, affects the

collision probability as well: the larger the TXOPlimit, the larger may be the duration of EDCF-TXOPs allocated by any station in the environment. With larger durations of EDCF-TXOPs, a player has to wait longer times until it can start its own resource allocation. While waiting for the channel to become idle, the opponent player may also decide to attempt an allocation once the channel will become idle again. As a result, the two players will observe a collision in this case. The TXOPlimit defines a granularity in medium access and must be kept small to achieve a small probability of collision. Note that in this thesis a single TXOPlimit is assumed that is valid across all QBSSs.

However, it must not be a poll frame that collides. According to the CCHC concept and the 802.11e draft standard (IEEE 802.11 WG, 2002a), it is up to the station that allocates resources, which MPDU it selects for initial transmission after the PIFS duration. Usually a CCHC detects a collision from the missing response of the station the MPDU was directed to. How much capacity is lost when a collision occurs is therefore dependent on the length of the first transmitted MPDU within a resource allocation, i.e., within the TXOP. Here, it is assumed that the duration of the first frame is very small compared to the duration of a resource allocation by a player. Such allocations typically last for a couple of milliseconds, whereas the duration of a single first MPDU typically is smaller than $100\mu s$.

It is not the intention of this thesis to discuss collision resolution protocols. As part of the CCHC coexistence problem of two players, a simple rule to solve collisions is used: in the case when two players detect a collision of their allocation attempts, the one which allocated a resource the last time before the collision refrains from repeating its attempt. The other player immediately transmits another MPDU in order to start its resource allocation before any EDCF-TXOP can start. In case a player's resource allocation attempt is unsuccessful because of a collision with a starting EDCF-TXOP, the player can repeat its attempt immediately, whereas the station that transmitted the colliding MPDU has to backoff according to the EDCF protocol.

The simple rule to solve collisions, as well as the relatively short duration of MPDUs that actually collide, allow ignoring collisions in the model of the SSG. No specific state in the Markov chain P represents the event of a collision.

8.1.2 Transition Probabilities Expressed with the QoS Demands

In this section, the QoS demands are used to determine the transition probabilities of P. The transition probability that player 1 allocates resources while the

channel is idle or allocated by low priority EDCF-TXOPs via contention is approximated as

$$P_{01} \simeq \frac{L^1}{L^1 + L^2}, \quad L^1, L^2 > 0 . \tag{8.3}$$

During an SSG, the more TXOPs, L^1, player *1* attempts to allocate compared to the number of all high priority TXOPs, L^1+L^2, the higher the probability of resource allocation of this player *1*. With $P_{03}=1-P_{01}$, the probability of resource allocation of player *2* can be calculated similarly.

It is further approximated that the transition probability that player *2* attempts to allocate resources during an ongoing allocation of player *1*, is given by

$$P_{12} \simeq \begin{cases} \dfrac{d^1}{D^2 - d^2} & , D^2 - d^2 > d^1 \\ 1 & else \end{cases} \Rightarrow P_{12} \simeq min\left(1, \frac{d^1}{D^2 - d^2}\right), \tag{8.4}$$

and equivalently,

$$P_{34} \simeq \begin{cases} \dfrac{d^2}{D^1 - d^1} & , D^1 - d^1 > d^2 \\ 1 & else \end{cases} \Rightarrow P_{34} \simeq min\left(1, \frac{d^2}{D^1 - d^1}\right). \tag{8.5}$$

These transition probabilities are declared in a piecewise way. The probability P_{12} is either $d^1 / D^2 - d^2$ or approximated to *1*, as expressed by Equation (8.4). The probability that player *1* decides to attempt a resource allocation while player *2* is allocating resources, depends on the ratio between the duration of this allocation d^1 and the duration of the time interval between two consecutive demanded resource allocations of player *2*, i.e., $D^2 - d^2$. In the case that the time interval between two consecutive demanded resource allocations of player *2*, given by $D^2 - d^2$, is smaller than the duration d^1 of a resource allocation by player *1*, the player *2* will attempt to allocate resources immediately after the ongoing resource allocation, with probability *1*. The same is valid for the reverse situation when player *2* allocates resources with duration d^2, as is stated in Equation (8.5), where P_{34} is equivalently defined.

The parameters L^i, D^i ,d^i determine the times of the resource allocations of player *i*. They are introduced in Section 7.2.1 and illustrated in Figure 7.1. These parameters can also be determined from the demanded QoS parameters:

$$
\begin{aligned}
L^i &= \left\lceil \frac{1}{\Delta^i_{dem}} \right\rceil, \quad \Delta^i_{dem} > 0; \\
D^i &= SFDUR \cdot \Delta^i_{dem}; \\
d^i &= SFDUR \cdot \Theta^i_{dem} \cdot \Delta^i_{dem}.
\end{aligned}
\tag{8.6}
$$

The operator $\lceil \cdot \rceil$ is neglected in the following for the sake of analytical tractability of the model. Any nonnegative real value $L > 0$ is allowed, as already explained in Section 7.2.1. With the QoS demands as given in Equation (8.6), the transition probabilities of P are

$$P_{01} = \frac{\Delta^2_{dem}}{\Delta^2_{dem} + \Delta^1_{dem}}, \quad \Delta^{1,2}_{dem} > 0,$$

$$P_{12} = min\left(1, \frac{\Delta^1_{dem}}{\Delta^2_{dem}} \cdot \frac{\Theta^1_{dem}}{1 - \Theta^2_{dem}}\right), \quad \Delta^2_{dem} > 0, \Theta^2_{dem} < 1,$$

$$P_{34} = min\left(1, \frac{\Delta^2_{dem}}{\Delta^1_{dem}} \cdot \frac{\Theta^2_{dem}}{1 - \Theta^1_{dem}}\right), \quad \Delta^1_{dem} > 0, \ \Theta^1_{dem} < 1,$$

with $0 \le P_{01}, P_{12}, P_{34} \le 1$. Most relevant for the CCHC coexistence problem are situations where the overall throughput demands of all involved players are high, i.e., $\sum_i \Theta^i_{dem} \to 1$. In such situations, the transition probabilities P_{12} and P_{34} can be simplified to

$$
\begin{aligned}
P_{12} &\to 1, \\
P_{34} &\to 1.
\end{aligned}
\tag{8.7}
$$

For this reason, $P_{21} \to 0$ and $P_{43} \to 0$ in situations of high offered traffic. The equilibrium analysis in Section 8.2 will make use of this simplification.

8.1.3 Average State Durations Expressed with the QoS Demands

The average state durations T_0, T_1, T_2, T_3, T_4 are further required to calculate the QoS observations from the stationary distributions of P.

The average duration of the model P being in the idle state, T_0, is approximated to

$$T_0 \simeq min\left(D^2 - d^2, D^1 - d^1\right),$$

which can be expressed using the QoS demands of Equation (8.6) as

$$T_0 \simeq SFDUR \cdot min\left(\Delta^1_{dem} \cdot \left(1\text{-}\Theta^1_{dem}\right), \Delta^2_{dem} \cdot \left(1\text{-}\Theta^2_{dem}\right)\right), \tag{8.8}$$

with SFDUR being the duration of an SSG, given in *ms*. This is understood as follows. If both players attempt to allocate resources periodically, the idle times between the resource allocations of a player i is denoted as $D^i - d^i$. In general, the player that requires shorter periods determines the average T_0 of the SSG. This is represented by Equation (8.8). The value of T_0 can be simplified to

$$T_0 \to 0 \tag{8.9}$$

for situations where the overall throughput demands of all involved players are relatively high, i.e., $\sum_i \Theta^i_{dem} \to 1$. In this case, it is very probable that the contention-based channel access through EDCF cannot allocate any resources due to its low priority in medium access. Therefore, if $\sum_i \Theta^i_{dem} \to 1$, resources are nearly always allocated by one of the two players; the channel is busy most of the time.

The mean state duration is given by

$$T_{Mean} = p_0 T_0 + p_1 T_1 + p_2 T_2 + p_3 T_3 + p_4 T_4,$$

and can be expressed by

$$T_{Mean} \simeq p_0 T_0 + p_1 \cdot d^1 + p_3 \cdot d^2,$$

because the duration of the process P being in state p_1 is determined by the duration of a resource allocation of player *1*, d^1, if the opponent player *2* does not decide to attempt resources during this allocation. In addition, if the opponent player decides to attempt a resource allocation during this allocation, the process changes to state p_2. The duration of the process P consecutively being in the states p_1 and p_2 is again determined by the duration of a resource allocation of player *1*, d^1. Therefore, it can be approximated that

$$p_1 T_1 + p_2 T_2 \approx p_1 \cdot d^1,$$

and equivalently,

$$p_3 T_3 + p_4 T_4 \approx p_3 \cdot d^2.$$

The mean state duration T_{Mean} can now be expressed by using the QoS demands of Equation (8.6) as

$$T_{Mean} \simeq SFDUR \cdot \left(p_0 \cdot min\left(\Delta^1_{dem} \cdot \left(1\text{-}\Theta^1_{dem}\right), \Delta^2_{dem} \cdot \left(1\text{-}\Theta^2_{dem}\right) \right) + p_1 \cdot \Theta^1_{dem} \cdot \Delta^1_{dem} + p_3 \cdot \Theta^2_{dem} \cdot \Delta^2_{dem} \right),$$

where p_0, p_1, and p_3 are given through the solution of P, see Section 8.1.1.3. With this definition of the mean state duration T_{Mean}, the observed throughput of the players is given by

$$\begin{aligned} \Theta^1_{obs} &= SFDUR \cdot \Delta^1_{dem} \cdot \Theta^1_{dem} \cdot \frac{p_1}{T_{Mean}}, \\ \Theta^2_{obs} &= SFDUR \cdot \Delta^2_{dem} \cdot \Theta^2_{dem} \cdot \frac{p_3}{T_{Mean}}. \end{aligned} \tag{8.10}$$

Assuming high offered traffic, with Equation (8.7) the throughput observation of player i is calculated as

$$\sum\nolimits_i \Theta^i_{dem} \to 1 \quad \Rightarrow \quad \Theta^i_{obs} = \frac{\Theta^i_{dem} \cdot \Delta^i_{dem}}{\Theta^i_{dem} \cdot \Delta^i_{dem} + \Theta^{-i}_{dem} \cdot \Delta^{-i}_{dem}}, \quad i, -i \in \mathrm{N} = \{1,2\}. \tag{8.11}$$

In any other case, $\Theta^i_{obs} = \Theta^i_{dem}$. The maximum resource allocation period a player may observe due to delayed allocations during an SSG is calculated as

$$\Delta^i_{obs} = \underbrace{\Delta^i_{dem}}_{\text{demanded allocation interval}} + \underbrace{\Delta^{-i}_{dem} \cdot \Theta^{-i}_{dem} + TXOPlimit}_{\text{unwanted increase of allocation interval (delay)}}, \quad i, -i \in \mathrm{N} = \{1,2\},$$

where the unwanted maximum increase of resource allocation intervals is dependent on the demand of the opponent player as well as the maximum duration of the EDCF-TXOPs. The latter is defined by the TXOPlimit. This TXOPlimit is neglected in the following as it was defined to be relatively small compared to the typical duration of resource allocations of the two players ($TXOPlimit \ll \Delta^i_{dem} \cdot \Theta^i_{dem}$ with $i \in \mathrm{N} = \{1,2\}$), and further because of the lower priority in medium access through EDCF. Thus, the maximum observed resource allocation period is given by

$$\Delta^i_{obs} = \Delta^i_{dem} + \Delta^{-i}_{dem} \cdot \Theta^{-i}_{dem}, \quad i, -i \in \mathrm{N} = \{1,2\}. \tag{8.12}$$

All calculations in the following are performed using this upper bound of Δ^i_{obs} instead of any mean or expected value. Such an expected value can be derived from P as well (see Hettich 2001), but is not a realistic approximation, mainly due to the fact that depending on the $\Delta^{i,-i}_{req}$-parameters, the process that is modeled by P may become periodic. The stationary distributions that are calculated from P are only true approximations if the process that is modeled by P, i.e., here the

allocations during an SSG, is aperiodic. As already stated in Section 7.2.2.1, p. 135, the observed delay variation Ξ^{i}_{obs} is not used here. An upper bound can be derived from the approximation, which is given in the following equation for the sake of completeness. Again, $TXOPlimit \ll \Delta^{i}_{dem} \cdot \Theta^{i}_{dem}$ for any $i \in \mathrm{N} = \{1, 2\}$. The upper bound of the observed delay variation is given as

$$\Xi^{i}_{obs} = \Delta^{-i}_{dem} \cdot \Theta^{-i}_{dem}, \quad i, -i \in \mathrm{N} = \{1, 2\}.$$

8.1.4 Result

As the result, the expected throughput observations $\Theta^{i,-i}_{obs}$ can be approximated by Equation (8.11), and for the observed allocation periods $\Delta^{i,-i}_{obs}$ an upper bound is given by Equation (8.12). In summary, with

$$\Theta^{i}_{obs} \leq \Theta^{i}_{dem}, \quad \Delta^{i}_{obs} \geq \Delta^{i}_{dem}, \quad i \in \mathrm{N} = \{1, 2\}. \tag{8.13}$$

The model P results in the following analytical approximation for the observation of an SSG:

$$P := \left(\begin{pmatrix} \Theta^{i}_{dem} \\ \Delta^{i}_{dem} \end{pmatrix}, \begin{pmatrix} \Theta^{-i}_{dem} \\ \Delta^{-i}_{dem} \end{pmatrix} \right) \rightarrow \left(\begin{array}{l} \Theta^{i}_{obs} = min\left(\Theta^{i}_{dem}, \dfrac{\Theta^{i}_{dem} \cdot \Delta^{i}_{dem}}{\Theta^{i}_{dem} \cdot \Delta^{i}_{dem} + \Theta^{-i}_{dem} \cdot \Delta^{-i}_{dem}} \right) \\ \Delta^{i}_{obs} = \Delta^{i}_{dem} + \Delta^{-i}_{dem} \cdot \Theta^{-i}_{dem} \end{array} \right), \quad i, -i \in \mathrm{N} = \{1, 2\} \tag{8.14}$$

Here, it is not necessary to indicate that the demand of the opponent player may be an estimation from the history of earlier games. This may be the case however if P is used by a player to decide what action to take next. A player does not have the knowledge about the demand of the opponent player, it estimates this from the history of actions with the prediction method as explained in Section 7.4, p. 152. In the following Section 8.1.5, the model is evaluated against simulation, before an analysis of the SSG is given in Section 8.2.

8.1.5 Evaluation

In this section, a comparison of the model with simulation results is presented to assess how accurate the Markov model P represents the outcome of the SSG. Three different scenarios have been selected to review all relevant configurations. In the first case scenario, the player *1* demands a smaller resource allocation interval than player *2*, and the demands for the share of capacity of player *1* are

varied. In the second case both players demand the same resource allocation interval, and in the third case player *1* demands a larger resource allocation interval than player *2*. In all cases, the demand for the share of capacity (demand for throughput) of player *1* is varied, and results are given with respect to this varying demand. In simulation, EDCF-background traffic of $1\,Mbit/s$, with a TXOPlimit of $100\mu s$ was assumed. The analytical approximation does not capture the EDCF specifically. With $SFDUR=200ms$, the maximum duration of the EDCF-TXOPs, defined by the TXOPlimit is smaller than the minimum duration of the resource allocations by the players. Hence, there are only minor influences on the game outcomes that result from the EDCF. The EDCF background traffic is nevertheless helpful in simulation. Even if it does not significantly influence the results of the observed shares of capacity and of the observed resource allocation intervals for the two players, simulation results becomes more realistic because of the random characteristic of the EDCF medium access.

8.1.5.1 First Case: Player 1 Demands Shorter Resource Allocation Intervals than Player 2

First, results are compared for a scenario where player *1* demands a shorter resource allocation interval $\Delta^1_{dem}=0.02$ than is demanded by player *2*, $\Delta^2_{dem}=0.03$, that means that $\Delta^1_{dem}<\Delta^2_{dem}$. Figure 8.2, p. 173, shows the resulting outcomes of an SSG for both players, calculated with the analytical model *P*, as well as simulated. The demand for share of capacity of player *1* is varied between $\Theta^1_{dem}=0$ and $\Theta^1_{dem}=0.9$. The left figure of Figure 8.2 shows the observed shares of capacity $\Theta^{1,2}_{obs}$ over the varying Θ^1_{dem}, and the right figure shows the observed resource allocation intervals $\Delta^{1,2}_{obs}$ over Θ^1_{dem}. It can be seen that the observed share of capacity increases with increasing demand up to a certain saturation point, according to simulation and analytical approximation (solid lines in the left figure). The observed share of capacity of player *2* keeps constantly at its demanded level, as long as the channel is not heavily overloaded (dotted lines in the left figure). This is captured by the simulation and the approximation. The reason for the result that player *2* achieves its demand in share of capacity is as follows. It is very unlikely that player *1* takes resources that player *2* wanted to allocate by itself: once player *2* successfully allocated a resource, it keeps operating for a relative long time of

$$d^2=\Theta^2_{dem}\cdot\Delta^2_{dem}\cdot SFDUR=0.4\cdot 0.03\cdot 200ms=2.4ms\,,$$

repeated every $D^2=\Delta^2_{dem}\cdot SFDUR=6ms$. According to Equation (7.14), the players tolerate delays of resource allocation of

$$SFDUR \cdot \Delta^2_{tolerance} = 200ms \cdot 10^{-4} \cdot (\sqrt{1+100} - 1) \approx 1,8ms \ .$$

Thus player *2*, although attempting to allocate resources more often, i.e., every $4ms$, with variable duration, cannot prevent player *2* from accessing the channel as long as the resource allocation attempts do not collide. This is indicated by the simulation results, and the results of the analytical approximation. With heavy overload ($\Theta^1_{dem} > 0.8$), the approximation fails to model the effect of repeated collisions, which in general results in a loss of capacity for the player that demands the longer resource allocations, here the player *2*.

The right figure in Figure 8.2 shows the observed resource allocation intervals $\Delta^{1,2}_{obs}$. It can be seen that the observed resource allocation interval of player *2* increases with the increasing demand for share of capacity of player *1*, which is again indicated by simulation and approximation. Note that an upper limit of the maximum observed resource allocation interval is approximated, according to Equation (8.12). The simulation results show some variations of the delay, which is a result of correlated resource allocation times and unpredictable collisions. Although demanding $\Delta^1_{dem} = 0.02$, the player *1* observes a larger resource allocation interval as this is obviously determined by the player that demands the longer resource allocations, here the player *2*. Simulation and analytical approximation show the maximum observed resource allocation interval within one SSG. Note that the duration of a SSG is defined by the superframe duration, which is set to $SFDUR = 200ms$ in this thesis.

8.1.5.2 Second Case: Player 1 and Player 2 Demand the same Resource Allocation Interval

In this section, results are compared for a scenario where player *1* and player *2* demand the same resource allocation interval $\Delta^1_{dem} = \Delta^2_{dem} = 0.02$. Figure 8.3, p. 173, shows the resulting outcomes of an SSG for both players, calculated with the analytical model *P*, and simulated. Whereas the results of the observed share of capacity show clear similarities in simulation and analytical approximation (left figure in Figure 8.3), it can be seen that the approximated observations of the maximum resource allocation intervals are satisfying for player *2*, but too pessimistic for player *2* (right figure in Figure 8.3). This is due to the limitation an upper limit instead of an expected value is approximated. Theoretically, without regarding the EDCF-TXOPs, a maximum delay of resource allocations of player *1* is approximated to $\Delta^1_{obs} = 0.02 + \Delta^2_{dem} \cdot \Theta^2_{dem} = 0.08$, see Equation (8.12). The simulation results show that this must not necessarily happen during an SSG, especially in times of low demand ($\Theta^1_{dem} < 0.2$). Note that when both players

demand the same resource allocation interval, correlations in time of resource allocation attempts are very likely, which make approximations difficult.

8.1.5.3 Third Case: Player 1 Demands larger Resource Allocation Intervals than Player 2

Finally, results are compared for a scenario where player *1* demands a longer resource allocation interval $\Delta^{1}_{dem} = 0.02$ than is demanded by player *2,* $\Delta^{2}_{dem} = 0.01$, that means that $\Delta^{1}_{dem} > \Delta^{2}_{dem}$. From Figure 8.4 it can be observed that in this case the simulation results and the analytical approximation are very close to each other in nearly all cases.

8.1.5.4 Conclusion

The Markov model *P* was introduced for an analytical approximation of the outcome (observation) of an SSG. The main motivation was (1) to allow an analysis of the game on a purely analytical basis, and (2) to allow a player to estimate possible outcomes of the game in advance, while decision taking. Both goals are met. The model *P* is accurate enough to allow players to capture the statistical characteristics of the SSG. Whereas the model is simple enough to allow players to estimate the outcomes of an upcoming game in advance, this model can also be used for the equilibrium analysis of the SSG, which is described in detail in the next section.

8.2 Nash[16] Equilibrium Analysis

Note again, that, in what follows, for any parameter that may change its value throughout the MSG, the dependency on the stage number *n* is not shown in the equations, for the sake of simplicity.

Having an accurately defined analytical approximation of the SSG, it is now possible to investigate the SSG in terms of stability, and payoff maximizing. The outcome of an SSG that is in the interest of the players is the payoff vector as defined in Equation (7.16). This payoff depends on the observed QoS parameters as defined in Equation (8.11) and Equation (8.12). A fundamental question to be answered is what action to take as best response to any action the opponent takes. Does this best response action, denoted as $a^{i}*$ for a player *i*, exist? If it exists, is it unique? A commonly used solution concept for the question of what action to be taken in an SSG is the Nash equilibrium solution concept (Nash 1950a, Nash 1950b).

---

[16] John F. Nash (*1928), mathematician, USA

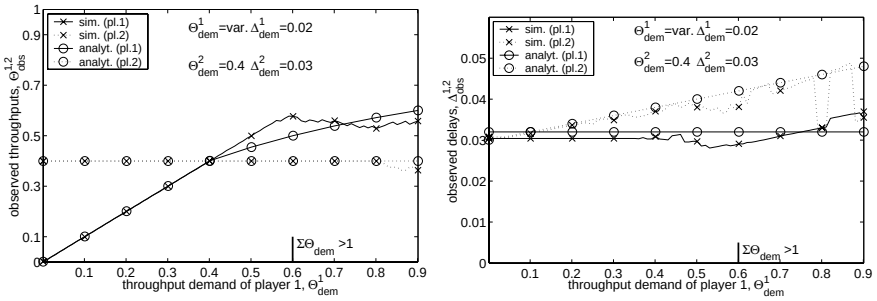

Figure 8.2: Resulting observed QoS parameters of an SSG for two interacting players via Θ^{1}_{dem}, calculated with *P,* and simulated. Left: observed share of capacity, right: observed resource allocation interval. In this figure, $\Delta^{1}_{dem} < \Delta^{2}_{dem}$.

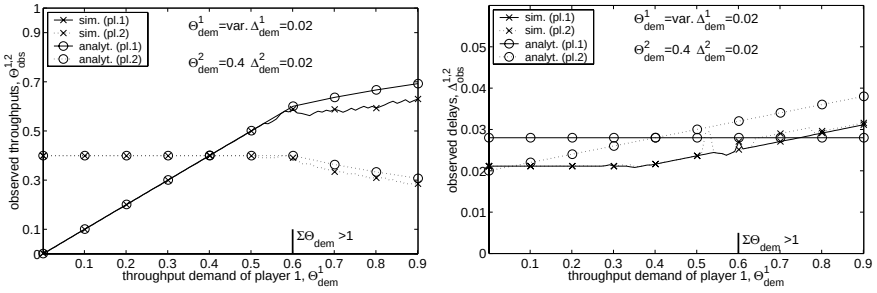

Figure 8.3: Resulting observed QoS parameters of an SSG for two interacting players via Θ^{1}_{dem}, calculated with *P,* and simulated. Left: observed share of capacity, right: observed resource allocation interval. In this figure, $\Delta^{1}_{dem} = \Delta^{2}_{dem}$.

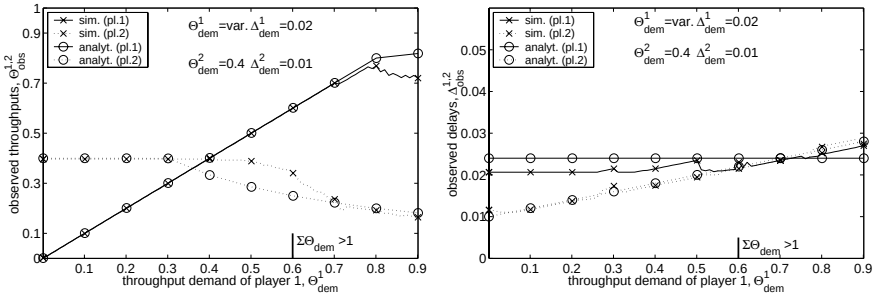

Figure 8.4: Resulting observed QoS parameters of an SSG for two interacting players via Θ^{1}_{dem}, calculated with P, and simulated. Left: observed share of capacity, right: observed resource allocation interval. In this figure, $\Delta^{1}_{dem} > \Delta^{2}_{dem}$.

8.2.1 Definition and Objective of the Nash Equilibrium

The Nash equilibrium is defined in the following Definition 8.1.

Definition 8.1 (Osborne and Rubinstein 1994) A *Nash equilibrium of actions in the Single Stage Game* is a vector of actions $\underline{a}^* = (a^i*, a^{-i}*) \in \mathrm{A}$, with $\mathrm{A} = \times_{i \in N} \mathrm{A}^i$ with the property that for every player $i \in \mathrm{N}$, the action a^i* is preferred to any other action a^i, provided that the opponent takes the action $a^{-i}*$, that means $(a^i*, a^{-i}*) \succsim_i (a^i, a^{-i}*)$ for all $a^i \in A^i, i \in \mathrm{N}$. Here, a^{-i} denotes $a^j, j \neq i$ with $i, j \in \mathrm{N}$.

The Nash equilibrium of actions in the SSG is characterized by the fact that for each player *i*, the particular action a^i* maximizes $V^i(\underline{a}) = V^i(a^i, a^{-i}*)$ in A^i for a given $a^{-i}*$. When operating in Nash equilibrium, no player can profitably deviate from its choice of action, thus the action taken by any player will remain stable as long as QoS requirements do not change. Given the action of the other players, no player has reason to take an action than the one that leads to the Nash equilibrium, as each player's action is an optimal, payoff maximizing response to the opponent player's action. In general, either none, or a unique, or multiple Nash equilibria may exist in a strategic game.

In a course of an MSG, if a Nash equilibrium exists in the SSG, players that adjust their demands rationally in the sense that they attempt to maximize their payoffs, will end up in an action profile that is a Nash equilibrium. If there is no Nash equilibrium in the SSG, then rational players keep adjusting their demands continuously without meeting a stable point of operation. If multiple Nash equilibria exist in the SSG, then it is not clear to which one the players are adjusting their demands throughout the course of an MSG.

8.2.2 Existence of the Nash Equilibrium in the SSG of Coexisting CCHCs

The SSG as it was defined in the previous Chapter 7 allows an uncountable number of actions per player. Such a game is referred to as infinite game (Fudenberg 1991). The analytical approximation of Section 8.1 works with a continuum of actions, whereas a simulation is performed with a large finite set of actions. During simulation, the size of the action set was chosen such that sensitivities to the precision of the discrete grid of actions are negligible. Therefore, the existence of a Nash equilibrium is verified by using a theorem that is known from the theory of infinite games, i.e., games that allow an infinite number of actions per player. The theorem uses an attribute of the payoff, which is referred to as quasi-concavity. Quasi-concavity of a payoff is defined in the following Definition 8.2. The Definition 8.3 recalls another necessary attribute, the continuity of the payoff.

Definition 8.2 For any two actions of a player *i*, $a^i, b^i \in A^i$, and any action of the opponent player *-i*, $a^{-i} \in A^{-i}$, if a payoff $V^i(a^i, a^{-i})$ of player *i* in an SSG satisfies $min(V^i(a^i, a^{-i}), V^i(b^i, a^{-i})) \leq V^i(\alpha \cdot a^i + (1-\alpha) \cdot b^i, a^{-i})$ for any vector of two real numbers $\alpha = (\alpha_1, \alpha_2) \in \mathbb{R}^2$, with $\alpha_1, \alpha_2 \in (0...1)$, then the payoff is said to be quasi-concave in A^i.

From this definition it follows that a payoff is quasi-concave if and only if every local maximum in A^i is a global maximum in A^i.

Definition 8.3 (Debreu 1959:15) Let the payoff $V^i(\underline{a})$ be a function from A to $\mathbb{R}$, and consider an action profile represented by the point $\underline{a}' = (a^i', a^{-i}') \in \mathrm{A}$. The payoff $V^i(\underline{a})$ is continuous at this point $\underline{a}'$ if, when $\underline{a}'' \to \underline{a}'$ and $y' = V^i(\underline{a}'), y'' = V^i(\underline{a}'')$ it follows that $\underline{y}'' \to \underline{y}'$. The function is continuous in A if it is continuous at every point of A.

With these two definitions, it is possible to formulate a sufficient condition for the existence of at least one Nash equilibrium in the SSG. The following Theorem 8.1 for the existence of a Nash equilibrium in an infinite game is taken from Fudenberg (1991).

Theorem 8.1 **(**Fudenberg 1991:34) Consider a strategic game of whose action spaces A^i are nonempty compact convex subsets of an Euclidean space, $i \in \mathrm{N} = \{1, 2\}$. If all payoffs $V^i(a^i, a^{-i})$ are continuous in A and quasi-concave in A^i, there exists a pure action Nash equilibrium $\underline{a}^* = (a^i*, a^{-i}*)$ in $\mathrm{A} = \times_{i \in \mathrm{N}} A^i$, $i, -i \in \mathrm{N}$.

The theorem is for example proven in Debreu (1952). Note that in the SSG competition model mixed actions are not defined, players take pure actions only (see Section 7.2). Nash equilibria can still exist in the SSG if the conditions of this theorem are not satisfied, as these conditions are sufficient but not necessary.

Proposition 8.1 postulates the existence of a Nash equilibrium in the SSG of two coexisting CCHCs. This proposition is proven underneath.

Proposition 8.1 In the Single Stage Game of two coexisting CCHCs exists a Nash equilibrium in $\mathrm{A} = \times_{i \in \mathrm{N}} A^i$.

Proof: By definition, the action spaces $\mathcal{A}^i$, $i \in \mathrm{N} = \{1, 2\}$, are each nonempty, compact, and convex sets, and they are subsets of an Euclidean space, as it was stated in the definition of the action spaces in Section 7.2.2.2. The outcome of an SSG for a player *i* is the payoff V^i, which is given by the observed utility U^i, as defined in Equation (7.16), page 148. The observed utility is given by the product $U^i = U^i_\Theta \cdot U^i_\Delta$ of the two utility terms $U^i_\Theta(\Theta^i_{dem}, \Theta^i_{obs}, \Theta^i_{req})$ and $U^i_\Delta(\Delta^i_{obs}, \Delta^i_{req})$, see Equation (7.11) on page 142. The two utility terms are continuous functions of QoS parameters by definition. Equation (8.14), page 169, defines a continuous function for the QoS parameters, thus, the payoff V^i is evidently continuous in A.

Since the two utility terms U^i_Θ, U^i_Δ are each concave functions of the observed QoS parameters for any shaping parameters $u, v \in \mathbb{R}^+$, with $u, v > 0$ (see Section 7.2.3.1), it remains to be shown that the functions for the observed QoS parameters, the share of capacity Θ^i_{obs}, and resource allocation interval Δ^i_{obs}, which are given by Equation (8.14), are concave functions of the selected demands, i.e., concave functions of action.

The observed resource allocation interval $\Delta^i_{obs} = \Delta^i_{dem} + \Delta^{-i}_{dem} \cdot \Theta^{-i}_{dem}$ is a concave function of Δ^i_{dem}, as it increases linearly with increasing demanded resource allocation interval Δ^i_{dem}. The observed resource allocation interval Δ^i_{obs} is not dependent on the share of capacity demanded by player *i*, i.e., Θ^i_{dem}. It can be concluded that Δ^i_{obs} is a concave function in $\mathcal{A}^i$.

The observed share of capacity Θ^i_{obs} increases linearly for small demands for share of capacity by player *i*, i.e., if $\Theta^i_{dem} \to 0$ then $\Theta^i_{obs} = \Theta^i_{dem}$, see Equation (8.14). Thus, it is a concave function of Θ^i_{dem} for small demands.

The function $\Theta^i_{obs} = \Theta^i_{dem}$ is called curve for smaller demands in the following. For small demands, this curve is not dependent on the demanded resource allocation interval Δ^i_{dem}.

It can be concluded that Θ^i_{obs} is a concave function in $\mathcal{A}^i$ for small demands of share of capacity, i.e., if $\Theta^i_{dem} \to 0$.

For large demands, i.e., if $\Theta^i_{dem} \to 1$, the observed share of capacity is defined by Equation (8.14) to

$$\Theta^i_{obs} = \frac{\Theta^i_{dem} \cdot \Delta^i_{dem}}{\Theta^i_{dem} \cdot \Delta^i_{dem} + \Theta^{-i}_{dem} \cdot \Delta^{-i}_{dem}} = \frac{1}{1 + \frac{\Theta^{-i}_{dem} \cdot \Delta^{-i}_{dem}}{\Theta^i_{dem} \cdot \Delta^i_{dem}}}.$$

This function is called the curve for larger demands in the following. This function is a concave function of Θ^i_{dem} and a concave function of Δ^i_{dem}. It can be concluded that Θ^i_{obs} is a concave function in A^i for large demands of share of capacity, i.e., if $\Theta^i_{dem} \to 1$.

The intersection point $\Theta^i_0 > 0$ between the two curves of Θ^i_{obs} is given by

$$\begin{aligned} \Theta^i_0 &= \Theta^i_{obs} = \Theta^i_{dem} \\ &= \frac{1}{1 + \frac{\Theta^{-i}_{dem} \cdot \Delta^{-i}_{dem}}{\Theta^i_{dem} \cdot \Delta^i_{dem}}} \\ \Rightarrow \Theta^i_{dem} &= \left(1 - \frac{\Theta^{-i}_{dem} \cdot \Delta^{-i}_{dem}}{\Delta^i_{dem}}\right) > 0 \end{aligned} .$$

The two curves intersect in the interval of interest, $0 < \Theta^i_0 < 1$, if $(\Theta^{-i}_{dem} \cdot \Delta^{-i}_{dem} / \Delta^i_{dem}) < 1$. At this intersection point, if it exists in the interval $0 < \Theta^i_0 < 1$, the gradient of the curve for a larger demand is required to be equal or smaller than the gradient of the curve for smaller demand, which is 1, in order to achieve that Θ^i_{obs} is a concave function of Θ^i_{dem} and Δ^i_{dem}. Since the gradient of the curve for a larger demand at point Θ^i_{obs} is given by

$$\underbrace{\left.\frac{\partial\Theta^i_{obs}}{\partial\Theta^i_{dem}}\right|_{\substack{\Theta^i_{dem}\to\Theta^i_0\\ \Theta^i_{dem}>\Theta^i_0}} = \left.\frac{\Theta^{-i}_{dem}\cdot\Delta^{-i}_{dem}\cdot\Delta^i_{dem}}{\left(\Theta^i_{dem}\cdot\Delta^i_{dem}+\Theta^{-i}_{dem}\cdot\Delta^{-i}_{dem}\right)^2}\right|_{\Theta^i_{dem}\to\Theta^i_0}}_{\substack{\text{gradient of the curve for larger demand}\\ \text{at intersection point } \Theta^i_0}}$$

$$= \frac{\Theta^{-i}_{dem}\cdot\Delta^{-i}_{dem}}{\Delta^i_{dem}}$$

Therefore,

$$\frac{\Theta^{-i}_{dem}\cdot\Delta^{-i}_{dem}}{\Delta^i_{dem}} < \underbrace{1 = \left.\frac{\partial\Theta^i_{obs}}{\partial\Theta^i_{dem}}\right|_{\Theta^i_{dem}<\Theta^i_0}}_{\substack{\text{gradient of the curve for smaller}\\ \text{demand at intersection point } \Theta^i_0}},$$

since it was required that $0<\Theta^i_0<1$. It can be concluded that Θ^i_{obs} is a concave function of Θ^i_{dem} for any demand. It can be concluded that Θ^i_{obs} is a concave function in A^i. ■

The Proposition 8.1 implies the existence of at least one Nash equilibrium, which may not be unique. The uniqueness of Nash Equilibria in the SSG is discussed in the next section.

8.2.3 Calculation of Nash Equilibria in the SSG of Coexisting CCHCs

A necessary condition for $\underline{a}$ to be a Nash equilibrium $\underline{a}^* = (a^i*, a^{-i}*) \in \mathrm{A}$ with the property that for every player $i \in \mathrm{N}$, the action a^i* is preferred to any other action a^i, is given by

$$\underline{a} = \underline{a}^* \Rightarrow 0 = grad^i\ V^i(\underline{a}) \quad \forall i \in \mathrm{N}, \quad with\ grad^i = \begin{pmatrix} \frac{\partial}{\partial\Theta^i_{dem}} \\ \frac{\partial}{\partial\Delta^i_{dem}} \end{pmatrix},$$

that means for every player $i \in \mathrm{N}$,

$$0 = grad^i\ U^i(\underbrace{\Theta^i_{req},\Delta^i_{req}}_{requirement},\underbrace{\Delta^i_{dem},\Theta^i_{dem}}_{demand},\underbrace{\Theta^{-i}_{dem},\Delta^{-i}_{dem}}_{opponent's\ demand}) \ \forall i \in \mathrm{N}. \qquad (8.15)$$

In the SSG, the utilities U^i are concave functions in A^i for any player *i*, therefore Equation (8.15) is a sufficient condition for a Nash equilibrium (Mangold et al. 2001h).

In a game of two players, Equation (8.15) describes a system of four equations with the four unknown variables $\Delta^i_{dem}, \Theta^i_{dem}, \Theta^{-i}_{dem}, \Delta^{-i}_{dem}$, given the requirements per player. In order to achieve differentiability, when calculating a Nash equilibrium, the utility functions have to be considered piecewisely. From Equation (8.15), the resulting vectors of demands in Nash equilibrium can be calculated numerically, if the requirements of all players and the shaping parameters *u, v* of the utility function are known. In general, the resulting vectors of demands in a Nash equilibrium can be given in closed form as function of all parameters of the game (resulting vectors of demands in a Nash equilibrium are given by the action profile that is selected when playing the Nash equilibrium). Because of the complexity of the general term of the Nash equilibrium, this is not explicitly shown here.

Depending on the profile of requirements, and given the shaping parameters of the utility function, Nash equilibria can be calculated with Equation (8.15). As an example for the calculation, in the following the Nash equilibrium is calculated for one example.

Let

$$\left(\begin{pmatrix}\Theta^1_{req}\\ \Delta^1_{req}\end{pmatrix},\begin{pmatrix}\Theta^2_{req}\\ \Delta^2_{req}\end{pmatrix}\right) = \left(\begin{pmatrix}0.4\\ 0.023\end{pmatrix},\begin{pmatrix}0.4\\ 0.04\end{pmatrix}\right)$$

be the matrix of requirements of the player *1* and *2*, both players select their actions out of the sets

$$a^i \in A^i = \begin{pmatrix}\Theta = [0...1]\\ \Delta = [0...0.1]\end{pmatrix},$$

as defined in Equation (7.8), with $i \in \mathbb{N}$. Equation (8.15) is used to calculate the Nash equilibria with the following set of equations, where the utility functions are shaped as stated in Equation (7.15).

$$\frac{\partial}{\partial \Theta^1_{dem}} U^1(\Theta^1_{req}, \Delta^1_{req}, \Delta^1_{dem}, \Theta^1_{dem}, \Theta^2_{dem}, \Delta^2_{dem}) = 0$$

$$\frac{\partial}{\partial \Delta^1_{dem}} U^1(\Theta^1_{req}, \Delta^1_{req}, \Delta^1_{dem}, \Theta^1_{dem}, \Theta^2_{dem}, \Delta^2_{dem}) = 0$$

$$\frac{\partial}{\partial \Theta^2_{dem}} U^2(\Theta^2_{req}, \Delta^2_{req}, \Delta^2_{dem}, \Theta^2_{dem}, \Theta^1_{dem}, \Delta^1_{dem}) = 0$$

$$\frac{\partial}{\partial \Delta^2_{dem}} U^2(\Theta^2_{req}, \Delta^2_{req}, \Delta^2_{dem}, \Theta^2_{dem}, \Theta^1_{dem}, \Delta^1_{dem}) = 0$$

This system of differential equations can be solved numerically for any specific requirement profile. With this solution, the resulting demands in Nash equilibrium are

$$\underline{a}^* = \left(a^1* = \begin{pmatrix} 0.42 \\ 0.018 \end{pmatrix}, a^2* = \begin{pmatrix} 0.44 \\ 0.032 \end{pmatrix} \right)$$

and with Equations (7.12)-(7.16), the resulting payoffs in Nash equilibrium are

$$V(\underline{a}^*) = (0.817, 1.000).$$

Both players achieve a high payoff in this example. However, player *1* suffers from the competition and the allocation process, and its payoff is $V^1(\underline{a}^*) = 0.817$. Therefore, it cannot completely achieve its QoS requirements in Nash equilibrium. It depends on the services the player *1* attempts to support if it is satisfied with this degradation or not. The Nash equilibrium is achieved either through complete knowledge in one SSG or through adjustment in repeated SSGs, when both players play rational. Playing rational means playing the best response action, i.e., attempting to optimize the payoff by taking the action that results in the highest payoff per SSG.

In general, multiple Nash equilibria can exist in the SSG, which may be the case for some QoS requirements the players attempt to support. Depending on the profile of requirements of the players, the Nash equilibrium in the SSG of two coexisting CCHCs is not always unique. A game with multiple Nash equilibria is given for example in games where both players have very high QoS requirements, such as

$$\left(\begin{pmatrix} \Theta^1_{req} \\ \Delta^1_{req} \end{pmatrix}, \begin{pmatrix} \Theta^2_{req} \\ \Delta^2_{req} \end{pmatrix} \right) = \left(\begin{pmatrix} 0.9 \\ 0.4 \end{pmatrix}, \begin{pmatrix} 0.9 \\ 0.4 \end{pmatrix} \right).$$

In this game, typically $\Theta^i_{obs} \ll \Theta^i_{req}$ for any *i*, and thus $V(\underline{a}^*) = (0, 0)$, for a large number of action profiles. This is a result of the shape of the utility function used in all games: for any shaping parameter, the utility function is concave, but not strictly concave.

8.3 Pareto[17] Efficiency Analysis, and Behaviors

In a SSG, Nash equilibria are stable and predictable points of operation. Players that take rational actions will automatically adjust into a Nash equilibrium, because it has been shown that at least one Nash equilibrium exists in the SSG. If the Nash equilibrium is unique, then the respective action profile can be predicted as point of operation, as a result of rational behavior. However, there may in general exist action profiles in the SSG that can lead to higher payoffs than what is achieved in Nash equilibrium. If such profiles do not exist, the Nash equilibrium is referred to as Pareto efficient, or equivalently, Pareto optimal. If such a profile exists, the Nash equilibrium is not Pareto efficient. In this case, payoffs may be optimized through actions taken by all players. This is discussed in the following.

The Definition 8.4 highlights the concept of Pareto efficiency, which is also referred to as Pareto optimality.

> **Definition 8.4** (Shubik 1981:347) Let the payoff $V^i(\underline{a})$ be a function from A to $\mathbb{R}$, and consider an action profile represented by point $\underline{a} = (a^i, a^{-i}) \in \mathrm{A}$, with $i \in \mathrm{N}$; N being the set of players of a game. The action profile (the point) is said to be Pareto efficient (or Pareto optimal) if there is no other action profile $\underline{a}' = (a^i{}', a^{-i}{}') \in \mathrm{A}$ such that $V^i(\underline{a}') \geq V^i(\underline{a})$ for all $i \in \mathrm{N}$ and $V^i(\underline{a}') > V^i(\underline{a})$ for at least one $i \in \mathrm{N}$.

Definition 8.4 indicates that there can be one or more Pareto efficient action profiles in the SSG. A unique Nash equilibrium in the SSG that is Pareto efficient is a desirable scenario in the sense that in this case there is no other action profile that allows the usage of radio resources more efficiently, i.e., with larger payoffs for all involved players. It depends on the requirements of the players in the CCHC coexistence game if a Nash equilibrium is Pareto efficient. In general, Nash equilibria are less probable to be Pareto efficient in games where all players require more resources than available, i.e., with high offered traffic.

In addition, in case the Nash equilibrium is not Pareto efficient, a Pareto efficient action profile is reached if all players deviate from the Nash equilibrium point. If one player alone deviates, it achieves a lower payoff than before, according to the definition of a Nash equilibrium. Thus, when deviating from action profiles that are Nash equilibria and not Pareto efficient towards action profiles that are not

---

[17] Vilfredo Pareto (1848-1923), Italian economist.

Nash equilibria but Pareto efficient, a coordinated change of action among all players is necessary. How this coordination is established is discussed in the context of behaviors and strategies in the following.

8.3.1 Bargaining Domain

The concept of Pareto efficiency can be illustrated in what is referred to as bargaining domain. In the bargaining domain of two players, the payoff of one player is drawn against the payoff of the other player for any action profile that may be demanded by the two players. The resulting figure is a pattern of payoffs that depends on the requirements of the players. Figure 8.5, p. 183, shows an example of a bargaining domain of the SSG, where resulting payoffs for both players are indicated for a number of action profiles. In this example, the game has one Nash equilibrium that is not Pareto efficient. This is the case because there are other action profiles that lead to higher payoffs for at least one of the players, compared to the payoffs in Nash equilibrium.

A helpful method to illustrate the efficiency of Nash equilibria is the set of payoffs in the bargaining domain with higher payoff results than in the Nash equilibria for one of the players, and the same payoff result as in the Nash equilibria for the other players. This is illustrated as a line in the bargaining domain that is referred to as Pareto boundary in the following. The payoffs observed in Nash equilibria in the SSG are located on this Pareto boundary. See Zbigniew and Mason (1996) for a discussion of Pareto boundaries.

The Pareto boundary in the example of Figure 8.5 indicates that there are action profiles that result in higher payoffs (outcomes) for both players than what is achieved in the Nash equilibrium. Any action profile that leads to payoffs outside that boundary, are more Pareto efficient than any Nash equilibrium that may exist in the game. However, these profiles are not Nash equilibria, they cannot be achieved through rational behavior. At least one player has the intention to unilaterally change its action as part of its rational behavior, when these Pareto efficient profiles have been selected before.

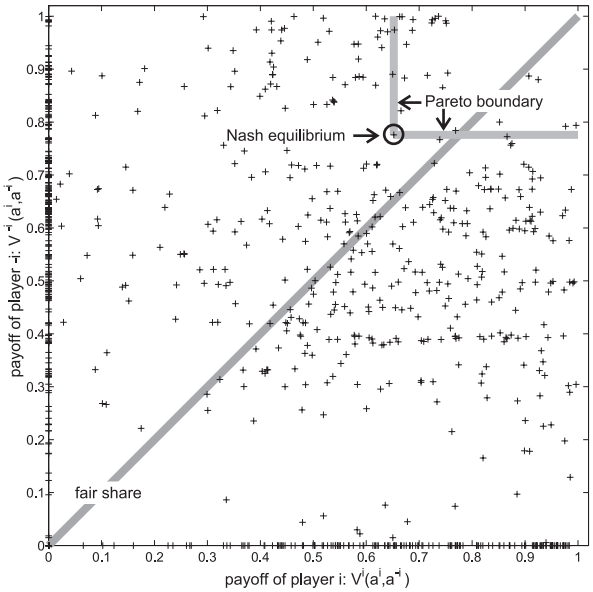

Figure 8.5: Bargaining domain of an example of an SSG. Indicated are the resulting payoffs of both players for a number of action profiles, i.e., demands. This game has one Nash equilibrium that is not Pareto efficient: there are action profiles that result for both players in higher payoffs than what is achieved in the Nash equilibrium.

One Nash equilibrium exists in the shown example. When multiple Nash equilibria exist, the Pareto boundary is given as the combined set of all action profiles that lead to payoffs higher than the payoffs in any Nash equilibrium.

To achieve Pareto efficiency, it is required that players cross the Pareto boundary, for example as a result of mutual cooperation in case the Nash equilibrium itself is not Pareto efficient. Once that boundary is crossed, there may be still action profiles that lead to higher payoffs than others, i.e., some action profiles may be more Pareto efficient than others. The Figure 8.5 further shows the line where both players observe the same payoff, which is referred to as action profile that leads to a fair share of radio resources.

In such outcomes, both players achieve the same payoffs according to their individual requirements, but not necessarily the same QoS. It is said that the interacting players achieve the same level of satisfaction when the resulting outcome of a SSG lies at this line. In symmetric games, where both players have exactly the same QoS requirements, the Nash equilibrium lies on this line.

Any action profile that improves the outcome of the SSG in the sense that, compared to the payoffs in Nash equilibria, the total sum of the payoffs of all players

is larger than what is achieved through rational behavior, i.e., in Nash equilibria, are considered as being more efficient in the sense of total utility. It is said that the interacting players achieve an improved social outcome of the game with such action profiles. In other words, payoffs outside the Pareto boundary form a subset of the payoffs with improved social outcome, given by the sum of all individual outcomes.

8.3.2 Core Behaviors

As result of the analysis of the SSG, the core behaviors are defined in this section. The behaviors capture all relevant aspects of the decision taking processes identified so far. They will allow the definition of strategies and the application of repeated SSGs with dynamically changing behaviors as part of the strategies.

8.3.2.1 Simple Core Behavior "Persist" (BEH-P)

A player *i* that behaves according to BEH-P will always select what is required:

$$\begin{pmatrix} \Theta^{i}_{dem} \\ \Delta^{i}_{dem} \end{pmatrix} := \begin{pmatrix} \Theta^{i}_{req} \\ \Delta^{i}_{req} \end{pmatrix}$$

This behavior achieves highest payoffs as result of the SSG if the opponent player -*i* does not require any radio resource, for example in an isolated QBSS. However, if all players behave according to BEH-P, the resulting payoffs are generally very low due to uncoordinated resource allocation attempts.

8.3.2.2 Rational Core Behavior "BestResponse" (BEH-B)

A player *i* that behaves according to BEH-B will always select what achieves the highest payoff in the SSG, considering its expectations of the action of its opponent.

$$\left(\begin{pmatrix} \Theta^{i}_{req} \\ \Delta^{i}_{req} \end{pmatrix}, \begin{pmatrix} \tilde{\Theta}^{-i}_{dem} \\ \tilde{\Delta}^{-i}_{dem} \end{pmatrix} \right) \rightarrow \begin{pmatrix} \Theta^{i}_{dem} \\ \Delta^{i}_{dem} \end{pmatrix}$$

This behavior is referred to as rational behavior. Player *i* achieves payoffs that can be sustained as result of the SSG if the opponent player -*i* also behaves rational. Depending on the requirements of the players, the resulting payoffs may not be Pareto efficient.

8.3.2.3 Cooperative Core Behavior "Coop" (BEH-C)

A player *i* that behaves according to BEH-C, attempts to cross the Pareto boundary by unilaterally deviating from the best response to an action that will allow the opponent player -*i* to better meet its individual requirements, without actually knowing the requirements of the opponent player. If the opponent also deviates from its own best response, all players can gain from this coordinated deviation in games where the Nash equilibrium is not Pareto efficient.

In order to define the behavior BEH-C, simulation campaigns are used to analyze what type of deviation from BEH-B towards a different behavior is beneficial for an opponent player, and what type of deviation has negative effects. Deviation can be the increase or the decrease of the demanded share of capacity Θ_{dem}, or the increase or decrease of Δ_{dem}.

The results of the analysis are illustrated in Table 8.1 and Table 8.2. The Table 8.1 shows the results taken from the analytical approximation, whereas the Table 8.2 shows the results of stochastic simulation. Instead of detailed results, the relative changes in payoff are given in the tables. They are indicated by "+", if the payoff increases as a result of deviation, "0", if it keeps constant while deviating, and "-", if the payoff decreases. Four cases are shown in four lines where the player *i* has different requirements relative to the opponent player -*i* (line 1, 2 vs. line 3, 4), and player -*i* takes actions either according to BEH-P (line 1, 3) or according to BEH-B (line 2, 4).

From Table 8.1 it can be concluded that increasing the demanded resource allocation interval Δ_{dem}, while keeping the demanded share of capacity Θ_{dem} constant, is positive for the player, as such a behavior has negative implications on the resulting payoff of the opponent player.

In contrast, reducing the demanded resource allocation interval Δ_{dem} is beneficial for the opponent player. Increasing the demanded share of capacity Θ_{dem}, while keeping the demanded resource allocation interval Δ_{dem} constant, has negative implications on the resulting payoff of the opponent. On the other hand, decreasing the demanded share of capacity Θ_{dem} is clearly beneficial for the opponent player, in any case.

These results are confirmed by the simulation results shown in Table 8.2, with some differences for the results when player *i* reduces its demanded share of capacity (right column). In this case, the simulation indicate that player *i* itself may observe smaller payoffs when deviating. This is not captured by the analytical approximation in Table 8.1 because of the simplified model of collisions of resource allocation attempts.

As result, cooperative behavior is defined as reducing the demand for share of capacity, and at the same time reducing the demanded resource allocation interval to smaller intervals. The two measures allow an opponent player to allocate resource more often at the demanded points in time. When player *i* cooperates, resource allocations of player *i* are shorter, due to the smaller resource allocation interval. Therefore, the opponent player -*i* now has to wait shorter times for the channel to become idle, when player *i* allocated the resources before. This is clearly beneficial for player -*i*, and can be referred to as cooperative behavior of player *i*. Cooperation means in the game context that the system of interacting players crosses the Pareto boundary from a Nash equilibrium towards an operation point that achieves higher payoffs for at least one player, and no payoff reduction for any player. The following expression indicates that the demands selected in cooperation are a result of the deviation from the rational behavior BEH-B:

$$\begin{pmatrix} \Theta^i_{dem}* \\ \Delta^i_{dem}* \end{pmatrix} \rightarrow \begin{pmatrix} \Theta^i_{dem,C} \leq \Theta^i_{dem}* \\ \Delta^i_{dem,C} \leq \Delta^i_{dem}* \end{pmatrix},$$

where the index "C" indicates the demand selected by a player in cooperation. As preliminary definition of the limits to which a player deviates when cooperating, $\Delta^i_{dem,C}$ and $\Theta^i_{dem,C}$ are defined in this thesis by

$$\Theta^i_{dem,C} \leq min\left(\Theta^i_{dem}*, \frac{1}{N}\right),$$
$$\tilde{\Delta}^{-i}_{dem} \leq \Delta^i_{dem,C} \leq \Delta^i_{dem}*,$$

N being the number of interacting players in the game. Here it is indicated that the demand of the opponent player is estimated by any player, therefore, players adapt to $\tilde{\Delta}^{-i}_{dem}$ instead of Δ^{-i}_{dem}. When cooperating, a player demands a maximum share of capacity of $\Theta^i_{dem,C} = 1/N = 0.5$, which can be interpreted as fair share when two players interact. Further, the demanded resource allocation interval in cooperation, $\Delta^i_{dem,C}$, is decreased until it reaches the value of the opponent's resource allocation interval. This simple definition implies that, in times of high offered traffic, players give their opponents a fair chance to allocate resources regularly. There are games where cooperation is not beneficial for the opponent, especially in games where the opponent achieved the maximum payoff already by playing rational, when the Nash equilibrium is Pareto efficient. In such a game, when player *i* does not meet its requirements in Nash equilibrium, player *i* is referred to as being weaker than player -*i*.

Table 8.1: Deviating behaviors – resulting pairs of payoffs per players *i, -i* as taken from the analytic approximation. Player *i* deviates the demands from its requirements by increasing or decreasing Δ, or Θ. The opponent player *-i* plays BEH-P or BEH-B.

	relative requirements	behavior of pl. *-i*	deviation of pl. *i* increase Δ	deviation of pl. *i* reduce Δ	deviation of pl. *i* increase Θ	deviation of pl. *i* reduce Θ
1	$\Delta^{i}_{req} < \Delta^{-i}_{req}$	*BEH-P*	*0* / –	*0* / +	*0* / –	*0* / +
2		*BEH-B*	*0* / –	*0* / +	*0* / –	*0* / +
3	$\Delta^{i}_{req} > \Delta^{-i}_{req}$	*BEH-P*	*0* / –	+ / *0*	*0* / –	*0* / +
4		*BEH-B*	*0* / –	+ / +	*0* / –	*0* / +

explanation:

0 /… ⇒ pl *i* observes the same payoff	…/ 0 ⇒ opp. pl. *-i* observes the same payoff
– /… ⇒ pl. *i* observes smaller payoff	…/ – ⇒ opp. pl. *-i* observes smaller payoff
+ /… ⇒ pl. *i* observes increased payoff	…/+ ⇒ opp. pl. *-i* observes increased payoff

for example, "– / +" means "pl. *i* observes a smaller payoff than before and player *-i* observes a higher payoff"

A weak player cannot gain from playing cooperatively. There are measures for a weak player *i* based on the behavior "defect" that will enable it to force the opponent player *-i* to cooperate, as part of dynamic strategies. The behavior "defect" is defined in the next section.

8.3.2.4 Punishing Core Behavior "Defect" (BEH-D)

A player *i* that behaves according to BEH-D will always select the demand that is most damaging to the payoffs of the opponent player *-i*, according to the analysis shown in Table 8.1 and Table 8.2:

$$\begin{pmatrix} \Theta^{i}_{dem} \\ \Delta^{i}_{dem} \end{pmatrix} := \begin{pmatrix} \Theta^{i}_{max} \\ \Delta^{i}_{max} \end{pmatrix} = \begin{pmatrix} 1 \\ 0.1 \end{pmatrix}$$

This behavior is likely to destroy any attempt of the opponent player to achieve some payoff in the SSG.

Table 8.2: Deviating behaviors – resulting utilities per players *i,-i* now taken from stochastic simulation instead of the analytic approximations.

	relative requirements	behavior of pl. *-i*	deviation of pl. *i* increase Δ	deviation of pl. *i* reduce Δ	deviation of pl. *i* increase Θ	deviation of pl. *i* reduce Θ
1	$\Delta^{i}_{req} < \Delta^{-i}_{req}$	*BEH-P*	*0* / –	*0* / +	*0* / *0*	*0* / *0*
2		*BEH-B*	*0* / –	*0* / *0*	*0* / –	*0* / *0*
3	$\Delta^{i}_{req} > \Delta^{-i}_{req}$	*BEH-P*	*0* / –	*0* / +	*0* / –	– / +
4		*BEH-B*	*0* / –	*0* / +	*0* / –	– / +

explanation: see Table 8.1.

However, this behavior cannot guarantee that player *i* itself may achieve a satisfying payoff. If one or all players behave according to BEH-D, the resulting payoffs are low due to the very long and many resource allocations.

8.3.2.5 Available Behaviors

In Figure 8.6, the action space of a player and the resulting consequences on the opponent players are indicated. The two illustrated cases at the left and right border of the action space, (a) deferring from resource access completely and (b) occupying all resources for the complete duration of the SSG, are not defined in the game model. Further, as part of the game model, $\Delta \leq 0.1$. Indicated in the figure are areas where a player may meet its requirement by playing the best response, where a player may cooperate, and where it behaves selfish by blocking the opponent. The collision probability depends on the number of resource allocation attempts and increases with decreasing Δ_{dem} of all players.

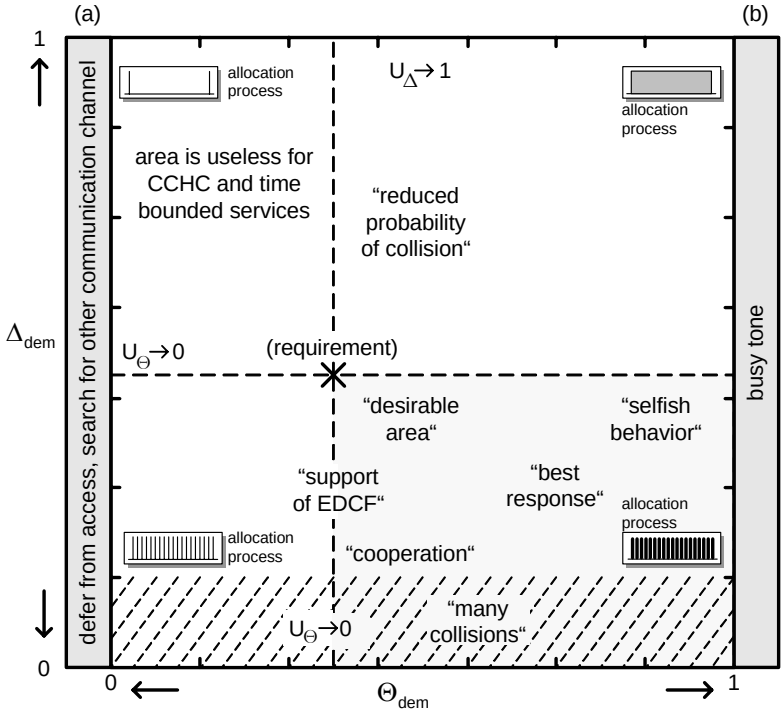

Figure 8.6: Portfolio of available actions, the corresponding utilities and the resulting consequences on the opponents. The extreme cases of (a) deferring from resource access as part of DFS and (b) occupying all resources all the time, are not part of the game model, and therefore not part of the action space.

Chapter 9

Coexisting Wireless LANs as Multi Stage Game

With the understanding of the SSG and the definition of behaviors that allow interacting players to dynamically take actions in order to achieve certain payoffs as the instantaneous outcome of an SSG, it is now possible to investigate realistic CCHC coexistence scenarios with the help of a *Multi Stage Game* (MSG). In an MSG, an SSG is played repeatedly with behaviors selected per SSG. All players take actions individually at the beginning of each stage. Players in an MSG follow a certain strategy. Strategies define what behavior to select in which SSG. Strategies can be understood as state machines where behaviors are selected from SSG to SSG based on the history of resulting payoffs. In general, an uncountable number of strategies and behaviors can be defined for an MSG; here the investigation is restricted to elementary strategies that will be defined in the following, and the behaviors defined in the previous chapter. These strategies and behaviors allow analyzing the concept of cooperation in this chapter, motivated by the analysis of Axelrod (1984). This chapter evaluates the advantages and drawbacks of the game approach developed in this thesis. The CCHC coexistence problem will be evaluated with and without the game approach that has been introduced in the previous chapters.

A strategy is a description of how a player intends to play by selecting behaviors throughout the MSG. The behaviors that are used by the strategies are BEH-P,

BEH-B, BEH-C, BEH-D, as defined in the previous chapter, see Section 8.3.2, p. 184. Static strategies, where one behavior is selected continuously throughout the complete MSG are studied first and discussed in Section 9.2. Dynamic strategies allow a player to select different behaviors as response to the behavior of the opponent player throughout the course of the MSG. Dynamic strategies are discussed in Section 9.3. This section concludes this chapter by discussing the advantages and drawbacks of the game approach taken in this thesis.

Before introducing static and dynamic strategies, the payoff calculation in the MSG and the Nash equilibrium in the MSG are introduced in the following Section 9.1.

9.1 Strategies in MSGs

In this thesis, strategies are defined as state machines that describe which behavior to select at what stage of the game. Payoffs in an MSG are calculated differently than payoffs in an SSG, which will be explained in Section 9.1.1. Further, Nash equilibria in the MSG are defined between strategies rather than between actions, as it was the case in the SSG. This is explained in Section 9.1.2.

9.1.1 Payoff Calculation in the MSGs, Discounting and Patience

In every stage n of the MSG, players take the decision of which action to take (or, what behavior to select out of the set of available behaviors). When taking the decision, the influence of the behavior in the present stage on the observed payoffs of the following stages must be taken into account. This is done in an MSG by discounting future expected payoffs (Osborne and Rubinstein, 1994), as explained in the following.

Players give present payoffs a higher weight than payoffs of future stages, as future payoffs are potentially uncertain and are estimated in the present stage. A general approach to model this preference is to discount the payoffs for each stage of a game. A discounting factor δ, with $0 \leq \delta \leq 1$ is used in the payoff calculation which reflects in the present stage the relative level of importance of the payoff of following stages.

As $\delta \to 1$, future payoffs have the same importance as the payoff of the present stage. A player that discounts with such a large discounting factor is referred to as being a patient player. On the other hand, with $\delta \to 0$, a player focuses on the present payoff only and pays no attention to potential future payoffs. Such a player is referred to as an impatient player.

Table 9.1: Discounting factors of different QoS characteristics (Berlemann 2003)

application	discounting factor δ
data, best effort	*0.5*
video, voice, CCHC (802.11 overlapping QBSS)	*0.9*
Network Control, CCHC (802.11 - HiperLAN/2)	*1.0*

The value of this discounting factor δ is determined with the help of the QoS requirements a player attempts to achieve throughout the MSG. As the QoS requirements remain constant during the course of the MSG, the discounting factor remains constant as well. Table 9.1 illustrates corresponding discounting factors for some typical applications.

The payoff a payer *i* observes in an infinitely often repeated SSG is then calculated with a discounting factor δ through

$$V^i_{infinite\ MSG} = V^i(0) + \delta V^i(1) + \delta^2 V^i(2) + \ldots = \sum_{n=0}^{\infty} \delta^t V^i(n). \tag{9.1}$$

With $\delta < 1$, the later the stages the smaller the contribution of this stage to the payoff in the present stage. Future payoffs are worth less in the present stage. A MSG consists of a finite number of repeated SSGs with an existing end. Thus, the MSG is not infinitely repeated. The interaction of two CCHCs in the coexistence scenario has a typical duration of some seconds or minutes, but is clearly not infinite. However, the end of the interaction is unknown to the players, because of the unknown situation of the opponent player: players can only define a certain probability *p* that there will be no next stage after the present stage. Assuming that *p* is the probability that the MSG ends after each stage, the payoff is calculated as

$$\begin{aligned} V^i_{finite\ MSG} &= V^i(0) + (1-p)V^i(1) + (1-p)^2 V^i(2) + \ldots \\ &= \sum_{n=0}^{N_{MSG}} (1-p)^t V^i(n) \end{aligned}, \tag{9.2}$$

where N_{MSG} is the unknown number of stages of the MSG. In literature of game theory, the probability *p* is often used as a measure for what is called the shadow of the future. The larger the value of *p* is, the more important the future stages are when taking a decision at a particular stage. Note that the payoff calculation by discounting in an infinite MSG, as shown in Equation (9.1), and the probability version of the payoff calculation in an finite MSG with unknown end, as shown in Equation (9.2), are very similar.

By setting the probability p, that the finite MSG continues, to $\delta = 1 - p$, and assuming that there is a large number of stages left to be played, i.e., $n \ll N_{MSG}$, the overall payoff V^i_{MSG} a player i observes in an MSG is derived from the infinite game with discounted payoffs, as shown in Equation (9.1). The discount version and the probability version of the payoff calculation are equivalent, hence, in the following the payoff V^i_{MSG} a player i observes in the MSG, is calculated by the following equation (Fuller, 2002).

$$(1-p) \overset{!}{=} \delta \quad \Rightarrow \quad V^i_{MSG} = \sum_{n=0}^{\infty} \delta^t V^i(n) \,. \tag{9.3}$$

9.1.2 Solution of the MSG of two Players: Nash Equilibrium of Strategy Pairs

It can be analyzed whether two strategies, each strategy selected by one player, form a *Nash equilibrium of Strategies in the MSG*. Here, the concept of Nash equilibrium differs from the definition for the SSG, as it was used in the previous chapters: a Nash equilibrium of Strategies in the MSG is given if no player has the incentive to unilaterally deviate from its strategy for any number of stages, taking into consideration the observed payoff as defined in Equation (9.3).

Players have the intention to establish a steady state in the MSG. The players attempt to influence this steady state to their advantage. The concept of a Nash equilibrium implies best response actions of the players. A result of the analysis of SSGs is that in many scenarios the Nash equilibrium is the Pareto optimal outcome of the SSG. In this context, the equilibrium is a *Nash equilibrium of actions in the SSG*.

To show that a strategy pair is not a Nash equilibrium in the MSG, at least one other strategy has to be identified that one player would prefer, i.e., a strategy that achieves a higher payoff. In contrast, to show that a strategy pair is a Nash equilibrium in the MSG, it has to be shown that there is no other strategy that one player would prefer to deviate to for any number of stages.

9.2 Static Strategies

Static strategies implement one single behavior constantly throughout the MSG. Therefore, static strategies are directly related to behaviors.

9.2.1 Definition of Static Resource Allocation Strategies

In this section, four fundamental strategies are defined and described in detail.

9.2.1.1 Static Strategy "Persist" (STRAT-P)

The strategy STRAT-P may be interpreted as the one selected by wireless LANs that are not following any game approach. A player representing such a wireless LAN selects actions as they are defined by its requirement, without taking into account the resource allocations of an opponent player. A player that follows STRAT-P is referred to as myopic, as it is not aware of any activity of other players in its environment. The Figure 9.1 illustrates this strategy as machine with a single state, using the notation of Osborne and Rubinstein (1994).

9.2.1.2 Static Strategy "Best Response" (STRAT-B)

The strategy STRAT-B implements the rational behavior, which attempts to maximize the payoff by estimating the opponent player's behavior. If all players select this strategy, players will adjust into a Nash equilibrium. How fast this adjustment process converges into the equilibrium depends on the success of the prediction, as explained in Section 7.4, p. 152.

9.2.1.3 Static Strategy "Coop" (STRAT-C)

The strategy STRAT-C implements the cooperative behavior without taking into account any effect of this behavior on the resulting outcome. Note that there are many games where cooperation is not the desirable behavior because it leads to very small observed payoffs for the cooperating players.

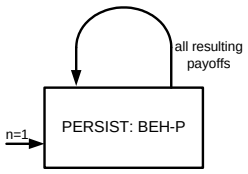

Figure 9.1: Strategy STRAT-P as machine in the notation of Osborne and Rubinstein (1994). There is one state labeled as PERSIST, which is the initial state at stage $n = 1$. In this state, the player plays the behavior BEH-P as defined in Section 8.3.2.1, p. 184. The strategy is static, thus, upon any outcome of a SSG, the player will play BEH-P in the complete MSG.

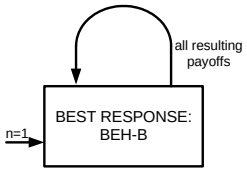

Figure 9.2: Strategy STRAT-B as machine. The state is labeled with BEST RESPONSE and the behavior is BEH-B as defined in Section 8.3.2.2, p. 184.

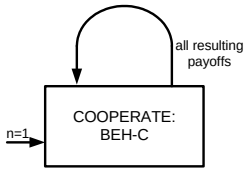

Figure 9.3: Strategy STRAT-C as machine. The state is labeled with COOPERATE and the behavior is BEH-C as defined in Section 8.3.2.3, p. 185.

9.2.2 Experimental Results

In the following, the static strategies STRAT-P, STRAT-B, and STRAT-C are analyzed and compared with each other.

9.2.2.1 Scenario

A game with the following requirements is analyzed:

$$\left(\begin{pmatrix}\Theta^1_{req}\\ \Delta^1_{req}\end{pmatrix},\begin{pmatrix}\Theta^2_{req}\\ \Delta^2_{req}\end{pmatrix}\right) = \left(\begin{pmatrix}0.6\\ 0.4\end{pmatrix},\begin{pmatrix}0.6\\ 0.23\end{pmatrix}\right).$$

Player *1* attempts to allocate resources for a longer duration than player *2*. Hence, as a result of the analysis in Section 8.3.2.3, p. 185, player *2* can be considered as the weaker player. The Nash equilibrium of this game is unique and given by the action profile

$$\underline{a}^* = \left(a^1* = \begin{pmatrix}0.6\\ 0.032\end{pmatrix}, a^2* = \begin{pmatrix}0.86\\ 0.02\end{pmatrix}\right), \tag{9.4}$$

and the resulting payoff in Nash equilibrium is

$$V^*\left(\left(a^1*\right),\left(a^2*\right)\right) = \left(0.81;\ 0.37\right). \tag{9.5}$$

Numerical searches indicate that this Nash equilibrium is not Pareto efficient, which means that in this particular game it may be beneficial for both players to cooperate rather than attempting to maximize the individual payoffs per SSG. This will be discussed in the following Section 9.2.2.2. In this section, the results given in Section 9.2.2.4–9.2.2.6 are reviewed. Results for three different approaches of the CCHC coexistence game of two overlapping BSSs are presented. Section 9.2.2.4, p. 202, shows the simulation and analytical results for the simplest

approach where both players take actions without dynamic behavior adaptation, according to the static strategy STRAT-P. This scenario represents two overlapping BSSs that follow their requirements when allocating resources, without taking into account the mutual influences between the competing BSSs. It is the scenario against which all other scenarios are evaluated and compared, because it represents behaviors that occur when players do not follow any game approach. Section 9.2.2.5, p. 203, shows the simulation and analytical results for the approach where both players take actions that attempt to maximize the individual payoffs, based on the history of their observations. This is referred to as best response, according to the static strategy STRAT-B. Finally, Section 9.2.2.6, p. 204, shows the simulation and analytical results for the approach where both players take actions cooperatively, according to the static strategy STRAT-C.

Three figures are given per section, each figure being comprised by some subfigures. The first figure at the beginning of each section illustrates the required, demanded, and observed QoS parameters (see for example for the first section, Figure 9.4, p. 202) as a result of the repeated interactions of the players. The second figure in each section indicates the behaviors that are selected by the players per stage, and the observed utilities and payoffs (see for example in Figure 9.5, p. 202). The third figure in each section illustrates in its left subfigure the probabilities of resource allocation delays that result if the respective static strategies are selected for a long duration (see for example Figure 9.6, p. 203, left subfigure). Finally, this third figure in each section illustrates in its right subfigure the throughput and payoff results that are typically found when the requirements for share of capacity of both players are varied. Note that in the latter figure the required resource allocation intervals remain as they have been defined in this section, but the required share of capacities are varied between *0.1* and *0.8*:

$$\left(\begin{pmatrix}\Theta^1_{req}\\ \Delta^1_{req}\end{pmatrix},\begin{pmatrix}\Theta^2_{req}\\ \Delta^2_{req}\end{pmatrix}\right) = \left(\begin{pmatrix}\Theta^1_{req}\\ 0.4\end{pmatrix},\begin{pmatrix}\Theta^2_{req}\\ 0.23\end{pmatrix}\right),$$

with $\Theta^1_{req} = \Theta^2_{req} = 0.1 \ldots 0.8$. In all games analyzed here, the EDCF background simulates an offered traffic of $5\,Mbit/s$, which is modeled through an Ethernet traffic trace file (see Appendix B for an explanation of the simulation environment). The TXOPlimit that defines the maximum duration of resource allocations of the EDCF is set to $300\,\mu s$, which is relatively small and therefore limits the influence of the EDF on the results. All results are discussed in the next section, each approach independently.

9.2.2.2 Discussion

The results of the three approaches STRAT-P, STRAT-B, and STRAT-C are discussed in the following sections 9.2.2.2.1-9.2.2.2.3.

9.2.2.2.1 Persistent Behavior

Section 9.2.2.4, p. 202, summarizes the results for two players that follow the strategy STRAT-P.

Figure 9.4 shows the required, demanded and observed QoS parameters for the first 40 stages of the MSG. The left figures show the results for player *1* and the right figures show the results for player *2*, with Θ-parameters in the top figure, and the Δ-parameters in the bottom figure, respectively. The dotted lines indicate that the players demand their requirements persistently throughout all stages. The demands are always identical to the requirements. The requirements remain constant throughout all stages and are indicated as light gray lines in the figure.

However, because of the interaction within the allocation process and because of the strong QoS demands of both players, the outcomes of the games, i.e., the observed QoS parameters $\Theta_{obs}^{1,2}$ and $\Delta_{obs}^{1,2}$, deviate significantly from the demanded parameters. Player *1* requires longer resource allocations than player *2*, and as a result, it is player *1* that can achieve its required share of capacity by playing STRAT-P in the presence of the opponent player *2*, i.e., $\Theta_{obs}^{1} \approx \Theta_{req}^{1}$. In contrast to player *1*, player *2* is considered as the weaker player and cannot achieve its required share of capacity by playing the persistent STRAT-P, therefore $\Theta_{obs}^{2} < \Theta_{req}^{2}$. The reason for this result is the longer duration of the resource allocations of the opponent player *1*: the player *2* has to wait considerably longer when player *1* allocates radio resources. Therefore, it is more likely to loose individual resource allocations by unacceptable long delays.

However, looking at the delay results it can be observed that both players suffer from the uncoordinated interaction with their opponents. For both players, the observed resource allocation delays are larger than what they require, i.e., $\Delta_{obs}^{1} > \Delta_{req}^{1}$ and $\Delta_{obs}^{2} > \Delta_{req}^{2}$, hence, both players cannot achieve their requirements because of the many resource allocations of their opponents.

The figures show minor dynamic variations of the observed QoS parameters, which are a result of the random EDCF background traffic. The influence of the EDCF is insignificant here because of the lower priority in resource allocation and the small TXOP durations of the EDCF due to the TXOPlimit.

All resulting observations that are indicated in Figure 9.4 are simulation results. In addition, the repeated interactions have been approximated with the help of the

analytical game model. The results of this approximation are given as dashed lines in the figure and show adequate conformity with the simulation results. This supports the conclusion taken in Section 8.1.5.4, p. 172, where it was stated that the Markov model developed for the approximation is accurate enough to capture all relevant characteristics of the SSG.

The Figure 9.5 indicates the behaviors that are selected by the players for each stage, and the observed utilities and payoffs for both players. As part of the static strategy STRAT-P, all players select the persistent behavior out of four possible behaviors, throughout all stages. The utilities can be directly derived from the observations and imply again the problematic situation: in summary, when comparing the payoffs given as utility $U^{1,2}_{\Theta\Delta}$, the player *2* suffers clearly from the uncoordinated interaction with its opponent, whereas player *1* can achieve a certain level of satisfaction, that means a certain payoff that may be sufficient for it.

Figure 9.6 indicates in its left subfigure the probability distributions of delay of resource allocation attempts, which can be compared to the backoff delays in 802.11. From this figure, any variation in the resource allocation periods can be derived, thus it indicates also the parameter Ξ_{obs}, which is not in the focus of this analysis. Clearly, because of the different durations of resource allocations, player *1* and player *2* observe different delays. Player *1* observes smaller delays because of the smaller durations of resource allocations of player *2*.

Results of more general experiments that have been obtained by applying the analytical model of the SSG, are presented in the right subfigure of Figure 9.6. Here, the observed share of capacity is shown as function of the required share of capacity, as explained in the scenario description. Here, the required resource allocation intervals remain constant, whereas the required durations of the resource allocations are varied ($\Delta^{1,2}_{req}$ remain constant, but $\Theta^{1,2}_{req}$ are varied). It can be seen in Figure 9.6, right subfigure, that player *1* outperforms player *2* as soon as the cumulative requirements do not allow both players to meet their requirements at the same time in the presence of the opponent. That is, for $\Theta^{1}_{req}+\Theta^{2}_{req} > 0.35 \cdot 2$, player *2* cannot achieve what it requires, whereas player *1* can still meet its required share of capacity as long as the scenario becomes not completely overloaded at $\Theta^{1}_{req}+\Theta^{2}_{req} \geq 1$. In addition, the higher the requirements of player *1* and player *2* for share of capacity, the smaller the throughput of the EDCF, as can be seen in the figure. The EDCF is not captured by the analytical model; the respective curves are a result of stochastic simulation. In Figure 9.6, in addition to the observed share of capacity (which corresponds to the resulting throughput), the payoffs of the two players are shown as they are the relevant outcomes of the games. As expected, the higher the requirements of player *1* and

player *2* for share of capacity, the smaller the payoffs. As long as the durations of resource allocations are relatively short, resulting payoffs are high, as both players can achieve what they require. However, with increasing requirements, the payoffs decline, again earlier for the weaker player *2* than for the stronger player *1*. The discussed payoff results of Figure 9.6 are to be evaluated against the resulting payoffs when strategies are selected by the players that differ from the persistent strategy STRAT-P, as it will be discussed in the following.

9.2.2.2.2 Rational Behavior

Section 9.2.2.5, p. 203 summarizes the results for two players that follow the strategy STRAT-B.

The four figures of Section 9.2.2.4 illustrate the parameters as before, in similar order. It can be observed from Figure 9.7 that, after 2 s (after 10 stages), the players switch from persistent actions to the best response actions. At the beginning of the simulation, the actions are taken according to STRAT-P, and after some stages, the players select their new strategies. This is necessary to allow players to assess the initial demand of their opponents before starting to adapt actions as estimated best responses to the predicted actions of their opponents, as part of STRAT-B. However, in real life, interacting players need some stages at the beginning of the interaction to estimate the behavior of the opponent. This is neglected here.

Interestingly, the QoS demands converge to the unique Nash equilibrium that can be calculated for this particular game and is given in Section 9.2.2.1. This is one of the beneficial characteristics of the game approach in the CCHC coexistence problem, which is developed in this thesis: if both players play rational and select always their best response to what their opponent player demands, the game converges towards a Nash equilibrium profile. If the Nash equilibrium is unique, as it is the case here, then this profile is the predicted outcome after some stages. In fact, players may select this Nash equilibrium action profile in advance, without slowly converging to it. To enable players to take those actions immediately, they have to know their opponent's requirements, however. This is generally not the case. Without this detailed knowledge about their opponent's requirements, by estimating their opponent's demands, players can nevertheless converge to the Nash equilibrium action profile. The speed and success of convergence depend on many parameters, such as the quality of the prediction method, and the actual requirements the players try to achieve.

As before, simulated and analytically approximated outcomes in Figure 9.7 are qualitatively similar.

Figure 9.8 illustrates the resulting utilities and payoffs of the games, and the behaviors the players selected during the first 40 stages. Comparing the results with the outcomes given in Figure 9.5, it can be observed that after converging to the equilibrium profile, player 2 improved its payoff compared to what it achieved when both players played STRAT-P, whereas player 1 did not achieve the same level of satisfaction as with STRAT-P. This is a result from the fact that now player 2 is able to take actions that maximize its payoff, at the cost of player 1's payoff. However, player 1 also attempts to maximize its payoff independently. This does not necessarily mean that it can achieve higher payoffs than before, when both players took persistent actions STRAT-P. No player can improve its outcome by unilaterally deviating from the Nash equilibrium action profile when all players take rational actions according to STRAT-B.

Figure 9.9, left subfigure, indicates the probabilities of delayed resource allocation attempts, in the scenario where both players play rationally. From this figure, it can be seen that again player *1* and player *2* observe different delays, but now it is player *2* that observes smaller delays because with STRAT-B player *1* demands smaller resource allocations than with STRAT-P. As before, Figure 9.9, right subfigure, shows the resulting shares of capacity and the resulting payoffs, for any share of capacity required by the two players. Comparing the results with the right subfigure of Figure 9.6, it can be seen that depending on the requirement, playing rational may be beneficial for both players, or only for the weaker player *2*. Particularly, as long as the players require relatively small shares of capacity, they cannot gain largely by adapting their behaviors rationally, according to the best response strategy STRAT-B.

9.2.2.2.3 Cooperative Behavior

Section 9.2.2.6, p. 205, summarizes the results for two players that follow the strategy STRAT-C, again in the same order as before.

In Figure 9.10, where simulation results and analytical approximations show very similar results, it can be seen that, as part of the cooperative behaviors, the players reduce their demands for share of capacity after *2* seconds, when they switch from STRAT-P to STRAT-C. Further, in accordance with the definition of how to take actions in cooperation, player *1* reduces its demanded resource allocation period, whereas the resource allocation period demanded by player *2* remains constant, as it is relatively small already. Because of the shorter resource allocations, now the players observe delays that are closer to their requirements than before.

The payoffs indicated in Figure 9.11 show the advantage of the cooperative behavior about the persistent, as well as about the rational best response behavior, especially for player *2*. By crossing the Pareto boundary, when playing cooperatively, the players achieve higher payoffs than before. However, the result that cooperation outperforms the rational behavior is valid in the analyzed example here, but it is not necessarily a valid assumption in general.

The left subfigure of Figure 9.12 shows the delays of resource allocations. The figure indicates that due to the shorter resource allocations of both players, the delays are smaller than before, which of course is beneficial in terms of observed resource allocation periods and observed share of capacity.

In contrast, Figure 9.12, right subfigure, clearly indicates that it cannot be generally stated, that it is always beneficial for a player to cooperate. As described already, only if the Nash equilibrium is not Pareto efficient, it is worth for the interacting players to cooperate. However, it depends on the requirements and utility functions if a Nash equilibrium is Pareto efficient. The fact that it is not always preferable for a player to cooperate can be seen in the right subfigure of Figure 9.12, where the results shown in the case of small requirements for share of capacity imply that mutual cooperation results in smaller payoffs compared to what can be achieved by rational behavior. The players achieve high payoffs by playing their best responses as part of the rational behavior, as discussed in the previous section, and as illustrated in Figure 9.9. A Nash equilibrium in such a game, may it be unique or not, is probably Pareto efficient, and in such a situation, rational behavior will be preferred over cooperation by a player.

9.2.2.3 Conclusion

Three static strategies, the simple persistent STRAT-P, the payoff maximizing STRAT-B, and the cooperative STRAT-C have been compared with each other. In summary, the following conclusions can be drawn from the analysis. A player that does not meet its requirements because of the allocation process and the competition with another player shall not allocate resources as defined by the QoS requirements; it shall in contrast play rational and attempt to maximize its payoff:

$$U^i(BEH\text{–}B) \geq U^i(BEH\text{–}P)$$
$$\Rightarrow \quad STRAT\text{–}B \quad \succsim^i \quad STRAT\text{–}P, \quad i \in \mathbb{N}.$$

The rational behavior weakly dominates the persistent behavior, however, only if resource allocations by the opponent player have implications on the resulting payoffs.

Cooperation is not always beneficial. Depending on the requirements, there may exist an action profile that is not a Nash equilibrium profile, but results in higher payoffs for at least one player. In such a game, where Nash equilibria are not Pareto efficient, cooperation is a desirable action profile:

$$U^i(BEH\text{–}C) \geq U^i(BEH\text{–}B)$$
$$\Rightarrow \quad STRAT\text{–}C \quad \gtrsim^i \quad STRAT\text{–}B, \quad i \in \mathrm{N}.$$

In any other case, playing rational will lead to a Nash equilibrium point, which is Pareto efficient, and thus rational behavior is preferred.

The QoS requirements of opponents are not known to the players. Therefore, without any history of interactions, players cannot assess if an outcome of a game is Pareto efficient or not. Further, it is difficult for players to assess if their opponent players are cooperating or not. Once a player concludes that cooperative behavior results in better outcomes (in higher resulting payoffs) than rational behaviors, it has to ensure that the opponent player will cooperate as well in future stages of the MSG.

Dynamic strategies are discussed in Section 9.3. Dynamic strategies allow players to switch between behaviors dynamically, as part of the strategies. In dynamic games, i.e., in games where players apply dynamic strategies, payoffs and Nash equilibria are calculated as defined in Section 9.1 for the whole duration of the MSG. The defective behavior BEH-D is used by players to coordinate the actions, and to prevent the opponent from not playing cooperatively once cooperation has been reached, as is shown in the next section.

9.2.2.4 Results: Two Overlapping BSS Coordinated by CCHCs, Without Dynamic Behavior Adaptation: STRAT-P Against STRAT-P

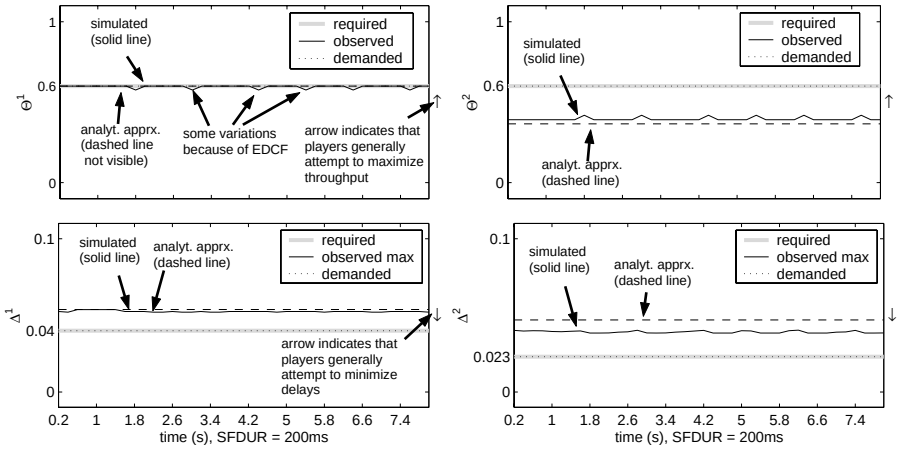

Figure 9.4: Required, demanded, and observed QoS parameters for player 1 (left) and player 2 (right). Top figures show the Θ parameter, bottom figures show the Δ parameters.

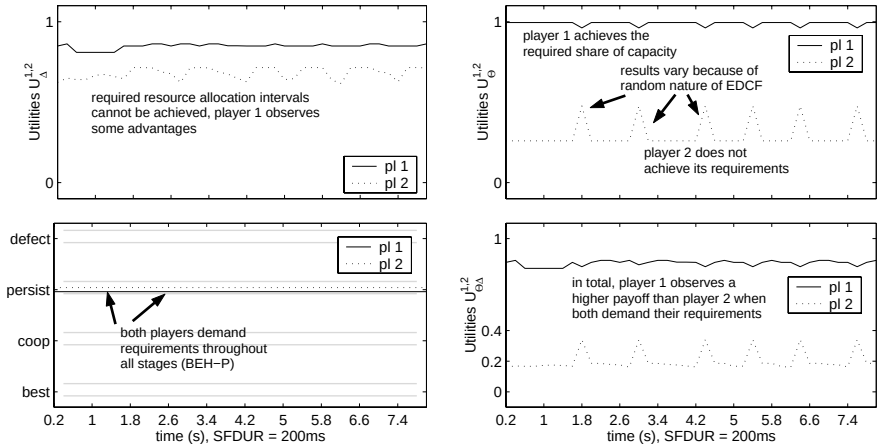

Figure 9.5: Selected behaviors throughout the game (bottom left). Resulting payoffs (=observed utilities) for player *1* and player *2*: U^i_Δ (top left) , U^i_Θ (top right), and the total payoff $V^i = U^i = U^i_\Theta \cdot U^i_\Delta$ (bottom right), $i = 1, 2$.

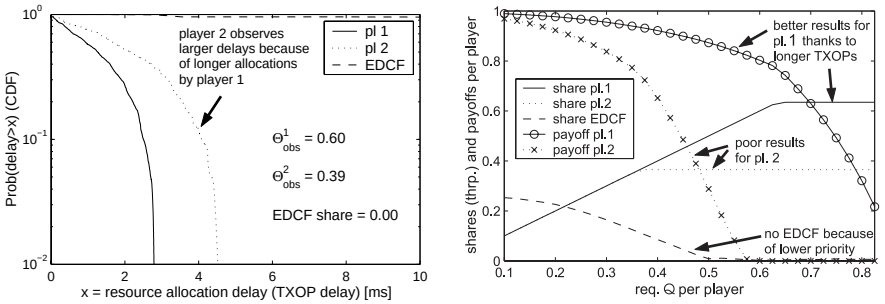

Figure 9.6: Probabilities of delay of resource allocation attempts, TXOP delay (left), and throughput and payoff results for varying requirements (right).

9.2.2.5 Results: Two Overlapping BSS Coordinated by CCHCs, Playing the Best Response: STRAT-B against STRAT-B

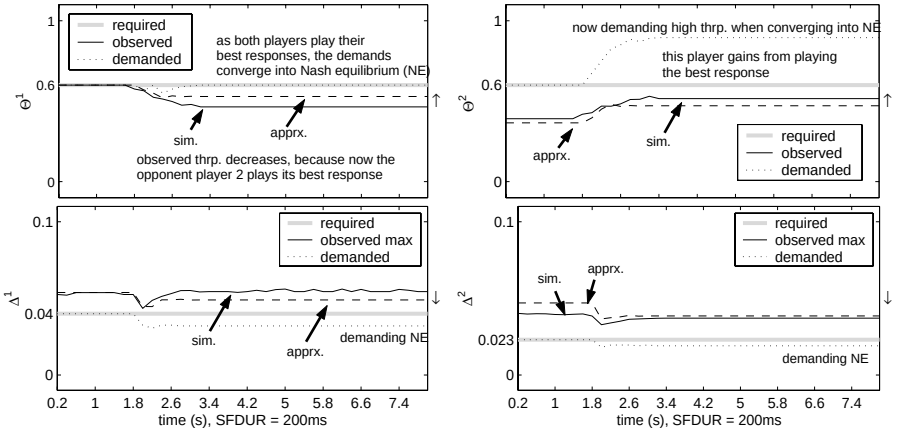

solid lines: analytics, dashed lines: YouShi simulation results

Figure 9.7: Required, demanded, and observed QoS parameters for player 1 (left) and player 2 (right). Top figures show the Θ parameter, bottom figures show the Δ parameters.

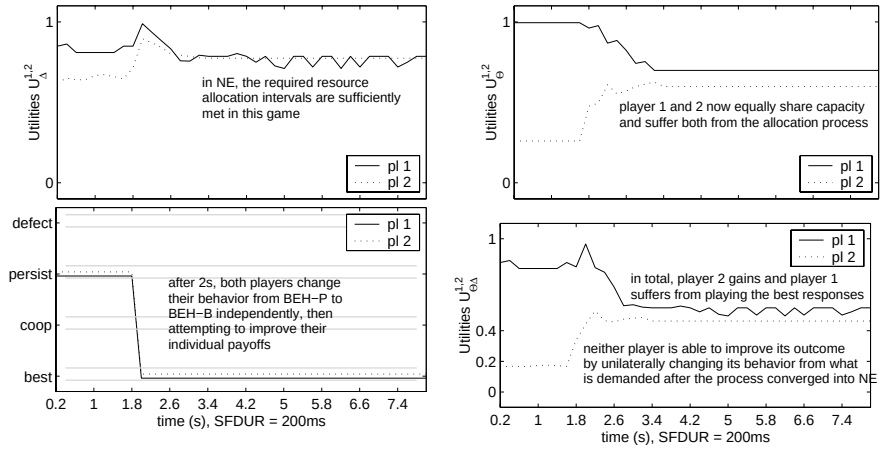

Figure 9.8: Selected behaviors throughout the game (bottom left). Resulting payoffs (=observed utilities) for player *1* and player *2*: U_{Δ}^{i} (top left) , U_{Θ}^{i} (top right), and the total payoff $V^i = U^i = U_{\Theta}^{i} \cdot U_{\Delta}^{i}$ (bottom right), $i = 1,2$.

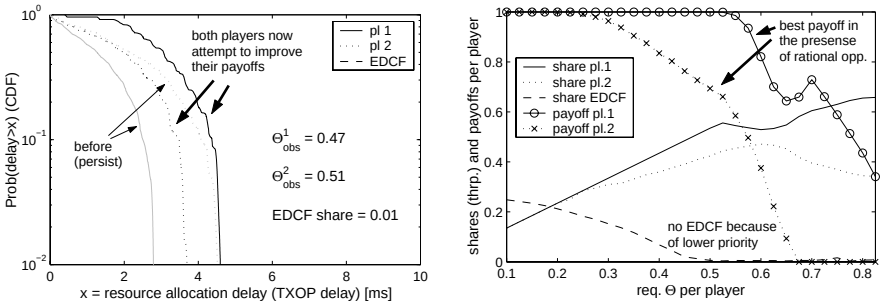

Figure 9.9: Probabilities of delay of resource allocation attempts, TXOP delay (left), and throughput and payoff results for varying requirements (right).

9.2.2.6 Results: Two Overlapping BSS Coordinated by CCHCs, Playing both Cooperatively: STRAT-C against STRAT-C

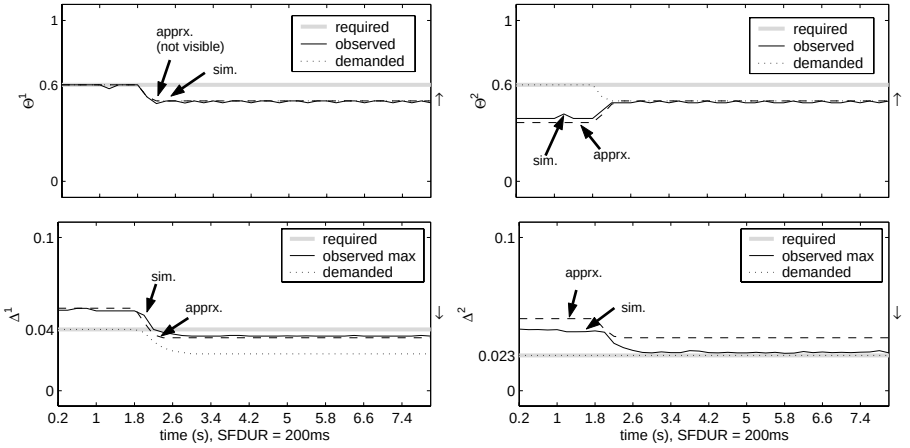

solid lines: analytics, dashed lines: YouShi simulation results

Figure 9.10: Required, demanded, and observed QoS parameters for player 1 (left) and player 2 (right). Top figures show the Θ parameter, bottom figures show the Δ parameters.

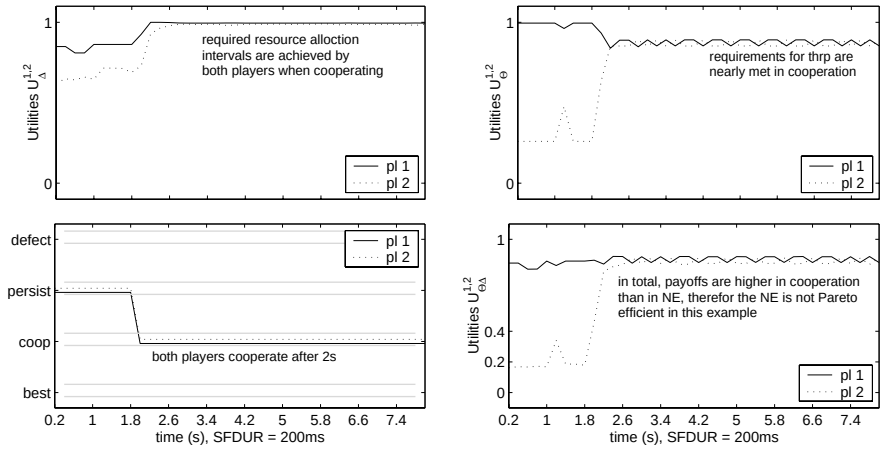

Figure 9.11: Selected behaviors throughout the game (bottom left). Resulting payoffs (=observed utilities) for player *1* and player *2*: U^i_Δ (top left) , U^i_Θ (top right), and the total payoff $V^i = U^i = U^i_\Theta \cdot U^i_\Delta$ (bottom right), $i = 1,2$.

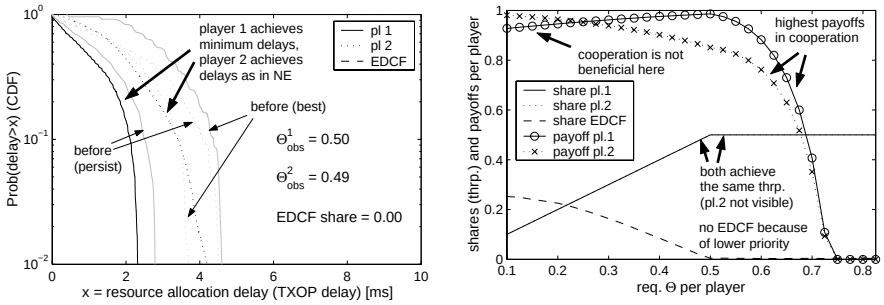

Figure 9.12: Probabilities of delay of resource allocation attempts, TXOP delay (left), and throughput and payoff results for varying requirements (right).

9.3 Dynamic Strategies

The analysis in the last section has shown that there are games in the CCHC coexistence scenario where one player requires the cooperation of the opponent player, to improve the achievable payoff for this player. Further, there are games in the CCHC coexistence scenario where both players benefit from cooperation. What has to be solved for such games are mechanisms to establish cooperation, once a player has concluded that cooperation will beneficial for all involved players. To establish cooperation, both players are required to cross the Pareto boundary. To motivate an opponent player to cooperate, punishments can be used as part of dynamic strategies. Dynamic strategies, where a player adaptively changes its behavior during the course of the MSG are discussed in the following. Dynamic strategies are also referred to as trigger strategies (Osborne and Rubinstein, 1994; Berlemann, 2003).

It is analyzed in the following under which condition deviating from cooperation will result in a higher payoff than not deviating, under the assumption that deviation will be punished as part of the dynamic strategy.

In the rest of this chapter, a scenario is assumed where cooperation is beneficial for all involved players.

9.3.1 Cooperation and Punishment

Players adopt their behavior for different purposes. In an MSG, the rational behind the decisions taken at the stages about what behavior to select is not the payoff per stage, but the discounted MSG payoff for the current and any following stages. It depends on the discounting factor if a player considers future stages, or if it attempts to optimize the instantaneous payoff of this stage.

Any behavior other than cooperation (denoted as BEH-C) is in the following interpreted as a defection. Defection may be the selection of punishments by playing BEH-D, but also the selection of BEH-B, the best response behavior. Playing the best response when the opponent is cooperating is a deviation from cooperation that is maximizing the payoff, but at the cost of the observed payoff of the opponent. Hence, it is interpreted as defection in the following.

It was defined in Section 9.1.2 that the MSG payoff is calculated with the help of the discounting factor, given by

$$V_{MSG}^{i} = \sum_{n=0}^{\infty} \delta^{n} V^{i}(n) \, .$$

Any player *i* cooperates during the MSG if it expects to observe a higher payoff with cooperation than without cooperation:

$$V_{MSG}^{i}(\mathit{STRAT\text{–}C}) \geq V_{MSG}^{i}(\mathit{any\ other\ strategy})$$
$$\Rightarrow \quad \mathit{STRAT\text{–}C} \quad \succsim^{i} \quad \mathit{any\ other\ strategy}, \quad i \in \mathrm{N}.$$

9.3.2 Condition for Cooperation

Let V_{CC}^{i} be the payoff player *i* observes at any stage when both interacting players cooperate, and let V_{CD}^{i} be the payoff when player *i* cooperates and at the same time player *-i* defects. Further, let V_{DC}^{i} be the payoff when only the opponent player cooperates, and V_{DD}^{i} be the payoff when neither player cooperates.

At any stage *n*, player *i* can expect the following discounted MSG payoff if it continues to cooperate, assuming that the opponent player will not deviate from cooperation:

$$V_{MSG}^{i} = \sum_{k=n}^{\infty} \left(\delta^{i}\right)^{k} \cdot V_{CC}^{i} \, .$$

This payoff gain must outweigh the payoff gain that results from a one-time defection, including the expected payoffs that follow when the opponent punishes this defection. As part of a dynamic strategy that seeks to establish cooperation, the payoff gain of defecting must be compensated through punishment over one or several following stages.

At any stage *n*, player *i* can expect the following discounted MSG payoff if it unilaterally deviates from cooperation to defection, assuming that the opponent player will punish this defection for the *n'* following stages:

$$V^i_{MSG} = \underbrace{V^i_{DC}}_{\substack{\text{one time}\\ \text{defection}}} + \underbrace{\sum_{k=n+1}^{n+n'+1} \left(\delta^i\right)^k \cdot V^i_{CD}}_{\text{punishment}} + \underbrace{\sum_{k=n+n'+1}^{\infty} \left(\delta^i\right)^k \cdot V^i_{CC}}_{\text{return to cooperation}} .$$

Comparing the last two equations, it can be defined under which condition player *i* does not deviate from established cooperation. The condition is

$$\sum_{k=n}^{\infty} \left(\delta^i\right)^k \cdot V^i_{CC} \quad > \quad V^i_{DC} + \sum_{k=n+1}^{n+n'+1} \left(\delta^i\right)^k \cdot V^i_{CD} + \sum_{k=n+n'+1}^{\infty} \left(\delta^i\right)^k \cdot V^i_{CC},$$

which can be rewritten as

$$\sum_{k=n}^{n+n'+1} \left(\delta^i\right)^k \cdot V^i_{CC} \quad > \quad V^i_{DC} + \sum_{k=n+1}^{n+n'+1} \left(\delta^i\right)^k \cdot V^i_{CD}. \tag{9.6}$$

The worst-case punishment is a game wide punishment, i.e., $n' \to \infty$, which would for example mean the end of cooperation because of the deviation. For a game wide punishment, Equation (9.6) can be solved to

$$V^i_{CC} \cdot \frac{1}{1-\delta^i} \quad > \quad V^i_{DC} + V^i_{CD} \cdot \frac{\delta^i}{1-\delta^i}.$$

With this condition, it is visible that it depends on the discounting factor if deviation from cooperation at one stage is preferred over cooperation, regardless of how long the punishment will take place. In conclusion, the condition that cooperation is preferred over defection is given by

$$\delta^i > \frac{V^i_{CC} - V^i_{DC}}{V^i_{CD} - V^i_{DC}}. \tag{9.7}$$

9.3.3 Experimental Results

In the following, a dynamic strategy that allows players to achieve cooperation under some conditions is discussed as an example. Let player *-i* play according to the dynamic strategy STRAT-CnP, which is illustrated as machine in Figure 9.13. Player *i* plays cooperates at any time (STRAT-C). At a stage *n*, it considers deviating to the best response for a single stage. The question to be answered is if it is worth to continue the cooperation or not.

Figure 9.14 shows the results obtained from the analysis as described here, as well as taken from simulation. A typical CCHC coexistence scenario is analyzed. Results are given for different discounting factors, i.e., different QoS requirements. The MSG outcomes of player i are shown in the figure.

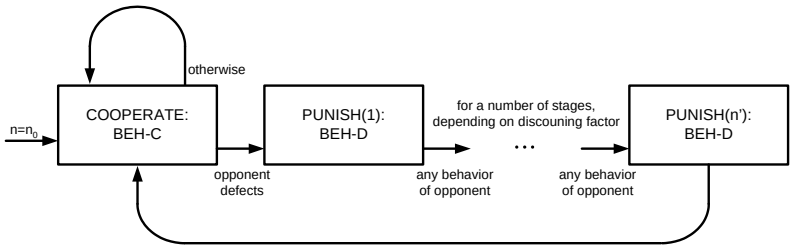

Figure 9.13: Strategy STRAT-CnP as machine. A player initially cooperates (state "COOPERATE"), and punishes for a number of stages (states PUNISH(1)...PUNISH(n')) upon defection of the opponent player.

All results are normalized to the cooperation payoff $V^i_{COOP}(\delta^i)$. The lines mark the expected payoffs, determined at stage n when the player's decision which behavior to select is taken. Player i deviates for a single stage and is consequently punished by the opponent player $-i$. Depending on the intensity of the punishment, i.e. the number of stages, the discounted MSG payoff for player $-i$ from this single deviation is higher than the payoff that results when continuing cooperation, as can be seen in all four subfigures. If the cooperation payoff that is in the figure denoted as $V^i_{COOP}(\delta^i)$, is higher than the deviation payoff, cooperation can be established.

For low values of δ^i, i.e., if the future is not very much considered compared to the current stage, the player i gives the short-term payoff gain through the deviation at this stage a higher value than the long-term payoff from cooperation, see Figure 9.14(d). In this case, cooperation cannot be established.

In this example, the player prefers cooperation to defection for discounting factors that are larger than ~ 0.7. This is indicated in Figure 9.14(a-c). The larger the discounting factor, the smaller the number of stages during which punishment takes place, until the single deviation from cooperation will be compensated.

9.3.4 Conclusion

Cooperation is more likely to be established, and maintained, if players consider the outcomes of future stages, when taking the decision about what behaviors to select. This confirms the empirical study in Axelrod (1984). As a consequence for the CCHC coexistence, cooperation is indeed a realistic assumption likely to be achieved in scenarios where the offered traffic is high, because of the CCHC characteristics. CCHCs will operate with larger discounting factors when they attempt to support multiple different MACs.

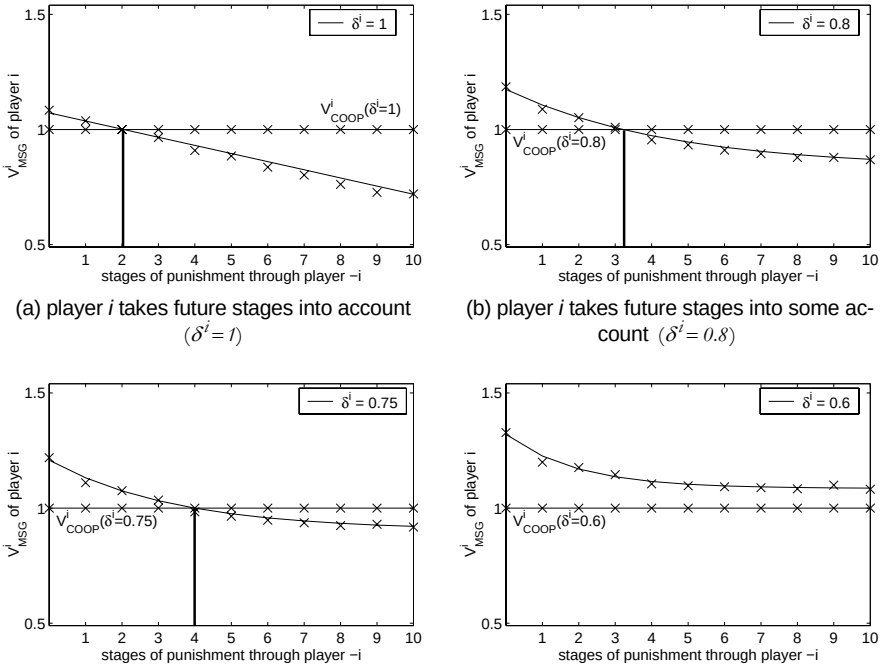

(a) player *i* takes future stages into account $(\delta^i = 1)$

(b) player *i* takes future stages into some account $(\delta^i = 0.8)$

(c) future is less important for player *i* $(\delta^i = 0.75)$

(d) mainly the current, instantaneous QoS is important to player *i* $(\delta^i = 0.6)$

lines: analytical results; markers: YouShi simulation results

Figure 9.14: MSG payoffs of player *i*, normalized to the payoff in cooperation. Results are given for various discounting factors. Player *i* deviates for a single stage and is consequently punished by the opponent. If the MSG payoff in cooperation is larger than the MSG payoff when deviating, cooperation can be established.

Chapter 10

CONCLUSIONS

WIRELESS communication in unlicensed frequency bands is a challenging task when QoS is required. This thesis discusses new technologies for wireless networks and new approaches for spectrum management. The IEEE 802.11e standard is described and analyzed with the help of a new analytical approach to approximate priorities. A mechanism to integrate other protocols such as ETSI BRAN HiperLAN/2 into 802.11e, the CCHC, is proposed as solution for coexistence and interworking of wireless networks in unlicensed bands. To analyze the CCHC coexistence, a game model is developed and comprehensively used.

10.1 Problem and Selected Method

Future wireless networks will meet many technical challenges in radio resource control, especially when radio resources are shared between different networks. Considering the growth of the wireless Internet, and the increasing demands of consumer products with typical audio-/video applications that have strong QoS requirements, and considering the increasing need for information at more and more places, wireless LANs such as IEEE 802.11 are discussed in this thesis as candidate systems to provide the services needed to meet those challenges.

Wireless LANs operate in unlicensed bands, which makes it difficult to support QoS. However, QoS is a key requirement in future wireless networks. The coexistence of wireless networks of different or the same type operating in unlicensed bands in competition for radio resources is a key challenge in the development of future wireless networks. It is natural to approach this problem with the help of the theory of games.

> *"Perhaps the word 'game' was an unfortunate choice for a technical term. Although many rich and interesting analogies can be made to Bridge and Poker, and other parlor games, the usual sense of the word has connotations of fun and amusement, and of removal from the mainstream and the major problems in life. These connotations should not be allowed to obscure the more serious role of game theory in providing a mathematical basis for the study of [...] interaction, from the viewpoint of the strategic potentialities of individuals and groups."* (Shubik 1982:7)

The cited statement considers human interaction, whereas in this thesis the interaction of technical systems is analyzed. However, the statement points to an often raised, but unwise concern when applying games for the analysis of technical problems. It should be emphasized in this context that "the game" is more related to strategies, whereas "the play" refers more to what is the common understanding of games between people.

Game models are developed in this thesis to analyze the CCHC coexistence. The developed methods are evaluated with stochastic simulation.

The CCHC concept relies on the upcoming enhancement of 802.11, the 802.11e. For this new protocol, an analytical model is developed and evaluated with stochastic simulation to approximate the expected achievable throughput that can be supported by 802.11e. Hence a complete analysis of this new protocol, including the analysis of the coexistence problem, is provided in this thesis.

10.2 Summary of Results

802.11e will be an efficient means for QoS support in wireless LANs. It will provide mechanisms to increase the protocol efficiency and the achievable throughput. The most promising and flexible approach to support future applications are wireless LANs such as IEEE 802.11, including its enhancements to support QoS, i.e., 802.11e. Integrated into cellular networks such as *Universal Mobile Telecommunications System* (UMTS), wireless LANs will make these networks *universal*.

A new analytical model to approximate the relative priority between different access categories when 802.11e stations operate with different QoS parameters, is

provided in this thesis. The model sufficiently approximates simulation results in nearly all scenarios.

The controlled channel access of 802.11e is analyzed by means of the analytical model, and simulation. The controlled channel access provides the means for supporting time-bounded traffic with strong QoS requirements, but does not work in coexistence scenarios. QoS support is problematic when multiple networks overlap.

This problem is discussed in detail in the context of coexisting CCHCs with the help of games. Competing networks are modeled as players. Behaviors and strategies are defined, and conditions under which a player selects certain types of behaviors are given. The concept of cooperation is discussed in the context of multi stage games. In cooperation, a CCHC seeks to establish the ability to guarantee -or at least to support- the allocation of radio resources at the requested points in time, by considering the demands of competing CCHCs, and by implicitly negotiating the behaviors to select. It is shown in this thesis that cooperation is an achievable situation even when CCHCs are not able to communicate with each other, in many scenarios.

10.3 Contributions of this Thesis

The analytical model to approximate the relative priority between different access categories will be helpful for future developments of wireless LANs.

The two simulation tools WARP2 and YouShi allow a detailed analysis of the protocol, and of the coexistence scenarios, respectively.

The games developed in this thesis, the Nash analysis of the single stage game, the strategy machines, and the discounting of payoffs are approaches that can be used for the analysis of many game problems, for example for scenarios with more than two networks operating at various channels in parallel, ad-hoc networks, and the EDCF.

10.4 Further Development and Motivation

Wireless communication networks that share the frequency spectrum can be seen as forming a virtual society in the unlicensed bands. This virtual society faces many challenges that have been already analyzed for real-life societies as for example interacting nations and groups of animals such as ant colonies. The theory of games is an efficient means for analyzing such societies. When developing future flexible and adaptive wireless networks that have to operate in unlicensed bands, the models developed in this thesis may be of help. Future wireless net-

works will be required to act *environment and interference aware* when operating with shared radio resources. Such networks will be required to operate *spectrum agile*, with high flexibility by also considering the implications of decisions on other networks.

Further developments may focus on the application of the developed models for cellular and ad-hoc networks with a larger number of players.

The motivation for wireless communication is to facilitate the exchange of information. However, the demands for exchanging information are increasing. In our world, communication must be improved to provide a better understanding of what too often appears to be unknown, and different, simply because of lack of information. New ways to provide communication have to be found to change this. In this view, wireless communication provides great benefits to our future. Communication is one of our key means for developing our future society. Communication is life.

Appendix A

IEEE 802.11a/e Simulation Tool "WARP2"

WARP2 stands for Wireless Access Radio Protocol, where the number 2 refers to the HiperLAN/2 protocol. The simulator was developed in Kadelka (2001) and Esseling et al. (2001) as simulation environment for the HiperLAN/2 protocol. In WARP2, the HiperLAN/2 protocol is specified in the graphical representation of the *System Description Language* (SDL) and the *Abstract Syntax Notation* (ASN.1) with the usage of the commercial tool Telelogic TAU SDT™. With this tool, stand-alone simulators can be generated that allow tests of the specified protocols. For in depth analysis and event driven simulation, a modified version of the *ComNets Class Library* (CNCL) and the ComNets ReadDefaults tool have been attached to the protocol specification, making WARP2 suitable for the simulation of large scenarios with detailed specifications of complete protocols.

For this thesis, the WARP2 simulator was extended by a complete specification of the 802.11 MAC protocol including the 802.11e QoS enhancements, and a model of the 802.11a PHY with the OFDM radio transmission scheme, which allows simulation of 802.11 in parallel to the HiperLAN/2 protocol. Further, the channel model as described in Section 2.4 and Appendix C was implemented, and a JAVA-based graphical user interface was added. Contributions from the following works have been integrated in the 802.11 part of the simulation tool WARP2:

Forkel (1999), Easo (1999), Wijaya (1999), Hmaimou (2000), Wiemann (2000), Badali (2001), Hiertz (2002), and Berlemann (2002).[18]

A.1 Traffic Models

Various models that generate typical Internet traffic can be used as offered traffic for MSDU Deliveries in single-hop station-to-station links or in multi-hop routes where MSDUs are forwarded over more than two stations. In WARP2, multi-hop routes are static, which means the list of stations by which a particular route is defined remains constant throughout a simulation. The traffic generators used in WARP2 allow the application of constantly distributed and negative-exponentially distributed inter-arrival times of the generated packets. The generated packets are fed into the MAC layers as part of the frame body of MSDUs. The constant inter-arrival time can be used to simulate highly correlated offers such as an N-ISDN voice source with a constant bit rate of *64 kbit/s*. The negative-exponentially distributed inter-arrival times can be used to simulate uncorrelated offers such as best-effort Ethernet traffic. In addition, traces of recorded real life inter-arrival processes of traffic sources, which include packet lengths, can be used to simulate realistic LAN and *Moving Pictures Expert Group* (MPEG) video, i.e., MPEG-1 offers (see Bellcore 2000 and Garret 2000).

To investigate the interaction between the protocols and the *Transport Control Protocol* (TCP) and *Internet Protocol* (IP) stack, a TCP/IP model with *File Transfer Protocol* (FTP) and *Hypertext Transfer Protocol* (HTTP) applications are available, but not used in this thesis. All traffic generators can be mixed to model complicated scenarios where each station carries multiple applications at the same time.

A.2 IEEE 802.11 MAC Implementation

Figure A.1 illustrates the implementation of the 802.11 protocol in WARP2. Shown are the models for MAC and PHY layers, that are connected to traffic generators, stochastic evaluation, and the radio channel model. However, any number of stations can be simulated by instantiating numerous entities of the 802.11 protocol. It is defined in some parameter files where the stations are positioned and in case they are mobile, along what route they move throughout the simulation.

---

[18] The diploma theses referred to in this thesis, including all cited diploma theses in the bibliography, have been supervised by the author of this thesis.

A.3 Radio Channel and PHY Capture Model

The channel model as described in Section 2.1 and Appendix C is implemented in WARP2, including power control, link adaptation, and a simplified mobility model. Further, a complex model of PHY capture is implemented in WARP2. This PHY capture happens when a receiving station is synchronizing its reception to a particular burst by receiving a valid preamble from that burst, and at some point in time during synchronization, this receiving station is detecting another preamble from another transmission of a second transmitting station, at a higher power level. In this case, it may happen that the second transmitting station captures the synchronization, and as a result, the receiving station attempts to receive the burst from the second transmitting station instead of the first burst. In the model that is implemented in the WARP2 simulator, it is assumed that the PHY capture occurs if the receiving power of the second burst is at least twice as high as the receiving power of the ongoing synchronization. The success of the synchronization itself is calculated based on the PER requirements of a short frame transmitted with BPSK1/2. A detailed model of the timing during synchronization is required in simulation of the 802.11 protocol, since according to the 802.11 standard, stations have to react differently when receiving bursts from stations that transmit simultaneously, but with different starting times. Received powers at a station depend on the transmitting powers and distances between stations. Throughout this thesis, the attenuation model as given in Equation (2.3) is used with $\gamma = 3.5$, if not stated otherwise. Transmit powers are typically $23\ dBm$, but may change dynamically from frame to frame when dynamic transmit power control is applied by a station.

A.4 Results

The results of the stochastic simulation are the throughput per route (a route may be a single hop), the backoff delays per access category at any backoff entity within any station, and the MSDU Delivery delays per route (per multi hop or per single hop). All results can be given per access category for every station individually, or averaged over all stations of the scenario.

Further, beacon delays and collision probabilities can be evaluated, as well as any parameters of the random backoff processes, such as contention window sizes. With WARP2, event-driven, stochastic simulation is used to calculate long runs of realistic scenarios. For the delay results of the MSDU Delivery and backoff delays, empirical distribution functions of the resulting stochastic data can be given, in this thesis presented as *Complementary Cumulative Distribution Func-*

tions (CCDFs). The discrete *Limited Relative Error* (LRE) algorithm that measures the local correlation of the stochastic data is used.

See Schreiber (1988) and Görg (1997) for an explanation of the LRE algorithm. With this algorithm, by measuring local correlations, the accuracy of empirical simulation results can be estimated. All WARP2 results that are presented in this thesis are within a maximum limited relative error of *5 %*. This maximum limited relative error is the level of confidence all WARP2 results are calculated with.

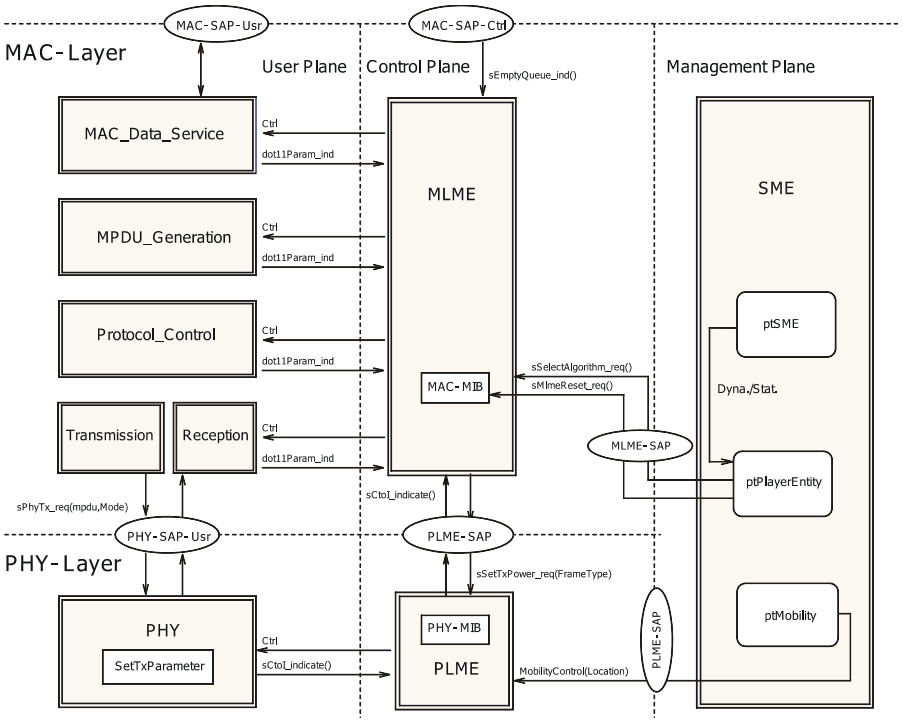

Figure A.1: Implementation of the IEEE 802.11 MAC and PHY layer. Shown are user, control, and management plane. Packets are fed into an instance of the MAC user plane by traffic generators. The physical layer forwards MPDUs through a channel to other stations.

A.5 User Interface

Figure A.2 shows the user interface of the WARP2 simulation tool.

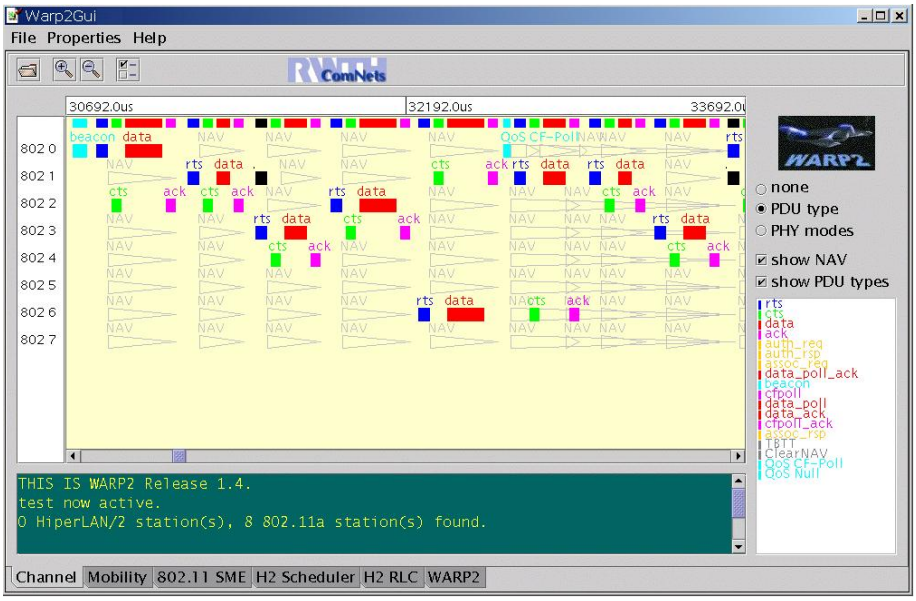

Figure A.2: User interface of the WARP2 simulation tool. Shown are frame exchanges between eight 802.11e stations, including beacon and QoS CF-Poll.

Appendix B

GAME ANALYSIS AND GAME SIMULATION TOOL "YOUSHI"

YOUSHI is Chinese for "the game". The tool has been developed by the author and Berlemann (2002), using the commercial tool MATLAB™. In this thesis, the results presented in Chapters 7-9 are produced with this tool to evaluate the game approach that was selected to analyze the CCHC coexistence problem, and to develop solution concepts for this problem. The tool allows stochastic simulation of the SSG and the MSG. In addition, it allows the analytical calculations with the Markov chain *P* (see Section 8.1.1, p. 160) of the SSG and the MSG.

B.1 Model of Offered Traffic and Requirements

Three player entities are implemented in the tool, where two player entities represent two CCHCs that share resources. A third player entity represents the EDCF background traffic. The requirements of the two players that represent the CCHCs are modeled as defined in Section 7.2.2.1, p. 135, by the QoS parameters Θ, Δ, Ξ for each player individually. The EDCF player attempts to carry the background traffic, which is modeled through an Ethernet traffic trace file (Bellcore 2000) which is also used in the WARP2 simulator. This trace file repre-

sents the offered traffic at the air interface generated through typical Internet applications and logged at the DLC layer. The maximum MSDU duration of the EDCF-traffic is therefore *1514 byte*. All MSDUs have the same priority, and fit into the TXOPlimit. The CFB concept as described in Section 5.2, p. 96, is not part of the implementation. MSDU Deliveries are not implemented in the simulation tool YouShi, as they are in the detailed 802.11 protocol simulator WARP2.

The resulting offered traffic can be selected such that shorter inter-arrival times generate higher offered traffic. In this thesis, the EDCF is typically overloaded, if not stated otherwise.

B.2 Implementation of Resource Allocation Process, and Collisions

Throughout this thesis, a superframe duration of *200 ms* is always assumed, as indicated in Figure B.1. This duration defines the duration of one SSG. The resource allocation process in the MSG can either be simulated, which means that after each SSG the observations are calculated from the TXOP allocations, or alternatively, the observations can directly be calculated using the approximation with the Markov chain. With simulation, CCDFs of the resource allocation delays can be given. With approximation, an upper bound of the resource allocation can be given.

Collisions of resource allocation attempts are modeled and resolved as follows. Player *1* and player *2* allocate resources with highest priority. In case the channel gets idle and provided that one of the two high priority players scheduled a resource allocation at that point in time or during the last resource allocation, this player immediately attempts to access the channel before the third player attempts at a slightly later time (hence, with less priority).

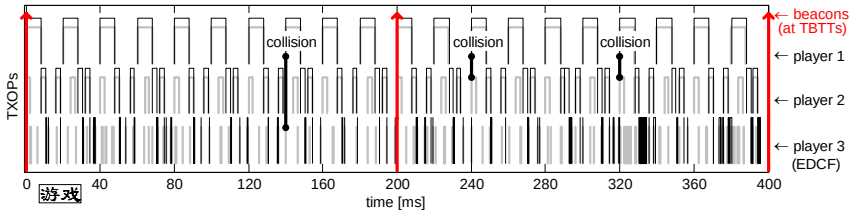

Figure B.1: MSG with two stages or two SSGs, with the EDCF as third player. Each SSG starts with a beacon. Demanded resource allocations are indicated as gray lines, and successful resource allocations are indicated as solid black lines. Three collisions occur during the two SSGs.

This attempt to allocate resources may be unsuccessful due to collisions of the first transmitted frame (which is not necessarily a QoS CF-Poll) with a frame transmitted by the other high priority player.

As there are only two players involved that access the channel with highest priority, collisions of allocation attempts of player *1* and *2* are more likely than collisions with allocation attempts of player *2*. In the case of collision of allocation attempts of player *1* and *2*, as part of the sharing approach, the player that allocated the last resource before the collision will refrain from reallocation. The other player's last resource allocation occurred earlier. Thus, it is allowed to immediately repeat its allocation attempt. This solves collisions between the resource allocation attempts of player *1* and player *2*. Note that these collisions are very unlikely in high offered scenarios because of the fact that in this case, once a (first) player finished its resource allocation, the opponent (second) player can immediately allocate resources before the first player will reallocate resources again.

However, collisions of resource allocation attempts of the two high priority players with attempts of the EDCF player *3* may also occur, as indicated in Figure B.1. In this case, it is obviously the high priority player *1* or player *2* that can reallocate the channel faster than the EDCF player after the allocation.

Note that while player *1* allocates resources, player *2* may attempt to allocate resources and thus waits for player *1* to finish its allocation. After finishing a resource allocation, a player does not attempt resource allocation immediately again.

As a result, collisions between resource allocation attempts of player *1* and player *2* can only happen after a resource allocation by player *3*, but not after a resource allocation by player *1* or player *2*. The probability of collision depends on the TXOPlimit. The higher the TXOPlimit, the higher the probability that player *1* and player *2* will attempt a resource allocation immediately after the allocation by player *3*.

In the YouShi simulator, an error-free radio channel is assumed. All stations are in range with each other, which means that the resource allocations of the opponent players are completely observed by any player.

B.3 Results

Results of the simulation and analysis are the QoS observations per stage, and the resulting payoffs (the utilities per player). With detailed simulation, probability functions for the delays of resource allocations can be given as CCDFs. The

analysis with the Markov chain gives an approximation for the upper bound of the delays.

However, all three players are evaluated, where for player *3* the QoS observations can be given, but a utility function is not applied, thus a payoff is calculated for player *1* and player *2* only.

In addition, the tool allows the calculation of Nash equilibria or a numerical search for Nash equilibria and the assessment of Pareto efficiency of action profiles, given a set of requirements. With the numerical search, players can calculate their best response to their opponent player's demand, out of a finite action space. In any stage n, $n>1$, of the MSG, players estimate their opponent player's demands of the last stage by using the predictor as described in Section 7.4, p. 152, or may have perfect knowledge about their opponents history of demands. The predictor requires information about earlier resource allocation attempts and can therefore not be applied if the SSG is approximated by the Markov chain P.

B.4 User Interface

Figure B.2 shows the user interface of the YouShi analysis tool.

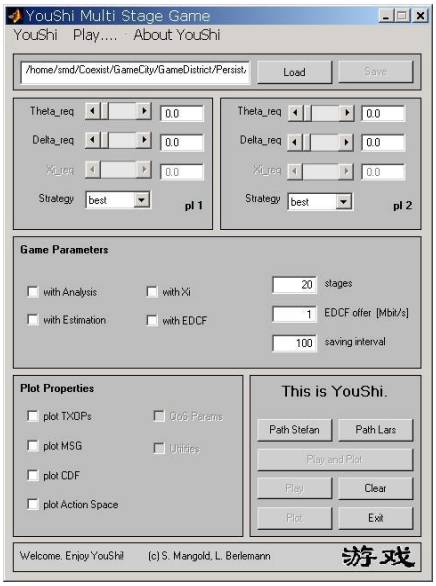

Figure B.2: User interface of the YouShi analysis tool.

Appendix C

The Qiao-Choi Transmission Error Probability Analysis

In this appendix, the approach presented in Qiao and Choi (2000) for calculating the probability of reception errors when transmitting packets of arbitrary lengths is summarized. This approach is referred to as the Qiao-Choi Transmission Error Probability Analysis. The approach takes into account the modulation and coding scheme used in HiperLAN/2 and 802.11a, without considering the underlying *Orthogonal Frequency Division Multiplexing* (OFDM).

With the extension of the analysis given in Mangold et al. (2001h), the analysis serves as channel model for the simulation that is discussed in this thesis. The extension includes a simplified model for the OFDM into the analysis, under some assumptions about the radio channel characteristics.

HiperLAN/2 and 802.11a apply *Quaternary Amplitude Modulation* (QAM) and binary punctured convolutional encoding. A punctured convolutional code is a high-rate code obtained by periodic elimination of specific code symbols from the output of the low-rate mother encoder (Haccoun and Begin 1989). The generator polynomials of the mother code applied in 802.11a and HiperLAN/2 are $G_1=133_8$ and $G_2=171_8$, thus the constraint length is *7*. Table C.1 summarizes the characteristics of the physical layers of both standards.

Table C.1: HiperLAN/2 and 802.11a PHY layer characteristics

PHY Mode m (modulation, encoding rate)	M	bit rate Mbit/s	data bits per symbol.	d_{free}	minimum sensitivity	used in
1 *BPSK 1 / 2*	*2*	*6*	*24*	*10*	*-86 dBm*	*11a, HiperLAN/2*
2 *BPSK 3 / 4*	*2*	*9*	*36*	*5*	*-85 dBm*	*11a*, HiperLAN/2*
3 *QPSK 1 / 2*	*4*	*12*	*48*	*10*	*-83 dBm*	*11a, HiperLAN/2*
4 *QPSK 3 / 4*	*4*	*18*	*72*	*5*	*-81 dBm*	*11a*, HiperLAN/2*
5 *16QAM 1 / 2*	*16*	*24*	*96*	*10*	*-78 dBm*	*11a*
6 *16QAM 9 / 16*	*16*	*27*	*108*	*10*	*-78 dBm*	*HiperLAN/2*
7 *16QAM 3 / 4*	*16*	*36*	*144*	*5*	*-74 dBm*	*11a*, HiperLAN/2*
8 *64QAM 2 / 3*	*64*	*48*	*192*	*6*	*-70 dBm*	*11a**
9 *64QAM 3 / 4*	*64*	*54*	*216*	*10*	*-69 dBm*	*11a*, HiperLAN/2**

The PHY mode indicates the modulation, and the coding rate. The minimum sensitivities depend on implementation; the values used here are taken as working assumption. Optional PHY modes that do not have to be supported by a terminal are marked with "*". Only data frames, not control frames are usually sent using the optional PHY modes.

C.1 Bit Error Probability

The bit error probability is also referred to as *Bit Error Ratio* (BER). The symbol error probability for an *M*-ary QAM with *M= 4, 16, 64* is given by

$$P_M = 1-(1-P_{\sqrt{M}})^2, \tag{C.1}$$

where

$$P_{\sqrt{M}} = 2\cdot(1-\frac{1}{\sqrt{M}})\cdot Q\left(\sqrt{\frac{3}{M-1}\cdot\frac{E_{av}}{N_0}}\right) \tag{C.2}$$

is the symbol error probability (*Symbol Error Ratio,* SER) for the $\sqrt{M}$ -ary QAM with the average signal-to-noise ratio per symbol, E_{av}/N_0. This representation of the SER is valid for single carrier systems, such as a single OFDM sub-carrier.

In general, one QAM symbol per useful OFDM sub-carrier is transmitted. The BER for an *M*-ary QAM with Gray coded constellation mappings can be approximated by

$$P_b^{(M)} \approx \frac{1}{log_2 M}\cdot P_M \tag{C.3}$$

For BPSK modulation, the BER is the same as the SER given by

$$P_b^{(2)} = P_2 = Q\left(\sqrt{2\frac{E_{av}}{N_0}}\right). \quad \text{(C.4)}$$

C.2 Packet Error Probability

The packet error probability is also referred to as *Packet Error Ratio* (PER).

The evaluation of the PER is complicated by the fact that the errors in the convolutional decoder output stream depend on each other. According to Pursley and Taipale (1987), errors occur in bursts at the output of a Viterbi decoder, even if the errors into the decoder are independent. For this reason, Pursley and Taipale (1987) give an upper bound on the PER, under the assumption of binary convolutional coding and hard-decision Viterbi decoding with independent errors at the channel input. Viterbi decoding is the recommended way of decoding of punctured codes. Given the received sequence of data from the channel, Viterbi decoding consists of computing the likelihood that a particular sequence has been transmitted for every possible encoder state, where at each state only the path with the largest metric (highest probability) is selected. In general, a gain of *2.5 dB* in the PER performance can be expected when using soft-decision instead of hard-decision decoding.

For a packet of length L to be transmitted using PHY mode m the upper bound on the PER at PHY mode m is

$$\begin{aligned} & P_e^m(L) = 1-((1-P_u^m)^{8L} + 8L(1-P_u^m)^{2\cdot 8L} + ...) \\ & \Rightarrow P_e^m(L) \le 1-(1-P_u^m)^{8L} \end{aligned}, \quad \text{(C.5)}$$

where the union bound of the first-event error probability is given by

$$P_u^m = \sum_{d=d_{free}}^{\infty} a_d \cdot P_d \,. \quad \text{(C.6)}$$

Here, d_{free} is the free distance of the convolutional code selected in PHY mode m, a_d is the total number of error events of Hamming weight d, and P_d is the probability that an incorrect path at distance d from the correct path being chosen by the Viterbi decoder. Note that m is used as index indicating the mode of operation.

When hard-decision decoding is applied, P_d is given by

$$P_d = \begin{cases} \sum_{k=\frac{d+1}{2}}^{d} \binom{d}{k} \cdot \rho^k \cdot (1-\rho)^{d-k}, & d = odd \\ \frac{1}{2}\binom{d}{d/2} \cdot \rho^{d/2} \cdot (1-\rho)^{d/2} + \sum_{k=\frac{d}{2}+1}^{d} \binom{d}{k} \cdot \rho^k \cdot (1-\rho)^{d-k}, & d = even \end{cases} \quad \text{(C.7)}$$

where ρ is the BER for the modulation scheme selected in PHY mode *m*, and is given by Equation (C.3) or Equation (C.4). The value of a_d can be obtained either from the transfer function or by a numerical search.

To use this analytical approach for calculating the PER from a given E_{av}/N_0, the coding parameters as given in Table C.2 are required.

Table C.2: Coding parameters for calculating the PER, as used in Qiao and Choi (2001)

	coding rate 1/2	coding rate 2/3	coding rate 3/4
d_{free} :	*10*	*6*	*5*
$a(d_{free})$:	*36*	*3*	*42*
$a(d_{free}+1)$:	*0*	*70*	*201*
$a(d_{free}+2)$:	*211*	*285*	*1492*
$a(d_{free}+3)$:	*0*	*1276*	*10469*
$a(d_{free}+4)$:	*1404*	*6160*	*62935*
$a(d_{free}+5)$:	*0*	*27128*	*379644*
$a(d_{free}+6)$:	*11633*	*117019*	*2253373*
$a(d_{free}+7)$:	*0*	*498860*	*13073811*
$a(d_{free}+8)$:	*77433*	*2103891*	*75152755*
$a(d_{free}+9)$:	*0*	*8784123*	*428005675*

Appendix D

BIANCHI'S LEGACY 802.11 SATURATION THROUGHPUT ANALYSIS

FOR THE CONTENTION of a finite set of legacy 802.11 backoff entities, Bianchi (1998a, 1998b, 2000), presents an analytical approximation based on a Markov model, that allows the analysis of the saturation throughput of a system of contending legacy 802.11 backoff entities. A similar approach for the analysis of legacy 802.11 is presented in Ho and Chen (1996). With this model (here referred to as "Bianchi's legacy 802.11 model"), the system saturation throughput in legacy 802.11 is approximated. As already explained in Chapter 5, the system saturation throughput is defined as expected sum of all throughputs of MSDUs delivered by contending backoff entities when all entities attempt to transmit at any time (all backoff entities have MSDUs to deliver, the queues are never empty). Calì et al. (2000a) refers to this throughput as achievable throughput in asymptotic conditions.

Hettich (2001) uses Bianchi's legacy 802.11 model and extends it to analytically approximate not only the expected saturation throughput, but also the backoff delays. In addition, Hettich (2001) provides an analysis and comparison of 802.11 and HiperLAN/2, with the help of the analytical approximations, confirmed by

stochastic simulation. See also Hettich and Schröther (2000) for the comparison of 802.11 and HiperLAN/2.

In this appendix, the analytical approximation of Bianchi's legacy 802.11 model is reviewed and summarized. A modified version of this model is used in Chapter 5 of this thesis to evaluate the concepts of the EDCF contention window. In this thesis, the focus of the discussion is the throughput approximation. The model extensions for backoff delays are not considered here.

D.1 Contention Window of one Backoff Entity in Saturation

Bianchi (1998a, 1998b, 2000) considers a finite number of N contending backoff entities in a legacy 802.11 network, without hidden stations, and assuming an error-free channel. However, in legacy 802.11, there is one backoff entity per station, hence, the number of stations and the number of backoff entities are the same.

In the initial version of Bianchi's legacy 802.11 model, it is assumed that all transmitted data frames (MSDUs) have the same frame body size, and are not fragmented.

Figure D.1, p. 232, illustrates the Markov model as described in Bianchi (1998a, 1998b). The Markov model represents the backoff process of one backoff entity (one station in legacy 802.11). A bidimensional stochastic process $\{s(t), b(t)\}$ is modeled, where $b(t)$ is the stochastic process representing the size of the contention window for a backoff entity at time t. The process of changing the backoff stage upon ACK timeouts (collisions) is represented by $s(t)$.

The collision avoidance times are time intervals with random durations, given by a number of slots, during which each backoff entity defers from attempting to transmit. During collision avoidance, all backoff entities down count their backoff counters until one or more backoff entities end the idle phase by initiating frame exchanges. Contention windows are used by the backoff entities to select random numbers that define the slot at which the respective backoff entity initiates a frame exchange. The contention window sizes per backoff stage are calculated based on the initial contention window size W_0 as

$$W_i = 2^{min(i,m)} \cdot W_0, \quad i \in 0,1,\ldots m. \tag{D.1}$$

Parameter i is the backoff stage, and m is the maximum value of the backoff stage. W_i is the maximum number of slots a backoff entity waits until initiating a

frame exchange, i.e., the contention window size at backoff stage i. Note that the model assumes an unlimited number of retries. Bianchi (1998a, 1998b, 2000) assumes that the collision probability p that more than one backoff entity transmits a frame is independent of the state $s(t)$, i.e., independent of the size W_i of the contention window. This assumption, which makes the process Markovian, is more accurate for longer sizes of contention windows, and for large numbers of backoff entities N (Bianchi, 1998a; Hettich, 2001). The process is illustrated as discrete-time Markov model, with the transition probabilities given by

$$\begin{aligned}
P\{i,k \mid i,k+1\} &= 1, && k \in (0, W_i - 2), \quad i \in (0,m),\\
P\{0,k \mid i,0\} &= \frac{1-p}{W_0}, && k \in (0, W_0 - 1), \quad i \in (0,m),\\
P\{i,k \mid i-1,0\} &= \frac{p}{W_i}, && k \in (0, W_i - 1), \quad i \in (1,m),\\
P\{m,k \mid m,0\} &= \frac{p}{W_m}, && k \in (0, W_m - 1), \quad i \in (1,m).
\end{aligned} \tag{D.2}$$

Here, $P\{i_1,k_1 \mid i_0,k_0\} = P\{s(t+1)=i_1, b(t+1)=k_1 \mid s(t)=i_0, b(t)=k_0\}$.
The solution of the Markov model for the stationary distributions is found as

$$\begin{aligned}
b_{i,0} &= p^i \cdot b_{0,0}, && i \in (0, m-1),\\
b_{m,0} &= \frac{p^m}{1-p} \cdot b_{0,0},\\
b_{i,k} &= \frac{W_i - k}{W_i} \cdot b_{0,0}, && k \in (0, W_i - 1),
\end{aligned}$$

where $b_{i,k} = lim_{t\to\infty} P\{s(t)=i, b(t)=k\}$.
The value of $b_{0,0}$ can be calculated as follows. The stationary distributions must satisfy

$$1 = \sum_{i=0}^{m} \sum_{k=0}^{W_i - 1} b_{i,k}, \quad m \in 0,1,2,\ldots \quad W_i \in 1,2,\ldots,$$

which can, by using the definitions of the stationary distributions, be written as (Bianchi, 2000)

$$1 = \sum_{i=0}^{m} b_{i,0} \cdot \sum_{k=0}^{W_i - 1} \frac{W_i - k}{W_i}.$$

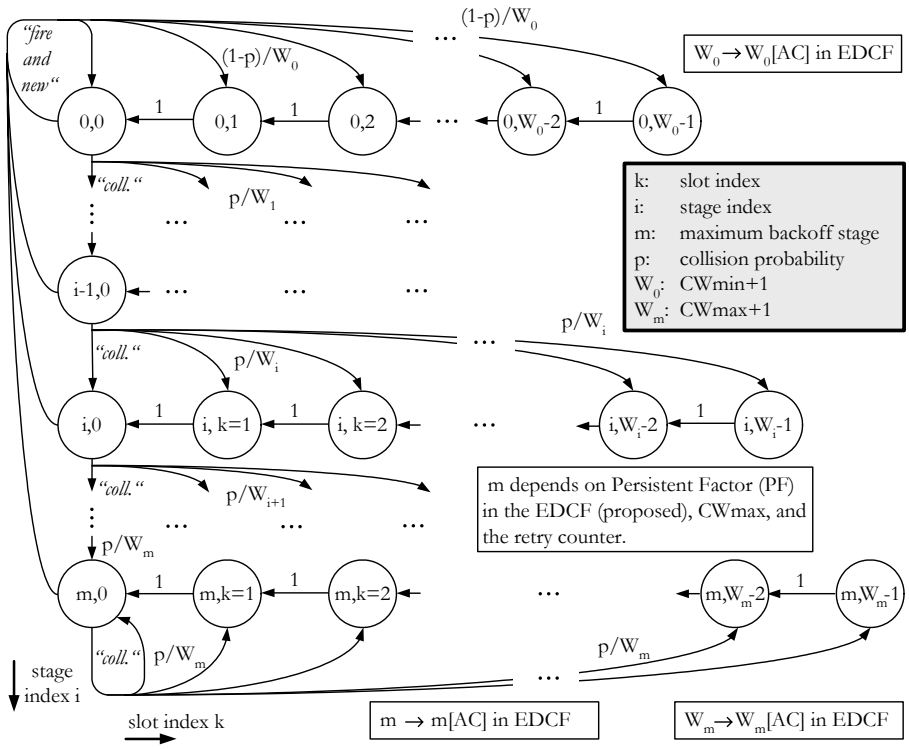

Figure D.1: Markov model of for the backoff window process in legacy 802.11 (Bianchi, 1998b). This model assumes an unlimited number of retries.

In legacy 802.11 with the 802.11a PHY, $m = 6$ and $W_0 = 16$. For any $0 \le i \le m,\ m \ge 0$,

$$1 = \sum_{i=0}^{m} \left(b_{i,0} \cdot \sum_{k=0}^{W_i - 1} \frac{W_i - k}{W_i} \right), \quad W_i \ge 1 \quad \forall 0 \le i \le m,\ m \ge 0 \quad \Rightarrow$$

$$1 = \frac{1}{2} \cdot \sum_{i=0}^{m} b_{i,0} \cdot (W_i + 1) = \tag{D.3}$$

$$= \frac{b_{0,0}}{2} \cdot \left[W_0 \cdot \left(\sum_{i=0}^{m-1} (2p)^i + \frac{(2p)^m}{1-p} \right) + \frac{1}{1-p} \right], \quad m \ge 0,\ W_0 \ge 1.$$

Note that the term $2p$ that occurs twice in Equation (D.3) is related to the fact that in legacy 802.11 the contention window is doubled upon collisions. Backoff entities that attempted to transmit a frame increase their backoff stage i by 1 after

unsuccessful transmission attempts, i.e., upon ACK timeout. When increasing the backoff stage, legacy backoff entities increase the size of their contention windows by the factor *2*.

For legacy 802.11, with Equation (D.1), it follows

$$1 = \frac{b_{0,0}}{2} \cdot \left[W_o \cdot \left(\frac{1-(2p)^m}{1-2p} + \frac{(2p)^m}{1-p} \right) + \frac{1}{1-p} \right], \quad m \geq 0, W_0 \geq 1, \tag{D.4}$$

which can be solved using the rule of L'Hospital, to

$$b_{0,0} \underset{L'Hospital}{=} \begin{cases} \dfrac{2 \cdot (1-p)}{W_o \cdot (1-p) \cdot m \cdot (2p)^{m+1} + W_o \cdot (2p)^m + 1}, & p = \dfrac{1}{2}, \\ \dfrac{2 \cdot (1-p)}{W_o \cdot (1-p) \cdot \dfrac{1-(2p)^m}{1-2p} + W_o \cdot (2p)^m + 1}, & else. \end{cases} \tag{D.5}$$

Increasing the contention window by the factor *2* may not be required in the case of 802.11e, as explained in Chapter 4. The *Persistence Factor* (PF) discussed in the context of the QoS enhancements of 802.11e adds a degree of freedom to the system, which helps to support QoS. With the PF, the contention window increases -upon collisions of transmission attempts- by a factor that can be set to other values than *2*. Different values per AC can be selected for the PF.

The probability τ that a backoff entity is transmitting in a generic slot is calculated by the summation of all stationary distributions $b_{i,0}$, given by

$$\tau = \sum_{i=0}^{m} b_{i,0} = \frac{1}{1-p}, \quad with\ m \geq 0.$$

This approximation becomes more accurate with smaller p. As explained in Chapter 5, a generic slot time may be an idle slot during the contention phase, or a busy phase during which a frame exchange is completed, or, alternatively, during which a collision occurs. It is referred to as generic slot to differentiate it from the backoff slots, because a generic slot can be a backoff slot, or a busy phase with a longer duration than the backoff slot duration.

D.2 Collision Probability

The probability p that a frame transmission at a generic slot is unsuccessful depends on the number of backoff entities, N, and the probability τ that a back-

off entity attempts to transmit at this generic slot. If more than one backoff entity transmit, frames collide. The collision probability is given by

$$p = 1 - (1-\tau)^{N-1} .$$

As expected, in the case of one isolated backoff entity, i.e., $N = 1$, the collision probability $p = 0$. If there is an ongoing transmission, regardless if it collided or not, the channel is busy, and the carrier sense mechanism in 802.11, *Clear Channel Assessment* (CCA), will detect the channel as busy *(CCAbusy)*. Equivalently, without ongoing transmission, the channel is idle *(CCAidle)*. Note that the CCA mechanism indicates the channel as busy also during the SIFS time intervals between consecutively transmitted frames (for example RTS and CTS), as they are part of an ongoing frame exchange during which the virtual carrier sensing mechanisms in the backoff entities set the NAV vector. The probability $P_{CCAbusy}$ that there is a transmission of at least one backoff entity in a generic slot time, and the probability $P_{CCAidle} = 1 - P_{CCAbusy}$ that there is no transmission, as well as the probability $P_{success}$ that the transmission attempt leads to a successful frame exchange (conditioned by the probability of transmission, $P_{CCAbusy}$), are obtained to

$$\begin{aligned} P_{CCAidle} &= (1-\tau)^N , \\ P_{CCAbusy} &= 1 - P_{CCAidle} = 1 - (1-\tau)^N , \\ P_{success} &= \begin{cases} 0, & P_{CCAbusy} = 0, \\ \dfrac{1}{P_{CCAbusy}} \cdot N \cdot \tau \cdot (1-\tau)^{N-1}, & else. \end{cases} \end{aligned} \tag{D.6}$$

Only collisions lead to unsuccessful transmissions here, because of the ideal channel conditions that are assumed in the model. The probability that a transmission attempt is unsuccessful, i.e., the collision probability P_{coll}, is given by

$$P_{coll} = 1 - P_{success} . \tag{D.7}$$

D.3 State Durations

In each generic slot, the system is in one of the three states, no transmission *(CCAidle)*, successful transmission *(success)*, or collision *(coll)*. The carrier sense indicates CCAbusy during transmission and during collision. The state durations $T_{CCAidle}, T_{success}, T_{coll}$ of the three respective states depend on many PHY and MAC parameters. The state duration $T_{CCAidle}$ is given by a slot duration *aSlotTime* that is defined by the standard (*aSlotTime*=9μs for 802.11a). The state durations $T_{success}$ and T_{coll} depend on the duration of a PPDU which is mainly defined by

the frame body sizes and the selected PHY modes. Further, the duration of a transmitted PPDU depends on the selected PHY mode, whether or not WEP encryption is used, and if the optional address 4 is used. The collision duration depends on the duration of the first fragment, or, if RTS/CTS is used, on the duration of the RTS frame. Figure D.2, p. 236, indicates how the state durations are calculated from the protocol and PHY parameters. The state durations are given by

$$T_{success} = \underbrace{T_{RTS} + T_{SIFS} + T_{CTS} + T_{SIFS}}_{only\ with\ RTS/CTS} + T_{MSDU} + T_{SIFS} + T_{ACK} + T_{DIFS},$$

$$T_{coll} = \underbrace{T_{RTS} + T_{DIFS}}_{only\ with\ RTS/CTS} \ or\ \underbrace{T_{PPDU} + T_{DIFS}}_{without\ RTS/CTS},$$

$$T_{CCAidle} = aSlotTime.$$

When transmitted frames of two or more backoff entities collide, the transmitting backoff entities detect the collision after a timeout of PIFS, while waiting for the ACK response from the addressed stations. Any other contending backoff entity, however, observes the collision as busy time as they are not able to detect and decode one of the colliding frames. It is assumed here that colliding frames cannot be detected by any station, due to the ideal channel conditions. The other contending backoff entities observe the collision time a PIFS duration earlier than the two or more transmitting backoff entities. The other stations do not wait for an acknowledgement, as the collision is observed as noise-like interference. Thus, they immediately start contenting after the channel is idle again, not at the ACK timeout. This is the reason why the duration of collisions, T_{coll}, is here defined without the PIFS timeout duration. See also the illustration of the collision time in Figure D.2.

A colliding RTS frame is shorter than a colliding data frame with typical frame body size. In case MSDUs are fragmented into a number of shorter MPDUs, the duration of a complete MSDU Delivery is longer than without fragmentation. The duration $T_{CCAidle}$ is not a random variable. It is the length of one slot within the contention window, defined by *aSlotTime*.

D.4 Legacy 802.11 Saturation Throughput

As result of the approximation, the normalized system saturation throughput of legacy 802.11 is given by

$$Thrp_{sat} = \frac{time\ used\ for\ successful\ transm.}{E\left[length\ of\ renewal\ interval\right]} = \\ = \frac{P_{CCAbusy} \cdot P_{success} \cdot FrameBody\,[\,Mbyte\,]}{P_{success} \cdot T_{success}[s] + P_{CCAbusy} \cdot \left(P_{coll} \cdot T_{coll}[s] + P_{CCAidle} \cdot T_{CCAidle}[s]\right)} \cdot {}^{1}\!/_{Mbyte/s}. \quad \text{(D.8)}$$

The saturation is normalized relative to the applied PHY mode, i.e., $Thrp_{sat} \in 0..1$. As the frame body size (payload) is assumed fixed and equal for all backoff entities, the durations $T_{success}, T_{coll}$ are not random variables, but constant values depending on the selected PHY mode. The duration T_{coll} is usually shorter with RTS/CTS than without. It is assumed that either all backoff entities together operate with RTS/CTS, or no backoff entity at all operates with RTS/CTS.

Figure D.3, p. 237, and Figure D.4 show the saturation throughput obtained through simulation and analytical approximation with Bianchi's legacy 802.11 model, which can be compared to the results given in Hettich (2001). The results show the expected characteristics. The throughput increases with increasing frame body sizes. The higher the number of backoff entities, the lower the saturation throughput, because of collisions. The higher the PHY mode, the smaller the efficiency of the carrier sense protocol. RTS/CTS increases the throughput for long frame body sizes, but not for short frame body sizes.

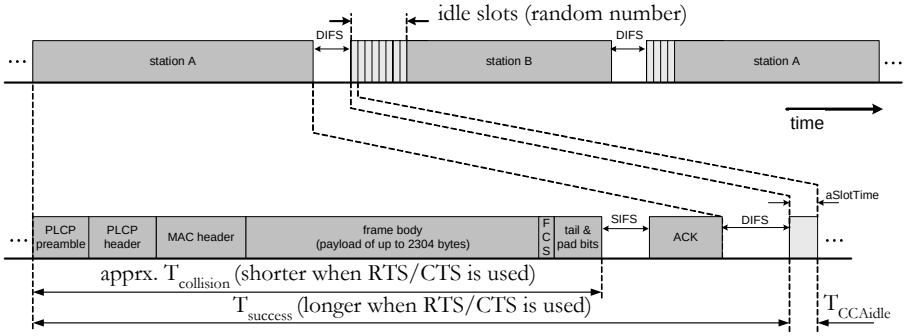

Figure D.2: State durations $T_{CCAidle}, T_{success}, T_{coll}$, as defined by the durations of the frames and the contention phase (Bianchi, 1998b). Note that the original figure in Bianchi (1998b) indicates a different definition of the collision time, although the original model works with the state duration as indicated here.

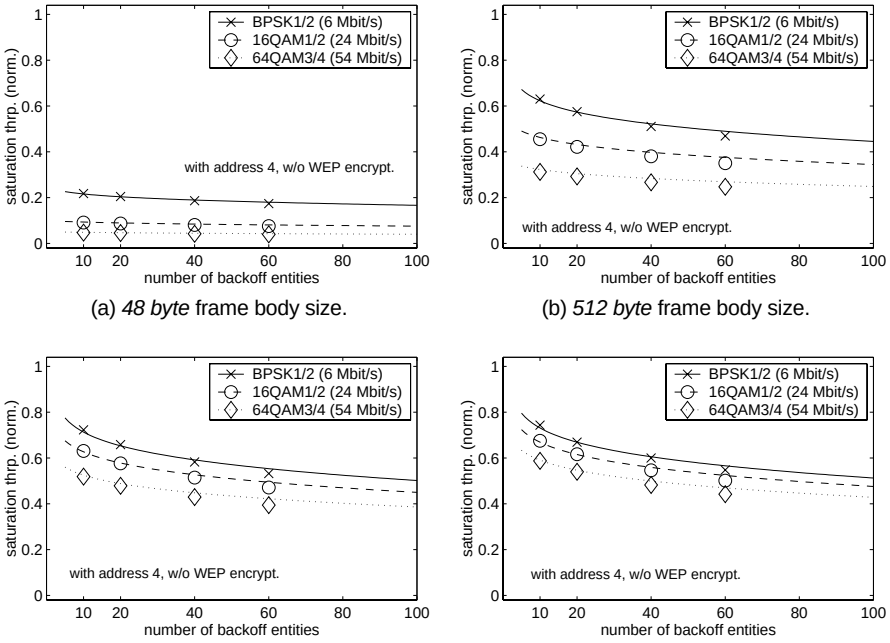

(a) *48 byte* frame body size.

(b) *512 byte* frame body size.

(c) *1514 byte* frame body size.

(d) *2304 byte* frame body size.

lines: Bianchi approx.; markers: WARP2 simulation results

Figure D.3: Normalized saturation throughput for different frame body sizes and PHY modes. Results are shown for legacy 802.11 (DCF).

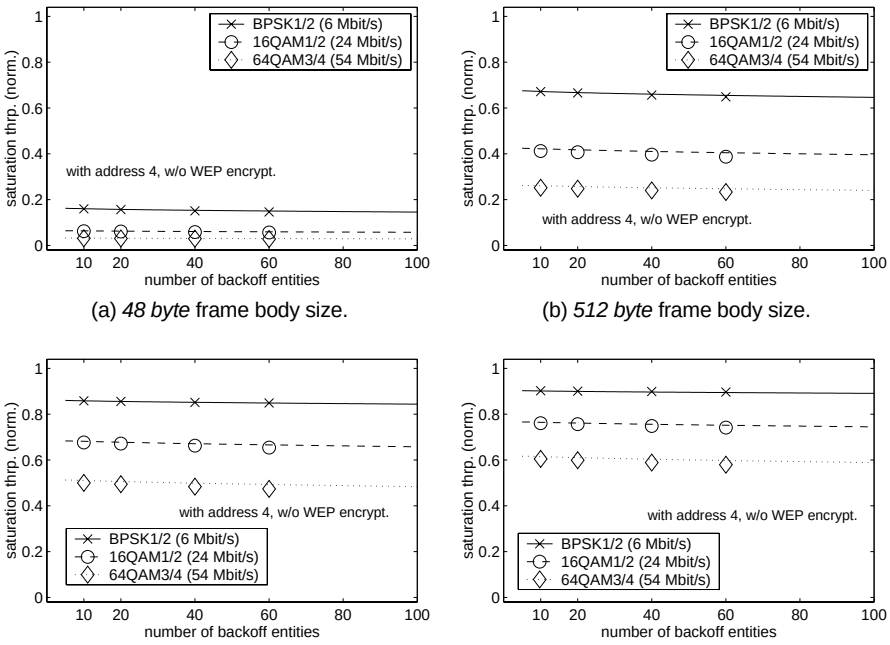

(a) *48 byte* frame body size.

(b) *512 byte* frame body size.

(c) *1514 byte* frame body size.

(d) *2304 byte* frame body size.

lines: Bianchi approx.; markers: WARP2 simulation results

Figure D.4: Normalized saturation throughput for different frame body sizes and PHY modes, now with RTS/CTS. Results are shown for legacy 802.11 (DCF).

Table of Symbols

symbol	meaning	context
$h(t,x)$	time domain channel response at receiver location x	PHY model
$H(f,x)$	frequency domain channel response at receiver location x	PHY model
t	time	PHY model
f	frequency	PHY model
B_D	Doppler spread	PHY model
f_c	center frequency	PHY model
v	velocity	PHY model
T_c	coherence time	PHY model
T_b'	OFDM symbol duration	PHY model
T_g	OFDM guard time (or: guard interval)	PHY model
T_b	OFDM block time (or: block interval)	PHY model
α_g	power loss	PHY model
E_{av}	energy per symbol	PHY model
ΣI	cumulated interference from multiple interferers	PHY model
N	background noise	PHY model
N_0	noise at receiver from interference and background noise	PHY model
T	1/(sampling rate)	PHY model
N_{total}	total number of OFDM sub-carriers	PHY model
D_f	OFDM sub-carrier spacing	PHY model
B	emission bandwidth	PHY model
C	power of a received signal	PHY model
d	distance between radio stations	PHY model
P_{Tx}	transmission power	PHY model
g_{Tx}	antenna gain at transmitter	PHY model
g_{Rx}	antenna gain at receiver	PHY model
γ	attenuation parameter	PHY model
G_1/G_2	the generator polynomials of the mother code	PHY model
N	number of backoff entities (stations)	Bianchi model
m	maximum number of backoff stages	Bianchi model
i	number of backoff stages	Bianchi model
$Thrp_{sat}$	normalized saturation throughput	Bianchi model
$T_{success}$	time of on successful frame exchange	Bianchi model

symbol	meaning	context
$P_{success}$	probability that frame exchange is successfully completed	Bianchi model
$P_{CCAbusy}$	probability of ongoing transmission in saturation	Bianchi model
$P_{CCAidle}$	probability that the channel is idle in saturation	Bianchi model
$T_{CCAbusy}$	duration of transmission, frame exchange or colliding frames	Bianchi model
$T_{CCAidle}$	random variable, duration of idle periods in saturation	Bianchi model
T_{coll}	duration of collision, depends on frame body size	Bianchi model
P_{coll}	probability, that a transmission attempts fails	Bianchi model
p	probability of collision at a particular slot	Bianchi model
τ	probability that a backoff entity transmits at a slot	Bianchi model
$s(t)$	stochastic process for the backoff stage	Bianchi model
$b(t)$	stochastic process for the contention window size	Bianchi model
$b_{i,k}$	stationary distribution of Markov chain	Bianchi model
W_i	contention window size in backoff stage i	Bianchi model
ξ_{slot}	slot access probability of the backoff entities	Bianchi model
n	stage of a game	game model
N	number of players that participate in the game	game model
$\mathbf{N}$	the set of N players	game model
N_{MSG}	number of stages in a multi stage game	game model
i	identifier of a player	game model
$-i$	identifier of all players but not player i	game model
A^i	infinite set of actions of player i	game model
$\mathbf{A}$	Euclidean space of actions	game model
Θ	share of capacity, related to the throughput	game model
Δ	resource allocation interval, related to the delay	game model
Ξ	variation of resource allocation interval	game model
a	action	game model
U	utility	game model
V	payoff	game model
u,v	shaping parameters of utility functions	game model
d	duration of a resource allocation, in ms	game model
D	time between two consecutive resource allocations, in ms	game model
L	number of resource allocations of one player per stage	game model
V^i_{MSG}	multi stage game payoff for player i	game model
δ^i	discounting factor for player i	game model
s	discrete sequence of resource allocation attempts	predictor
φ	autocorrelation function	predictor

symbol	meaning	context
W	window size of calculation of autocorrelation function	predictor
K	ratio of SFDUR to aTimeUnit	predictor
aTimeUnit	defines precision of autocorrelation function	predictor

List of Figures

List of Tables

Abbreviations

AC	Access Category
ACF	Auto Correlation Function
ACK	Acknowledgement
AID	Association Identifier
AIFS	Arbitration Inter Frame Space (measured in us)
AIFSN	Arbitration Inter Frame Space Number (measured in slots)
ALOHA	Ala Lokahi Oia'i'o Ha'aha'a Ahonui
AP	Access Point
APC	Access Point Controller
APSD	Automatic Power-Save Delivery
APT	Access Point Transceiver
ARQ	Automatic Repeat Request
aSlotTime	contention window slot duration
ASN.1	Abstract Syntax Notation
ATM	Asynchronous Transfer Mode
BE	Best Effort
BER	Bit Error Ratio
BRAN	Broadband Radio Access Networks
BSA	Basic Service Area
BSS	Basic Service Set
BSSID	Basic Service Set Identification
C/I	Carrier to Interference ratio
CA	Collision Avoidance
CAP	Controlled Access Phase
CBR	Constant Bit Rate
CC	Central Controller
CCA	Clear Channel Assessment
CCHC	Central Controller Hybrid Coordinator
CCK	Complementary Code Keying
CCDF	Complementary Cumulative Distribution Function
CDF	Complementary Cumulative Distribution Function, synonym for CCDF
CEPT	Conference of Postal and Telecommunications Administrations
CF	Coordination Function
CFB	Contention Free Burst
CF-End	Contention Free-End
CFP	Contention Free Period
CF-Poll	Contention Free-Poll
CF-Pollable	Contention Free-Pollable
CL	Controlled Load (802.1D)
CL	Convergence Layer (ETSI BRAN HiperLAN/2)
CNCL	ComNets Class Library
CP	Contention Period
CRC	Cyclic Redundancy Check
CSMA	Carrier Sense Multiple Access
CSMA/CA	Carrier Sense Multiple Access / Collision Avoidance
CSMA/CD	Carrier Sense Multiple Access / Collision Detection
CTS	Clear To Send
CW	Contention Window
CWmax	Contention Window Maximum
CWmin	Contention Window Minimum
DA	Destination Address

DCA	Dynamic Channel Allocation
DCC	DLC Connection Control
DCF	Distributed Coordination Function
DCS	Dynamic Channel Selection
DF	Distribution Function
DFS	Dynamic Frequency Selection
DIFS	Distributed Coordination Function Interframe Space
DiL	Direct Link
DL	Downlink
DLC	Data Link Control
DLCC	DLC Connection
DLP	Direct Link Protocol
DQPSK	Differential QPSK
DS	Distribution System
DSM	Distribution System Medium
DSS	Distribution System Services
DSSS	Direct Sequence Spread Spectrum
DTIM	Delivery Traffic Indication Message
EC	Error Control
EDCF	Enhanced Distributed Coordination Function
EE	Excellent Effort
EIFS	Extended Interframe Space
EIRP	Equivalent Isotropically Radiated Power
ERC	European Radiocommunications Committee
ERO	European Radiocommunications Office
ESS	Extended Service Set
ETSI	European Telecommunications Standards Institute
FCC	Federal Communication Commission
FCCH	Frame Control Channel
FCH	Frame CHannnel
FCS	Frame Check Sequence
FDM	Frequency Division Multiplexing
FHSS	Frequency Hopping Spread Spectrum
FTP	File Transfer Protocol
HC	Hybrid Coordinator
HCF	Hybrid Coordination Function
HiperLAN/2	High Performance Local Area Network Type 2
HR-DSSS	High Rate Direct Sequence Spread Spectrum
HTTP	Hypertext Transfer Protocol
IAPP	Inter AP Protocol
IBSS	Independent Basic Service Set
ICI	Inter-Channel Interference
IEEE	Institute of Electrical and Electronics Engineers, Inc.
IFFT	Inverse Fast Fourier Transform
IFS	Interframe Space
IMT-2000	International Mobile Telecommunications-2000
IP	Internet Protocol
IR	Infrared
ISI	Inter-Symbol Interference
ISM	Industrial, Science, Medical
ISO	International Organization for Standardization
ITU	International Telecommunications Union
LA	Link Adaptation
LAN	Local Area Network
LBT	Listen Before Talk

LCCH	Link Control Channel
LCH	Long transport Channel
LLC	Logical Link Control
LOS	Line of Sight
LRC	Long Retry Counter
LRE	Limited Relative Error
MAC	Medium Access Control
MAC-SAP	MAC Service Access Point
MCM	Multi Carrier Modulation
MF	MAC Frame
MLME	MAC Layer Management Entity
MLME-SAP	MLME - Service Access Point
MMPDU	MAC Management Protocol Data Unit
MPDU	MAC Protocol Data Unit
MPEG	Moving Pictures Expert Group
MSDU	MAC Service Data Unit
MSG	Multi Stage Game
NAV	Network Allocation Vector
NC	Network Control
OFDM	Orthogonal Frequency Division Multiplexing
OSI	Open System Interconnection
PC	Point Coordinator
PCF	Point Coordination Function
PDU	Protocol Data Unit
PER	Packet Error Ratio
PF	Persistence Factor
PHY mode	Physical Layer mode, coding and modulation scheme
PHY	Physical Layer
PIFS	Point Coordination Function Interframe Space
PLCP	Physical Layer Convergence Protocol
PLME	PHY Layer Management Entity
PMD	Physical Medium Dependent
PPDU	Physical (layer) Protocol Data Unit
PSDU	PHY Service Data Unit
QAM	Quaternary Amplitude Modulation
QAP	QoS Access Point
QBSS	Quality of Service Basic Service Set
QIBSS	Quality of Service Independent Basic Service Set
QoS	Quality of Service
QPSK	Quaternary Phase Shift Keying
QSTA	QoS Station
RA	Random Access (HiperLAN/2)
RA	Receiving station Address (802.11)
RCP	Radio link Control Protocol
RetryCnt	Retry Counter
RLC	Radio Link Control
RR	Resource Request
RRC	Radio Resource Control
RTS	Request to Send
SA	Source Address
SAP	Service Access Point
SAR	Segmentation and Reassembly
SBCH	Slow Broadcast Channel
SCH	Short Transport Channel
SDL	System Description Language
SDU	Service Data Unit
SER	Symbol Error Ratio
SFDUR	Superframe Duration
SIFS	Short Interframe Space
SME	Station Management Entity
SRC	Short Retry Counter

SS	Station Service
SSG	Single Stage Game
STA	Station
TA	Transmitting station Address
TBTT	Target Beacon Transmission Time
TCLAS	Traffic Classification
TCP	Transport Control Protocol
TID	Traffic Identifier
TPC	Transmitter Power Control
TS	Traffic Stream
TSF	Timing Synchronization Function
TSID	Traffic Stream Identifier
TSPEC	Traffic Specification
TXOP	Transmission Opportunity
TXOPlimit	Transmission Opportunity Limit
UL	Uplink
UMTS	Universal Mobile Telecommunications System
U-NII	Unlicensed-National Information Infrastructure
U-SAP	User Service Access Point
VBR	Variable Bit Rate
VI	Video < *100 ms* delay
VO	Voice, video < *10 ms* delay
WEP	Wired Equivalent Privacy
Wi-Fi	Wireless Fidelity
WSS	Wide Sense Stationary
WSTA	Wireless STA

Bibliography

ALTMAN, E. AND BASAR, T. (1998) Multiuser Rate-Based Flow Control. *IEEE Transactions on Communications*, 46 (7), 940-949.

AXELROD, R. (1984) *The Evolution of Cooperation*. New York: Basic Books.

BADALI, B. (2001) Entwicklung von Management-Funktionen für 802.11 und HiperLAN/2 zur Funkressourcen-Verwaltung und Erweiterung einer JAVA-basierten Simulationsumgebung. Thesis (Diploma), ComNets Aachen University.

BELLCORE (2000) *Ethernet Tracefile pAug.TL*. Bellcore (now Telcordia). Available from (anonymous ftp):
ftp.telcordia.com/pub/world/wel/lantraffic [1.1.2003]

BENVENISTE, M. (2001) Neighborhood Capture in Wireless LANs. *IEEE Working Document 802.11-01/596r1*. Available from:
http://www.ieee802.org/11 [1.1.2003]

BENVENISTE, M. (2002) Wireless LANs and 'Neighborhood Capture'. *In: IEEE Personal Indoor Mobile Radio Conference,* Lisbon Portugal 15-18 September 2002. 2148-2154.

BERLEMANN, L. (2002) Coexistence and Interworking in IEEE 802.11e in Competition Scenarios of Overlapping Wireless Networks. Thesis (Diploma), ComNets Aachen University.

BERLEMANN, L. (2003) Microeconomic Scope of Modeling and Evaluation of the Radio Resource Competition of IEEE 802.11e Wireless Networks. Thesis (Diploma), Institute for Microeconomics, Aachen University.

BERTSEKAS, D. AND GALLAGER, R. (1992) *Data Networks*. 2nd ed. New Jersey USA: Prentice Hall.

BIANCHI, G. (1998a) Throughput Evaluation of the IEEE 802.11 Distributed Coordination Function. *In: 5th Workshop on Mobile Multimedia Communications ,* Berlin Germany 12-14 October 1998. 307-318.

BIANCHI, G. (1998b) IEEE 802.11 – Saturation Throughput Analysis. *IEEE Communications Letters,* 2 (12), 318-320.

BIANCHI, G. (2000) Performance Analysis of the IEEE 802.11 Distributed Coordination Function. *IEEE Journal of Selected Areas in Communications,* 18 (3), 535-547.

BRONSTEIN, I. N. AND SMEDJAJEW, K. A. (1991) *Taschenbuch der Mathematik*. Moskow Russia: Nauka.

CHOI, S. AND GRAY, S. AND KASSLIN, M. AND MANGOLD, S. AND SOOMRO, A. (2001) Transmitter Power Control (TPC) and Dynamic Frequency Selection (DFS) Joint Proposal for 802.11h WLAN. *IEEE Working Document 802.11-01/169r1*. Available from:
http://www.ieee802.org/11 [1.1.2003]

CHOI, S. AND DEL PRADO, J. AND GARG, A. AND HOEBEN, M. AND MANGOLD, S. AND SHANKAR, S. AND WENTINK, M. (2002) Multiple Frame Exchanges during EDCF TXOP. *IEEE Working Document IEEE 802.11-01/566r3*. Available from: http://www.ieee802.org/11 [1.1.2003]

CIMINI, L. J. (1985) Analysis and simulation of a digital mobile channel using orthogonal frequency division multiplexing. *IEEE Transactions on Communications*, 33 (7), 665-675.

CALÌ, F. AND CONTI, M. AND GREGORI, E. (2000a) Design and Performance Evaluation of an Adaptive Backoff Mechanism. *IEEE Journal on Selected Areas in Communications*, 18 (9), 1774-1786.

CALÌ, F. AND CONTI, M. AND GREGORI, E. (2000b) Dynamic Tuning of the IEEE 802.11 Protocol to Achieve a Theoretical Throughput Limit. *IEEE/ACM Transactions on Networking*, 8 (6), 785-799.

DEBREU, D. (1952) A social equilibrium existence theorem. *Proceedings of the National Academy of Sciences*, 38, 886-893.

DEBREU, D. (1959) *Theory of value. An axiomatic analysis of economic equilibrium*. New Haven USA, London England: Yale University Press.

DZIONG, Z. AND MASON, L.G. (1996) Fair-Efficient Call Admission Control Policies for Broadband Networks - A Game Theoretic Framework. *IEEE/ACM Transactions on Networking*, 4 (1), 123-136.

EASO, R. (1999) Evaluation of Dynamic Channel Allocation Schemes for TDMA and Comparison with CDMA Systems for Broadband ATM in Radio-Local-Loop Environments. Thesis (Diploma), ComNets Aachen University.

ERC (1999) Decision of 29 November 1999 on the harmonised frequency bands to be designated for the introduction of High Performance Radio Local Area Networks (HiperLANs). ERC/DEC/(99)23. Copenhagen Denmark: Electronic Communications Committee (European Radiocommunications Committee). Available from: http://www.ero.dk/documentation [1.1.2003]

ESSELING, N. AND VANDRA, H.S. AND WALKE, B. (2001) A Forwarding Concept for HiperLAN/2. *Computer Networks*. 37, 25-32. Available from: http://www.comnets.rwth-aachen.de/publications/N_Esseling.html [1.1.2003]

ETSI (2000a) Broadband Radio Access Networks (BRAN); HIPERLAN Type 2; Physical (PHY) Layer, Technical Specification ETSI TS 101 475. Sofia Antipolis France: European Telecommunications Standards Institute.

ETSI (2000b) Broadband Radio Access Networks (BRAN); HIPERLAN Type 2; Data Link Control (DLC) Layer; Part 1: Basic Data Transport Functions, Technical Specification ETSI TS 101 761 1. Sofia Antipolis France: European Telecommunications Standards Institute.

ETSI (2000c) Broadband Radio Access Networks (BRAN); HIPERLAN Type 2; Data Link Control (DLC) Layer; Part 2: Radio Link Control Protocol Basic Functions, Technical Specification ETSI TS 101 761 2. Sofia Antipolis France: European Telecommunications Standards Institute.

FCC (2003) Office of Engineering and Technology rule, part 15: Unlicensed RF Devices. *Title 47 of the Code of Federal Regulations*. Federal Communications Commission. Updated Mar-13 2003.

FISCHER, M. (2001) Hybrid Coordination Function (HCF) Frame Exchange and NAV Details. *IEEE Working Document 802.11-01/109r2*. Available from: http://www.ieee802.org/11 [1.1.2003]

FORKEL, I. (1999) Channel and Transmission Scheme Modeling for Wireless Local Loop and Powerline Communication Systems. Thesis (Diploma), ComNets Aachen University.

FORKEL, I., AND EASO, R., AND MANGOLD, S. (2000) Computer Simulation of Performance Enhancing Methods in ATM based Fixed Wireless Access Networks. *In: Symposium on Performance Evaluation of Computer and Telecommunication Systems*, Vancouver Canada 16-20 July 2000. 465-472. Available from: http://www.comnets.rwth-aachen.de/publications/S_Mangold.html [1.1.2003]

FORKEL, I., AND MANGOLD, S., AND EASO, R. AND WALKE, B. (2001) Traffic based Dynamic Channel Allocation Schemes for W.L.L.. *In:* P. STAVROULAKIS, ed. *Wireless Local Loops - Theory and Applications*. New York USA: John Wiley & Sons, 163-190. Available from: http://www.comnets.rwth-aachen.de/publications/S_Mangold.html [1.1.2003]

FUDENBERG, D. AND TIROLE, J. (1991) *Game Theory*. Cambridge Massachusetts USA, London England: The MIT Press.

FUDENBERG, D. AND LEVINE, D. K. (1998) *The Theory of Learning in Games*. Cambridge Massachusetts USA, London England: The MIT Press.

FULLER, C. (2002) *Iterated/Repeated Games*. Online Presentation. University of Rochester, Rochester USA.

GARRETT, M. W. (2000) *MPEG Tracefile MPEG.data*. Available from (anonymous ftp): ftp.telcordia.com/pub/vbr.video.trace [1.1.2003]

GANESH, A. AND LAEVENS, K. AND STEINBERG, R. (2000) Dynamics of congestion pricing. *Microsoft Research Technical Journal,* June 2000.

GAST, M. S. (2002) *802.11 Wireless Networks*. Sebastopol CA USA: O'Reilly & Associates, Inc.

GEIER, J. (2002) *Wireless LANs*. Indianapolis USA: Sams Publishing.

GLANCE, N. AND HUBERMAN, B. (1994) The Dynamics of Social Dilemmas. *Scientific American*, March 1994, 58-63.

GÖRG, C. (1997) *Verkehrstheoretische Modelle und Stochastische Simulationstechniken zur Leistungsanalyse von Kommunikationsnetzen*. Thesis (Habilitation), ComNets Aachen University. Aachen Germany: Wissenschaftsverlag Mainz.

GOODMAN, D. AND MANDAYAM, N. (2000) Power Control for Wireless Data. *IEEE Personal Communications Magazine*, 7 (2), 48-54.

GREEN, J. AND HELLER, W. P. (1981) Mathematical Analysis and Convexity with Applications to Economics. In: K. J. ARROW AND M. D. INTRILIGATOR, eds. *Handbook of Mathematical Economics, Vol. I*. Amsterdam The Netherlands: North-Holland Publishing, 15-52.

HABETHA, J. AND MANGOLD, S. AND WIEGERT, J. (2001) 802.11 vs. HiperLAN/2 – a comparison of decentralized and centralized MAC protocols for multihop ad hoc radio networks. *In: 5th World Multiconf. on Systemics, Cybernetics and Informatics*. Orlando 22-25 July 2001. Available from: http://www.comnets.rwth-aachen.de/publications/S_Mangold.html [1.1.2003]

HABETHA, J (2002) *Entwurf eines cluster-basierten ad hoc Funknetzes*. Thesis (PhD), ComNets Aachen University. Aachen Germany: Wissenschaftsverlag Mainz.

HACCOUN, D. AND BEGIN, G. (1989) High-rate punctured convolutional codes for Viterbi and sequential decoding. *IEEE Transactions on Communications*, 37 (11), 1113-1125.

HASHEMI, H. (1993) The indoor radio propagation channel. *Proceedings of the IEEE,* 81 (7), 942-967.

HEEGARD, C. AND COFFEY, J. AND GUMMADI, S. AND MURPHY, P. A. AND PROVENCIO, R. AND ROSSIN, E. J. AND SCHRUM, S. AND SHOEMAKER, M. B. (2001) High-Performance Wireless Ethernet. *IEEE Communications Magazine*, 39 (11), 64-73.

HENRY, P. S., AND LUO, H. (2002) Wi-Fi: What's Next? *IEEE Communications Magazine*, 40 (12), 66-72.

HETTICH, A. AND SCHRÖTHER, M. (1999) IEEE 802.11 or ETSI BRAN HIPERLAN/2: Who will win the race for a high speed wireless LAN standard? *In: European Wireless*. Munich Germany 6-8 October 1999. 169-174. Available from:
http://www.comnets.rwth-aachen.de/publications/A_Hettich.html [1.1.2003]

HETTICH, A. (2001) *Leistungsbewertung der Standards HIPERLAN/2 und IEEE 802.11 für drahtlose lokale Netze*. Thesis (PhD), ComNets Aachen University. Aachen Germany: Wissenschaftsverlag Mainz.

HIERTZ. G. R. (2002) Development and Evaluation of QoS Schemes in IEEE 802.11e Considering Competition Scenarios of Overlapping Wireless Networks. Thesis (Diploma), ComNets Aachen University.

HMAIMOU, M. (2000) Leistungsbewertung von Verfahren zur Koexistenzunterstützung von HiperLAN/2 und IEEE 802.11a. Thesis (Diploma), ComNets Aachen University.

HO, T.-S. AND CHEN, K.-C. (1996) Performance Analysis of IEEE 802.11 CSMA/CA Medium Access Control Protocol. *In: IEEE Personal Indoor Mobile Radio Conference,* Taipei Taiwan 15-18 October 1996. 392-396.

HOEBEN, M. AND WENTINK, M. (2000) Suggested 802.11 PCF Enhancements and Contention Free Bursts. *IEEE Working Document 802.11-00/113*. Available from:
http://www.ieee802.org/11 [1.1.2003]

HÖHER, P. (1992) A statistical discrete-time model for the WSSUS multi-path channel. *IEEE Transactions on Vehicular Technology*, 41 (4), 461-468.

IEEE 802 (1998) ANSI/IEEE Std 802.1D, 1998 Edition. IEEE Standard for Information technology - Telecommunications and information exchange between systems - Local and metropolitan area networks - Common specifications - Part 3: Media Access Control (MAC) Bridges. Adopted by the ISO/IEC and redesignated as ISO/IEC 15802-3:1998. New York USA: The Institute of Electrical and Electronics Engineers, Inc. Available from:
http://www.ieee802.org/11 [1.1.2003]

IEEE 802.11 WG (1999a) IEEE Std 802.11a, 1999 edition. Supplement to IEEE Standard for Information Technology - Telecommunications and information exchange between systems - Local and metropolitan area networks-Specific Requirements - Part 11: Wireless LAN Medium Access Control (MAC) and Physical Layer (PHY) specifications: High-speed Physical Layer in the 5 GHz Band. New York USA: The Institute of Electrical and Electronics Engineers, Inc. Available from: http://www.ieee802.org/11 [1.1.2003]

IEEE 802.11 WG (1999b) IEEE Std 802.11b, 1999 edition. Supplement to IEEE Standard for Information Technology-Telecommunications and information exchange between systems-Local and metropolitan area networks-Specific Requirements- Part 11: Wireless LAN Medium Access Control (MAC) and Physical Layer (PHY) specifications: Higher-Speed Physical Layer Extension in the 2.4 GHz Band. New York USA: The Institute of Electrical and Electronics Engineers, Inc. Available from:
http://www.ieee802.org/11 [1.1.2003]

IEEE 802.11 WG (1999c) Reference number ISO/IEC 8802-11:1999(E) IEEE Std 802.11, 1999 edition. International Standard [for] Information Technology-Telecommunications and information exchange between systems-Local and metropolitan area networks-Specific Requirements- Part 11: Wireless LAN Medium Access Control (MAC) and Physical Layer (PHY) specifications. New York USA: The Institute of Electrical and Electronics Engineers, Inc. Available from:
http://www.ieee802.org/11 [1.1.2003]

IEEE 802.11 WG (2002a) Draft Supplement to STANDARD FOR Telecommunications and Information Exchange Between Systems - LAN/MAN Specific Requirements - Part 11: Wireless Medium Access Control (MAC) and Physical Layer (PHY) specifications: Medium Access Control (MAC) Enhancements for Quality of Service (QoS), IEEE 802.11e/D3.3. New York USA: The Institute of Electrical and Electronics Engineers, Inc.

IEEE 802.11 WG (2002b) Draft Supplement to STANDARD FOR Telecommunications and Information Exchange Between Systems - LAN/MAN Specific Requirements - Part 11: Wireless Medium Access Control (MAC) and Physical Layer (PHY) specifications: Spectrum and Transmit Power Management extensions in the 5GHz band in Europe, IEEE 802.11h/D2.0. New York USA: The Institute of Electrical and Electronics Engineers, Inc.

IEEE 802.11 WG (2002c) Draft Supplement to STANDARD FOR Telecommunications and Information Exchange Between Systems - LAN/MAN Specific Requirements - Part 11: Wireless Medium Access Control (MAC) and Physical Layer (PHY) specifications: Medium Access Control (MAC) Enhancements for Quality of Service (QoS), IEEE 802.11e/D4.0. New York USA: The Institute of Electrical and Electronics Engineers, Inc.

KADELKA, A. (2002) *Entwurf und Leistungsanalyse des mobilen Internetzugangs über HIPERLAN/2*. Thesis (PhD), ComNets Aachen University. Aachen Germany: Wissenschaftsverlag Mainz.

KHUN-JUSH, J. AND SCHRAMM, P. AND WACHSMANN, U. AND WENGER, F. (1999) Structure and performance of the HIPERLAN/2 physical layer. *In: 50th IEEE Vehicular Technology Conference Fall-1999*, Amsterdam The Netherlands 22-24 September 1999. 2667-2671.

KITCHEN, D. (2001) HCF channel access rules. *IEEE Working Document 802.11-02/015r1*. Available from:
http://www.ieee802.org/11 [1.1.2003]

KLEINROCK, L. AND TOBAGI, F. A. (1975) Packet Switching in Radio Channels: Part 1: CSMA Modes and Their Throughput-Delay Characteristics. *IEEE Transactions on Communications,* 23, 1400-1416.

KYRIAZAKOS, S. (1999) *Position of Mobile Terminals in GSM and UTRA based on Pattern Recognition Techniques*. Thesis (Diploma), ComNets Aachen University.

LI, H. AND MALMGREN, G. AND PAULI, M. (2000) Performance comparison of the radio link protocols of IEEE 802.11a and HIPERLAN/2. *In: 52nd IEEE Vehicular Technology Conference Fall-2000*, Boston USA 24-28 September 2000. 2185-2191.

LOTT. M., AND MANGOLD, S. (1998) Indoor Radio Channel Characteristics. *In: Joint Workshop on Wireless Broadband In-house Digital Networks*, Ulm Germany 22-23 January 1998. Available from: http://www.comnets.rwth-aachen.de/publications/S_Mangold.html [1.1.2003]

LOTT. M., AND SEIDENBERG, P. AND MANGOLD, S. (1998) BER Characteristic for the Broadband Radio Channel at 5.2 GHz. *In: ITG-Workshop Wellenausbreitung bei Funksystemen und Mikrowellensystemen*, Oberpfaffenhofen Germany 11-13 May 1998. 53-60. Available from: http://www.comnets.rwth-aachen.de/publications/S_Mangold.html [1.1.2003]

LOTT. M., AND MANGOLD, S., AND EVANS, D. AND FIfiELD, R. (1998) Radio Transmission at 5.2 GHz: Channel Modelling and Performance Results for the Wireless ATM LAN Prototype. *In: MTT-S European Wireless*, Amsterdam The Netherlands 8-9 October 1998. 181-185. Available from: http://www.comnets.rwth-aachen.de/publications/S_Mangold.html [1.1.2003]

MACKENZIE, A. B. AND WICKER, S. B. (2001) Game Theory and the Design of Self-Configuring, Adaptive Wireless Networks. *IEEE Communications Magazine*, 39 (11), 126-131.

MANGOLD, S. (1997) Evaluation of the OFDM Multicarrier Transmission Scheme for Radio Channels by Means of Ray-Tracing. Thesis (Diploma), ComNets Aachen University.

MANGOLD, S., AND LOTT, M. (1998) Indoor Radio Channel Models based on Measurements and Ray-Tracing at 5.2 GHz. *In: ITG-Workshop Wellenausbreitung bei Funksystemen und Mikrowellensystemen*, Oberpfaffenhofen Germany 11-13 May 1998. 49-52. Available from: http://www.comnets.rwth-aachen.de/publications/S_Mangold.html [1.1.2003]

MANGOLD, S. AND LOTT, M. AND EVANS, D. AND FIfiELD, R. (1998) Indoor radio channel modeling - Indoor Radio Channel Modeling - Bridging from Propagation Details to Simulation. *In: IEEE Personal Indoor Mobile Radio Conference*, Boston Massachusetts USA 8-11 September 1998. 625-629. Available from: http://www.comnets.rwth-aachen.de/publications/S_Mangold.html [1.1.2003]

MANGOLD, S., AND FORKEL, I. (1999) Optimal DLC Protocol Configuration for Realistic Broadband Fixed Wireless Access Networks based on ATM. *In: International Conference on ATM,* Colmar France 22-24 June 1999. 15-21. Available from: http://www.comnets.rwth-aachen.de/publications/S_Mangold.html [1.1.2003]

MANGOLD, S., AND SIEBERT, M. AND KIESEL, C. (1999) Fair Coexistence of DECT and PHS Working in the same Frequency Band in Fixed Wireless Access Networks. *In: IEEE Personal Indoor Mobile Radio Conference,* Osaka Japan 12-15 September 1999. 347-352. Available from: http://www.comnets.rwth-aachen.de/publications/S_Mangold.html [1.1.2003]

MANGOLD, S., AND KYRIAZAKOS, S. (1999) Applying Pattern Recognition Techniques based on Hidden Markov Models for Vehicular Position Location in Cellular Networks. *In: 50th IEEE Vehicular Technology Conference Fall-1999*, Amsterdam The Netherlands 19-22 September 1999. 780-784. Available from:
http://www.comnets.rwth-aachen.de/publications/S_Mangold.html [1.1.2003]

MANGOLD, S., AND SIEBERT, M. (1999) Sharing Rules for DECT and PHS Providing Fair Access to the Commonly used Frequency Band. *In: European Wireless*, Munich Germany 6-8 October 1999. 367-372. Available from:
http://www.comnets.rwth-aachen.de/publications/S_Mangold.html [1.1.2003]

MANGOLD, S. (2000) Game Theoretical Approaches for Spectrum Sharing in Wireless Communication. In: 7th Viennese Workshop on Optimal Control, Dynamic Games and Nonlinear Dynamics: Theory and Applications in Economics and OR/MS, Vienna Austria 24-26 May 2000. Available from:
http://www.comnets.rwth-aachen.de/publications/S_Mangold.html [1.1.2003]

MANGOLD, S. AND HMAIMOU, M. AND WIJAYA, H. (2000) Coexistence of IEEE 802.11a and ETSI BRAN H2: The Problem of Fair Resource Sharing in the License Exempt Band at 5GHz. *In: IEEE International Conference on Third Generation Wireless Communications,* San Francisco USA 30 May-2 June 2000. 530-536. Available from:
http://www.comnets.rwth-aachen.de/publications/S_Mangold.html [1.1.2003]

MANGOLD, S. AND FORKEL, I. (2000) Configuration optimale d'un protocole de liaison de données pour réseaux d'accès fixes sans fil basés sur ATM. *Annales des Télécommunications*, 55 (11-12), 567-576. Available from:
http://www.comnets.rwth-aachen.de/publications/S_Mangold.html [1.1.2003]

MANGOLD, S. AND CHOI, S. AND WIEMANN, T. (2001a) 802.11a/e and H2: Coexistence and Interworking using Enhanced PCF. *European Telecommunications Standardization Institute ETSI Working Document BRAN22d096*.

MANGOLD, S. AND CHOI, S. AND WIEMANN, T. (2001b) Contention-Free Scheduling of H2 Frames without QoS Limitations. *IEEE Working Document IEEE 802.11-01/13*. Available from:
http://www.ieee802.org/11 [1.1.2003]

MANGOLD, S. AND CHOI, S. AND WIEMANN, T. (2001c) 801.11a/e and H2 interworking via CCEPC. *IEEE Working Document IEEE 802.11-01/067*. Available from:
http://www.ieee802.org/11 [1.1.2003]

MANGOLD, S. AND CHOI, S. AND BUDDE, W. AND NGO, C. (2001d) 802.11a/e and H2 Interworking using HCF. *IEEE Working Document 802.11-01/414r0*. Available from:
http://www.ieee802.org/11 [1.1.2003]

MANGOLD, S. AND MATHEUS, A. AND BEINE, M. (2001e) Powerline Communications: Adopting Protocols of Wireless Access Networks. *In: 5th Africom Conference*, Cape Town South Africa 28-31 May 2001. Available from:
http://www.comnets.rwth-aachen.de/publications/S_Mangold.html [1.1.2003]

MANGOLD, S. AND CHOI, S. AND ESSELING, N. (2001f) An Error Model for Radio Transmissions of Wireless LANs at 5GHz. *In: 10th Aachen Symposium on Signal Theory*, Aachen Germany 20-21. September 2001. Berlin Germany: VDE Verlag, 209-214. Available from: http://www.comnets.rwth-aachen.de/publications/S_Mangold.html [1.1.2003]

MANGOLD, S. AND HABETHA, J. AND CHOI, S. AND NGO, C. (2001h) Co-existence and Interworking of IEEE 802.11a and ETSI BRAN HiperLAN/2 in MultiHop Scenarios. *In: IEEE 3rd Workshop on Wireless Local Area Networks* Boston USA 27-28. September 2001. Available from: http://www.comnets.rwth-aachen.de/publications/S_Mangold.html [1.1.2003]

MANGOLD, S. AND FORKEL, I. AND EASO, R. AND WALKE, B. (2001i) Traffic Considerations in Comparing Access Techniques for W.L.L.. *In:* P. STAVROULAKIS, ed. *Wireless Local Loops - Theory and Applications*. New York USA: John Wiley & Sons, 141-161. Available from: http://www.comnets.rwth-aachen.de/publications/S_Mangold.html [1.1.2003]

MANGOLD, S. AND CHOI, S. AND MAY, P. AND KLEIN, O. AND HIERTZ, G. AND STIBOR, L. (2002a) IEEE 802.11e Wireless LAN for Quality of Service. *In: European Wireless* Florence Italy 26-28 February 2002. 32-39. Available from: http://www.comnets.rwth-aachen.de/publications/S_Mangold.html [1.1.2003]

MANGOLD, S. AND BERLEMANN, L. AND HIERTZ, G. (2002b) QoS Support as Utility for Coexisting Wireless LANs. *In: International Workshop on IP Based Cellular Networks*, Paris France 23-26 April 2002. Available from: http://www.comnets.rwth-aachen.de/publications/S_Mangold.html [1.1.2003]

MANGOLD, S. (2002c) IEEE 802.11e: Coexistence of Overlapping Basic Service Sets. *In: Mobile Venue'02*, Athens Greece 30-31 May 2002. 131-135. Available from: http://www.comnets.rwth-aachen.de/publications/S_Mangold.html [1.1.2003]

MANGOLD, S. AND CHOI, S. AND MAY, P. AND HIERTZ, G. (2002d) IEEE 802.11e - Fair Resource Sharing between Overlapping Basic Service Sets. *In: IEEE Personal Indoor Mobile Radio Conference,* Lisbon Portugal 15-18 September 2002. 166-171. Available from: http://www.comnets.rwth-aachen.de/publications/S_Mangold.html [1.1.2003]

MITTAG, L. (2002) Guide to IEEE 802.11 Wireless LAN Standards. In: Embedded Systems Conference, Rosemont IL USA, 3-6 June 2002. Available from: http://www.chipcenter.com/wireless/tn002.html [1.1.2003]

NASH, J. F. (1950a) *Non-cooperative Games*. Thesis (PhD), Princeton University.

NASH, J. F. (1950b) Equilibrium points in N-person games. *Proceedings of the National Academy of Science of the United States of America*, 36, 48-49.

O'HARA, B. AND PETRICK, A. (1999) *The 802.11 Handbook – A Designer's Companion*. New York USA: The Institute of Electrical and Electronics Engineers, Inc.

ORDA, A. AND ROM, R. AND SHIMKIN, N. (1993) Competitive Routing in Multiuser Communication Networks. *IEEE/ACM Transactions on Networking*, 1 (5), 510-521.

OSBORNE, M. J. AND RUBINSTEIN, A. (1994) *A Course in Game Theory*. Cambridge Massachusetts USA, London England: The MIT Press.

PURSLEY, M. B. AND TAIPALE, D. J. (1987) Error probabilities for spread-spectrum packet radio with convolutional codes and Viterbi decoding. *IEEE Transactions on Communications*, COM-35 (1), 1-12.

QIAO, D. AND CHOI, S. (2001) Goodput enhancement of IEEE 802.11a wireless LAN via link adaptation. *In: IEEE International Conference on Communications*, Helsinki Finland 11-14 June 2001, 7, 1995-2000.

REGTP (2002) Vfg Nr. 35/2002: Allgemeinzuteilung von Frequenzen in den Bereichen 5150 MHz – 5350 MHz und 5470 MHz – 5725 MHz für die Nutzung durch die Allgemeinheit un lokalen Netzwerken; Wireless Local Area Networks (WLAN-Funkanwendungen). *Amtsblatt der Regulierungsbehörde für Telekommunikation und Post,* 22. Bonn Germany: Regulierungsbehörde für Telekommunikation und Post, 1634-1637.

SALGADO-GALICIA, H. AND SIRBU, M. AND PEHA, J. (1997) A Narrowband Approach to Efficient PCS Spectrum Sharing Through Decentralized DCA Access Policies. *IEEE Personal Communications Magazine*, 4(1), 24-34. Available from: http://www.comsoc.org/%7Edl/jhtmls/ieee/comm/pc/1997004/01feb/0024salg/0024salg.html [1.1.2003]

SCHREIBER, F. (1988) Effective Control of Simulation Runs by a New Evaluation Algorithm for Correlated Random Sequences. *AEÜ International Journal of Electronics and Communications*, 42 (6), 347–354.

SHUBIK, M. (1981) Game Theory Models and Methods in Political Economy. In: K. J. ARROW AND M. D. INTRILIGATOR, eds. *Handbook of Mathematical Economics, Vol. I*. Amsterdam The Netherlands: North-Holland Publishing, 285-330.

SHUBIK, M. (1982) *Game Theory in the Social Sciences*. Cambridge Massachusetts USA, London England: The MIT Press.

SOBRINHO, J. L. AND KRISHNAKUMAR. A. S. (1996) Real-time traffic over the IEEE 802.11 medium access control layer. *Bell Labs Technical Journal,* Autumn 1996, 172–187.

SOBRINHO, J. L. AND KRISHNAKUMAR. A. S. (1999) Quality-of-Service in ad hoc carrier sense multiple access networks. *IEEE Journal on Selected Areas in Communications*, 17 (8), 1353–1368.

STEER, D. G. (1994) Coexistence and Access Etiquette in the United States Unlicensed PCS Band. *IEEE Personal Communications Magazine*, 1(4), 36–43.

STEPHENS, D. W. AND ANDERSON, J. P. (1997) Reply to Roberts: cooperation is an outcome, not a mechanism. *Journal on Animal Behavior*, 53, 1363-1364.

TAKAGI, H. AND KLEINROCK, L. (1985) Throughput Analysis for Persistent CSMA Systems. *IEEE Transactions on Communications,* 33(7), 627-638.

TOURRILHES, J. (1998) Packet Frame Grouping : Improving IP multimedia performance over CSMA/CA. *In: IEEE International Conference on Universal Personal Communications*. Florence Italy October 5-9, 1998. Available from: http://www.hpl.hp.com/personal/Jean_Tourrilhes/Papers [1.1.2003]

VON NEUMANN, J. AND MORGENSTERN, O. (1953) *Theory of games and economic behavior*. 3rd ed. Princeton New Jersey: Princeton University Press.

WALKE, B. (2002) *Mobile Radio Networks*. 2nd ed. New York USA: John Wiley & Sons.

WALKE, B. AND ESSELING, N. AND HABETHA, J. AND HETTICH, A. AND KADELKA, A. AND MANGOLD, S. AND PEETZ, J. AND VORNEFELD, U. (2001) IP over Wireless Mobile ATM - Guaranteed Wireless QoS by HiperLAN/2. *Proceedings of the IEEE*, 89, 21-40. Available from:
http://www.comnets.rwth-aachen.de/publications/S_Mangold.html [1.1.2003]

WEIBULL, J. W. (1995) *Evolutionary Game Theory*. Cambridge Massachusetts USA, London England: The MIT Press.

WIEMANN, T. (2000) Development of techniques to support QoS in ad hoc scenarios of competing HiperLAN/2 and IEEE 802.11a systems. Thesis (Diploma), ComNets Aachen University.

WIJAYA, H. (1999) Development of Framework Methods based on Game Theory to provide Fair Coexistence of Future Mobile Radio Communication Networks within Unlicensed Frequency Bands with respect to HiperLAN/2 and IEEE 802.11. Thesis (Diploma), ComNets Aachen University.

ZBIGNIEW, D. AND MASON, L. G. (1996) Fair-Efficient Call Admission Control Policies For Broadband Networks-A Game Theoretic Framework. *IEEE/ACM Transactions on Networking*, 4 (1), 123-136.

Acknowledgement

This thesis is an outcome of five exciting years of intensive work at the Chair of Communication Networks, Aachen University, Germany. During my time at ComNets, I was honoured with the privilege to work for Prof. Dr.-Ing. Bernhard Walke. My most sincere appreciation goes to Prof. Walke for his support, the many helpful advises, and for providing me with the opportunity to work in the challenging environment of ComNets.

I further thank Prof. Dr. Petri Mähönen, Chair of Mobile Networks, Aachen University, for his support from the very first day we met, and for evaluating my thesis.

I thank my fellow colleagues Dipl.-Ing. Lars Berlemann and Dr.-Ing. Ian Herwono, as well as Dr.-Ing. Jörg Habetha of Philips Research, for checking large parts of my thesis and giving many valuable comments.

I thank Dipl.-Ing. Guido Hiertz for his very good master thesis, and for taking over the numerous projects from me. My appreciation also goes to Dipl.-Ing. Lars Berlemann for his very good master thesis, and our many stimulating discussions about the exciting field of the theory of games.

A deep thank you is forwarded to all students I had the opportunity to work with, for their many contributions. I wish all of them, Guido, Lars, Bahman, Mohamed, Thorsten, Roger, Alexander, Yao, Arnd, Michael, Wolfgang, Harianto, Sofoklis, Matthias, Ingo, Carsten, Yang, Yu, the very best for their future.

Thanks to my friend Dr.-Ing. Ian Herwono for helping me to make my stay at ComNets so comfortable and for spending a great time together!

A very sincere thanks to the people I worked with at Philips Research Aachen, Germany. Special thanks are due to Dr.-Ing. Wolfgang Budde and Dipl.-Ing. Peter May for their support.

Further, I am grateful to Steven Hanft, ConUS, for his uncountable helpful advices during the last years.

It remains to be sent a very warm thank you to the other side of our world. I thank Ass.-Prof. Dr. Sunghyun Choi, Seoul National University, Korea, for the remarkable years of joint research, standardization, and the many papers we wrote together.

Finally I wish to thank my friends, and my family, Beate and Benjamin, the Mangolds, the Hoppes and Phillips, for having them on my side. I thank my father-in-law, Dr. rer. nat. Klaus Hoppe for his overwhelming support and educating.

I am gifted with a father and a mother who have been believing in me throughout my entire life. I thank both for their continual support and love.

However, there is one person left. I thank you, Hella, for your love, for your inspirations, for being with me.

New York USA, June 2003 Stefan Mangold

Biography

Name, Vorname:	Mangold, Stefan
Geburtsdatum:	30. März 1968
Geburtsort:	Goch
Familienstand:	verheiratet
Staatsangehörigkeit:	Deutsch

Schule

1974–1978	Grundschule Holzlar, Bonn
1978–1987	Kardinal Frings Gymnasium Bonn, Abitur 1987

Berufsausbildung

1987–1990	Elektrogerätemechaniker und Energiegeräteelektroniker bei der Klöckner Moeller AG, Bonn

Studium

10/1991–12/1997	Elektrotechnik, Fachrichtung Nachrichtentechnik an der RWTH Aachen Diplomarbeit: „Evaluation of the OFDM Multicarrier Transmission Scheme for Radio Channels by Means of Ray-Tracing“ bei den Philips Research Laboratories Redhill, England

Beruf

1/1998–2/2003	Wissenschaftlicher Mitarbeiter am Lehrstuhl für Kommunikationsnetze der RWTH Aachen (Lehrstuhlinhaber: Prof. Dr.-Ing. B. Walke)
seit 3/2003	Senior Member Research Staff bei den Philips Research Laboratories Briarcliff Manor NY, USA